

The Farinograph Handbook

Advances in Technology, Science, and Applications

Fourth Edition

Edited by

Jayne E. Bock and Clyde Don



The Farinograph Handbook

This page intentionally left blank

Woodhead Publishing Series in Food Science,
Technology and Nutrition

The Farinograph Handbook

Advances in Technology, Science, and Applications

Fourth Edition

Edited by

Jayne E. Bock

Wheat Marketing Center, Portland, OR, United States

Clyde Don

FoodPhysica Laboratory, Malden, The Netherlands



WP
WOODHEAD
PUBLISHING

An imprint of Elsevier



**CEREALS
& GRAINS
ASSOCIATION**

Woodhead Publishing is an imprint of Elsevier
50 Hampshire Street, 5th Floor, Cambridge, MA 02139, United States
The Boulevard, Langford Lane, Kidlington, OX5 1GB, United Kingdom

Copyright © 2022 Cereals & Grains Association. Published by Elsevier Inc. All rights reserved.

No part of this publication may be reproduced or transmitted in any form or by any means, electronic or mechanical, including photocopying, recording, or any information storage and retrieval system, without permission in writing from the publisher. Details on how to seek permission, further information about the Publisher's permissions policies and our arrangements with organizations such as the Copyright Clearance Center and the Copyright Licensing Agency, can be found at our website: www.elsevier.com/permissions.

This book and the individual contributions contained in it are protected under copyright by the Publisher (other than as may be noted herein).

Notices

Knowledge and best practice in this field are constantly changing. As new research and experience broaden our understanding, changes in research methods, professional practices, or medical treatment may become necessary.

Practitioners and researchers must always rely on their own experience and knowledge in evaluating and using any information, methods, compounds, or experiments described herein. In using such information or methods they should be mindful of their own safety and the safety of others, including parties for whom they have a professional responsibility.

To the fullest extent of the law, neither the Publisher nor the authors, contributors, or editors, assume any liability for any injury and/or damage to persons or property as a matter of products liability, negligence or otherwise, or from any use or operation of any methods, products, instructions, or ideas contained in the material herein.

ISBN: 978-0-12-819546-8 (print)

ISBN: 978-0-12-819571-0 (online)

For information on all Woodhead publications
visit our website at <https://www.elsevier.com/books-and-journals>

Publisher: Nikki Levy
Acquisitions Editor: Nancy Maragioglio
Editorial Project Manager: Lindsay Lawrence
Production Project Manager: Sruthi Satheesh
Cover Designer: Miles Hitchen

Typeset by STRAIVE, India



Working together
to grow libraries in
developing countries

www.elsevier.com • www.bookaid.org

Dedication

This handbook is respectfully dedicated to Carl Wilhelm Brabender, who once stated ([Brabender, 1965](#)), “I have devoted the last 40 years to the design and application engineering of physical and rheological test methods, and I intend to do so for the rest of my life.” No one can ever say that he did not remain faithful to this statement. He became a member of the AACC in 1931 and was made an Honorary Member in 1965. The Cal Wilhelm Brabender Award was established in his honor to encourage research in applied milling and baking rheology.

Will became acquainted with the flour milling industry by designing and introducing an electrical high-voltage arc bleacher producing N_2O_4 for flour bleaching. He had been trained as an electrical engineer and physicist. In 1929 he met Professor Jeno von Hankóczy, who had developed a disk-type dough-testing machine and an apparatus to determine water absorption. From this meeting developed a lifelong friendship and mutual interest in measuring elastic and plastic properties of doughs.

In about 1927, Hankóczy observed in a bakery a motor-driven dough mixer to which an ammeter was attached; he noted that the greater the ammeter reading, the higher the consistency of the dough. This observation led to the design of the first forerunner of the Farinograph. Hankóczy realized that the basic problem with the design of instruments that followed was due to small differences in power consumption in mixing different doughs, compared with the energy required to drive the whole instrument.

Then, in Will’s own words ([Brabender, 1965](#)), “In 1929 and 1930 I made many trips from my native Germany to Budapest, spending a total of more than six months with my friend Hankóczy ‘learning the ropes’ of wheat

breeding, experimental milling and baking tests. Hankóczy taught me nearly 30 years of his own experience and that of his teachers, especially Kosutany. I knew then that the next goal was to design the most accurate dynamometer for measuring the torque of a little dough mixer, but still no one spoke of temperature control or of recording the results on a strip chart. – Within five months I went back to Budapest with the first prototype of this instrument. – This design already showed basic elements of the present day farinograph. – Development then went step by step. The first discovery was that water absorption as strength measurement was not reliable. There were too many exceptions. – A little recording drum from a thermograph was attached to the farinograph. – The chart we obtained on this drum was, more or less, today's farinogram. We learned very soon that the time to peak was in line with the dough mixing requirements of a certain flour, and the weakening characteristics of the curve beyond the peak was an indication of general strength. In addition, the machine would produce the water absorption figure. It was an immediate success all over Europe.”

“The next disappointment came when this machine was introduced in 1930–1931 in the United States. Again it produced very confusing results. Sometimes it would duplicate well, sometimes not at all. – We found that the general strength of wheat flours in the United States was several times that of European wheat, and the heat produced during mixing would, of course, change the rheological properties of the dough and introduce a strongly disturbing factor into the whole measurement. – I went back to Europe and redesigned the machine for close temperature control, resulting in the present jacketed mixer and jacketed damper and the circulating pressure thermostat. At the same time, the rather primitive thermograph drum recorder was replaced by a larger 7-inch strip chart recorder which has been standard on farinographs for the last 35 years. – From then on, the Farinograph was introduced quickly all over the world.”

The impact and influence of Cal Wilhelm Brabender on the milling and other industries by the introduction of the Farinograph, as well as many other testing instruments, will never be forgotten.

Will Brabender will remain fresh in the memory of cereal chemists for his many contributions to the advancement of cereal science.

REFERENCE

Brabender, C.W., 1965. Physical dough testing—past, present, and future. *Cereal Sci. Today* 10, 291–304.

This page intentionally left blank

Contents

Contributors	xv
About the editors	xvii
Preface	xix

SECTION A INSTRUMENT

CHAPTER 1 The Farinograph: Its origins	3
C.W. Wrigley, S. Tömösközi, F. Békés, and M. Bason	
1.1 Introduction.....	3
1.2 Dough properties and baking quality.....	4
1.3 The wheat breeder's needs	6
1.4 Hooke, Newton, Hogarth and Dough	6
1.5 Hankóczy's Farinograph	9
1.6 The Valorigraph—Still in production and use	10
1.7 The Hankóczy-Brabender relationship	11
1.8 Ongoing development and expansion for Brabender	11
1.9 Ongoing development and adoption of the Farinograph.....	13
1.10 The transition from chart paper to computer screen	15
1.11 The Breeder's and Researcher's needs—Very small-scale analysis	15
1.12 Dough in the “real life” of the bakery.....	17
1.13 Beyond the recording of torque	18
1.14 Conclusion.....	18
References.....	20
CHAPTER 2 Principles of Farinograph operation and factors affecting performance	23
Jayne E. Bock	
2.1 What influences Farinograph results?.....	23
2.1.1 The temperature factor	23
2.1.2 The water absorption factor	24
2.1.3 The operator factor	25
2.1.4 Instrumental factors	26
2.2 Communicating meaningful Farinograph results between millers and bakers	27
2.2.1 Communicating for decision making	27
2.2.2 Communicating for relevancy to a process	27
2.3 Putting it all together.....	31

CHAPTER 3 The Farinograph: Understanding Farinograph curves	33
Jayne E. Bock	
3.1 Flour composition basics and beyond.....	33
3.2 Assessing flour quality	34
3.3 What does the Farinograph measure?.....	34
3.4 How do we read the Farinograph torque curve?	35
3.5 Using Farinograph parameters to classify flours.....	36
3.6 The double-peak conundrum.....	37
3.7 Comparing different Farinograph methods.....	37
3.8 The bottom line	41
CHAPTER 4 Dough rheology and the Farinograph:	
The mechanism underlying dough development.....	43
Clyde Don	
4.1 Dough rheological insights in the third edition.....	44
4.2 Dough development—The disaggregation of gel-protein	46
4.3 Developing dough—The interaction of glutenin aggregates	52
4.4 Dough physical properties—Glutenin polymer size or glutenin aggregates?	58
4.4.1 Observed changes in the SP fraction	60
4.4.2 Observed changes in the insoluble glutenin-gel fraction	61
4.4.3 Fate of the gel-proteins and functionality in dough	63
4.4.4 The mechanism underlying dough peak resistance in the Farinograph	64
4.5 Conclusions.....	66
Acknowledgments	68
References.....	68
SECTION B APPLICATIONS	
CHAPTER 5 The Farinograph as a tool for wheat-milling operations: Current and potential uses.....	73
Curtis Bartell, Angie Anyieni, and Gang Guo	
5.1 Introduction.....	73
5.1.1 Using the Farinograph to optimize mill input	74
5.1.2 Using the Farinograph to optimize in-process stream selection	76
5.1.3 Using the Farinograph to optimize final product flour blends	77

5.2	Limitations of Farinograph testing in wheat milling operations.....	79
5.3	Summary	80
CHAPTER 6	Using the Farinograph in daily bakery operations	81
	Stanley P. Cauvain	
6.1	Key elements of bread production	81
6.2	Dough consistency in bakery practice	82
6.3	Water absorption and recipe water level	83
6.4	Water absorption, recipe water level, and dough processing	84
6.5	Dough development and commercial dough mixing.....	85
6.6	Dough temperature	87
6.7	Alternate commercial uses for the Farinograph	87
6.8	Conclusion	88
	References.....	89
CHAPTER 7	Using the Farinograph for soft wheat products	91
	Jayne E. Bock	
7.1	Soft wheat and its uses.....	91
7.2	Cracker processing	92
7.3	Flour-quality requirements for crackers.....	92
7.4	Making the Farinograph method relevant to cracker applications	94
	References.....	97
CHAPTER 8	Farinograph applications for whole wheat flour: Exploring the influence of circulating water temperature and mixing speed on dough mixing properties in the Farinograph	99
	Lingzhu Deng and Gary G. Hou	
	References.....	108
CHAPTER 9	Use of the Farinograph for gluten-free grains	111
	Andrea Bresciani, George Amponsah Annor, Mattia Gardella, and Alessandra Marti	
9.1	Introduction.....	111
9.2	Use of the Farinograph for GF cereals	113
9.3	Pseudocereals.....	118
9.4	Pulses	119
9.5	Conclusions.....	124
	Acknowledgment	124
	References.....	125

CHAPTER 10 Using the Farinograph and other Brabender torque rheometers to measure the rheological properties of complex biological materials	127
R.K. Connelly, S. Burlawar, D.J. Klingenberg, and C.T. Scott	
10.1 Introduction	128
10.2 Equipment.....	129
10.2.1 Torque rheometer basics	129
10.2.2 Brabender torque rheometers and accessories in use in the food industry	129
10.2.3 Brabender torque rheometer modifications for high solids biomass research	131
10.3 Procedure	132
10.3.1 Calibration procedure	132
10.3.2 Fitting data with rheological models.....	133
10.3.3 Data collection.....	134
10.3.4 Sample results.....	138
10.4 Representative results from high solids biomass research.....	143
10.4.1 Rheology of suspensions of acid-hydrolyzed corn stover	143
10.4.2 Effect of rheological modifiers	145
10.4.3 Effect of biomass type.....	146
10.4.4 Effect of enzymatic hydrolysis.....	148
10.5 Conclusions	149
Appendices.....	150
Appendix I: Instrument calibration	150
Appendix II: Fitting rheological models.....	155
References.....	158
CHAPTER 11 Advanced research applications.....	161
Jose C. Bonilla, Neslihan Bozdogan, and Jozef L. Kokini	
11.1 Gluten and gluten subfraction contributions in dough development during mixing	163
11.1.1 Gluten protein classification and impact in wheat flour and dough	163
11.1.2 Gliadin and glutenin classification and contribution to mixing	164
11.1.3 Glutenin macropolymer behavior during mixing	165
11.2 Visualization of gluten proteins during dough mixing/development	166

11.2.1	Gluten and starch visualization at different mixing regimes through fluorescence fingerprint	166
11.2.2	Visualization of gluten with nano-fluorescent quantum dots.....	166
11.3	Visualization of gliadin during dough mixing using fluorescent nanoparticles.....	168
11.3.1	Quantum dots as tracers for cereal proteins with confocal laser scanning microscopy as a detection system	168
11.3.2	Imaging of gliadin subfraction during mixing and in baked bread	169
11.4	Current research in visualization of gluten subfractions during dough mixing	170
11.4.1	Immunofluorescent imaging of HMW and LMW glutenins through specifically developed antibodies	170
11.4.2	Detection of gliadins, HMW glutenins, and LMW glutenins in wheat dough with autofluorescence and nongluten controls	172
11.5	Distribution of extension rate and shear rate and prediction of maximum stable bubble size inside the C.W. Brabender Farinograph.....	184
	References.....	188

SECTION C APPENDICES

Appendix A	Bowl cleaning and maintenance	195
Appendix B	Troubleshooting.....	197
Appendix C	Legacy information	199
I	Prefaces to prior editions	199
II	The Farinograph.....	201
III	Theoretical aspects of the Farinograph	212
IV	AACC physical testing methods committee Farinograph collaborative study	226
V	Farinograph procedures of the AACC, ICC, and RACI.....	232
VI	Selected references concerning the Farinograph that have appeared in cereal chemistry and cereal foods world	240
	Index	247

This page intentionally left blank

Contributors

George Amponsah Annor

Department of Food Science and Nutrition, University of Minnesota, Saint Paul, MN, United States

Angie Anyieni

Ardent Mills, Denver, CO, United States

Curtis Bartell

Ardent Mills, Denver, CO, United States

M. Bason

Perten, Sydney, NSW, Australia

F. Békés

FBFD Pty Ltd, Sydney, NSW, Australia

Jayne E. Bock

Wheat Marketing Center, Portland, OR, United States

Jose C. Bonilla

Department of Food Science, Purdue University, West Lafayette, IN, United States

Neslihan Bozdogan

Department of Food Science, Purdue University, West Lafayette, IN, United States

Andrea Bresciani

Department of Food, Environmental and Nutritional Sciences (DeFENS), Università degli Studi di Milano, Milan, Italy

S. Burlawar

International Flavors and Fragrances, Inc., St. Louis, MO, United States

Stanley P. Cauvain

BakeTran, Witney, United Kingdom

R.K. Connelly

International Flavors and Fragrances, Inc., St. Louis, MO, United States

Lingzhu Deng

Wheat Marketing Center, Portland, OR, United States

Clyde Don

FoodPhysica Laboratory, Malden, The Netherlands

Mattia Gardella

Department of Food, Environmental and Nutritional Sciences (DeFENS), Università degli Studi di Milano, Milan, Italy

Gang Guo

Ardent Mills, Denver, CO, United States

Gary G. Hou

Wheat Marketing Center, Portland, OR, United States; SPC Group, Seoul, South Korea

D.J. Klingenberg

Department of Chemical and Biological Engineering, University of Wisconsin, Madison, WI, United States

Jozef L. Kokini

Department of Food Science, Purdue University, West Lafayette, IN, United States

Alessandra Marti

Department of Food, Environmental and Nutritional Sciences (DeFENS), Università degli Studi di Milano, Milan, Italy

C.T. Scott

Department of Chemical and Biological Engineering, University of Wisconsin, Madison, WI, United States

S. Tömösközi

Budapest University of Technology and Economics, Department of Applied Biotechnology and Food Science, Research Group of Cereal Science and Food Quality, Budapest, Hungary

C.W. Wrigley

University of Queensland, Brisbane, QLD, Australia

About the editors

Jayne E. Bock, PhD, is the Technical Director at the Wheat Marketing Center and an adjunct professor at Oregon State University. She previously served as the Global Technical Leader of the Food Division for C.W. Brabender Instruments, Inc. and as an adjunct professor at the University of Guelph. Her expertise is in grain and flour quality, baking science, gluten structure-function, and the influence of bran on product structure and quality in whole-grain products. She works extensively with wheat breeders, agronomists, growers, millers, and food processors at the interface of academia and industry to find solutions for emerging quality issues in the global milling and baking industries. Jayne earned her BSc and MSc degrees from Kansas State University and her PhD from the University of Wisconsin-Madison.

Clyde Don, PhD, studied chemical engineering in The Hague/Delft (BSc degree) and chemistry at the University of Amsterdam (MSc degree). He obtained his PhD degree in food chemistry from Wageningen University. He has worked in applied research and technology (e.g., TNO) and in analytical service labs in various leadership functions. As an active member of AACCI, he has chaired scientific initiatives and divisions, co-chaired courses, conducted workshops, and led technical committees and working groups. For IFT he is the co-founder and leadership team member of the IFT Protein Division (2015). Clyde is also currently a member of the AOAC Expert Review Panel on gluten methods. Since 2009 he has been the managing director of Clyde Don Consultancy FoodPhysica, and since 2016 has served as director of the FoodPhysica R&D Laboratory, providing consulting and contract R&D services in sustainable food science and technology, biobased products, processing and interactions, food machinery and NPD, protein functionality and applications, analytical chemistry, and food safety and quality.

This page intentionally left blank

Preface

As editors we are honored to have taken part in this new edition of *The Farinograph Handbook*. Both of us share a past with the specific rheology in cereal science and the role of the Farinograph. In this preface, we would like to share a few personal notes as editors, followed by a note from Sal Iaquez, who has been the face and connector of C.W. Brabender for more than 30 years. With his optimism and energy, he has helped many of us taking the first steps into the use of the Farinograph.

Having spent time as a scientist within TNO for a decade and being able to interact with Dr. A.H. Bloksma before his passing, it was without hesitation that I agreed to help with this edition and add the new knowledge on the mechanism underlying dough development.

Clyde Don

The opportunities I had to study under Dr. Robin K. Connelly and interact with Dr. Clyde Don fundamentally shaped my understanding of dough rheology in the formative years of my career. I gladly accepted the opportunity to assist with this edition to further the use and exploration of dough rheology in both practical and unconventional applications.

Jayne E. Bock

The Farinograph is fundamentally a torque rheometer used all over the world as a standard means of communication between the flour miller and the baker. It's important for these types of publications, such as the Farinograph, Extensograph, and Amylograph handbooks, just to name a few, to exist so they can provide an objective understanding of an instrument's operation and standard methodology. But, more importantly, this handbook provides information on what the "actual" farinogram means, and how the numbers it yields, like "stability, MTI, etc." may relate to your individual process, which can ultimately create a consistent end product.

I've spent decades participating in many industry (AACC) workshops/conferences and, as a longtime member of the AACC Physical Testing Methods Committee, I tend to have a different perspective on the use, and requested uses, of the Farinograph in various segments of the food and unrelated industries. Over the years, there have been many inquiries about the Farinograph for what I refer to as "unconventional" applications and/or testing, which basically means any use of the Farinograph, outside of the typical standard methodologies, which are outlined by AACC 54-21.02 and ICC 115, ISO, etc. Of course, the basis for this 4th edition of *The Farinograph Handbook* is, and should be, the proper use of the Farinograph for standard applications, such as water absorption and the evaluation points generated when conducting a standard test. That said, not mentioning and/or dedicating chapters to the other "nonconventional" uses and

applications of the Farinograph that are often requested would be a disservice to this 4th edition, as this edition of *The Farinograph Handbook* should be a representation of how industries portray and “actually use” this worldwide standard instrument.

It’s been a great privilege early in my career to work, organize, and contribute at many of the AACR Rheology Workshops, with Bert D’Appolonia, Vladimir Rasper, Robin Connelly, and Jozef Kokini. These are well-known industry professionals who have contributed to many publications that have used the Farinograph, both “conventionally” and “unconventionally,” and the unconventional applications side is often not known, or not mentioned as often. A special thank you to my colleagues Wolfgang Sietz, Markus Loens, and Jessica Wiertz, from our headquarters, Brabender GmbH and Co. KG (Duisburg, Germany), that have helped me over many years to support Brabender’s food product portfolio, which includes the Farinograph, to our North American customers.

Sal Iaquez
Gemelli Scientific

Section A

Instrument

This page intentionally left blank

The Farinograph: Its origins

C.W. Wrigley^a, S. Tömösközi^b, F. Békés^c, and M. Bason^d

^a*University of Queensland, Brisbane, QLD, Australia* ^b*Budapest University of Technology and Economics, Department of Applied Biotechnology and Food Science, Research Group of Cereal Science and Food Quality, Budapest, Hungary* ^c*FBFD Pty Ltd, Sydney, NSW, Australia* ^d*Perten, Sydney, NSW, Australia*

CHAPTER OUTLINE

1.1	Introduction	3
1.2	Dough properties and baking quality	4
1.3	The wheat breeder's needs	6
1.4	Hooke, Newton, Hogarth and Dough	6
1.5	Hankóczy's Farinograph	9
1.6	The Valorigraph—Still in production and use	10
1.7	The Hankóczy-Brabender relationship	11
1.8	Ongoing development and expansion for Brabender	11
1.9	Ongoing development and adoption of the Farinograph	13
1.10	The transition from chart paper to computer screen	15
1.11	The Breeder's and Researcher's needs—Very small-scale analysis	15
1.12	Dough in the "real life" of the bakery	17
1.13	Beyond the recording of torque	18
1.14	Conclusion	18
	References	20

1.1 INTRODUCTION

There was a time when “wheat was wheat,” with little concern for its grain quality, apart from checking for possible contamination with weed seeds or other undesirable matter. A change in those attitudes appears to have occurred during the 19th century, when various technological advances accentuated the possibilities of assessing and improving the suitability of flour for bread making and other food uses. Concern for flour quality in Britain prompted James Hogarth to develop and patent a recording dough mixer (Hogarth, 1892).

One of these changes of attitude resulted from the introduction of roller milling, which was gradually replacing the stone grinding of whole grain

(Walker and Eustace, 2016). Roller milling provided a cleaner white flour that could then be examined for its dough properties and for bread making. Thus it may be no coincidence that a further invention of dough-testing equipment occurred in Hungary (Hankóczy, 1914a,b), in association with the Hungarian commercial exploitation of roller milling (Wrigley et al., 2011). Hankóczy's invention appears to have been independent of Hogarth's recording mixer.

The Museum of Hungarian Agriculture has exhibited some of the earliest designs of equipment for cereal chemistry testing. One of these is pioneering dough-testing equipment developed early in the 20th century in Hungary by Professor Jenő von Hankóczy (Pénzes, 1970; Kenyeres, 2006) (Fig. 1.1), who was then the Director of the Hungarian Cereal and Milling Research Station (Gabona- és Lisztkísérleti Állomás) in Budapest. Among other test machines, Hankóczy developed the principles and the prototypes of the Farinometer, Farinograph, and Extenzograph, which was improved and produced later (from 1930) by Brabender in Duisburg. Hankóczy patented one of his dough-testing items of equipment for the determination of optimal water addition in 1929. The modified dough-mixing apparatus based on the Hankóczy principle began to be produced as the "Valorigráf" in Hungary from the 1960s.

Hankóczy's dough-testing equipment was used extensively for the breeding of Austro-Hungarian wheats and in the quality control of the country's wheat for export.

1.2 DOUGH PROPERTIES AND BAKING QUALITY

Central to the interest in testing dough properties was the realization that baking quality is related to dough quality. Thus there was the need to test grain for these basic quality attributes—milling (+hardness) and dough strength (+water absorption). Initially, the need for these forms of evaluating wheat quality required a kilogram of flour for bulk-scale testing, following harvest, at the flour mill and bakery, and also for quality control at export. These developments arose because interregion and international transport was becoming significant, in contrast to the traditional village-scale use of wheat: local farmer → village miller → home baking.

An additional stimulus for Hankóczy in about 1914 was the opening of a large-scale bakery in Budapest. This level of baking lifted bread making from an artisan operation (in which variations in dough quality were accommodated by the baker's skill) to the level of manufacture (in which uniformity of dough consistency was critical for trouble-free operation). Predictive dough testing was thus a great advantage for quality control.

**Profile of Professor Jenő von Hankóczy,
inventor of the Farinometer and the Valorigraph, forerunners of the Farinograph**

Jenő Hankóczy was born in 1879 in Western Hungary into a family where the head of the family had been a farm manager, following generations before him. Having completed his studies as an agronomist in Mosonmagyaróvár, an Agricultural Academy founded in the late 18th century, the talented Hankóczy was invited to work as an assistant at the Experimental Station of Plant Production of the Academy in 1903. He worked under the famous Sandor Cserhati and Ignac Kossutany on a project to improve the yield of wheat in Hungary.

The project also involved comparing of the gluten content of 50 Hungarian and 50 foreign wheat cultivars. To replace the tedious methodology used in those days, in 1905 he developed his first item of equipment, "Farinometer", which was capable of measuring the stretching properties of gluten washed out from dough. The use of this equipment at the Academy was so successful that Hankóczy received an award from the Minister of Agriculture. The success stimulated Hankóczy to further developments in dough testing: after long experimenting, he completed equipment suitable for the determination of water absorption in dough formation.

Hankóczy worked for more than twenty years, at the experimental station in Mosonmagyaróvár, in a well-equipped laboratory where he even established a pilot-scale bakery to evaluate wheat samples. In these years, he was already recognised as the most skilled expert in the quality evaluation of wheat. This reputation was the basis of his appointment as Research Director at the National Institute of Chemistry, with the duty to establish an independent Experimental Institute for wheat and flour research.

Hankóczy was active advocate of the quality evaluation of cereals, he presented lectures and published several papers not only for research purposes but for the experts in the whole wheat-production and processing chain. In his new institute, he continued his developmental work on numerous testing equipments: in 1926 he finalised the completely modernised Farinometer and in 1928, he introduced the Farinograph which made him world famous.

Not being able to financially establish the mass-production of his machine, he was obliged to pass the rights of further improvements and production of the Farinograph in Germany to C.W. Brabender.

Later on, Hankóczy developed several more items of dough-testing equipment, including the "Fermentometer", suited to investigating the gas-production and gas-holding capacity of dough, and the very first version of the "Extenzograph". Each of these machines has been further developed and manufactured in Brabender's factory. Because of his early death in 1939, he was unable to finish his last item of equipment, the Laborograph, designed to measure the resistance of the dough during sheeting. This was completed by Hankóczy's colleague, Ferenc Gruzl.

Beyond his pioneer achievements as designer of numerous types of dough-testing equipment, Hankóczy's legacy is his role as organising the modernised quality-oriented wheat testing system in Hungary, benefiting breeding, seed production, grain production, quality evaluation and quality control. It is also to his merit that in the 1930s, the world renowned Hungarian wheat cultivar, Bankuti 1201, comprised more than 80% of Hungarian wheat production. Hungary's whole wheat classification system was developed by him, forming the basis of the present network of well equipped laboratories all around the country.

■ FIG. 1.1 A profile of Professor Jenő von Hankóczy (Hankóczy, 1914a) in relation to his contributions to the early days of dough-testing methodology. (Translated and adapted from Kenyeres, Á., 2006. Hankóczy Jenő. In: Hungarian Biographical Glossary, 1000–1990. Akadémiai Kiadó, Budapest, pp. 345–347 and Pénzes, I., 1970. Who Was Hankóczy Jenő? ÉT Publ., Budapest (in Hungarian).)

1.3 THE WHEAT BREEDER'S NEEDS

A contrasting situation developed in parallel of testing these quality attributes on a much smaller scale for the new technology of breeding wheat to improve baking quality. Until this stage of working toward quantitative evaluation, it was said that “a wheat breeder requires a good set of teeth” ([Buller, 1919](#)) to crush several grains of a new wheat line to test grain hardness; next came the making of a tiny dough piece by mixing the crushed grain with saliva. This primitive dough piece was then taken out to test dough strength and extensibility by stretching it with the fingers.

A less subjective approach was obviously needed. Thus enters the cereal chemist, whose task it was to interact with the breeder in the objective evaluation of grain quality for the breeder's advanced wheat lines. Consequently, interactions between breeder and cereal chemist needed to develop into instrumental testing of milling quality and dough consistency. The Australian Farrer-Guthrie collaboration of the 1890s has been claimed as the first such collaboration ([Blakeney and Wrigley, 1993](#)), although the initial attention of Farrer and Guthrie was focused on milling and baking, giving less attention to the intermediate stage of dough properties ([Wrigley, 1978](#)).

1.4 HOOKE, NEWTON, HOGARTH AND DOUGH

Early studies of the elastic deformation of solids by the English scientists Hooke and Newton in the 1600s related to ideal solids and liquids, but their studies did not relate well to food substances such as dough ([Bourne, 1982](#)). James Hogarth, in Kirkcaldy, Scotland ([Bailey, 1944](#)), was the first to “obtain a patent for a device that measured the consistency of dough using the same principles as the modern Farinograph” ([Bourne, 1982](#)). This first recording dough mixer was patented by Hogarth in the United Kingdom in 1889 and again in the United States in 1892 ([Hogarth, 1892](#)). The US patent commences:

“Be it known that I, JAMES HOGARTH, miller and corn merchant, of West Mills, Kirkcaldy, Fifeshire, Scotland, a subject of the Queen of Great Britain and Ireland, have invented a Mechanism for Testing and Graphically Recording the Properties of Flour, of which the following is a specification.” There follow five pages of text, plus nine pages of detailed drawings.

This instrument had a belt-driven drive connected to a differentially geared sigma-arm mixing bowl ([Fig. 1.2](#)). A dynamometer was attached to the drive

(No Model.)

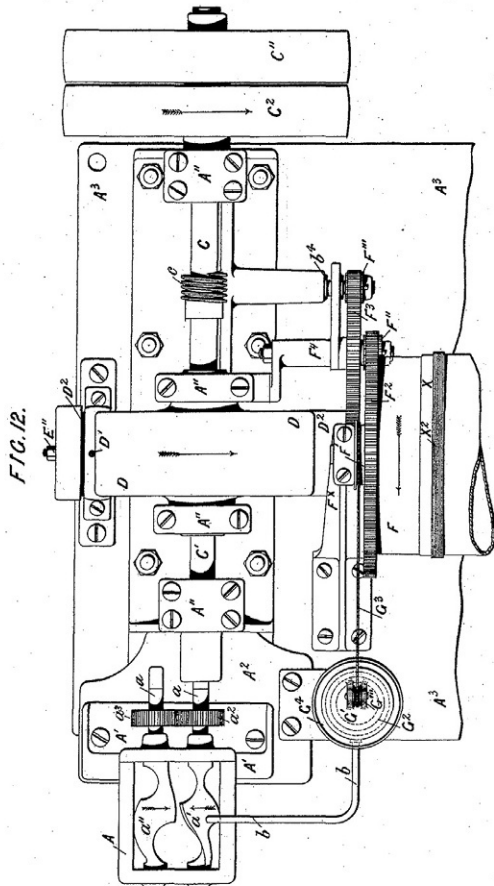
9 Sheets—Sheet 9.

J. HOGARTH.

MECHANISM FOR TESTING AND RECORDING THE PROPERTIES OF FLOUR.

No. 474,636.

Patented May 10, 1892.



WITNESSES.

George Baumann
S. C. Connor

INVENTOR

James Hogarth
By his attorneys
Hoveon and Hoveon

THE HORNBACH PETERS CO., PHOTOLITHO., WASHINGTON, D. C.

■ FIG. 1.2 Detailed illustration of Hogarth's recording dough mixer, viewed from above. The mixing bowl ("kneading machine") can be seen at the bottom, labeled "A," with its two Z-arm mixing paddles. The automatic water-dispensing mechanism ("G") can be seen at bottom right, with a delivery tube entering from the right. (From Fig. 12, Sheet 9, of Hogarth, J., 1892. Mechanism for Testing and Recording the Properties of Flour. U.S. Patent 474,636, May 10, 1892.)

shaft to detect the mixing torque, driving a pen up a chart connected to a rotating drum. It even included an automatic water dispenser!

For the first test, the water was metered in slowly (the test took some hours) and when the dough developed to peak consistency, this was recorded on the graph and the corresponding amount of water required was calculated. Then, in a second test, the required water was added at the start of the test, the dough allowed to develop, and then the rate of reduction in dough consistency after the peak was measured as an index of the dough's mixing tolerance. So, the instrument measured water absorption, development time, and mixing tolerance—all the key measures we still use today.

Hogarth's small dough mixer was "provided with a dynamometer attached to the drive, and a stylus recording on a chart the force applied at all times throughout the extended mixing process" thus "measuring the power of flour to absorb water to yield a dough of a given consistency" ([Bailey, 1944](#)).

By inventing this equipment, Hogarth, in the late 19th century "appears to have anticipated certain fundamental characteristics of several of the devices which made an appearance considerably later. Strangely enough Hogarth's invention attracted no interest at the time. So far as the author [Bailey] can learn, no reference was made to it in the literature between 1892 and 1930, nor were any results published based upon its application to flour testing" ([Bailey, 1944](#)).

[Bailey \(1944\)](#) and [Bourne \(1982\)](#) also described a succession of inventions for evaluating the texture of food substances, including many dough-testing inventions, such as puncture testers, the Plastometer based on air pressure, the Shortometer to test the shortness of cookies, the Swanson-Working recording dough mixers (large and micro sizes—the Mixograph), the Chopin Extensimeter, the Chopin Alveograph (see [Fig. 1.3](#)), the Buhler Comparator, Barbade's Aleurographe, etc., in addition to the Farinograph and later the Valorigraph.

Now, long after these developments, some of these names are much more familiar to us than others. In particular, the Mixograph (no longer manufactured by TMCO) has found greater popularity in North America, whereas the Farinograph is more familiar in Europe, probably because the Mixograph has traditionally been better suited to the dough-strength characteristics of the Dark Northern Spring wheat class of the United States and the Hard Red Spring class of Canada. The Farinograph is distinct because of its added ability to provide water-absorption details for the test flour.

The Chopin Alveograph

Chapter 1.

In 1905, Hungarian scientist Hankóczy designed an apparatus that became known as "Hankóczy's gluten tester" (Hankóczy, 1920). The apparatus provided a means for pressing moist, crude gluten into a thin sheet between two plates that each had a round opening 2 cm in diameter. The plates, with gluten pressed in between, then were mounted in a device that joined the lower plate to a vessel into which air could be compressed, while the upper plate joined another vessel from which air could be displaced. Air in the lower vessel was compressed by introducing mercury from a bulb elevated to a height that provided enough pressure to stretch the gluten. The gluten expanded into a bubble through the round opening in the upper plate. A simple gasometer measured the air displaced from the upper vessel by the expansion of the gluten bubble. Thus, the maximum volume of the bubble before it burst could be measured.

Hankóczy later improved this instrument so that the pressure of the air in the lower vessel also could be measured; thus improving the precision of the evaluation of the "strength" of the gluten sample. A later version of the testing device allowed a disk of dough to be stretched instead of a disk of gluten. Because the importance of temperature in the rheological testing of doughs had not yet been recognized, none of these early instruments had any temperature control.

In the 1920s, Marcel Chopin became interested in the possibility of using dough-testing instruments in place of baking tests to assess the baking quality of French wheats. With no prior knowledge of Hankóczy's developments, he attempted to develop a test that would simulate as closely as possible, the process that dough undergoes in bread baking.

FIG. 1.3 The opening paragraphs of Chapter 1, "The Chopin Alveograph," in *The AlveoConsistograph Handbook*, Second Edition. They describe Hankóczy's invention of equipment similar to the later-invented Chopin Alveograph. (Based on Dubois, M., Dubat, A., Launay, B., 2016. *The AlveoConsistograph Handbook*, second ed. AACC International/Chopin Technologies/Elsevier Publishing, St Paul, USA/Paris, France.)

1.5 HANKÓCZY'S FARINOGRAPH

Jenő von Hankóczy's first invention for these purposes related to testing the viscoelastic properties of wet gluten (washed from dough) (Kosutány, 1907; Bailey, 1944). The mechanism was based on monitoring air pressure changes during the stretching of a thin sheet of wet gluten, eventually being automatically recorded on a chart as the pressure changes with gluten extension. This invention was a forerunner to the Alveograph, as explained in Fig. 1.3. Hankóczy developed the Farinometer (in 1905) and then the Farinograph (in 1912 and modified it until 1928). The Valorigráf was produced from the 1960s, but only by Labor MIM, Hungary.

Hankóczy developed a succession of dough-testing machines initially for determining the optimum water absorption for a specific flour sample (Hankóczy, 1914a,b; Tibor, 1933). Hankóczy's main activity focused on a recording dough mixer using a pair of intermeshing Z-shaped blades that rotated in a double spherical trough. According to Bailey (1944), "the attention of Hankóczy and his colleagues was not strongly attracted to this possibility [of observing progressive time-based changes in consistency] until the torsion dynamometer was attached to the dough mixer." The resulting

curves thus resembled what are also referred to as “farinograms.” The patent: “Method for the determination of the amount of water to produce wheat flour dough with optimal consistency.” (in Hungarian). Hungarian Patent No. 100245 (1930).

1.6 THE VALORIGRAPH—STILL IN PRODUCTION AND USE

Despite the subsequent transfer of Hankóczy’s attention to the Brabender operations, the Valorigraph continued to be produced, used, and further developed in Hungary and beyond. In the late stages of Hankóczy’s career, a new generation of young cereal chemists grew up under his influence. One of them, István Tibor, summarized the principles of Hankóczy’s equipment in a research paper that is exciting to read, even today (Tibor, 1933).

Hankóczy’s dream of mass-producing dough-testing equipment in Hungary was realized in the 1960s, partly because of the Cold War of that time. Purchasing any equipment made in the West in those days required hard currency, and therefore it was extremely difficult for the countries then behind the Iron Curtain. An alternative solution was needed.

Relying on the principles of Hankóczy’s Farinograph, engineers (L. Török, I.J. Hegedűs, and G. Kard) of the Labor MIM company (Budapest) redeveloped the Valorigraph as equipment suitable to characterize wheat samples essentially in the same way as the Farinograph (Telegdy-Kováts and Lásztity, 1967; Ruttkay, 1967). While the mixing action in the refabricated equipment is the same, there are several technical differences that distinguish the Farinograph from the “new” Valorigraph. The two most important differences are related to:

- (i) the measurement of the resistance of the dough during dough development, and
- (ii) the mechanism for keeping the system at 30°C during the experiment.

The following Standard Methods for use of the Valorigraph have been established:

- Valorigraph use is standardized by the International (ISO) and national Hungarian Standard MSZ ISO 5530-3:1995.
- The following Valorigraph Standard Method is given as an ISO (ICC) standard method (1988) and was confirmed in 2018.
 - <https://www.iso.org/obp/ui/#iso:std:iso:5530:-3:ed-1:v1:en>.
 - This part of ISO 5530 has been drawn up on the basis of the Labor-MIM Valorigraph. Wheat flour—Physical characteristics of

doughs—Part 3: Determination of water absorption and rheological properties using a Valorigraph. It is based on Standard No.115 of the International Association for Cereal Science and Technology (ICC). The method consists in measuring and recording of the consistency of a dough as it is formed from flour and water, as it is developed, and as it is broken down. Annex A gives a description of the Valorigraph.

1.7 THE HANKÓCZY-BRABENDER RELATIONSHIP

Hankóczy could see the value and potential of his dough-testing equipment, so he sought a suitable backer—a combination of financial backing, engineering design, and manufacturing ability. But this combination was not available in his native Hungary.

When he turned his attention elsewhere, he found what he needed in Carl Wilhelm Brabender ([Fig. 1.4](#)), who “operated a technical and scientific instrument factory in Duisburg, Germany” ([Tibor, 1933](#)). According to [Bailey \(1944\)](#) the “first commercial exploitation of this device” was in the 1930s.

The story of the ongoing development of Hankóczy-Brabender interactions is told eloquently in the dedication statement to Will Brabender (as he was known by his many cereal-chemist friends) in the third edition of *The Farinograph Handbook*. It is reproduced complete as [Fig. 1.5](#). In “Will’s own words” in the Dedication, the depth and harmony of the relationship are told:

- “In 1929 and 1930, I made many trips from my native Germany to Budapest, spending a total of more than six months with my friend Hankóczy ‘learning the ropes’.”
- “Hankóczy taught me nearly 30 years of his own experience.”
- “I knew that the next goal was to design the most accurate dynamometer for measuring the torque of the little dough mixer.”
- Attention was also paid to “temperature control and recording the results on a strip chart.”
- “Within five months, I went back to Budapest with the first prototype of this instrument.”

1.8 ONGOING DEVELOPMENT AND EXPANSION FOR BRABENDER

The following decades have seen the expansion of Brabender’s scope into quality control for a range of food and plastic products (motto: “Where quality is measured”). The current summary for the company is:

Carl Wilhelm Brabender, prominent engineer and contributor to cereal technology, honorary AACC member and founder-sponsor of the AACCI's C.W. Brabender Award, died October 27, 1970, at his home in Duisburg, Germany. He was 73 years old.

Brabender's important contributions to cereal technology were numerous. He was the designer of the Farinograph, the Extensograph, the Fermentograph, Amylograph, over-rise recorder, the Matuograph, rapid-test experimental mill, moisture ovens, and in recent years, the Quadrumat Junior and Senior test mills. During his lifetime his name synonymous with precision-made instrumentation for physical testing all over the world, not only in cereal chemistry, but for such diverse fields as plastics, rubber, ceramics, textiles, paper, paint, and pharmaceuticals.

He received his university education in Germany, graduating with an engineering degree. In 1929 he met Peno Von Hankoczy, a Hungarian who some 20 years previously had designed an apparatus for measuring flour quality which washed gluten from wheat flour, stretched it by means of an air bubble, and then measured the volume of air before the gluten membrane burst. The device was of limited utility, however. A later attempt to use a motor-driven dough mixer with an ammeter to measure power requirements also proved ineffective, because differences in power consumed in mixing the doughs were too small. After meeting Hankoczy, Brabender began work on the same concept, culminating in a mechanical dough-mixing machine with a dynamometer, the forerunner of the Farinograph. He began manufacturing the instrument in a small factory in Duisburg, and it soon became a universally-accepted standard in cereal technology. Other Brabender-designed and manufactured instruments followed in rapid succession.

Prior to World War II he was active in establishing and funding the Institute for Flour Physics at Duisburg, offering short courses on a regular schedule, and training laboratory technicians from all over the world. Under his influence, the Institute employed many extremely competent young scientists to assist with the school and provide new ideas.

The war halted production in the plant, which was later destroyed during an Allied bombing raid on the industrial areas along the Rhine River.

When the war ended, Brabender's worldwide scientific reputation and expert knowledge, particularly in the construction and operation of environmental chambers, ranked him among the first scientists scheduled for removal from Germany by the Allied Military Government. With his manufacturing plant in Duisburg in ruins and his property in the United States expropriated under the Alien Property Act, he arrived in the United States virtually penniless.

His first assignment was to work in the Army Quartermaster Corps Laboratory in Chicago. At first his freedom of action was greatly restricted because he was considered an enemy alien. He was later allowed to join the Pillsbury Company, Minneapolis as a full-time consultant.

In 1950, during frequent short trips to Germany, he began the difficult task of rebuilding the Duisburg plant. By the time he returned there permanently, the plant was turning out all of the devices previously produced, along with Do-Corders, moisture meters, continuous flour and wheat moisture recorders, and flour-bleaching, wheat conditioning and dough oxidizing equipment, including scales and feeders.

Brabender earned many honors during his lifetime. In addition to his election to Honorary Membership in the AACC, he was an honorary lifetime member of the Scandinavian Cereal Chemists Association; member of the Association of Operative Millers; and honorary senator of the Technical University in Breslau, where he received his early training. He was also awarded the Honorary Presidency and the Neumann Prize for his accomplishments in cereal science by the Arbeitsgemeinschaft fur Getreideforschung, of which he was also the first president. He was also an honorary member of Alpha Mu, the milling fraternity at Kansas State University. The C.W. Brabender Award of the AACC for outstanding work in the field of applied milling and baking rheology was established in his honor.

Carl Wilhelm Brabender is remembered by an award that bears his name. It is awarded every three years as part of the activities of AACC International, St Paul, MN, USA.

The Carl Wilhelm Brabender Award

The Carl Wilhelm Brabender Award was established to honor the distinguished contributions to the application of rheology in milling and baking. Sponsored jointly by C.W. Brabender Instruments, Inc. (South Hackensack, NJ) and Brabender OHG (Duisberg, Germany), the award is presented every three years and is administered alternately by AACCI and the Arbeitsgemeinschaft Getreideforschung (Detmold, Germany). The award provides a plaque and a travel grant to enable the recipient to visit scientists and laboratories in other parts of the world to increase the awardee's knowledge and experience in the field. The only qualification is to be professionally active in rheology, specifically those engaged in the milling and baking industry. The awardee will address attendees at the AACCI Annual Meeting or at one of the three annual meetings of the AG at which the award is given.

Previous Award Winners

1967	Isydore Hlynka	1968	Arnoldus Crommetuyn
1970	William Shuey	1972	Egon Drews
1974	Walter Bushuk	1978	Keith Tipples and R. Henry Kilborn
1985	Seiichi Nagao	1988	Dorian Weipert
1990	Vladimir Rasper	1993	Rolf Kieffer
1996	Bert D'Appolonia	2002	Jozef Kokini
2008	Ton van Vliet	2014	Juan de Dios Figueroa Cárdenas

■ FIG. 1.4 A profile of Carl Wilhelm Brabender in relation to his contributions to the commercial development of the Brabender Farinograph. (From Brabender's obituary, published in the AACCI's Cereal Foods World: Anon, 1970. C.W. Brabender, Honorary AACC Member, dead at 73. Cereal Foods World 15, 422–423.)

Dedication

This handbook is respectfully dedicated to Carl Wilhelm Brabender who once stated,¹ "I have devoted the last 40 years to the design and application engineering of physical and rheological test methods, and I intend to do so for the rest of my life." No one can ever say that he did not remain faithful to this statement. He became a member of the AACC in 1931 and was made an Honorary Member in 1965. The Carl Wilhelm Brabender Award was established in his honor to encourage research in applied milling and baking rheology.

Will became acquainted with the flour milling industry by designing and introducing an electrical high voltage arc bleacher producing N_2O_4 for flour bleaching. He had been trained as an electrical engineer and physicist. In 1929 he met Professor Jeno von Hankóczy, who had developed a disk-type dough-testing machine and an apparatus to determine water absorption. From this meeting developed a lifelong friendship and mutual interest in measuring elastic and plastic properties of doughs.

In about 1927, Hankóczy observed in a bakery a motor-driven dough mixer to which an ammeter was attached; he noted that the more the ammeter would show, the higher the consistency of the dough. This observation led to the design of the first forerunner of the Farinograph. Hankóczy realized that the basic problem with the design of instruments that followed was due to small differences in power consumption in mixing different doughs, compared with the energy required to drive the whole instrument.

Then in Will's own words,¹ "In 1929 and 1930 I made many trips from my native Germany to Budapest, spending a total of more than six months with my friend Hankóczy 'learning the ropes' of wheat breeding, experimental milling and baking tests. Hankóczy taught me nearly 30 years of his own experience and that of his teachers, especially Kosutany. I knew then that the next goal was to design the most accurate dynamometer for measuring the torque of a little dough mixer, but still no one spoke of temperature control

or of recording the results on a strip chart. - Within five months I went back to Budapest with the first prototype of this instrument. - This design already showed basic elements of the present day farinograph. - Development then went step by step. The first discovery was that water absorption as strength measurement was not reliable. There were too many exceptions. - A little recording drum from a thermograph was attached to the farinograph. - The chart we obtained on this drum was, more or less, today's farinogram. We learned very soon that the time to peak was in line with the dough mixing requirements of a certain flour, and the weakening characteristics of the curve beyond the peak was an indication of general strength. In addition, the machine would produce the water absorption figure. It was an immediate success all over Europe.

"The next disappointment came when this machine was introduced in 1930–1931 in the United States. Again it produced very confusing results. Sometimes it would duplicate well, sometimes not at all. - We found that the general strength of wheat flours in the United States was several times that of European wheat, and the heat produced during mixing would, of course, change the rheological properties of the dough and introduce a strongly disturbing factor into the whole measurement. - I went back to Europe and redesigned the machine for close temperature control, resulting in the present jacketed mixer and jacketed damper and the circulating pressure thermostat. At the same time, the rather primitive thermograph drum recorder was replaced by a larger 7-inch strip chart recorder which has been standard on farinographs for the last 35 years. - From then on, the Farinograph was introduced quickly all over the world."

The impact and influence of Carl Wilhelm Brabender on the milling and other industries by the introduction of the Farinograph, as well as many other testing instruments, will never be forgotten.

Will Brabender will remain fresh in the memory of cereal chemists for his many contributions to the advancement of cereal science.

¹C. W. Brabender. 1965. Physical Dough Testing—Past, Present, and Future. Cereal Sci. Today 10:291–304.

■ FIG. 1.5 The Dedication statement to "Will Brabender" (as he was known to his many cereal-chemist friends) in the third edition of *The Farinograph Handbook*, indicating the development of good relationships between Hankóczy and Brabender. (Reproduced with permission from D'Appolonia, B.L., Kunerth, W.H., 1984. *The Farinograph Handbook*, third ed., revised and expanded. American Association of Cereal Chemists, Inc., St Paul, MN, USA.)

Founded in 1923 by Carl Wilhelm Brabender, Brabender® GmbH & Co. KG is the leading company for the development, manufacture, and distribution of instruments and equipment for testing material quality and physical characteristics in all fields of research, development, and industrial production in the chemical and food industries all over the world.

(www.brabender-mt.de)

1.9 ONGOING DEVELOPMENT AND ADOPTION OF THE FARINOGRAPH

The growth in use of the Farinograph is described by Tömösközi and Békés (2016) as follows:

"The huge success of the Farinograph spreading all around the wheat chain as early as the 1930's derived from the idea of using this direct relationship between the amount of water in the system and [mixing] resistance for the determination of the most important quality attribute of the flour: water absorption [which] is the amount of water needed to be added to the flour to reach the constant consistence (500 or 600 Farinograph or Brabender Unit, BU) of dough." Consequently, the "500 line" on the chart thus became a characteristic part of Farinograph jargon.

How the traditional Farinograph has impacted cereal chemistry is indicated by the extensive collaborative standardization and approval of methods for using the Farinograph (Miskelly et al., 2010). These are listed below for two prominent associations of grain scientists. The collaborative procedures for evaluating and standardizing such testing methods are described by Bridges and Wrigley (2016). Such collaborations have also been used by other associations of wheat scientists around the world to provide national agreements on how the Farinograph should be used.

Standardized Testing Method of the International Association for Cereal Science and Technology (ICC). https://www.icc.or.at/standard_methods.

No. 115/1 Method for using the Brabender Farinograph.

Standardized Testing Methods of AACC International, from AACCI Approved Methods of Analysis, 11th Edition. <https://www.aaccnet.org/Pages/default.aspx>.

38-20.01	Farinograph Test for Vital Wheat Gluten
54-21.02	Rheological Behavior of Flour by Farinograph: Constant Flour Weight Procedure
54-22.01	Rheological Behavior of Flour by Farinograph: Constant Dough Weight Procedure
54-28.02	Farinograph Table for Constant Dough Weight Method Only
54-29.01	Approximate Corrections for Changing As-Is Farinograph Absorption to 14.0% Moisture Basis, for Constant Dough Weight Method Only
82-21.01	Table: Conversion of Farinograph Absorption to 14.0% Moisture Basis (Constant Weight Method Only)

1.10 THE TRANSITION FROM CHART PAPER TO COMPUTER SCREEN

For many years the Farinograph and similar instruments were inextricably linked to a chart recorder as the means of providing a record of the time-based changes in dough properties. Consequently, the typical dough-testing laboratory had chart traces festooning the walls! With the proliferation of the personal computer into every area of our lives in the later decades of the 20th century, a computer screen soon replaced chart paper as a digital recording of dough quality.

This revolutionary step permitted the next breakthrough of intensive analysis of the trace. Automatic (objective) analysis of the mixing curves soon followed, including automatic recording of derived results (R_{max} , water absorption, development time, etc.), also providing the basis for regulating industrial on-line mixing systems. Further developments of this nature are now represented by the Farinograph-TS.

Electronic recording opened up wider opportunities, such as the ability to analyze the detailed trace, which had been no more than a solid blur on the chart recorder and even on the computer screen. This fresh revelation is illustrated in Fig. 1.6, which shows the distinctive traces with high-speed recording for various stages of the mixing trace, permitting the development of mathematical modeling of the distinct stages of hydration, dough development, and overmixing, as indicated in Fig. 1.6. This new approach has permitted analysis, for example in the Mixograph, of the individual stretching action of each pin movement as the pin interacts with the dough at these stages of dough measurement (Anderssen et al., 1996; Tömösközi and Békés, 2016).

1.11 THE BREEDER'S AND RESEARCHER'S NEEDS— VERY SMALL-SCALE ANALYSIS

At the start of this chapter, there was mention of the contrasting situations for which dough-mixing analysis is required, namely:

- (1) factory scale—by the tonne!
- (2) for bulk-scale testing—by the kilogram;
- (3) for breeding—when only small amounts of flour or wheatmeal are available, and
- (4) in research on very small-scale testing of dough and additives or components isolated from flour.

Correlation of results is required across these extremes of scale. The conventional Farinograph is designed to cater to situations (1) and (2), but

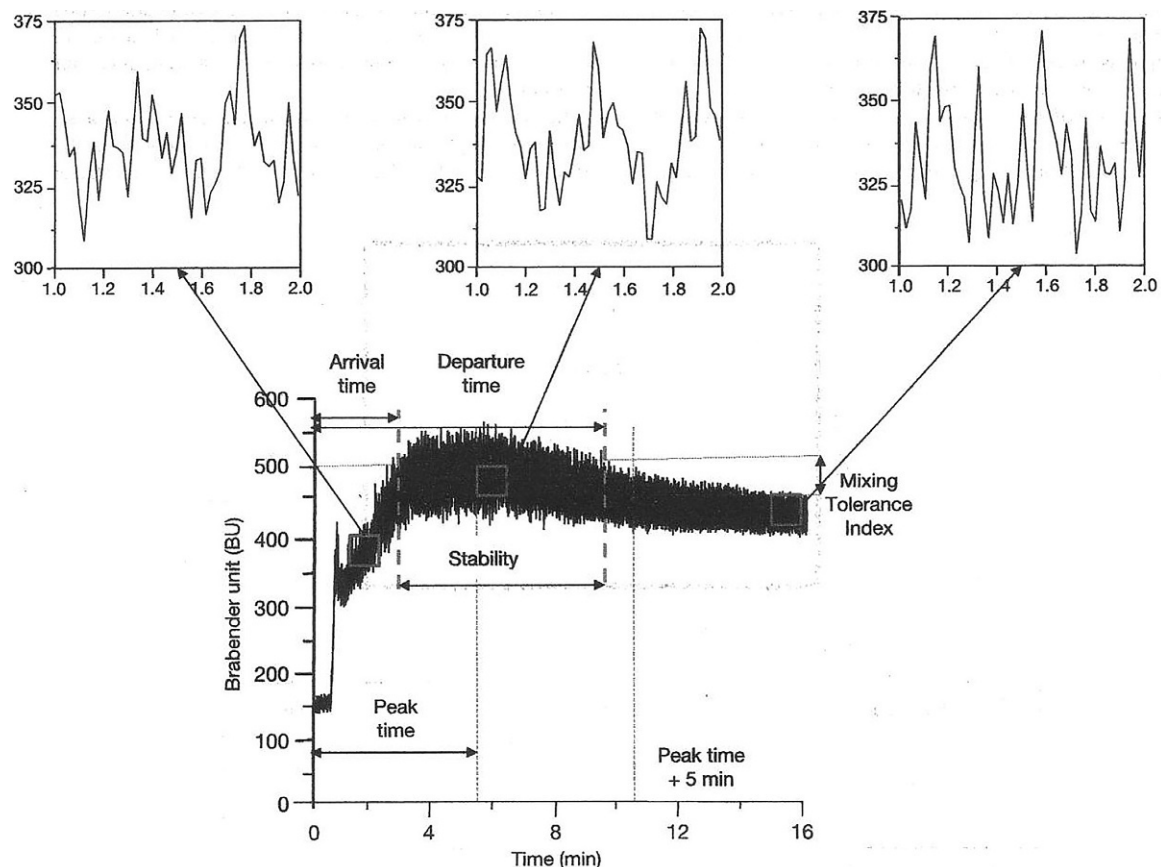


FIG. 1.6 Expansion of the Farinograph mixing curve at specific stages of mixing, due to fast-speed recording, which had not previously been possible with chart recording. (Reproduced with permission from Tömösközi, S., Békés, F., 2016. *Bread: dough mixing and testing operations*. Encyclopedia of Food and Health, vol. 1. pp. 490–499 (Fig. 1).)

insufficient amounts of flour are available for Farinograph testing in the early stages of breeding (3) and for research situations (4).

Given the evident need for Farinograph-type dough testing with small flour samples, Brabender developed a semimicro Farinograph equipped with a 10-g bowl, which was found to be extremely useful in the early stages of wheat breeding. At the same time, CSIRO Plant Industry scientists in North Ryde, Australia, Peter Gras and Ferenc Békés (both recipients of the 2000 Perten Award for their pioneering work on small-scale dough testing research and development), together with engineer Chris Rath, set about developing a microscale Z-arm mixer, mimicking the Farinograph.

The choice of collaborating partners for this work was obvious: a generation of specialized experts in laboratory testing of cereals grew up in the Department of Biochemistry and Food Technology of the Budapest University of Technology and Economics (BUTE), under the mentorship of the famous food rheologist and equipment developer, Radomir Lásztity. The final team was made up of BUTE scientists Sándor Tömösközi, András Salgó, and János Varga with József Nánási and Dezső Fodor, the engineers-founders of the small firm METEFEM (the successor of Labor MIM, which had several decades of experience in producing the Valorigraph).

The machinery and engineering design of the prototypes—even the bowl and the Z-arms of the equipment today—came from Budapest, while the electronics and software of the original version were developed in Australia. The fully computerized microequipment required not more than 4 g of flour to determine the water absorption and mixing characteristics of dough (Tömösközi et al., 2000). This novel mixer permitted the specific contributions to dough properties by purified subfractions of gliadin and glutenin polypeptides (Haraszi et al., 2004). This instrument was subsequently commercialized as the micro-doughLAB by Newport Scientific (now Perten).

The micro-doughLab has become an essential tool in academic and applied wheat research, providing indispensable data on the mixing parameters in large population studies where this information could not be achieved with regular-sized equipment (Cavanagh et al., 2010; Newberry et al., 2018). Similarly, in cases such as additional/incorporation studies, where the effects of a few milligrams of individual proteins on the water absorption and mixing properties are monitored (Békés, 2012a,b), or genetic engineering studies where often the crop of one single plant is available (Oszvald et al., 2013), the application of micro methods like this equipment are the only way to characterize the samples.

According to one report (Anon, 2007), “Today’s fully computerised micro-equipment, requiring not more than 4 g of flour to determine water absorption and mixing characteristics of dough, hopefully will prove as popular as its ‘grandfather’, the Farinograph.”

1.12 DOUGH IN THE “REAL LIFE” OF THE BAKERY

Nevertheless, dough testing on a modest or small scale (applications 2–4) are all directed toward satisfying the requirements of commercial baking—at level (1)—the “real world” of the plant bakery. In this situation, mixing speeds are often much faster than the speed used for Farinograph testing. In addition, heat production in the commercial dough may differ from the laboratory testing system.

The need for considering commercial high-speed mixing in predictive testing is described by Elliott (2010), with the further considerations of mixing to optimum consistency for pasta and noodle doughs, as well as considering the practical complications of added fats. Weipert (2006) points out the further “real life” factor of heat in an oven, an essential part of baking. His criticism is aimed at present dough-testing methods that “only describe the properties of the dough in the cold phase of the baking process, ignoring the pasting properties of the cereal starch as a function of alpha-amylase activity at high temperatures.” Simulation of the complete baking process is an ongoing challenge that is being addressed, but that at any rate brings us back full circle to bake testing.

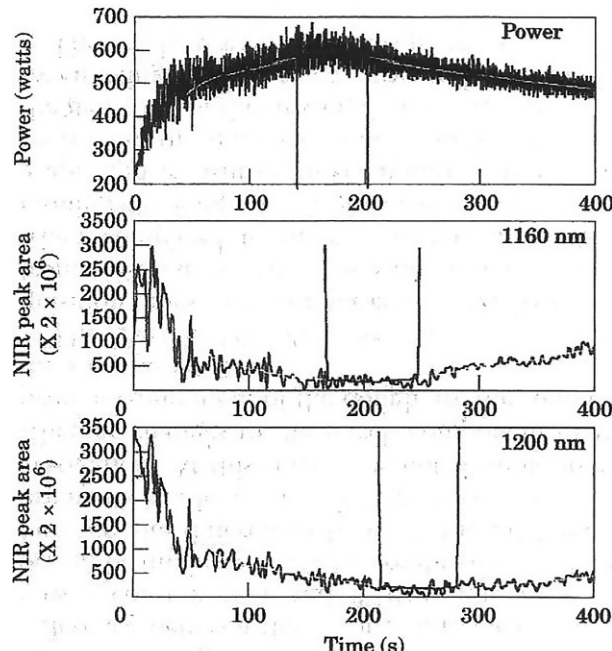
1.13 BEYOND THE RECORDING OF TORQUE

The question has been asked long ago (Tracey, 1968): “What is the most important ingredient in dough?” The answer could well be the ingredient that is present in the highest proportion, namely, water. During mixing the nature of the water phase continues to change, and it is these changes that contribute most to dough properties. So why not monitor the status of the water phase (free or bound)? This has been the revolutionary approach of Wesley et al. (1998), by using near infrared spectroscopy as a means of noninvasive monitoring (Fig. 1.7). Variations in two specific wavelengths in the near infrared have been found to provide mixing curves (Fig. 1.7) similar to those produced by measuring torque on other dough-mixing equipment. This observation opens up a vista of new approaches to the monitoring and investigation of dough properties, especially for continuous monitoring during commercial dough processing.

1.14 CONCLUSION

“Wheat dough has both elastic and flowing properties; therefore, it shows a complex viscoelastic behaviour” and “the main challenge in the development of empiric rheological methods and instruments has been” to “apply adequate external forces on the dough to measure both elastic and viscous flow in one system” (Tömösközi and Békés, 2016). Are these the basic reasons for the proliferation of dough-testing equipment during the past century or so?

Our interest in dough testing is principally practical—to predict the behavior of a flour sample in the production of food products, mainly bread. “What, then, is the relationship between bread and the rheology of the dough?” asks Weipert (2006), who continues: “Rheology has a sub-discipline, rheometry,



■ FIG. 1.7 Farinograph-like dough-mixing traces (Z-arm mixer), obtained by NIR sensing. (Reproduced with permission from Wesley, I.J., Larsen, N., Osborne, B.G., Skerritt, J.H., 1998. Non-invasive monitoring of dough mixing by near infrared spectroscopy. *J. Cereal Sci.* 27, 61–69 (Fig. 7).)

whose task is to make and explain measurements. We speak of **empirical** (also known as descriptive or imitative) rheometry [including the Farinograph] and **fundamental** (absolute) rheometry, depending on the measuring principle and the possibilities offered by the instruments used” (Weipert, 2006).

Cynically, Weipert offers the quote:

- “With the empirical methods we don’t know what we are measuring, but it works”;
- “with the fundamental methods we know exactly what we are measuring, but it doesn’t work.”

Weipert cites Finagle’s Law (perhaps it sometimes reflects the feelings of many of those who test dough properties):

- “The information we have is not the information we want”;
- “The information we want is not the information we need”;
- “And the information we need is not available.”

But Weipert contrasts this cynicism with the statement:

The viscosity and viscoelastic behaviour of doughs and the end products is and will always be the information we have and the information we need. And since it is available, it offers a guarantee of reliable production and good quality in the end products.

REFERENCES

- Anderssen, R.S., Gras, P.W., MacRitchie, F., 1996. Modelling the mixing of wheat flour dough. In: Wrigley, C.W. (Ed.), Gluten 96. Proceedings of 6th International Gluten Workshop. Australian Royal Australian Chemical Institute, Melbourne, pp. 249–252.
- Anon, 2007. The ‘Hungarian connection’. In: Newport Scientific World No 11. October, 2007.
- Bailey, C.H., 1944. The Constituents of Wheat and Wheat Products. Van Nostrand-Reinhold, Princeton, NJ.
- Békés, F., 2012a. New aspects in quality related wheat research: I. Challenges and achievements (review). *Cereal Res. Commun.* 40, 159–184.
- Békés, F., 2012b. New aspects in quality related wheat research: II. New methodologies for better quality wheat (review). *Cereal Res. Commun.* 40, 307–333.
- Blakeney, A.B., Wrigley, C.W., 1993. One hundred years of cereal chemistry: the centenary of a chemical discipline. *Chem. Aust.* 60, 459–460.
- Bourne, M.C., 1982. Food Texture and Viscosity: Concept and Measurement. Academic Press Inc., New York.
- Bridges, A.R., Wrigley, C., 2016. Standardized test methods for grains and grain-based products. In: Wrigley, C., Corke, H., Seetharaman, K., Faubion, J. (Eds.), second ed. Encyclopedia of Food Grains, vol. 2. Elsevier Ltd, Oxford, UK, pp. 300–307.
- Buller, A.H.R., 1919. Essays on Wheat. The MacMillan Co, New York.
- Cavanagh, C.R., Taylor, J., Larroque, O., Coombes, N., Verbyla, A.P., Nath, Z., Kutty, I., Ramplin, L., Butow, B., Ral, J.P., Tömösközi, S., Balázs, G., Békés, F., Mann, G., Quail, K., Southan, M., Morell, M.K., Newberry, M., 2010. Sponge and dough bread making: genetic and phenotypic relationships with wheat quality traits. *Theor. Appl. Genet.* 121, 815–828.
- Elliott, B., 2010. Better modelling of high-speed commercial mixing. *Cereal Foods World* 55, 136–138.
- Hankóczy, J., 1914a. Evaluation of wheat flour. I. *Magyar Mérnök- és Építész-Egylet Közlönye* 18 (16), 307–311.
- Hankóczy, J., 1914b. Evaluation of wheat flour. I. *Magyar Mérnök- és Építész-Egylet Közlönye* 18 (17), 321–331.
- Haraszti, R., Gras, P.W., Tömösközi, S., Salgo, A., Békés, F., 2004. Application of a micro Z-arm mixer to characterise mixing properties and water absorption of wheat flour. *Cereal Chem.* 81, 555–560.
- Hogarth, J., 1892. Mechanism for Testing and Recording the Properties of Flour. U.S. Patent 474,636, May 10, 1892.

- Kenyeres, Á., 2006. Hankóczy Jenő. In: Hungarian Biographical Glossary, 1000–1990. Akadémiai Kiadó, Budapest, pp. 345–347.
- Kosutány, T., 1907. Der ungarische Weizen und das ungarische Mehl. (Budapest, 1907).
- Miskelly, D., Batey, I.L., Suter, D.A.I., Batey, I.L., 2010. Processing wheat to optimise product. In: Wrigley, C.W. (Ed.), *Cereal Grains: Assessing and Managing Quality*. Woodhead Publishing, Cambridge, UK, pp. 431–457.
- Newberry, M., Verbyla, A., Verbyla, K., Appels, R., Diepeveen, D., Cato, L., Howitt, C., 2018. Understanding the genetics of wheat quality using MAGIC populations. In: Presented at the 68th Australasian Grain Science Association Conference, Wagga Wagga.
- Oszvald, M., Balázs, G., Pólya, S., Tömösközi, S., Appels, R., Békés, F., Tamás, L., 2013. Wheat storage proteins in transgenic rice endosperm. *J. Agric. Food Chem.* 61, 7606–7614.
- Pénzes, I., 1970. Who Was Hankóczy Jenő? ÉT Publ, Budapest (in Hungarian).
- Ruttkay, L., 1967. Role of the Valorigraf in laboratories for the investigation of cereals and flour. *Élelmiszervizsgálati Közlemények* 13, 46–52 (in Hungarian).
- Telegdy-Kováts, L., Lásztity, R., 1967. Valorigraf, a novel Hungarian instrument for dough investigation and flour evaluation. *Élelmiszervizsgálati Közlemények* 13, 5–9 (in Hungarian).
- Tibor, I., 1933. The methodology of the quality of wheat and flour. MKGL, Budapest (in Hungarian).
- Tömösközi, S., Békés, F., 2016. Bread: dough mixing and testing operations. In: Caballero, B., Finglas, P.M., Toldra, F. (Eds.), *Encyclopedia of Food and Health*. vol. 1. Academic Press, Oxford, UK, pp. 490–499 (Chapter 86).
- Tömösközi, S., Varga, J., Gras, P.W., Rath, C., Salgó, A., Nánási, J., Fodor, D., Békés, F., 2000. Scale down possibilities in development of dough testing methods. In: Shewry, P.R., Tatham, A.S. (Eds.), *Wheat Gluten*. Cambridge, UK, Royal Soc. Chem, pp. 321–325.
- Tracey, M.V., 1968. Fitting the environment by modifying water structure. *Proc. R. Soc. B* 171, 59–65.
- Walker, C.E., Eustace, W.D., 2016. Milling and baking: history. In: Wrigley, C., Corke, H., Seetharaman, K., Faubion, J. (Eds.), *Encyclopedia of Food Grains*, second ed. vol. 3. Elsevier Ltd, Oxford, UK, pp. 299–306.
- Weipert, D., 2006. Fundamentals of rheology and spectrometry. In: Popper, L., Schafer, W., Freund, W. (Eds.), *Future of Flour: A Compendium of Flour Improvement*. Agrimedia, Hamburg, pp. 117–146.
- Wesley, I.J., Larsen, N., Osborne, B.G., Skerritt, J.H., 1998. Non-invasive monitoring of dough mixing by near infrared spectroscopy. *J. Cereal Sci.* 27, 61–69.
- Wrigley, C.W., 1978. W.J. Farrer and F.B. Guthrie: the unique breeder-chemist combination that pioneered quality wheats for Australia. *Rec. Aust. Acad. Sci.* 4, 7–25.
- Wrigley, C.W., Tömösközi, S., Békés, F., 2011. Hungarian-Australian collaborations in flour milling and test milling over 120 years. *Cereal Res. Commun.* 39 (2), 216–225. <https://doi.org/10.1556/CRC.39.2011.2.5>.

This page intentionally left blank

Principles of Farinograph operation and factors affecting performance

Jayne E. Bock

Wheat Marketing Center, Portland, OR, United States

CHAPTER OUTLINE

- 2.1 What influences Farinograph results? 23
 - 2.1.1 The temperature factor 23
 - 2.1.2 The water absorption factor 24
 - 2.1.3 The operator factor 25
 - 2.1.4 Instrumental factors 26
 - 2.2 Communicating meaningful Farinograph results between millers and bakers 27
 - 2.2.1 Communicating for decision making 27
 - 2.2.2 Communicating for relevancy to a process 27
 - 2.3 Putting it all together 31
-

2.1 WHAT INFLUENCES FARINOGRAPH RESULTS?

2.1.1 The temperature factor

One of the first factors to consider when looking at what can influence Farinograph results is the temperature. This includes the temperature of the thermostat, flour, and titrating water. It is critical to maintain a constant temperature throughout the test.

The thermostat is the first temperature checkpoint. It should be set to 30.0° C ± 0.5°C and not located near air vents or external windows. Beyond this, it's important to ensure that the thermostat reservoir is filled with only distilled water. Mineral deposits can affect circulation over time and cause variation in temperature. One final point is to check the thermostat reservoir fill level every day and refill as needed before starting the Farinograph.

The flour being tested should be at ambient (room) temperature. Flour that has been in refrigerated or frozen storage should be removed early enough to allow for the sample to reach room temperature. The easiest way to do this is to leave the samples out overnight the day before testing. During the test, flour should be premixed for 1 minute prior to water addition. The mixing action of the blades and heat transfer from the water-jacketed bowl will increase the flour temperature to the 30.0°C target.

Titrating water should reach 30.0°C before beginning tests for the day. Some Farinograph units and thermostats have mechanisms to automatically control titrating water temperature. In instances where these features are not available, it is acceptable to place a beaker of titrating water directly into the thermostat for temperature equilibration. Any operators using a buret for water addition should be careful not to add the titrating water to the buret until premixing of the flour has begun. This prevents large temperature drops prior to water addition during the test. Once premixing is complete, the titrating water should be added within 30 seconds to prevent any further temperature drop.

This may seem excessive, but a decrease in the temperature of the flour and/or titrating water results in decreased arrival time, peak time, and stability, and increased torque. This can have a significant effect on the accuracy of the farinogram.

Once the test is fully initiated, dough temperature is dictated by the initial flour and titrating water temperature, heat exchange with the bowl, and heat generated by mixing. The desired steady-state temperature is 30.0°C.

Steady-state dough temperature is typically achieved within 2–4 minutes of mixing. The exact length of time is dependent on initial flour and titrating water temperature as well as the dough mass. A dough mass of 80 g in a 50-g mixer will achieve steady-state temperature more rapidly than a 460-g dough mass in a 300-g mixer. Mixing action will always result in an increase in the dough temperature. The excess heat is absorbed by the mixing wall. The lower limit of initial dough temperature is 23°C to achieve steady state within the allotted time, and this initial dough temperature is always achieved if flour and titrating water temperature requirements are met.

2.1.2 The water absorption factor

The second factor to consider when comparing farinograms is the water absorption of the curve. This is especially important when comparing the same flour across multiple locations. For every increase in water absorption

there will be an increase in arrival time, dough development time, and stability. Torque will concomitantly decrease. Operators should therefore expect values to differ slightly if they are comparing farinograms of the same flour from the extremes of the acceptable torque range (500 ± 20 BU, or 480–520 BU).

2.1.3 The operator factor

A third factor to take into account is operator error. Even highly trained operators will occasionally make a mistake during a test that affects the results. Some sources of error include:

- (1) Weighing of flour,
- (2) Use of the bowl cover,
- (3) Dispensing of titration water,
- (4) Scraping of bowl walls,
- (5) Peak selection, and
- (6) Bowl cleaning.

Of these, the last four are the most common and can be overcome with better training programs. Weighing of flour is more commonly an issue of proper scale calibration, but is sometimes caused by the operator weighing out the wrong amount (e.g., transposing numbers or forgetting to correct for flour moisture content). Use of the bowl cover minimizes moisture loss from the dough during testing and is sometimes overlooked by operators after scraping of the bowl.

Dispensing of titration water is primarily an issue when a buret is used to add water. Automatic titrating units are available and reduce this source of error. Titration water should be added in less than 30 seconds at the start of the test, but some operators struggle to achieve this rate of water addition.

The method also requires that the bowl walls be scraped with a special spatula after water addition to ensure that all flour particles are incorporated into the dough. Operators can sometimes insert the spatula too deep and hit the mixing blades. This not only causes a jump in the torque measured on the blades, but can also bend or otherwise damage the blades.

After the test is complete, the software automatically identifies the greatest torque value as the peak of the farinogram, and the associated time is recorded as the dough development time. However, double-peak curves routinely require operators to manually select the appropriate peak in the software. Many operators struggle with this and a written protocol with

examples of double-peak curves can help improve operator identification of the correct peak.

Incomplete bowl cleaning after the test can result in material being left behind on the mixing blades, especially if they are not removable. This leftover material can cause the blades to catch and thereby skew torque readings. Use of floss to clean behind nonremovable blades can reduce this issue. Another common problem with bowl cleaning is the use of abrasive chemicals or materials to remove dough residue. Abrasive materials damage the bowl surface, resulting in incorrect water absorption values and/or changes in dough stability and breakdown.

2.1.4 Instrumental factors

The final thing to consider is that the instrument itself can influence the accuracy of test results. Bowl geometry and surface conditions, speed of the drive shaft, accuracy of the load cell, accuracy of the buret, and temperature control are all instrumental parameters that can influence test results. Those that can be controlled by proper maintenance and calibration are bowl geometry and surface conditions, speed of the drive shaft, and accuracy of the load cell. The accuracy of the buret is typically not an issue so long as the standard Farinograph buret is used. Finally, temperature is primarily under operator control as described earlier.

The primary concern among instrumental factors is determining when the mixing bowl requires maintenance (i.e., bowl geometry and surface conditions). In general, a mixing bowl should be serviced every 2 years to keep it in good operating condition. This assumes an average number of operating hours and no damage to the bowl. A shorter time span is recommended for mixing bowls that accrue a high number of operating hours. Bowls should be immediately sent in for service and/or repair if any of the following are observed:

- (1) Leakage of dough behind the blades—This indicates that the mixing blade bushings are worn.
- (2) Rough or irregular farinograms—This is a sign of worn or damaged mixing blades or bearings.
- (3) Excessively high water absorption values—This can be caused by bowl surface damage.
- (4) Excessive smearing of dough on bowl walls—This signifies a clearance issue between the blades and the bowl.

2.2 COMMUNICATING MEANINGFUL FARINOGRAPH RESULTS BETWEEN MILLERS AND BAKERS

The basic function of the Farinograph test in industry is to serve as a tool to communicate the properties of a given flour between two parties. The standard Farinograph methods set out by AACCI, ICC, ISO, and other standards organizations are meant to allow for comparisons between labs and facilitate this type of communication. However, these standard methods are not always meaningful in the context of using the flour in a commercial bakery.

2.2.1 Communicating for decision making

Figuring out how to identify the optimal flour for a product is a daunting task. Use of tools such as a Pugh matrix can help with comparisons between different flours and sources in a single document. An example of a Pugh matrix is provided in [Fig. 2.1](#). Most of these tools require identification of key parameters and assigning a weight based on their importance to decision making. Communication between parties regarding critical parameters, values, and weightings is essential to the development of an accurate matrix. The end of the exercise should result in a numerical value or other comparative factor that ranks the potential options against one another.

2.2.2 Communicating for relevancy to a process

Creating decision-making tools is one exercise millers and bakers can go through. Other options include changing the Farinograph test parameters to better reflect actual conditions during processing. One example is to change the test temperature. All standard methods have a temperature setting of 30°C. However, some bakeries may use ice or have water-jacketed mixers to keep the temperature closer to 20°C. Others may lack temperature control in the facility itself and have limited access to ice, resulting in dough temperatures close to 40°C on exceptionally hot summer days. This can substantially change the shape of farinograms, as shown in [Fig. 2.2](#), and may provide more useful information on water absorption and mixing properties.

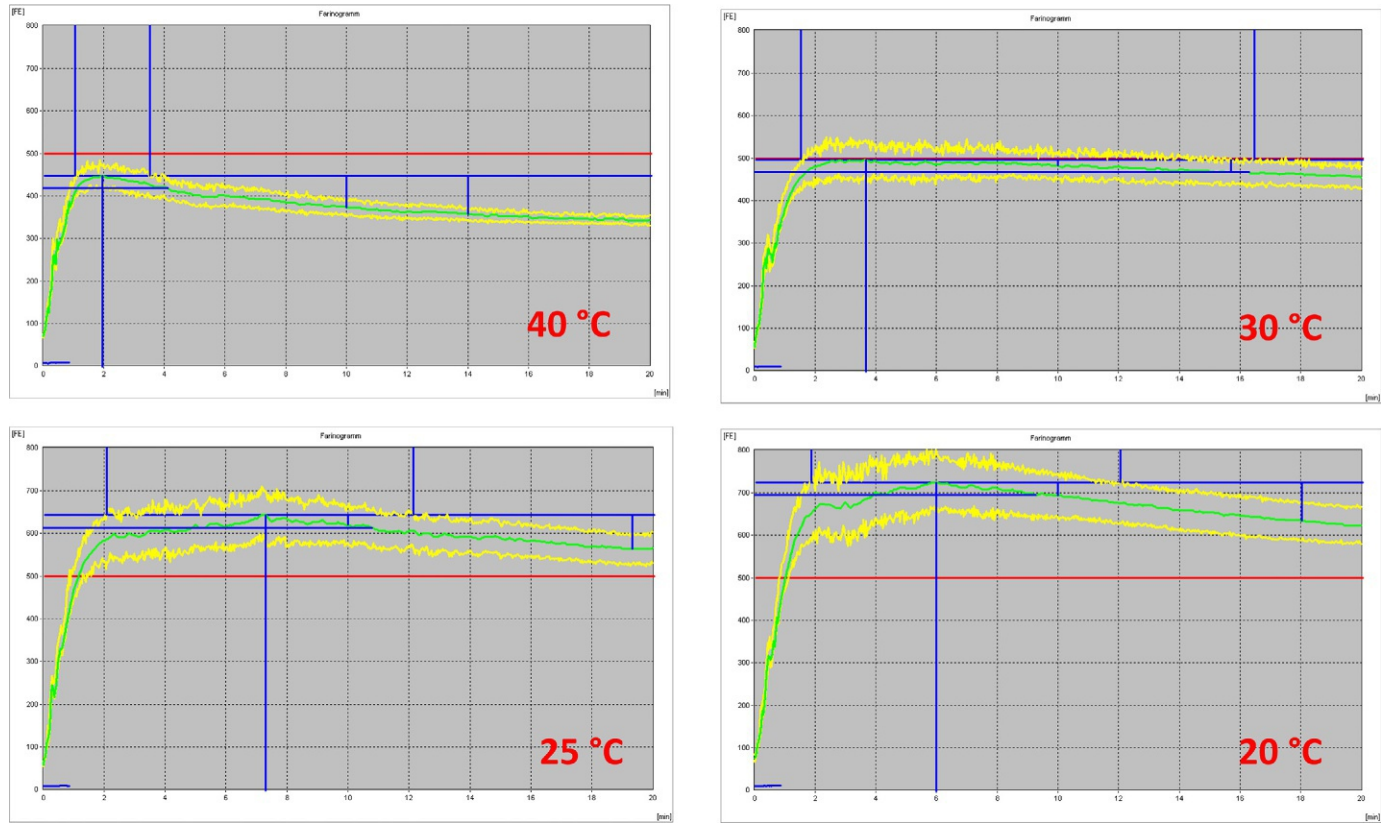
Bakeries also generally mix at higher speeds than the 63 rpm used in the standard Farinograph methods. Again, the mixing speed of the test can be adjusted to better reflect actual mixing speeds employed in the bakery. Dough development and stability times are significantly altered by changing the mixing speed ([Fig. 2.3](#)).

Pugh Matrix		Options						
Specification (Example)	Importance - Factor	Wish	Mill 1	Mill 2	Mill 3	Mill 4	Mill 5	Mill 6
Better +								
Same S								
Less good -								
Price	10	S	S	+	S	S		
Color	7	S	-	S	+	-		
Water absorption	9	S	+	S	S	+		
Dough Development Time (DDT)	8	S	+	S	-	-		
Mixing stability	10	S	S	-	+	S		
Maximum stretching (500)	5	S	S	-	-	S		
Maximum stretching 90 min 600	7	S	S	+	S	+		
Amylograph maximum (600)	9	S	-	+	-	+		
Amylograph temperature (70°C)	10	S	-	S	+	+		
Gluten index (38)	5	S	-	+	+	S		
Counts plus points	10	2	4	4	4	0	0	
Counts minus points		4	2	3	2	0	0	
Neutral counts		4	4	3	4	0	0	
Sum		80	52	112	100	120	0	0

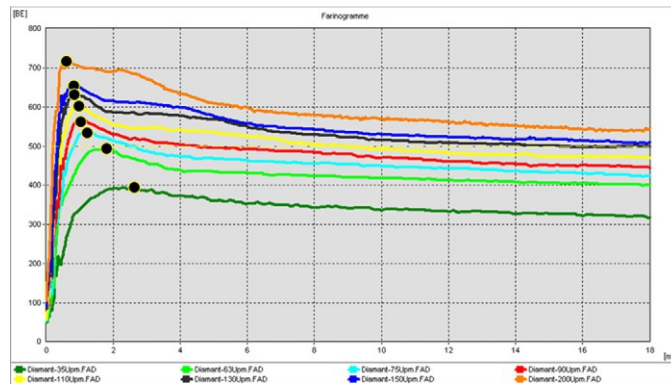
■ FIG. 2.1 An example of a Pugh matrix comparing flours from four different mills.

Another issue that arises, especially when evaluating whole-wheat flours, is the influence of particle size. Comparing farinograms from whole-wheat flours using more realistic mixing settings (Fig. 2.4) can reveal potential issues that may influence dough-mixing properties and final product quality. The reader is directed to Chapter 8 for additional reading on adaptations for whole-wheat flour Farinograph testing.

These are all examples of ways the Farinograph test can be adapted or modified to aid communication between millers and bakers. The key here is to keep the lines of communication open. Both parties need to ask questions:

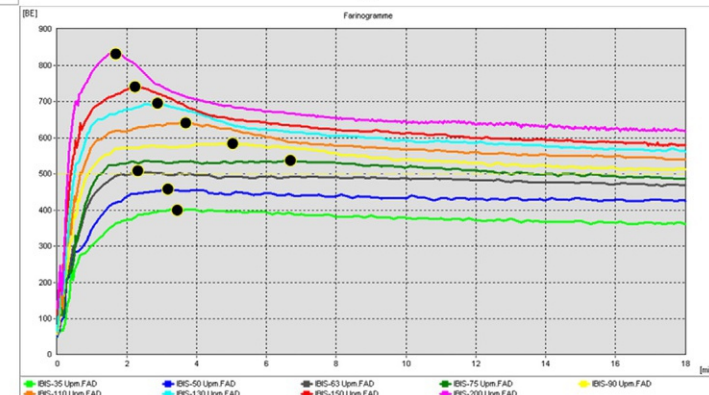


■ FIG. 2.2 Farinograms of the same flour run at different temperatures.

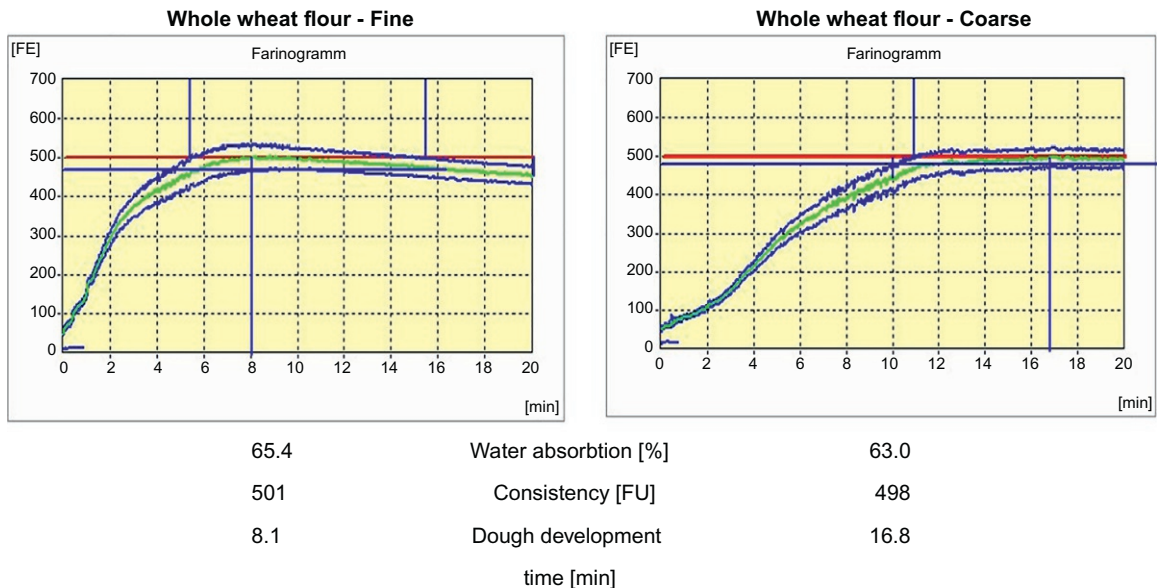


Weak flour

Strong flour



■ FIG. 2.3 Farinograms of the same flour using different mixing speeds. (A) Example of a weak flour, and (B) example of a strong flour.



■ FIG. 2.4 Sample farinograms of the same whole-wheat flour ground to fine or coarse particle size.

- What adds value to the results?
- What makes sense for the process?
- How can you move forward collaboratively?

2.3 PUTTING IT ALL TOGETHER

The Farinograph and its results have been misunderstood in recent years due to the slow but steady loss of knowledge surrounding the instrument and its use in industry. Experts have retired, operator turnover is much higher than in decades past, and nonconventional Farinograph applications have been forgotten. However, harnessing the full power of the Farinograph is possible with just a little knowledge, training, and communication.

This page intentionally left blank

The Farinograph: Understanding Farinograph curves

Jayne E. Bock

Wheat Marketing Center, Portland, OR, United States

CHAPTER OUTLINE

- 3.1 Flour composition basics and beyond 33
 - 3.2 Assessing flour quality 34
 - 3.3 What does the Farinograph measure? 34
 - 3.4 How do we read the Farinograph torque curve? 35
 - 3.5 Using Farinograph parameters to classify flours 36
 - 3.6 The double-peak conundrum 37
 - 3.7 Comparing different Farinograph methods 37
 - 3.8 The bottom line 41
-

3.1 FLOUR COMPOSITION BASICS AND BEYOND

A wheat kernel is composed of bran (~14% w/w), starch (~70% w/w), protein (~14% w/w), and lipids (~2% w/w) on a dry matter basis. The bran and germ are removed during milling of refined flour, leaving starch (amylopectin and amylose) and proteins (albumins, globulins, gliadin, and glutenin) with small amounts of pentosans (soluble fibers), minerals, enzymes, and lipids. These can be measured by traditional standard methods or estimated with NIR spectroscopy to give a representation of the raw flour composition. Understanding the composition of a specific flour can give some indication of its performance potential, but it is not a substitute or stand-in for flour quality.

Flour composition and its influence on quality becomes questionable after milling because of the addition of ingredients at the mill as well as the bakery. Ingredients like ascorbic acid, cysteine, malt flour, lipids, and enzymes can all be added at various points after milling to improve flour performance.

Additional characteristics such as protein quality, starch damage, and flour granulation or particle size all influence flour performance beyond composition. It's also important to remember that flour is a biological material that changes, or ages, over time. Once the wheat kernel is reduced to flour, all the internal components are disrupted and exposed to air. Ambient conditions at the mill, during transport, and at the bakery will determine how quickly biochemical reactions take place. These biochemical reactions will change the functional properties of the flour in ways that are measurable, and they will influence flour quality and performance during processing.

3.2 ASSESSING FLOUR QUALITY

With all of this to keep in mind, how do we assess variation in flour? The short answer is that we use approved, standardized methods to assess different aspects of flour functionality that are relevant to the product and process. There are numerous methods for specific flour functional properties—most commonly bulk rheological properties—utilizing instruments with different measurement principles. The focus here will be the Brabender Farinograph, used most commonly to assess dough-mixing properties.

The Farinograph, as mentioned earlier, measures dough-mixing properties by answering two key questions:

- (1) What is the water absorption of this flour? and
- (2) How stable is the dough during mixing?

These and other measurements, which we will go into shortly, can be taken directly from the farinogram, but other indirect assessments include things like protein quality and enzyme activity.

3.3 WHAT DOES THE FARINOGRAPH MEASURE?

The first item to address is what the Farinograph physically measures. The instrument is essentially a torque meter, specifically measuring the torque on the mixing blades from a dough at a given water absorption during mixing. Water absorption is key, because it dictates dough plasticity.

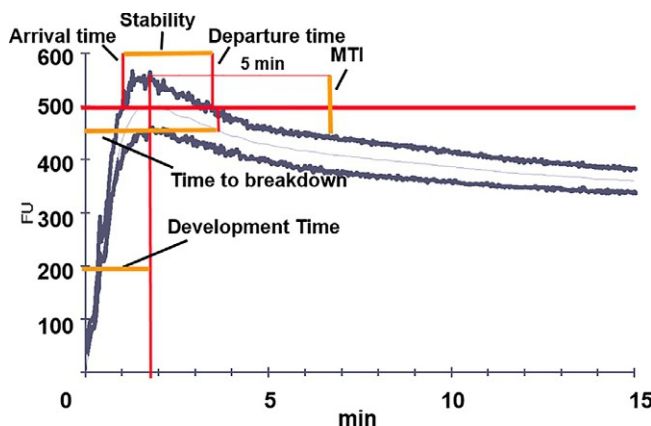
Another question is how that torque is harnessed for information on dough properties. Torque is plotted as a function of time to generate a torque curve, or farinogram. Flour-mixing performance is determined by close analysis of the changes in torque over time. For example, the farinogram produced by a flour intended for white pan bread looks different from those for flours intended for artisan rolls/bread or cookies/pastries.

3.4 HOW DO WE READ THE FARINOGRAPH TORQUE CURVE?

The Farinograph method is documented and accessible as AACCI Approved Method 54-21.02/54-22.01, ICC Standard 115/1, and ISO 5530-1/5530-2. We will focus on reading the farinograms and discuss the methods later. We'll begin by walking through the various measurements that can be taken from a farinogram and what they tell us about the flour.

Following is an example of a farinogram collected from a flour sample (Fig. 3.1). The water absorption (WA) value of the flour is adjusted until the torque curve achieves 500BU (± 20 BU). (Readers should note that BU stands for Brabender units and is an arbitrary unit of measure.) As seen in this example, the peak of the torque curve rises as the flour and water are mixed into a dough and achieves a maximum of 500BU at the midline of the torque curve. Water absorption (WA) is the amount of water that is added to a defined quantity of flour (typically 300g or 50g of flour at 14% moisture basis, or mb) to generate a torque of 500BU expressed as a percent of the amount of flour. (e.g., 180mL of water added to 300g flour equates to 60% WA.)

The arrival time is defined as the point in time where the top line of the torque curve first reaches 500BU. This occurs at approximately 1.0 minute in this farinogram. The corresponding departure time is the point where the top line of the torque curve last touches the 500BU line. The departure occurs at about 3.5 minutes in this example. These two points establish the stability of



■ FIG. 3.1 Sample farinogram showing a breakdown of evaluation points.

the dough to mixing: subtracting the arrival time from the departure time gives the length of time the dough is stable during mixing before breaking down. Stated another way, mixing stability determines how long a dough will resist breakdown due to overmixing.

The dough development time (DDT) is the point of maximum torque for a flour at a given WA. The dough is considered to be optimally developed by the mixing process and would be ready for continuing on with the baking process. However, should the dough continue to be mixed beyond this point it will eventually begin to break down. How long a dough can be mixed beyond the DDT is dependent on its mixing stability.

A parameter related to dough-mixing stability and breakdown is the mixing tolerance index (MTI). It is measured as the drop in the torque value, measured in BU, of the top line 5 minutes after the DDT. A larger MTI indicates more weakening of the dough during mixing than a smaller MTI. We would correspondingly expect mixing stability to be shorter if the MTI is larger.

We can also directly measure time to breakdown (TBD). This is the amount of time from the start of mixing until the dough breaks down, measured as the time required for the torque to drop 30BU from its maximum at DDT. This is measured from the midline, not the top line.

Another parameter that is similar to MTI and TBD is the 20-minute drop. This is expressed as the drop in torque from the DDT to 20 minutes after the addition of water. Again, this is measured from the midline of the torque curve and indicates the strength of the flour. A larger 20-minute drop value corresponds to a weaker dough that is not as tolerant to overmixing.

3.5 USING FARINOGRAPH PARAMETERS TO CLASSIFY FLOURS

Some general guidelines for classifying the strength of flour using these Farinograph parameters is included in [Table 3.1](#). Each company and operation will define these categories with different cut-off values, but this is intended to give a sense as to how the values would look for flours of different strength profiles.

You can also gather information about the strength of a flour simply by looking at the torque curve shape. In many instances, the parameters may turn out to be similar, but the overall farinogram shape will tell you if the flours are truly comparable or significantly different ([Fig. 3.2](#)).

Table 3.1 General guidelines for classifying flour strength using the Farinograph.

	Weak flour	Medium flour	Strong flour	Very strong flour
Water absorption (%)	<55	55–60	60–63	>63
Dough development time (min)	<2.5	2.5–4	2.5–14	>14
Dough stability (min)	<3	3–5	5–10	>10
MTI (FU)	>100	60–100	15–50	<10

3.6 THE DOUBLE-PEAK CONUNDRUM

This brings us to the double-peak shape observed in some farinograms. Certain flours show an exceptionally large hydration peak followed by a second later peak. It can be very subtle in some cases, and Fig. 3.2 is a good example of this more subtle double peak where the hydration peak obscures the second peak. In this case, the Farinograph operator should look for a plateau region, as this is the location of the second peak. A more obvious double peak is shown in Fig. 3.3. The second peak should be considered the true dough development time for the curve, as it correlates more directly with baking performance. The Farinograph operator will need to manually select the peak in the software in almost all double-peak farinograms.

3.7 COMPARING DIFFERENT FARINOGRAPH METHODS

Several methods have been developed over the decades of use to help standardize the operation of the Farinograph as well as the interpretation of the results. However, those methods can be a source of confusion when comparing farinograms, because different methods will yield different results.

The constant flour weight method (AACCI Method 54-21.02) is the most common method used for Farinograph testing. The method consists of weighing out a consistent amount of flour (50g or 300g) by correcting the flour moisture content to 14% mb. Water is then added to achieve a torque of 500BU at the peak of the curve. The amount of water added determines the water absorption value.

The key advantages to this method are that the flour moisture content correction to 14% mb allows for a constant amount of dry matter to be added for every test, and this allows for comparisons across a range of flours. However, the total dough weight is not held constant because the total amount of flour

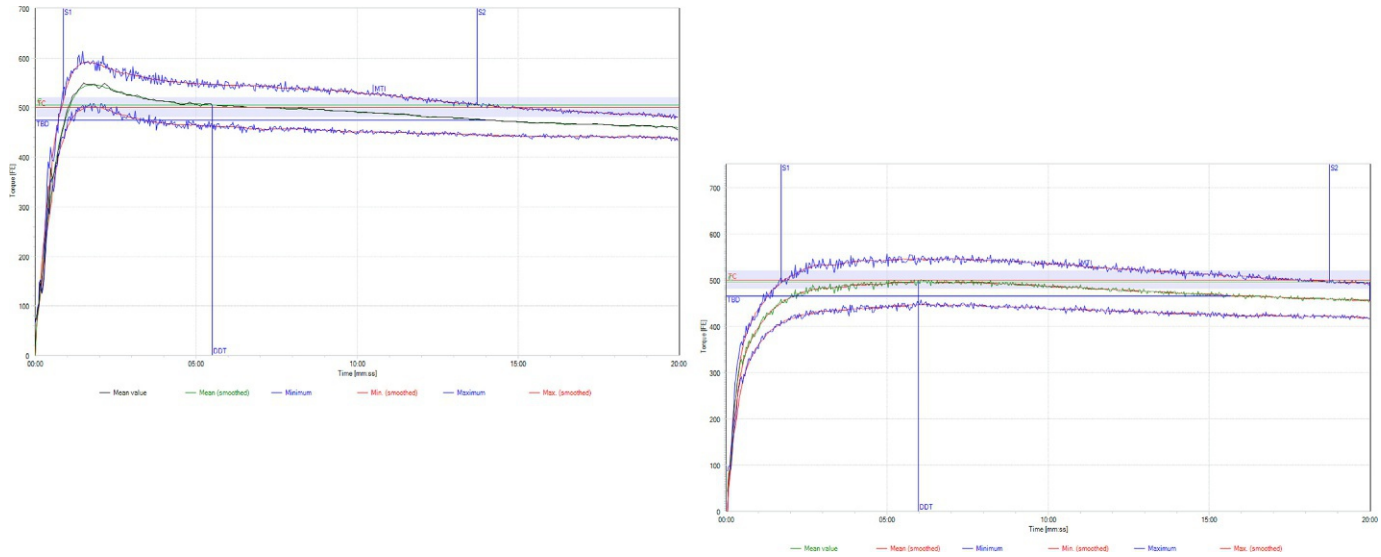
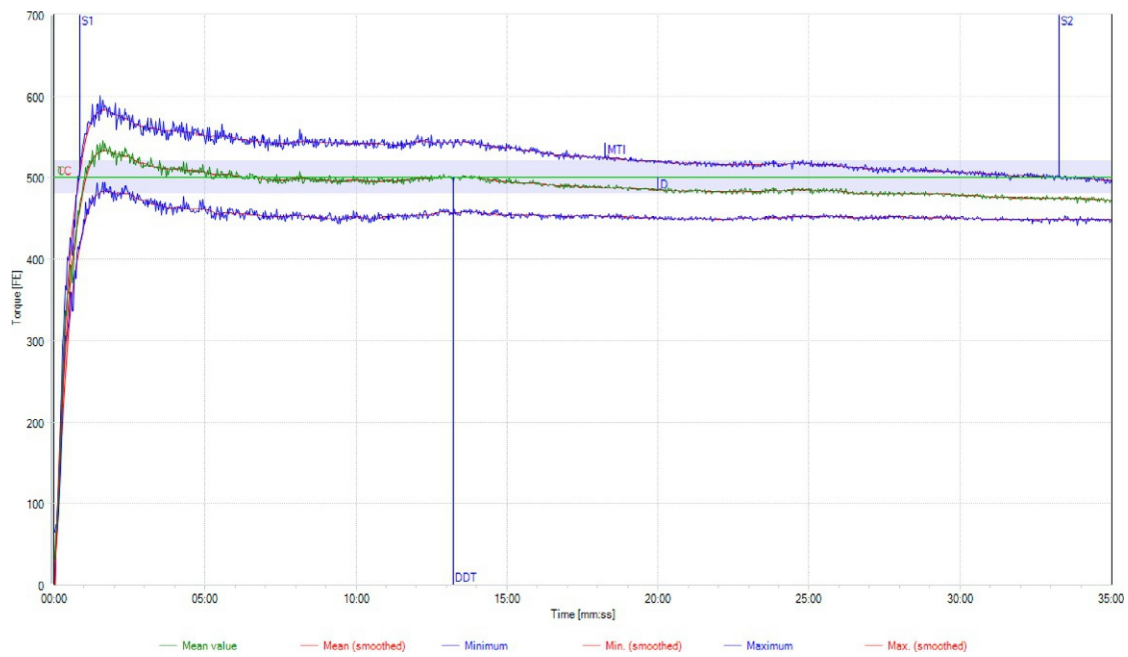


FIG. 3.2 Example of two strong flour farinograms giving relatively similar Farinograph values but having different shapes and end-use applications.



■ FIG. 3.3 Example of a double-peak farinogram.

and water changes. This variation in dough weight means that the same mechanical energy is being imparted to a different amount of dough in each test, and this has implications for the stability and breakdown of the dough.

The constant dough weight method (AACCI Method 54-22.01), on the other hand, consists of adding a specific amount of flour and water to provide a targeted dough weight. In this case, the flour moisture content is not corrected to 14% mb. The same 500 BU torque value is targeted at the peak of the farinogram curve. Again, the amount of water added determines the water absorption value.

The advantages of this method are that it is usually requires less time because the moisture content of the flour does not need to be known before the test, and the same amount of dough is being tested every time. However, the flour weight is not constant and the water absorption must be corrected to 14% mb in order to make comparisons across flours.

As a result, the constant flour weight method is not the same thing as the constant dough weight method. The correct method must be specified in the Farinograph software in order for the correct farinogram values to be calculated. The value most significantly affected is the water absorption.

Both methods present three different water absorption values:

- (1) The WZ, or the water absorption actually added during the test,
- (2) The WAC, or the water absorption necessary to correct the midline of the farinogram to the 500BU line, and
- (3) The WAM, or the water absorption corrected to 14% mb.

The WZ is straightforward and is determined by the operator. The WAC is calculated by the software and can be used directly in subsequent tests to better target the 500BU line. (A good rule of thumb for the WAC is that a 20BU difference is equivalent to $\sim 0.5\%$ WZ.) The WAM is the most important, however, because it is a normalized value that can be used to make comparisons between different flours. Therefore the WAM is the water absorption value that is reported in formal communications and specifications.

The WAM calculation for the constant flour weight method (AACCI Method 54-21.02) is given here and is designed to correct for differences in dough weight:

- (1) For a 300g bowl:

$$\text{Absorption \%} = (x + y - 300)/3$$

- (2) For a 50g bowl:

$$\text{Absorption \%} = 2(x + y - 50)$$

where

x = mL of water added, and

y = g of flour added.

The WAM calculation for the constant dough weight method (AACCI Method 54-22.01) is designed to correct for the flour moisture content:

$$\text{Absorption (14\%mb)} = 86 \times [(B + M)/(100 - M)] - 14$$

where

B = absorption (as-is), and

M = flour moisture content (as-is).

The ICC standard method (ICC-Standard No. 115/1) is similar to the AACCI Method 54-21.02 (constant flour weight), whereas ISO 5530-1:2013 includes both AACCI Methods 54-21.02 (constant flour weight) and 54-22.01 (constant dough weight). The only difference is in the parameters extracted from the farinograms. A degree of softening is extracted for ICC and ISO instead of a time to breakdown.

There is one final method that is commonly run in bakeries and we will refer to it here as the as-is method. This is not a standardized method and is typically used internally wherever it is conducted. It is run using a set amount of flour without moisture correction, with water added to achieve a desired torque value (not necessarily 500BU). This method is meant to simulate the baker's experience with the flour by identifying the amount of actual formula water needed to achieve a given consistency. It lacks scientific rigor and cannot be used for comparison of results, but it does provide a meaningful water/bake absorption for the flour going into the mixer.

3.8 THE BOTTOM LINE

Learning how to read the information contained in a farinogram and how it relates to processing and baking performance is a skill that requires time and experience. However, it's a skill worth the investment since it can significantly impact the bottom line of an operation. The following chapter will explore factors that affect the Farinograph and its curves, including ideas around how to modify the method to make results more meaningful.

This page intentionally left blank

Dough rheology and the Farinograph: The mechanism underlying dough development

Clyde Don

FoodPhysica Laboratory, Malden, The Netherlands

CHAPTER OUTLINE

4.1 Dough rheological insights in the third edition	44
4.2 Dough development—The disaggregation of gel-protein	46
4.3 Developing dough—The interaction of glutenin aggregates	52
4.4 Dough physical properties—Glutenin polymer size or glutenin aggregates?	58
4.4.1 Observed changes in the SP fraction	60
4.4.2 Observed changes in the insoluble glutenin-gel fraction	61
4.4.3 Fate of the gel-proteins and functionality in dough	63
4.4.4 The mechanism underlying dough peak resistance in the Farinograph	64
4.5 Conclusions	66
Acknowledgments	68
References	68

SYMBOLS AND ABBREVIATIONS

CSLM	confocal scanning laser microscopy
DDT or TTP	dough development time or dough peak time
DTT	dithiothreitol
G^*	complex modulus
G''	loss modulus
G'	storage modulus/stiffness
GMP	glutenin macropolymer

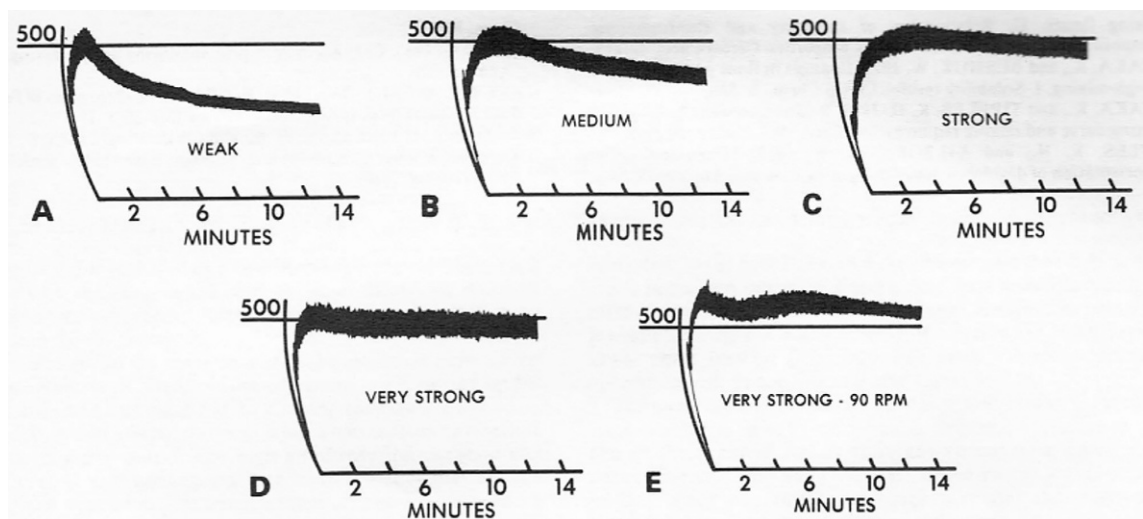
HMW-GS	high molecular weight-glutenin subunits
K_H	Huggins constant
LMW-GS	low molecular weight-glutenin subunits
M_n	number average molecular weight
M_w	polymer weight average molecular weight
M_w/M_n	p , the polydispersity or size heterogeneity
R_g	radius of gyration
R_h	hydrodynamic radius
SIP	insoluble glutenin
SP	dispersible glutenin
SP*	soluble glutenin
SUP	SDS dispersible glutenin aggregates
UPP	unextractable polymeric protein
$[\eta]$	voluminosity

4.1 DOUGH RHEOLOGICAL INSIGHTS IN THE THIRD EDITION

It has long been established that only wheat flour shows the typical dough peak when mixed with water in the Farinograph ([Bushuk, 1998](#)). Today, dough development time and/or energy to peak is still an important factor for any researcher or quality assurance manager in wheat technology. The empirical quality assignments—weak, strong, and overstrong—are part of the cereal chemist’s daily vocabulary. In their overview on dough rheology and the Farinograph, [Preston and Kilborn \(1984\)](#) concisely reviewed the typical results from flours with different strength ([Fig. 4.1](#)).

In addition to explaining the usefulness of having such empirical results from an accepted methodology (e.g., [AACC Method 54-21.01/2, n.d.](#) or [ICC Standard Methods, 1992](#)), with which cereal chemists around the globe can discuss their findings on wheat flour strength, mixing requirements, and water absorption, the authors of the previous edition pointed out some of the unknowns that underlie the typical shape of the Farinograph curve, the well-known dough development time, dough stability, and weakening/softening. An important insight from the third edition of the handbook is the following:

Qualitative properties of the proteins are considered to be the major factor determining flour mixing requirements. In particular the amount of high molecular weight acid unextractable “gel” protein appears to be closely related to inherent mixing strength. During mixing this gel protein is disaggregated, as demonstrated by increasing protein extractability in dilute acids. It has been



■ FIG. 4.1 Examples of farinogram dough curves. (Reproduced from the third edition of this handbook.)

suggested that the high molecular weight gel protein imparts strength in the gluten structure during mixing, and that after that this gel is broken down, mixing stability decreases. However 'recent' (Preston & Kilborn in 1984 eds.) studies suggest that it is the disaggregation products of the gel protein produced during mixing that impart mixing strength. Obviously this area requires additional study before more definitive answers are available.

It should be mentioned that such an insight had been advocated beforehand by Mecham et al. (1965), suggesting that gluten protein aggregates or particles had a pronounced influence on the mixing stability of wheat flour. On the other hand, Goldstein (1957) claimed to have evidence that the reactions involving sulphydryl groups and disulfide bond reshuffling are dominant in the specific mixing-rheology of wheat flour dough. This did influence the conceptualization of a generation of cereal chemists and rheologists such as Bloksma and Bushuk (1988) on the possible mechanisms underlying dough strength, although the same coauthor (Bloksma, 1972, 1975) did provide some nuances in suggesting that the effect of disulfide bonds/disulfide interchange reactions may not always be so controlling and rheologically effective. In a review on dough rheology and the bread-making process, Dobraszczyk and Morgenstern (2003) points at a polymeric structuring mechanism that could explain wheat flour dough rheology, because it shows striking similarities with the rheological response of (synthetic) branched polymers.

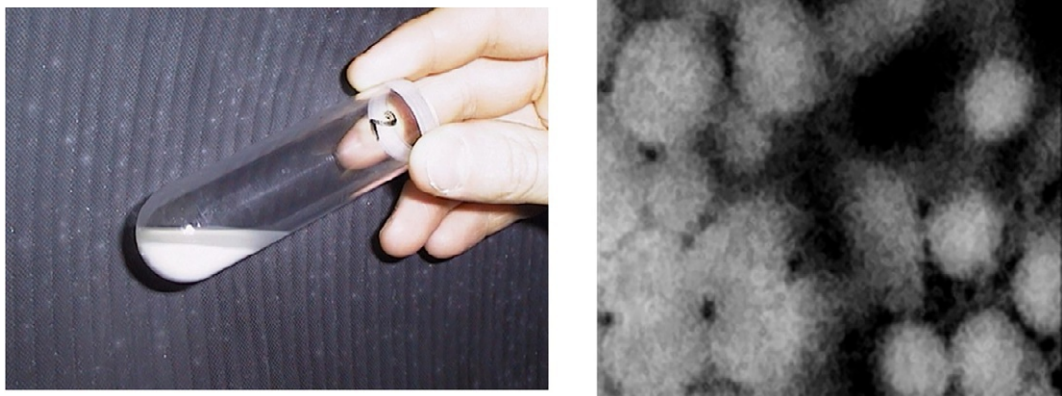


FIG. 4.2 Opaque GMP-gel protein on top of starch (left), Glutenin particles in wheat cultivar Soissons (right).

In this chapter on factors affecting dough development in the Farinograph, further evidence is discussed to underpin how unextractable gel-protein is indeed the key factor in dough mixing. Moreover, a mechanism relying more on protein particle/aggregate aspects is also presented. The basic gel-protein in this chapter is obtained by the isolation method of SDS gel-proteins by Graveland et al. (1982), called glutenin macropolymer or GMP-gel. The method is based on centrifuging flour in aqueous SDS (Fig. 4.2); the supernatant contains readily SDS-soluble wheat proteins and may also contain highly dispersible wheat protein particles that are kept buoyant in the solvent, resisting sedimentation by centrifugal forces. The GMP-gel fraction on top of the starch is very similar to the acid unextractable proteins and the fraction known as UPP (Lafiandra and MacRitchie, 1997). Since there is more supporting evidence that glutenins are indeed highly aggregated particles originating from wheat endosperm (Don et al., 2003a), the additional answers are available to further unravel the mechanism underlying dough peak resistance that is so characteristic of wheat flour dough.

4.2 DOUGH DEVELOPMENT—THE DISAGGREGATION OF GEL-PROTEIN

Undoubtedly, without the presence and unique properties of wheat gluten it would not be possible to prepare a viscoelastic dough from wheat flour suitable for bread making (Wrigley, 2009). Native gluten consists of gliadins and glutenins (Schofield, 1994). The gliadin fraction has been reported to contribute to the viscous properties of wheat flour dough; the glutenin fraction of wheat gluten has been shown to have a prominent role in the

Table 4.1 Protein content, HMW-GS composition, and dough development time.

Wheat variety	Flour protein content (%)	HMW subunit composition	Dough peak (DDT) (min)
Estica	12.4	6+8, 2+12	5
Soissons	10.6	2*, 7+8, 5+10	10
Baldus	12.5	1, 14+15, 5+10	27

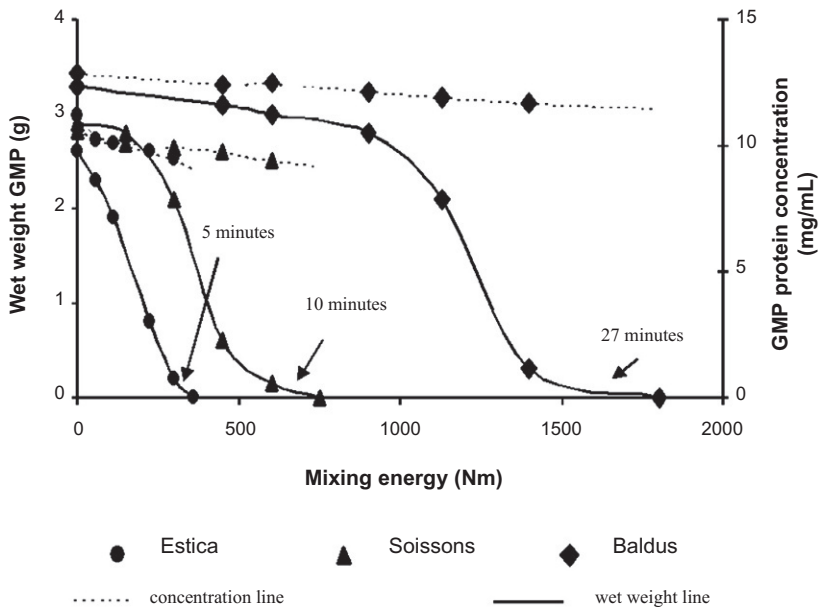
strengthening of dough (MacRitchie, 1980). The glutenin fraction consists of high molecular weight glutenin subunits HMW-GS and low molecular weight glutenin subunits LMW-GS (Lászity, 1996).

The observation of large glutenin particles in the protein gel fraction called GMP (Don et al., 2003a) opened up new possibilities for revealing the mechanism that links the properties of glutenin-gel with dough-mixing properties (Fig. 4.2 right).

The composition and mixing requirements of the three wheat flour varieties used in the studies that have revealed more about the mechanism underlying dough development are shown in Table 4.1.

This set of three was used in a thorough analysis of GMP-gel properties and the effect on dough properties in the Farinograph. Soissons can be seen as a fairly strong flour; although low in protein, it bakes reasonably. Some differences in dough peak time from the previous work and followed up on in this chapter are probably related to differences in bowl and mixing speed. This does not jeopardize the principles underlying the factors affecting dough development. In Fig. 4.3 it is shown how, as suggested by Preston and Kilborn (1984), the SDS extractability of the gel-proteins (here GMP-gel) increases with mixing.

It is also clear from Fig. 4.3 that the SDS unextractable GMP-gel amount decreases with mixing time, nearing zero at dough peak resistance (DDT). It has already been known since the mid-1980s that mixing leads to a decrease in GMP (Graveland, 1984). Fig. 4.3 confirms this for Estica, Soissons, and Baldus. Although the wet weight of GMP is decreased, protein concentration in the SDS unextractable GMP-gel left does not decrease as much as the wet weight. This result shows that gel quantity is affected, but not its concentration, indicating that there is a gradual disruption or disaggregation of the insoluble glutenin. It also suggests that the initial size distribution of the glutenin particles in flour could be broad and that the larger glutenin particles take longer to disrupt into smaller SDS (1.5%) dispersible



■ FIG. 4.3 Insoluble glutenin-gel protein (GMP) decrease due to Farinograph mixing.

glutenin. The framework of the hyperaggregation model from Hamer and van Vliet (2000) describes events taking place at the molecular level, the mesoscopic level, and the macroscopic level. In this framework the mesoscopic level is regarded as the scale wherein the most important glutenin dynamics takes place. In this framework it is also emphasized that noncovalent interactions are dominant in dough rheology, which is more in agreement with the suggestions made by Preston and Kilborn (1984) and Mecham et al. (1965). The GMP-gel fraction can be measured in the quantity (g wet gel/g flour), but also the stiffness of the GMP-gel can be measured by placing it between the two parallel plates of a small deformation rheometer (Pritchard, 1993). The resulting values from such an experiment, namely G^* (Pa), G' (Pa), G'' (Pa), and phase angle δ (degrees), respectively represent the GMP-gel's complex modulus, the storage modulus, the loss modulus, and the ratio between the loss modulus and storage modulus. At low strain the storage modulus of a GMP-gel is on a so-called plateau with a phase angle typically <20 degrees, but >10 degrees for weak to medium flour and <10 degrees for strong flour, confirming that the GMP-gel at low deformation is more elastic, where $G' \text{ (Pa)} \gg G'' \text{ (Pa)}$. Kelfkens and Lichtendonk (2000) showed how the use of small deformation rheology on glutenin-gel (GMP) helps predict mixing requirements and bread-making quality. Bekkers et al. (2000) have shown a strong positive correlation between

Farinograph dough development time and G' plateau values of GMP isolated from flour. It was therefore concluded that the mixing behavior of flour under the conditions applied is related to the nature of the glutenin proteins as present in GMP-gel, rather than the total amount of gel protein. Now with the additional data that the GMP-gel from flour consists of glutenin particles that originate from wheat endosperm, it is likely that GMP-gel stiffness (G') represents the resistance to disaggregation of the gel proteins in a Farinograph test. [Don et al. \(2003b\)](#) showed how in a semilog plot there is a linear decline for $\log G_{\text{gmp}}'$ versus mixing energy, indicating that GMP stiffness decreases with increasing mixing energy input. The negative slopes of the lines indicate the rate of G' decrease, or the gel stiffness; respectively for Estica, Soissons, and Baldus, the rate of (G') decrease (slope) was: -20.8, -6.9, and -3.1. Given the fact that GMP gel protein concentration does not decrease much ([Fig. 4.3](#)), the decrease in G' must be due to changes in GMP particle properties. GMP-gel can be disrupted by cleavage of di-sulfide bonds, as known from analytical techniques using mercapto-ethanol or DTT to completely solubilize glutenin proteins into its subunits (in SDS). [Ewart \(1979\)](#) noted a fall in viscosity of gluten dispersions treated with excess mercapto-ethanol, suggesting a covalent glutenin disruption that turns glutenin into a more soluble polymer in dough systems. It is also possible that in the absence of strong reducing agents, GMP particles are disrupted by a more physical mechanism, as in the noncovalent disaggregation of the gel-proteins affecting the mesoscopic level of the glutenin network in dough. Current knowledge also has established that the G' plateau (Pa) of a GMP-gel is related to the glutenin particle voluminosity ($[\eta]$) as follows: $G_{\text{plateau}}'(\text{Pa}) \approx (c_{\text{gmp}} \cdot [\eta])^{3.3}$ ([Don et al., 2003b,c](#)). Subsequently, close parallels have been shown between glutenin aggregate size determined by laser light scattering and the voluminosity found by viscometry, bringing the concept of downsizing a particulate structure back to mind, which is depicted in [Fig. 4.4](#). The interesting finding here is that the average particle size where the glutenins turn from 1.5% SDS unextractable to 1.5% SDS dispersible is a specific size. When we regard the dough peak time of the respective flour varieties, it becomes clear that the average voluminosity of the GMP particles is approximately the same near peak development. Completely in parallel, the average voluminosity of the SDS-dispersible fraction (SUP) increases. The presented dotted lines in [Fig. 4.4](#) do not “touch” because the SUP fraction also contains some water-soluble proteins, like wheat albumin; this slightly decreases the average protein voluminosity of the SUP fraction. When—as a control—a reducing agent like DTT was added to the GMP dispersion of Baldus, a dramatic decrease in viscosity was observed (“stars” shown in [Fig. 4.4](#)), which agrees with [Ewart’s \(1979\)](#) earlier observations on dispersed gluten. This confirms that

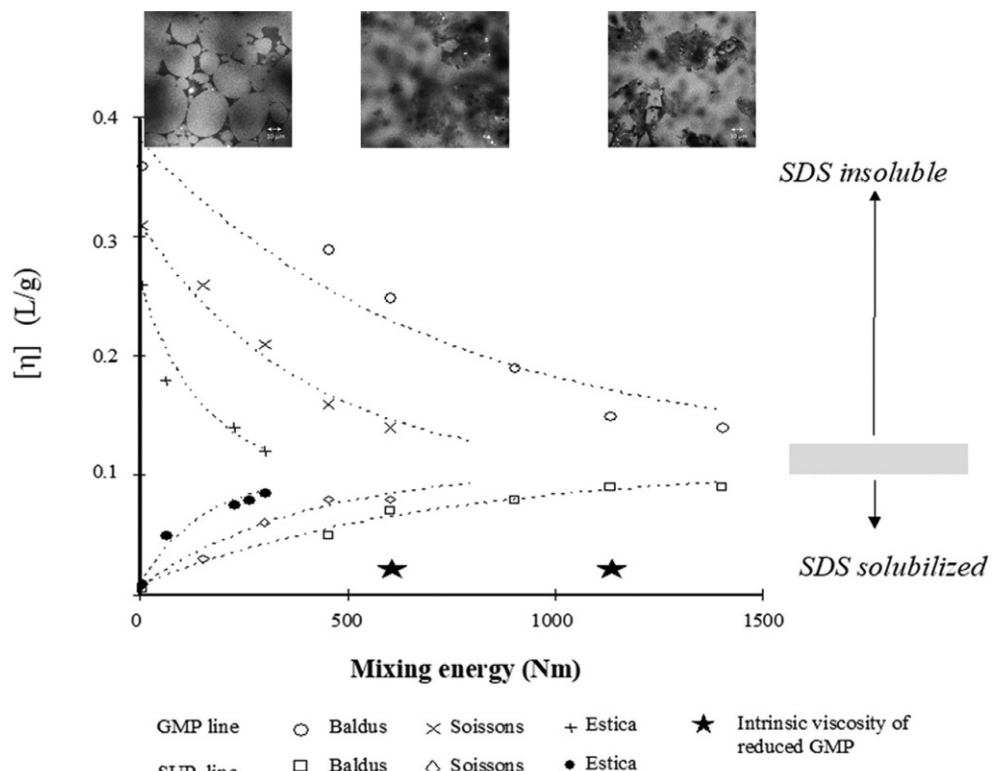


FIG. 4.4 Disruption of GMP gel during mixing and viscosity of SDS-soluble protein fraction. On top, an impression of the GMP-gel particles from very strong flour versus mixing.

disulfide-stabilized glutenin particles are still present in fully developed dough. The CSLM micrographs for GMP from Baldus corroborate the disruption of gel proteins becoming functional in dough, affecting dough strength.

The results presented in Figs. 4.3 and 4.4 indicate that the decrease of glutenin particle voluminosity and size is a fundamental step in dough development. In engineering, Kick's law (Eq. 4.1) is generally accepted to relate particle size reduction to energy input (Perry, 1997):

$$\frac{[x]}{[x]_0} = \exp(-E/C) \quad (4.1)$$

where E is the energy input in Nm, $[x]$ is average particle size vs. E , $[x]_0$ is the initial particle size (at $E=0$), and C is the rate constant. Assuming that this principle is applicable here, the decrease in glutenin particle voluminosity vs. energy is expected to follow Kick's law. It can also be deduced that

the rate of particle voluminosity decrease, C , is linked with the initial glutenin particle voluminosity. As a result, the following proportionality describes glutenin particle size disruption vs. energy (Eq. 4.2):

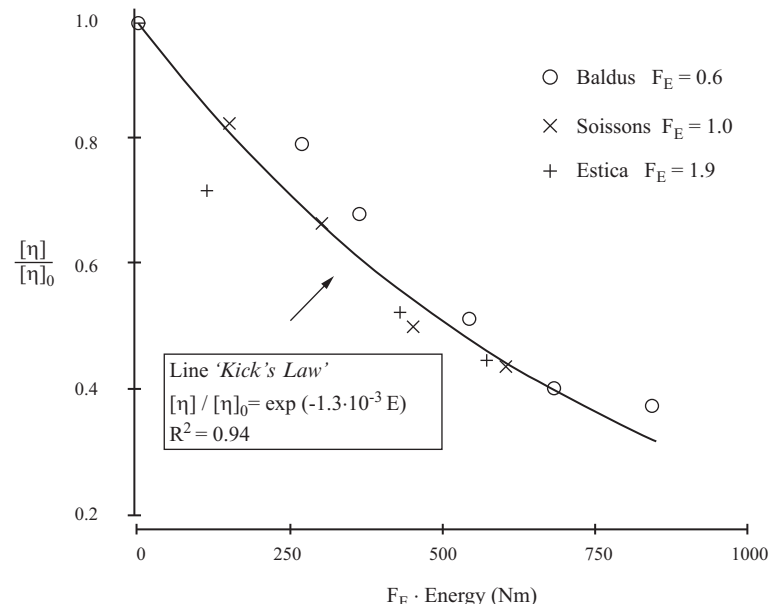
$$\frac{[\eta]}{[\eta]_0} \propto \exp \frac{-E}{[\eta]_0} \quad (4.2)$$

with $[\eta]_0$ as initial particle voluminosity at $E=0$ and $[\eta]$ as the average voluminosity vs. E . When the results observed for Estica, Soissons, and Baldus agree with the proportionality in Eq. (4.2), the experimental data is superimposable. The derivation of shift factor F_E from Eq. (4.2) leads to Eq. (4.3):

$$\ln(F_E) = \frac{1}{[\eta]_0} - \frac{1}{[\eta]_{\text{ref}}} \quad (4.3)$$

where $[\eta]_0$ is the initial voluminosity of the sample and $[\eta]_{\text{ref}}$ is the initial voluminosity of a reference sample. With Eq. (4.3), the shift factors F_E can be estimated, relative to Soissons ($[\eta]_{\text{ref}}=0.31 \text{ L/g}$). Hence, for Soissons $F_E=1$, for Estica F_E becomes 1.9, and for Baldus $F_E=0.6$.

The superposition shown in Fig. 4.5 indicates that the mechanism of particle size reduction vs. mixing energy is the same for the three varieties.

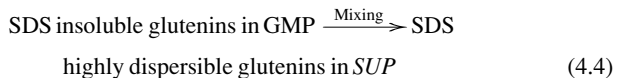


■ FIG. 4.5 Glutenin particle voluminosity vs. energy superposition for particle voluminosity decrease vs. mixing energy in a Farinograph.

The agreement with Eqs. (4.2) and (4.3) confirms that mechanical force is the predominant actuator in GMP breakdown (Hamer et al., 1994) during mixing toward dough peak. It is the initial glutenin particle voluminosity that largely determines the required mixing energy. Also, the phase angle of the GMP-gel from weak flour Estica (+) is higher than that of Baldus (○), indicating that there are internal gel-particle structure differences that affect the disruption pattern. This can be seen in Fig. 4.5 because the (○) symbols of the overstrong flour are slightly above the master-curve fit, and the symbols representing the weak flour (+) are slightly under the master-curve fit. Although only three flour varieties have been used, the fact that the widely differing mixing requirements for dough development could all be fitted with an R^2 of 0.94 gives further support to the idea that the insoluble gel fraction, the internal structure, and size of the glutenin particles in this gel govern wheat flour dough rheological properties.

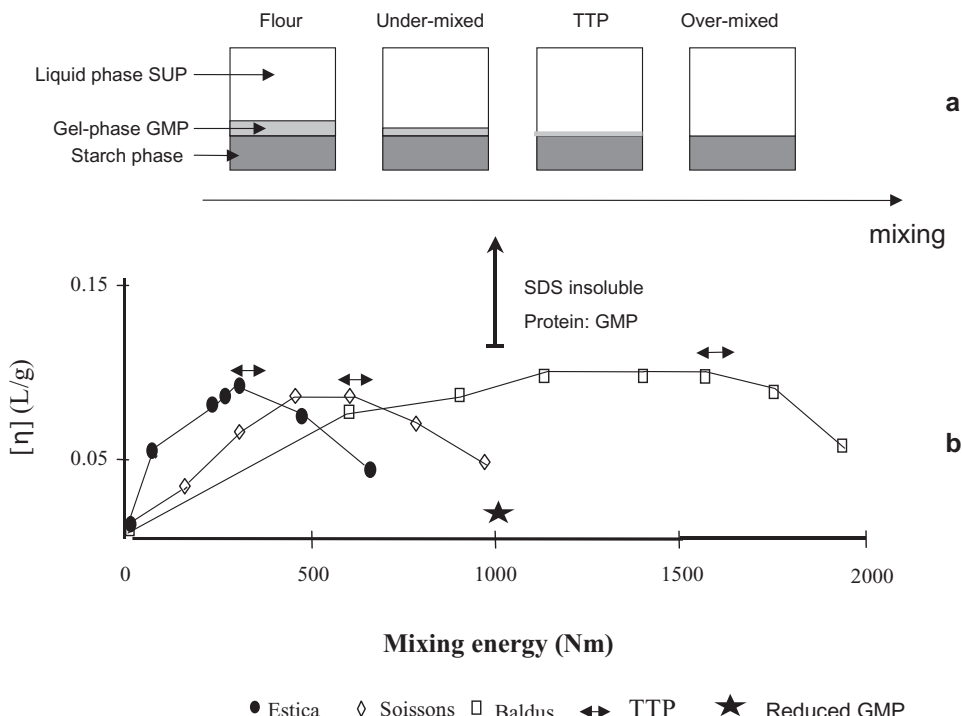
4.3 DEVELOPING DOUGH—THE INTERACTION OF GLUTENIN AGGREGATES

The SDS insoluble glutenin particles are converted to so-called SDS-dispersible glutenin aggregates so that at and past dough peak the glutenin particles have become dispersed in SDS, i.e., disaggregated glutenin-gel particles. Eq. (4.4) schematically describes this process:



The $[\eta]_{\text{gmp}}$ of GMP particles is typically $0.10 < [\eta]_{\text{gmp}} < 0.40 \text{ L/g}$. With mixing, both GMP particle size (measured with Coulter LS 130) and $[\eta]_{\text{gmp}}$ decrease (Don et al., 2003b), rendering the gel-proteins into smaller SDS-dispersible size (Fig. 4.6A). When $[\eta]_{\text{gmp}} < \sim 0.11 \text{ L/g}$, very little GMP ($< 0.1 \text{ g}$) can be isolated from $\sim 20 \text{ g}$ of dough (Don et al., 2003b). Earlier papers have focused on the SDS-insoluble GMP (Don et al., 2003a; Graveland, 1984; Weegels et al., 1996). To better understand the behavior of glutenin particles dissociated into the SDS dispersible and/or soluble phase, the viscosity changes in this phase as a function of mixing have been measured. Fig. 4.6B shows that the average intrinsic viscosity of the SDS soluble protein fraction increases with mixing. This is due to improved dispersibility in SDS of the glutenin particles during mixing and coincides with the mixing-driven decrease of GMP-gel particle voluminosity $[\eta]_{\text{gmp}}$ (Don et al., 2003b).

Fig. 4.6B further illustrates that the intrinsic viscosity of the SDS-soluble part ($[\eta]_{\text{sup}}$) can be followed in the undermixed regime, optimal mixing regime



■ FIG. 4.6 (A) Schematic view of GMP loss vs. mixing (A) and glutenin voluminosity in supernatant phase vs. mixing energy for Estica, Soissons, and Baldus flour (B).

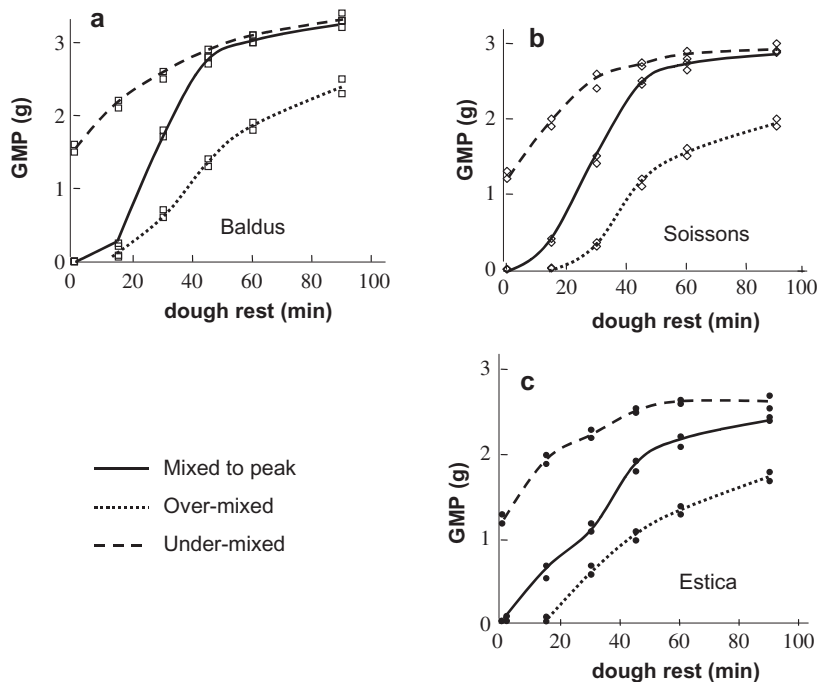
(dough peak), and, more importantly, also for the overmixed regime. These results show that when the glutenin particles have been sufficiently dissociated into SDS highly dispersible glutenin particles, $[\eta]_{\text{sup}}$ is maximal and closely parallels dough peak time (Fig. 4.6B). Thus TTP in the mixer is close to the maximal $[\eta]_{\text{sup}}$ observed for the SDS “solubilized” fractions. When dough is overmixed (i.e., beyond dough peak), a decrease in $[\eta]_{\text{sup}}$ is observed, presumably the result of further disruption of the SDS-dispersible glutenin aggregates into more soluble glutenin polymers. For comparison, the typical minimal intrinsic viscosity measured for dithioreitol-reduced SUP fractions is just ~ 0.02 L/g (indicated by the star in Fig. 4.6B). With undermixing, GMP particles are disrupted to a limited extent. Optimal mixing renders almost all GMP dispersible in SDS, and overmixing disrupts the SDS glutenin aggregates so that the $[\eta]_{\text{sup}}$ approaches the $[\eta]$ of ideally soluble reduced SUP fractions. Water absorption and development time are the two important measurements in a Farinograph. Especially in bread-making, the point where the gluten network is optimally developed with “optimal elasticity” seems crucial to also reach optimal flour functionality in terms of bread loaf volume (Frazier et al., 1975). Since the proposition of the

gel-protein disruption hypothesis (Mecham et al., 1965; Preston and Kilborn, 1984), it is now clear that this is the case. However, what happens to the disrupted glutenin gel-proteins when we stop the mixer? Another known factor is the reaggregation of GMP/glutenin-gel proteins during dough rest, schematically shown in Eq. (4.5).



In a simplified manner, Eq. (4.5) shows the equilibrium between the disruption of glutenin gel-proteins during mixing and the return of the glutenin gel during dough rest, or when the mixer has been stopped. For undermixed, mixed to peak (DDT), and overmixed doughs, the reaggregation of SDS-insoluble glutenin gel proteins is depicted in Fig. 4.7A–C.

For all three varieties from weak to overstrong, glutenin reassembles during dough rest. However, differences exist between varieties and between mixing regimes in terms of the rate of reaggregation and the final quantity of

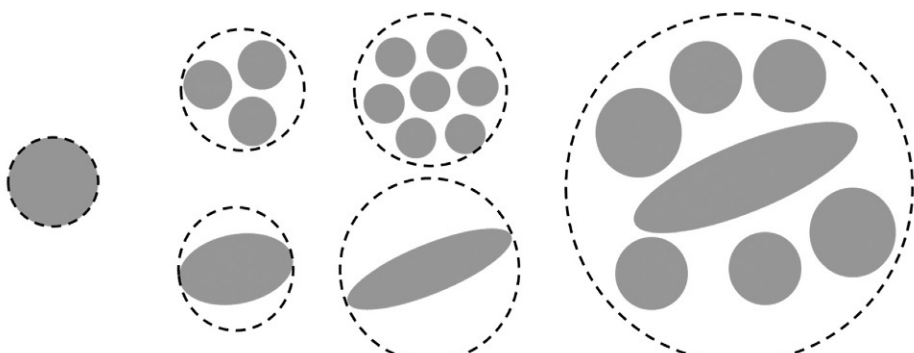


■ FIG. 4.7 (A–C) Recovery of GMP-gel protein vs. rest time for undermixed, optimal mixed, and overmixed dough prepared from Baldus (A), Soisson (B), and Estica (C) flour.

GMP recovered at the end of dough rest. It should also be noted that the shown balance (Eq. 4.5) does not imply that reformed glutenin-gel particles are the same as the original glutenin particles in flour. When mixed to peak, the reassembly of glutenins in SUP into GMP-gel appears to occur the most rapidly. When undermixed, only part of the GMP is rendered soluble: SDS gel-protein glutenins could be recovered 60 min after dough rest. Overmixing leads to a much slower GMP formation: a lag-time of ca. 15 min was observed and the recovery of GMP was not complete after 90 min rest. The balance of GMP recovery, speed of reassembly (Eq. 4.5), and dough resistance are clearly affected by the applied mixing energy (Campos et al., 1997). Conceptually, it can be suggested that glutenin-aggregate morphology in dough should play a role in the structuring properties of the gluten network and the subsequent dough physical properties. Schematically, changes such as increase in the number of glutenin particles with smaller size and the elongation of deformable glutenin gel particles ultimately lead to heterogeneity in sizes and shapes and the effective volume of these systems is sketched in Fig. 4.8.

After dough development, the glutenin gel-proteins have changed and this provokes the thought that the effect of downsizing of gluten particles in flour must somehow have affected the effective volume and interaction properties. Another way to look at glutenin aggregate interaction properties is the so-called Huggins constant (Eq. 4.6):

$$\left[\frac{n_8}{c} \right] = [n] + K_H [n]^2 c \quad (4.6)$$



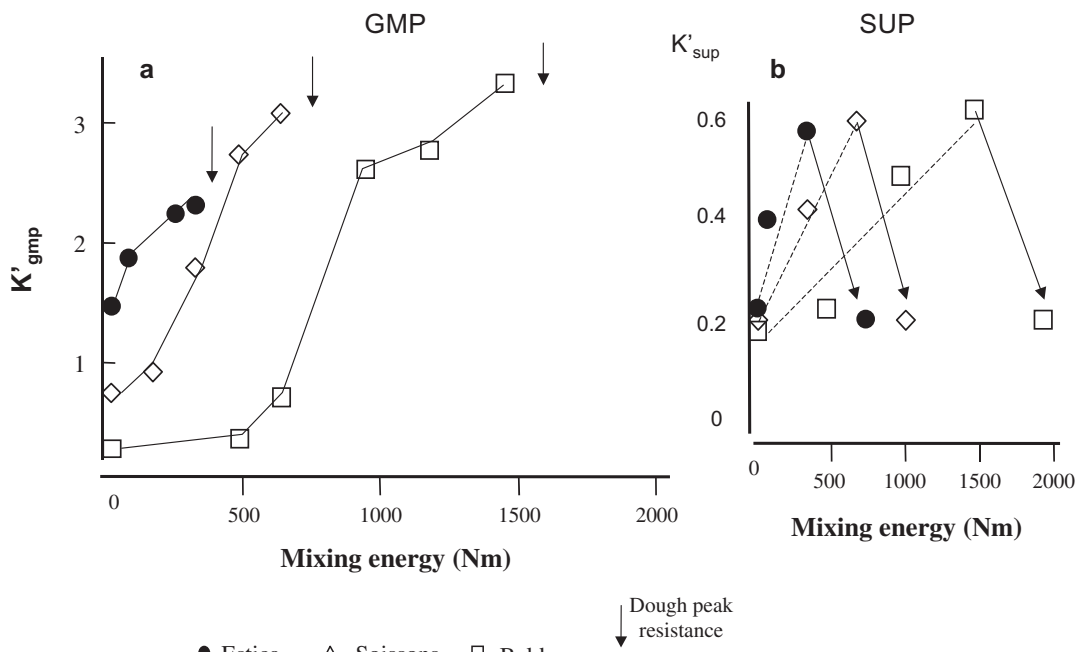
From dense sphere to more small spheres effective volume increases

From sphere to more elongated shapes, effective volume increases

From sphere to more heterogeneity, effective volume increases

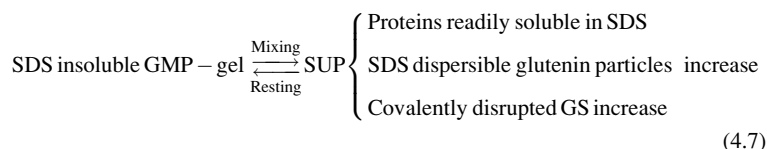
■ FIG. 4.8 Highly schematic: the effect of shapes, size, and heterogeneity of glutenin gel-proteins on effective volume; dotted lines indicate the effective radius.

The Huggins constant (Huggins, 1942), K_H , is an empirical factor that reflects the tendency of the glutenin particles to interact and/or increase effective volume as protein concentration increases. Interestingly, Wang (2003) revealed that K_H of glutenin particles isolated from gluten is strongly correlated with gluten extensibility, also indicating that average glutenin gel aggregate size is more related to dough strength. Extension of dough deals with the interaction property “connectivity” on a longer distance, beyond that of the scale of covalent bonds. Corneç et al. (1994) suggested earlier that connectivity is governed by glutenin interactions. The glutenin-gel protein’s heterogeneity after mixing must therefore be a factor in the subsequent interactions and dough rheological properties. In order to see how mixing affects glutenin particle interactions, the Huggins constant of glutenin particles extracted from the mixed dough samples (freeze dried), the K_{Hgmp} , has been calculated. The effect of mixing on the K_H of both SDS gel-proteins (GMP) and 1.5% SDS-soluble wheat proteins + dispersed glutenin (SUP) is shown in Fig. 4.9.



■ FIG. 4.9 The change in K_H of SDS-insoluble glutenin (left) and SDS-soluble glutenin (right).

The $K_{\text{Hgmp-flour}}$ (particles extracted from flour) is taken to reflect initial GMP particle interactions. The Huggins constant of GMP from dough, $K_{\text{Hgmp-dough}}$, shows a strong increase vs. mixing for all three varieties. Usually, a K_H of ~ 0.3 is reported (Niezette et al., 1984) for flexible polymers in a good solvent. Particle systems that do show interactions have a $K_H > 0.5$. A K_H larger than unity is indicative of strong particle-particle interactions (Russel et al., 1989). Our experiments show that $K_{\text{Hgmp-dough}}$ reaches values greater than unity, indicating that mixing strongly promotes glutenin particle interactions. The increase of $K_{\text{Hgmp-dough}}$ follows Baldus > Soissons > Estica. With resting, glutenin particle aggregates are reassembled from smaller, SDS-soluble glutenin particles or oligomers, that are present in the supernatant (SUP) fraction of the SDS extraction. Eq. (4.7) describes this relation:

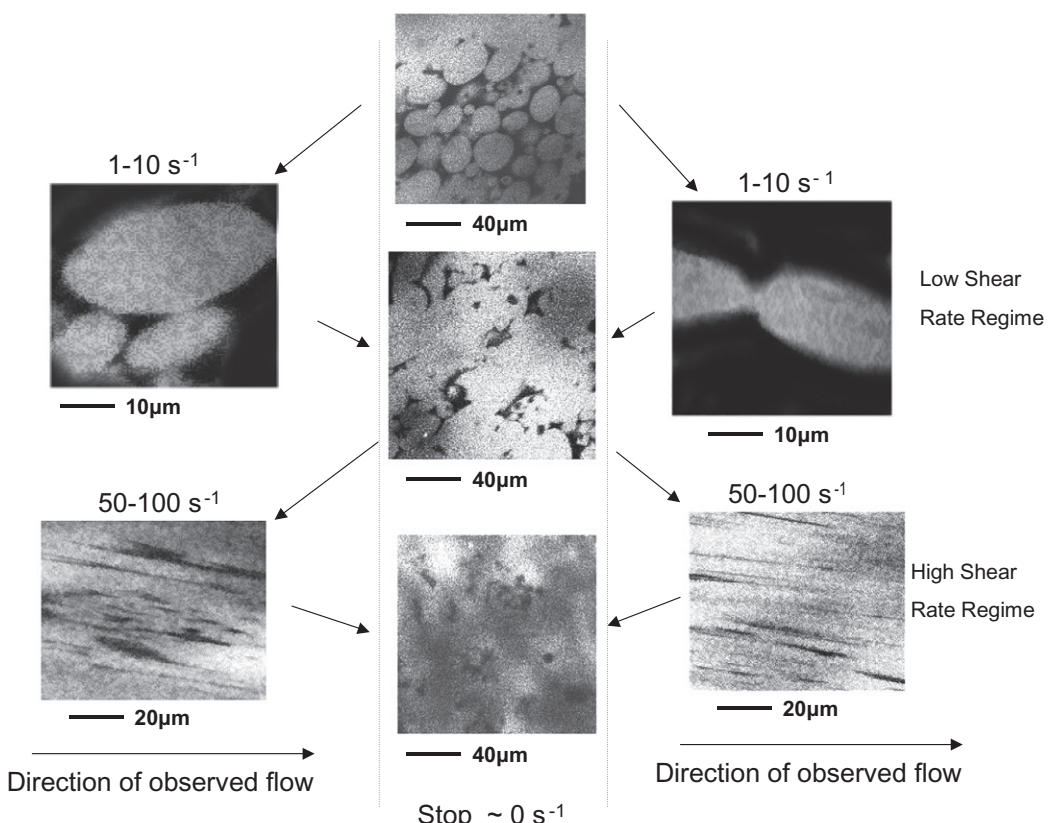


The changes in K_{Hsup} vs. mixing are shown in Fig. 4.9 (right panel). The SUP from flour has a $K_{\text{Hsup-flour}} \sim 0.2$ for all three varieties. The K_H of a DTT reduced SUP fraction (star symbol in Fig. 4.6) also has a K_H of 0.2. Such K_H values indicate behavior like soluble polymers (Niezette et al., 1984). Due to the predominance of readily SDS-soluble proteins in the SUP, the K_{Hsup} vs. mixing is typically lower than the K_{Hgmp} vs. mixing. For all three varieties, the K_{Hsup} showed an increase, from $K_{\text{Hsup}} \sim 0.2$ for flour, to a $K_{\text{Hsup}} \sim 0.6$ at dough peak. This can only result from an increase of extractable glutenin particles. This is followed by a decrease of K_{Hsup} from ~ 0.6 to ~ 0.2 when mixed past dough peak. This is important, since such a decrease indicates a transition from more physical particle-particle interactions to more soluble polymer behavior. In this respect, the increase in K_{Hgmp} during mixing can be explained by a change: first large spherical particles representing the initial status of the GMP fraction (flour), then into smaller irregular aggregates representing the status of the GMP-gel proteins in a mixed and rested situation, as schematically depicted in Fig. 4.8. This does raise the questions: On which scale are the glutenin-gel proteins actually rheologically effective in a dough, and when should we rely on polymer models for explaining wheat flour dough's unique properties? Further investigations have been done to unravel the SDS-insoluble glutenin polymer's deformability, molecular weight, heterogeneity, and shape factors (R_g/R_h) to see how results at this scale could connect with Farinograph mixing rheology.

4.4 DOUGH PHYSICAL PROPERTIES—GLUTENIN POLYMER SIZE OR GLUTENIN AGGREGATES?

In a special measuring cell that has an orifice to film protein aggregates (Nicolas et al., 2003) in motion in a suspension under shear (cone-plate rheometer), more details on glutenin can be observed (Don et al., 2005). The direct view of the glutenin particles in the GMP-gel protein-fraction shows how the glutenin particles behave, clearly showing the gel particles are deformable/stretchable (Fig. 4.10).

Under the initial static condition, the spherical glutenin particles are clearly visible (light areas in Fig. 4.10). In the low shear (10^0 – 10^1 s $^{-1}$) regime, the particles change from spherical to elliptic, and some particle-particle adhesion is observed (right panel in Fig. 4.10). The glutenin-gel particles are clearly deformed. When the shear is changed to zero, the system does not



■ FIG. 4.10 Observing glutenin particles under various flow regimes.

return to its initial state; contours of particles are still visible, but some aggregation has occurred. At a higher shear rate ($\sim 10^2 \text{ s}^{-1}$), deformation is larger, leading to a seemingly stretched and more continuous GMP phase, resembling the findings of Lee et al. (2001) for dough. When the rotating movement is stopped, the system relaxes, no glutenin particles are visible, and a more connected aggregate network has been formed. So far, the observations on glutenin-gel protein morphology, changes during mixing, and glutenin disaggregation and reaggregation are at the mesoscopic level, and only the overmixed doughs show ideally SDS-soluble glutenins that could behave more like a polymer system. This is reflected in the K_{Hsup} showing values < 0.3 , which is consistent with a polymer in good solvent. Viscometry and microscopy have proven to be powerful tools to deepen our understanding of the insoluble gel-proteins. In an experiment using a strong Chinese wheat flour with 11.3% protein (Hebei Jinshahe Flour Industry) taking samples at specific times during Farinograph mixing, light-scattering experiments (Li et al., 2020) have been performed on SDS-soluble, SDS-dispersible, and SDS-gel fractions from mixed dough. In Fig. 4.11, the farinogram shows a reasonably strong Chinese flour.

For some time, further research on wheat flour's unique properties seemed “stagnant” according to MacRitchie (2016). This seemed to have prompted a few new investigations of the role of wheat proteins (Li et al., 2020).

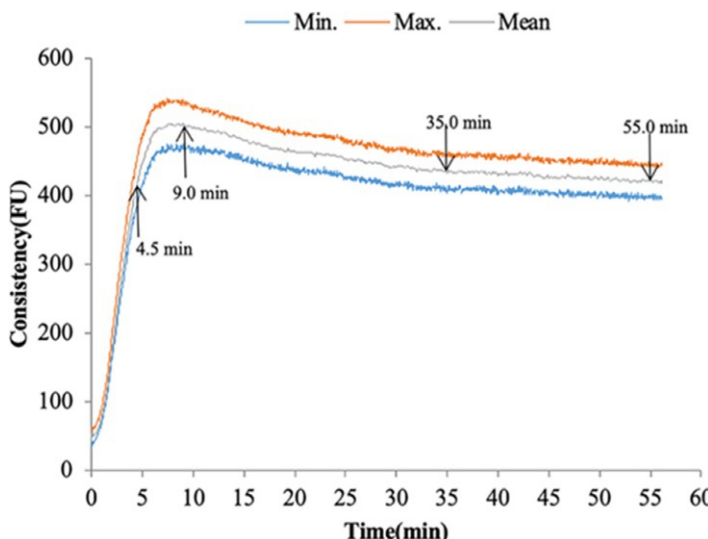


FIG. 4.11 Farinograph curve obtained at 30°C. The upper line (yellow (dark gray in print version)), the lower line (blue (light gray in print version)), and the mean resistance value (gray). Arrows indicate sampling points, 9 min = DDT or peak.

The dynamic wave-scattering results by Li et al. (2020) confirmed the formation of a more continuous gluten network at dough peak, coinciding with a minimum movement space for starch. In their in-depth light-scattering study of fractions (DLS, SLS) and assessment of how SDS-extractable and SDS-unextractable wheat gel-proteins change during Farinograph mixing, the researchers looked to see what the polymeric effect would be of glutenins in the unique dough rheology of wheat flour. The sampling points were taken before, at, and after dough peak resistance. Similar to the methodology used with Soissons flour with 10 min to dough peak (Don et al., 2003a,b, 2005), SDS-dispersible/extractable (SP) and SDS-gel protein (SIP) were prepared from mixed doughs of the Chinese flour (peak at 9 min). Placing the extracts in the instrument for LS/size measurements (static, dynamic, and multiangle) allows for the assessment of: R_h , R_g , polymer M_w , and M_n of both SDS-extractable glutenins and SDS-unextractable glutenin gel-proteins. These more recent methodologies that follow on the studies of gel-protein disaggregation done by Don et al. (2003a,b,c) are quite sophisticated and intricate, and here the main findings are described in a simplified manner.

4.4.1 Observed changes in the SP fraction

As has been discussed and shown in Figs. 4.4 and 4.6, the GMP-gel proteins gradually become SDS-dispersible during mixing. The voluminosity of the SDS-extractable fraction increases, but when overmixed the voluminosity of the gel-proteins decreases, indicating a change from dispersible to ideally soluble glutenin. Fig. 4.12 shows the main results for the changes in the SDS-extractable fraction SP. The M_w , as derived from LS, first increases and then decreases in the far overmixed region of 55 min. This is further from dough peak than the results found for voluminosity $[\eta]$, which seems to reach a maximum closer to the dough peak in the Farinograph. The viscometrically determined voluminosity $[\eta]$ is more affected by glutenin aggregates' effective volume, which could explain the difference between LS and viscometry. The radius of gyration (R_g) of SP increases rapidly toward dough peak, then seems to level out. The polydispersity, reflecting the heterogeneity of the calculated mass distribution, increases rapidly toward the Farinograph dough peak, and after dough peak this also levels out at ~18 min. The mixing effect can be viewed as increasing the heterogeneity of the size distribution, with average R_g of the SP fraction increasing. These are clear indications that the gel-proteins are disaggregated and rendered SDS extractable/dispersible by mixing forces. The pattern of the calculated M_w does not seem to justify the idea of an optimal polymer size, in terms of M_w , that affects the maximal dough consistency at dough peak;

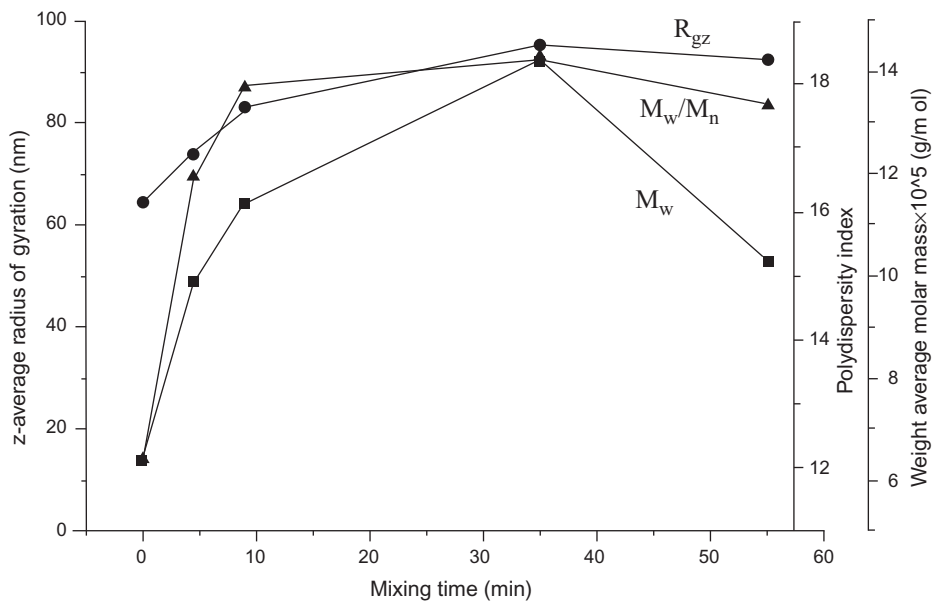


Fig. 4.12 Changes in radius of gyration (R_g), molecular weight (M_w), and polydispersity (M_w/M_n) assessed by LM on SDS-extractable protein versus Farinograph mixing time.

perhaps other factors are at play here. For SP the calculated M_w ranges between 1.0 and 1.4×10^6 g/mol, where HMW-GS are $8\text{--}10 \times 10^4$ g/mol and LMW-GS $3\text{--}5 \times 10^4$ g/mol. The other readily soluble wheat proteins in SP (gliadins, albumins, and globulins) are relatively lower in M_w . The glutenin present in SP is apparently a polydisperse construct of multiple HMW-GS and LMW-GS that pushes the estimated average M_w of the SP extract to higher values during mixing. These glutenin aggregates or disaggregated gel-proteins, dispersible in SDS, can be regarded to be rheologically functional glutenins.

4.4.2 Observed changes in the insoluble glutenin-gel fraction

Fig. 4.13 shows the pattern of the results of LS on SDS-insoluble gel protein (SIP). During mixing, it can be seen that the insoluble gel glutenins are around 10 times larger than the soluble glutenins, but similar to the result in Fig. 4.12, the highest insoluble glutenin M_w is estimated with LS at 35 min of mixing. The R_g of the insoluble glutenin particles is not really affected by mixing, consistent with a more or less constant glutenin concentration in isolatable GMP-gel (Fig. 4.3) versus mixing. However, the M_w of

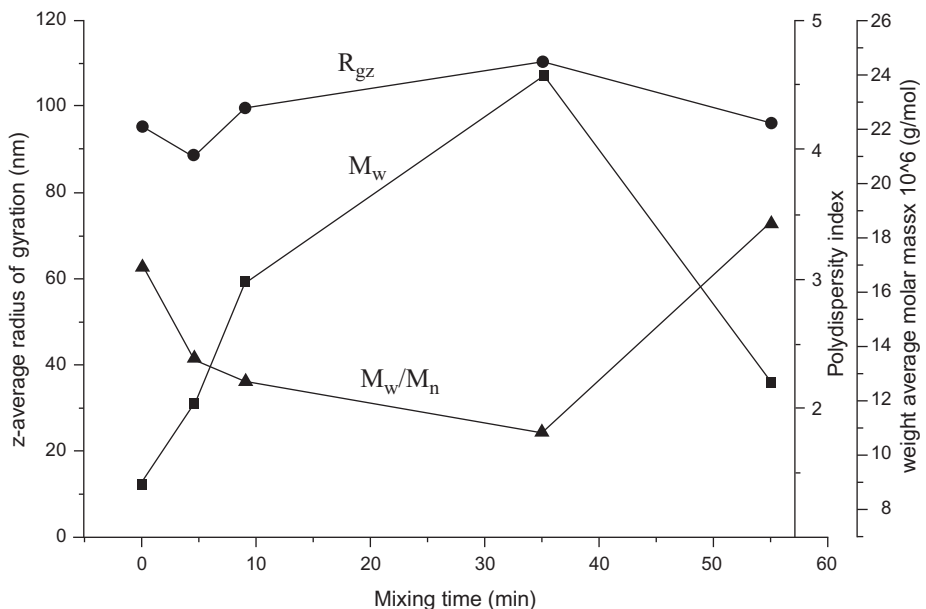


FIG. 4.13 Changes in radius of gyration (R_g), molecular weight (M_w), and polydispersity (M_w/M_n) assessed by LM on SDS-unextractable protein versus Farinograph mixing time.

insoluble glutenin first increases as the dough develops and then decreases after dough peak, indicating that first the smaller glutenin particles in flour become dispersible, while the larger glutenin particles that are disrupted at a later stage stay behind, following the principle of Kick's law (Fig. 4.5). Only after prolonged mixing do the mixing forces disrupt the glutenins to such an extent that M_w goes down. In contrast with the SP glutenins, the polydispersity of the SIP decreases with mixing. This can also be seen as a decrease of size heterogeneity due to further mixing past peak resistance, leaving just a small number of the difficult-to-disrupt glutenin aggregates to centrifuge down. SIP M_w 's of $12\text{--}24 \times 10^6$ g/mol show the highly aggregated state of the insoluble glutenin-gel that is 100–200 times the M_w of a single HMW-GS. This large size and high complexity of glutenin structure constructed of multiple HMW-GS + LMW-GS, moreover with SDS not always being the ideal solvent for glutenin (water as used in the Farinograph is even worse as a solvent!), could challenge the validity of trying to calculate a polymer type of M_w from the LS data on SDS-gel protein and/or SDS-dispersible glutenin aggregates.

4.4.3 Fate of the gel-proteins and functionality in dough

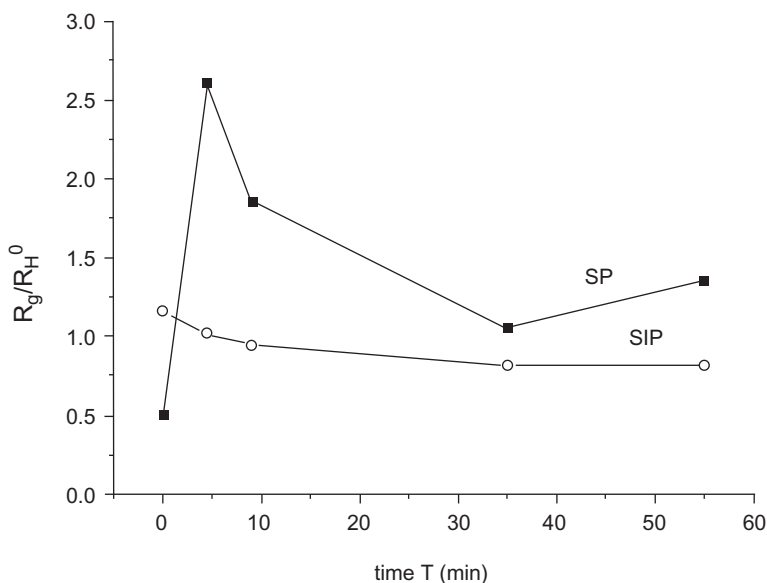
Macro-rheological phenomena as we know from the Farinograph can now be better understood. However, when using the polymeric size data that could be derived from LS techniques, it seems that gluten network consistency, connectivity, and dough peak resistance cannot be assigned to an optimal glutenin polymer molecular weight (Frazier et al., 1975). Actually, the highest glutenin M_w derived from light-scattering data was at 35 min, a moment at which the dough has already weakened/softened. We need to keep in mind that the mixture of SP extracts contains more soluble protein constituents than glutenins/HMW-GS and LMW-GS. Furthermore, Weegels et al. (1997) and Skerrit et al. (1999) indicated that first LMW-GS are released when S–S bonds are cleaved and then HMW-GS are released, indicating that the SDS-soluble HMW-GS polymer backbone could only be present in the extracts of overmixed dough. This can explain the delay of an increasing M_w in the SP extracts, because it could be related to the moment of extended mixing where the largest glutenin particles are covalently disrupted and rendered ideally soluble as dilute polymers in SDS, becoming part of the soluble mixture of albumins, globulins, gliadins, and further disrupted glutenins. A tipping-point where the disrupted glutenin-gel proteins are turned from dispersible in SDS (SP) to ideally soluble polymers in SDS (SP*) is also supported by the K_H results in Fig. 4.9. It could also confirm that the model assumptions for calculating polymeric M_w from protein size data from LS should be viewed very cautiously for the highly complex glutenin fraction before and around Farinograph peak resistance. The notion of a highly complex, covalently stabilized glutenin aggregate being dominant in the macroscopic strength of the gluten network at dough peak does not necessarily conflict with the model for the internal glutenin particle/aggregate structures and the readily soluble/extractable, or perhaps just partially covalently disrupted, glutenins. This allows room for the glutenin polymeric model proposed by Graveland et al. (1985), of a backbone consisting of multiple HMW-GS for the *internal* glutenin particle/“gel-protein” structure. These covalently stabilized macropolymers exist as further non-covalently aggregated larger glutenin structures in the mesoscopic size range in dough. The SP extract also contains the other soluble wheat proteins, so the M_w calculated reflects an average of all these protein constituents, and in view of such protein diversity of the SP fraction, it can still contain glutenin aggregates far beyond the polymeric size assessed by LS, but around 10^{6-7} g/mol for the disaggregated glutenin-gel proteins. Disulfide bond breaking and repolymerizing may therefore not be the dominating mechanism at mixing times until dough peak, or some time past peak

resistance (Goldstein, 1957). The mixing time of 55 min certainly provides the reaction time and energy-input for breaking down the glutenin backbone structure of disulfide-linked HMW-GS that is indeed most detrimental to glutenin functionality in dough, explaining dough weakening when mixing further past dough peak.

4.4.4 The mechanism underlying dough peak resistance in the Farinograph

Pinaud (1987) stated that the rheological properties of polymers depend on their molecular weight. Now that it has been learned that wheat glutenin polymer M_w does not “simply” explain the DDT/peak, what would be the mechanism that underlies the dough peak? The current knowledge supports the idea that dough resistance in the farinogram, the dough peak, is more likely due to physical connectivity between glutenin aggregates, as in a colloidal particle network suggested by Lefebvre and van Vliet (2003). It is also interesting to mention here that in the context of Farinograph mixing, mixing to peak or slightly past it could still bring the dough back to consistency in a so-called “unmixing” experiment, but further beyond the dough peak, recovering dough peak/strength was not possible (Kilborn and Tipples, 1975; Kieffer and Stein, 1999). Physical processes are reversible in nature, whereas chemical processes are irreversible. Therefore when we look at the gluten network’s optimal consistency and connectivity in dough, it is at the optimal balance of disrupting, modifying the glutenin aggregate size, polydispersity/heterogeneity, and shape factors.

We can further derive from the results presented here that glutenins becoming part of the SP fraction can be viewed as rheologically functional disaggregated gel-proteins. The particle size and LS techniques also give insight in the R_g and R_h of a protein particle, where R_g is the radius of gyration and R_h is the hydrodynamic radius. When the R_g/R_h is close to unity, the protein particles are more spherical. In Fig. 4.14 before mixing, a more monodisperse, noninteracting spherical shape of the SP is observed. As mixing proceeds and glutenin-gel turns SDS soluble, we see the SP fraction change to an extended rod shape/cigar shape with $sf = 2.6$ (Niu et al., 2000) at 4.5 min, and then to more monodisperse, elongated ellipsoid shapes close to 2 at 9.0 min. After dough peak, the shape factors go down closer to unity, representing more spherical shapes (Kok and Rudin, 1981) like globular proteins. The glutenin heterogeneity increases toward dough peak as well. As shown in Fig. 4.8, when glutenin aggregates are elongated from a spherical to an extended ellipsoid shape or even cigar shape, the glutenin effective volume increases. When glutenin sizes and shapes become more heterogeneous, the



■ FIG. 4.14 Shape factor of SP and SIP versus Farinograph mixing time.

glutenin effective volume also increases. Furthermore, the viscometry results for the empirical Huggins constant K_H (Fig. 4.9) show a similar pattern to the shape factors of SP in Fig. 4.14. The mixing-induced changes on shape and K_H strongly suggest that the glutenin aggregate heterogeneity and shape are more important in conveying gluten network consistency (dough peak resistance), connectivity (bandwidth), and dough strength, than LS assessed glutenin polymer molecular weight. The SIP fraction shows an R_g/R_h close to unity during mixing, confirming a more spherical glutenin particle shape of undisrupted glutenin-gel particles. For completeness, for the insoluble glutenin-gel it is noticed that K_H also increases versus mixing. This could be due to the viscometric measuring technique where aggregates are perhaps more sheared and easily elongated (Fig. 4.10) than in the assessments based on LS techniques.

In Fig. 4.15A–D, the x -axis shows the increase of dispersible glutenins in SP from dough at the specific mixing times, meaning the rheologically effective disaggregated gel-proteins; the y -axes show macro-rheological changes on the Farinograph and the mesochanges in glutenin increase in the respective SP fractions as SIP-flour → SP dough (Eq. 4.4). The mesoscopic changes in shape and heterogeneity (p) are shown left of the macrochanges in the

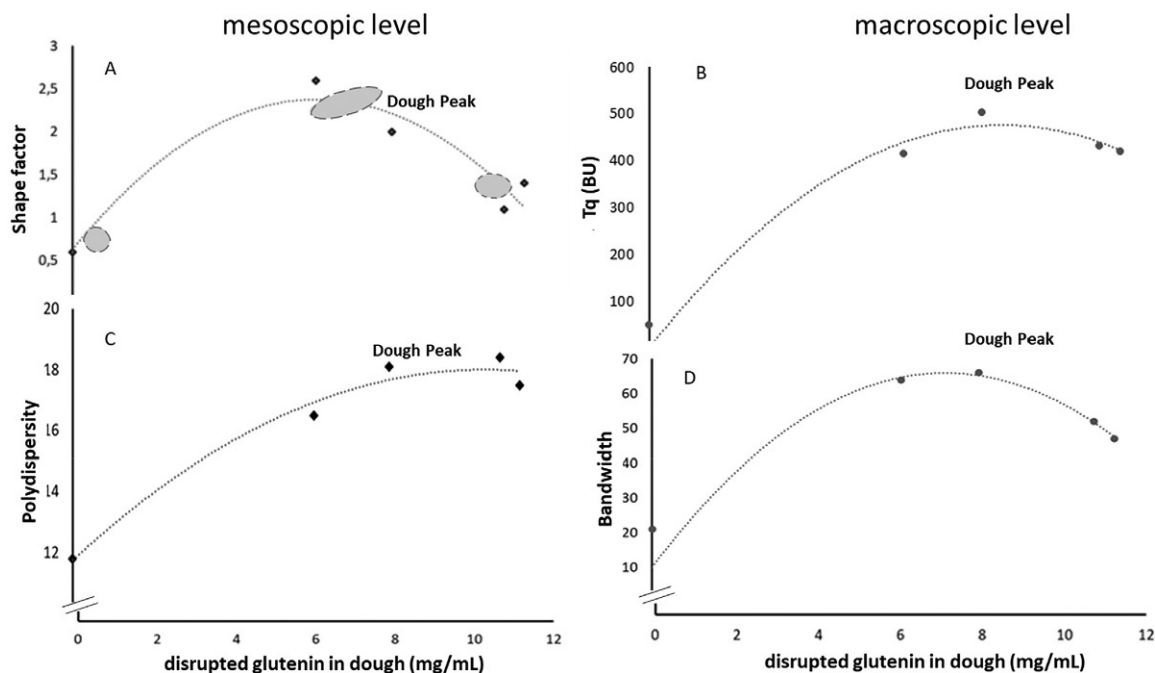


FIG. 4.15 (A–D) Mesoscopic and macroscopic glutenin changes versus solubilized glutenin [$SIP(0) - SIP(t)$] in dough at specific dough mixing times (x-axis). (A) Shape factor change (y-axis) with sketches of suggested and schematic shape changes. (B) Farinograph torque (y-axis) versus solubilized glutenin in dough. (C) Disaggregated glutenin polydispersity/heterogeneity (y-axis) versus solubilized glutenin in dough. (D) Farinograph bandwidth (y-axis) versus solubilized glutenin. Remark: Dotted lines through the datapoints are only to guide the eye to help recognize the pattern of the meso- and macrolevel changes.

dough, dough consistency (BU), and bandwidth (BU). The dough consistency (BU) can be viewed as an apparent bulk viscosity of the dough mass, while the bandwidth indicates how the dough resists the twists and extension movements during Farinograph mixing. The stretched glutenin aggregates are elongated from a spherical to an extended ellipsoid shape or even cigar shape, and the glutenin effective volume increases and aggregate interactions are amplified. This suggests that the glutenin aggregate size heterogeneity and shape are indeed predominant in conveying the unique gluten network rheology readings in the Farinograph: dough peak resistance and connectivity reflected in the bandwidth (at peak).

4.5 CONCLUSIONS

The discussed experiments and papers following on the notion of Preston and Kilborn (third edition) on the importance of insoluble gel-proteins have shown that the physical properties of the initially spherical glutenin

particles present in GMP-gel extracted from flour are changed by mixing to smaller, more irregularly shaped and extended ellipsoid glutenin aggregates. The measurable parameters: size, K_H , radius of gyration, and hydrodynamic radius, p , and shape factors, in combination with observable changes in the glutenin aggregates, helps us understand how dough rheological properties are linked with glutenin-gel properties. In the hyperaggregation model proposed by [Hamer and van Vliet \(2000\)](#) to describe the different scales in the glutenin protein network by aggregation from individual glutenin subunits (nm) to the macroscopic network, three levels of organization are distinguished:

- The molecular level (Level I) where only covalent interactions are encountered, and interactions are between the individual HMW and LMW glutenins, and the covalently disrupted SDS-soluble glutenin polymers (or SP*).
- The mesoscopic level (Level II) where physical aggregation is more important than covalent aggregation. At this level the interactions are between glutenin particles, affecting the glutenin-gel disaggregation, GMP-aggregate shape, and interactions.
- The macroscopic level (Level III) where aggregate formation is influenced by processing conditions. Here the mesoscopic glutenin particles interact in larger network formation, affecting the subsequent macroscopic dough properties.

At Level II, we can safely assume the glutenin network is composed of soft interacting glutenin particles or particle aggregates as in insoluble gel-protein ([Fig. 4.10](#)). These soft particles form a network by interaction with one another and are capable of exhibiting similar rheological behavior in small and large deformation as polymeric networks ([Flickinger et al., 1999](#)). However, this rheological similarity does not prove that the glutenin network of developed dough should be defined as being a polymer system, as past and current evidence points more toward a glutenin aggregate network. Moreover, in contrast with polymer theory, glutenin M_w does not closely reflect the Farinograph mixing rheology. It is more similar to the proposal of [Lefebvre and van Vliet \(2003\)](#), who suggested that a network of soft and deformable colloidal gluten particles determine the macro-rheological properties of dough at Level III of the HA model. By referring to the disaggregation of insoluble gel-proteins in combination with the framework of the hyperaggregation model, it is possible to provide better fitting physical-mechanical explanations for the typical rheological observations in a Farinograph dough curve.

ACKNOWLEDGMENTS

Permission from my coauthors, Robert J. Hamer and Bo Zhang, to reuse parts of our key collaborative papers on insoluble glutenin in this chapter is greatly appreciated.

REFERENCES

- AACC Method 54-21.01/2, n.d. Rheological Behavior of Flour by Farinograph.
- Bekkers, A.C.A.P.A., Lichtendonk, W.J., Graveland, A., Plijter, J.J., 2000. Mixing of wheat flour dough as a function of the physico-chemical properties of the SDS-gel proteins. In: Shewry, P.R., Tatham, A.S. (Eds.), *Wheat Gluten—Proceedings of the 7th International Workshop Gluten 2000*. Royal Society of Chemistry, Cambridge, pp. 408–412.
- Bloksma, A.H., 1972. The relation between the thiol and disulphide contents of dough and its rheological properties. *Cereal Chem.* 49, 104–118.
- Bloksma, A.H., 1975. Thiol and disulfide groups in dough rheology. *Cereal Chem.* 52, 170r–183r.
- Bloksma, A.H., Bushuk, W., 1988. Rheology and chemistry of dough. In: Pomeranz, Y. (Ed.), *Wheat: Chemistry and Technology II*, third ed. AACC, St. Paul, MN, USA, pp. 219–370.
- Bushuk, W., 1998. Interactions in wheat dough. In: Hamer, R.J., Hoseney, R.C. (Eds.), *Interactions: The Keys to Cereal Quality*. AACC, St. Paul, MN, USA, pp. 1–14.
- Campos, D.T., Steffe, J.F., Ng, P.K.W., 1997. Rheological behaviour of undeveloped and developed wheat dough. *Cereal Chem.* 74, 489–494.
- Corne, M., Popineau, Y., Lefebvre, J., 1994. Characterisation of gluten subfractions by SE-HPLC and dynamic rheological analysis in shear. *J. Cereal Sci.* 19, 31.
- Dobraszczyk, B.J., Morgenstern, M.P., 2003. Rheology and the breadmaking process. *J. Cereal Sci.* 38 (3), 229–245.
- Don, C., Lichtendonk, W.J., Plijter, J.J., Hamer, R.J., 2003a. Glutenin macropolymer: a gel formed by particles. *J. Cereal Sci.* 37, 1–7.
- Don, C., Lichtendonk, W.J., Plijter, J.J., Hamer, R.J., 2003b. Understanding the link between GMP and dough: from glutenin particles in flour towards developed dough. *J. Cereal Sci.* 38, 157–165.
- Don, C., Lichtendonk, W., Plijter, J.J., Hamer, R.J., 2003c. Glutenin macropolymer is a gel formed by particles: average particle size determines the gel rigidity. In: Dickinson, E., van Vliet, T. (Eds.), *Food Colloids—Biopolymers and Materials 2002*. Royal Society of Chemistry, Cambridge, pp. 275–281.
- Don, C., Lichtendonk, W.J., Plijter, J.J., Vliet, T.V., Hamer, R.J., 2005. The effect of mixing on glutenin particle properties: aggregation factors that affect gluten function in dough. *J. Cereal Sci.* 41, 69–83.
- Ewart, J.A.D., 1979. Glutenin structure protein complex in wheat flour responsible for dough viscoelasticity. *J. Sci. Food Agric.* 30, 482–492.
- Flickinger, G.L., Dairanieh, I.S., Zukoski, C.F., 1999. The rheology of aqueous polyurethane dispersions. *J. Non-Newtonian Fluid Mech.* 87, 283–305.
- Frazier, P.J., Daniels, W.R., Russel Eggitt, P.W., 1975. Rheology and the continuous breadmaking process. *Cereal Chem.* 52, 106r–130r.

- Goldstein, S., 1957. Sulphydryl und Disulfidgruppen der Klebereiweisse und ihre beziehung zur Backfahigkeit der Brotmehle. *Mitt. Gebiete Lebensm. Hyg.* 48, 87–93.
- Graveland, A., 1984. In: Graveland, A., Moonen, J.H.E. (Eds.), *Proceedings of the 2nd International Workshop on Gluten Proteins*. Pudoc, Wageningen, pp. 59–67.
- Graveland, A., Bosveld, P., Lichtendonk, W.J., Moonen, J.H.E., 1982. Extraction and fractionation of wheat flour proteins. *J. Sci. Food Agric.* 33, 1117–1128.
- Graveland, A., et al., 1985. A model for the molecular structure of the glutenins from wheat flour. *J. Cereal Sci.* 3, 1–16.
- Hamer, R.J., van Vliet, T., 2000. Understanding the structure and properties of gluten: An overview. In: Shewry, P.R., Tatham, A.S. (Eds.), *Wheat Gluten—Proceedings of the 7th International Workshop Gluten 2000*. Royal Society of Chemistry, Cambridge, pp. 125–131.
- Hamer, R.J., Weegels, P.L., Orsel, R., 1994. The polymerisation of glutenin in relation to end-use quality. In: *Proceedings of the International Meeting—Wheat Kernel Proteins: Molecular and Functional Aspects*, Viterbo, pp. 139–144.
- Huggins, M., 1942. The viscosity of long chain molecules. IV dependence on concentration. *J. Am. Chem. Soc.* 64, 2716–2718.
- ICC Standard Methods, 1992. *Standard Methods of the ICC (International Association for Cereal Science and Technology)*. Schäfer, Detmold, Germany.
- Kelfkens, M., Lichtendonk, W.J., 2000. Verbesserungen in der Beurteilung der Backfahigkeit von Weizensorten. *Getreide Mehl Brot* 54, 363–365.
- Kieffer, R., Stein, N., 1999. Demixing in wheat doughs—its influence on dough and gluten rheology. *Cereal Chem.* 76 (5), 688–693.
- Kilborn, R.H., Tipples, K.H., 1975. Unmixing—the disorientation of developed bread doughs by slow speed mixing. *Cereal Chem.* 52, 248–262.
- Kok, C.M., Rudin, A., 1981. Relationship between the hydrodynamic radius and the radius of gyration of a polymer in solution. *Macromol. Rapid Commun.* 2, 655–659.
- Lafiandra, D., MacRitchie, F., 1997. Structure function relationships of wheat proteins. In: Damodaran, S., Paraf, A. (Eds.), *Food Proteins and Their Applications*. Marcel Dekker, New York, USA, pp. 293–324.
- Lászity, R., 1996. *The Chemistry of Cereal Proteins*, second ed. CRC Press, Boca Raton, FL, USA, pp. 78–79.
- Lee, L., Ng, P.K.W., Whallon, J.H., Steffe, J.F., 2001. Relationship between rheological properties and microstructural characteristics of non-developed, partially developed and developed doughs. *Cereal Chem.* 78, 447–452.
- Lefebvre, J., van Vliet, T., 2003. Physico-chemical aspects of gluten proteins. In: Albersberg, W.Y., Hamer, R.J., Jasperse, P., de Jongh, H.H.J., de Kruijf, C.G., Walstra, P., de Wolf, F.A. (Eds.), *Industrial Proteins in Perspective. Progress in Biotechnology*, vol. 23. Elsevier, Amsterdam, pp. 94–102.
- Li, F., Zhang, Y., Guo, B., Wei, Y., Don, C., Pan, W., Zhang, B., 2020. The mesoscopic structure in wheat flour dough development. *J. Cereal Sci.* 95.
- MacRitchie, F., 1980. Studies of gluten protein from wheat flours. *Cereal Foods World* 25, 382–385.
- MacRitchie, F., 2016. Seventy years of research into breadmaking quality. *J. Cereal Sci.* 70, 123–131.
- Mecham, D.K., Cole, E.G., Pence, J.W., 1965. Dough-mixing properties of crude and purified glutenins. *Cereal Chem.* 42, 409–420.

- Nicolas, Y., Paques, M., Van den Ende, D., Dhont, J.K.G., Van Polanen, R.C., Knaebel, A., Steyer, A., Munch, J.P., Blijdestein, T.B.J., Van Aken, G.A., 2003. Monitoring the structure of flocculated emulsions under shear by DWS and CSLM. *Food Hydrocoll.* 17, 907–913.
- Niezette, J., Vanderschueren, J., Aras, L., 1984. Dilute solution behaviour of n-butyl methacrylate ionomers. *J. Polym. Sci. Polym. Phys. Ed.* 22, 1845–1848.
- Niu, A., Liaw, D.-J., Sang, H.-C., Wu, C., 2000. Light-scattering study of a zwitterionic polycarboxybetaine in aqueous solution. *Macromolecules* 33, 3492–3494.
- Perry, R.H. (Ed.), 1997. *Chemical Engineers' Handbook*, seventh ed. McGraw-Hill.
- Pinaud, F., 1987. Effect of molecular parameters on the viscoelastic properties of polymer melts. *J. Non-Newtonian Fluid Mech.* 23, 137–149.
- Preston, K.R., Kilborn, R.H., 1984. Dough rheology and the farinograph. In: D'Appolonia, B.L., Kunerth, W.H. (Eds.), *The Farinograph Handbook*, third ed. American Association of Cereal Chemists, St. Paul, MN, pp. 38–42.
- Pritchard, P.E., 1993. The glutenin fraction (gel-protein) of wheat protein—a new tool in the prediction of baking quality. *Asp. Appl. Biol.* 36, 75–84.
- Russel, W.B., Saville, S.A., Schowalter, W.R., 1989. *Colloidal Dispersions*. Cambridge University, Cambridge.
- Schofield, J.D., 1994. In: Bushuk, W., Rasper, V.F. (Eds.), *Wheat Production, Properties and Quality*, first ed. Blackie Academic and Professional, Glasgow, UK, pp. 73–99.
- Skerrit, J.H., Hac, L., Bekes, F., 1999. Depolymerization of the glutenin macropolymer during dough mixing: I. Changes in levels, molecular weight distribution, and overall composition. *Cereal Chem.* 76, 395–401.
- Wang, M.-W., 2003. *Effect of Pentosans on Gluten Formation and Properties (Thesis)*. Wageningen University, The Netherlands.
- Weegels, P.L., Van de Pijpekamp, A.M., Graveland, A., Hamer, R.J., Schofield, J.D., 1996. Depolymerisation and repolymerisation of wheat gluten during dough processing I. Relationships between GMP content and quality parameters. *J. Cereal Sci.* 23, 103–111.
- Weegels, P.L., Hamer, R.J., Schofield, J.D., 1997. Depolymerisation and re-polymerisation of wheat glutenin during dough processing. II. Changes in composition. *J. Cereal Sci.* 25, 155–163.
- Wrigley, C.W., 2009. *Wheat: Chemistry and Technology*, fourth ed. AACC, pp. 1–17.

Section

B

Applications

This page intentionally left blank

The Farinograph as a tool for wheat-milling operations: Current and potential uses

Curtis Bartell, Angie Anyieni, and Gang Guo
Ardent Mills, Denver, CO, United States

CHAPTER OUTLINE

5.1. Introduction	73
5.1.1. Using the Farinograph to optimize mill input	74
5.1.2. Using the Farinograph to optimize in-process stream selection	76
5.1.3. Using the Farinograph to optimize final product flour blends	77
5.2. Limitations of Farinograph testing in wheat milling operations	79
5.3. Summary	80

5.1 INTRODUCTION

The Farinograph can be used as a planning tool in wheat-milling operations (Fig. 5.1). This includes pre-, during, and postmilling decisions. The main use of the Farinograph is on the final milled flour as a predictor of functionality of that flour in different baking/cooking applications.

- A. Premilling: Used to help screen the grain materials and make the right wheat blend/mix for finished final flour product with targeted specifications and functionalities.
- B. During milling: Used to select the proper mill streams needed to produce the targeted final flour product with required farinogram specifications.
- C. Postmilling: Used to choose suitable flour products and properly blend them together to meet the quality specifications and/or application functionalities.



Within the milling industry, the Farinograph is one of the most widespread quality testing tools for analyzing flour dough rheology characteristics during mixing. Flour water absorption, dough development time, stability time, tolerance to overmixing, and overall dough strength are measured. The farinogram parameters generated are useful and practical predictors of wheat flour bake performance short of actual baking. As such, most bakeries and flour mill customers have farinogram specifications that they expect to be met.

On the wheat grain side, there are many varieties commercially available within each of the US six classes of wheat. Due to Mother Nature, each year can produce different quality crops. In order to produce quality and consistent flour products, blending and mixing different sources of wheat is a common industry practice.

Farinograph testing before, during, and after the milling process can serve as a guide to better achieve final flour product quality and consistency targets. Farinogram data can also be used to increase mill efficiency and efficacy.

5.1.1 Using the Farinograph to optimize mill input

Target Farinograph performance parameters can be controlled at various points before, during, and after the milling process, with differing impacts on cost and operational efficiency. The broadest adjustments would most easily be made when sourcing incoming material that would be blended to the desired targets ([Table 5.1](#)).

Table 5.1 Farinograph data for blends of two wheats.^a

Blend	Flour protein (%)	Water absorption (%)	Dough stability (min)
100% A	12.8	62.7	13.0
100% B	10.7	57.4	10.7
10% A/90% B	11.2	59.2	9.73
20% A/80% B	11.3	60.3	12.1
80% A/20% B	12.5	62.8	12.3
90% A/10% B	12.5	63.6	13.4

^aAll data on 14% moisture basis.

The closer incoming wheat is to the target flour specifications, the fewer adjustments need to be made during and after milling. The Farinograph can be used as an aid in initial wheat selection, as well as during wheat blending. Targeting flour absorption and dough mixing stability characteristics during wheat blending can minimize the need to cut valuable quality mill streams and avoid milling extraction losses. Experimentally milling and testing incoming wheat allows the consistency of incoming material to be monitored over time. This is important, as wheat from the same origin will change as the crop changes or ages. This is especially noticeable at the end of the crop year due to aging, when stabilities are generally higher. All this data is extremely valuable for making binning and blending decisions, which will minimize the need to make yield-reducing downstream process adjustments to meet target final product functionality requirements.

One important perspective is the farinogram difference between experimentally milled flour and commercial product. This includes two major aspects. (1) Experimental mill-refined flour is straight grade, while the commercial refined flour can be either straight grade or patent flour. Commercial milling is much more efficient than experimental milling. For an apples-to-apples comparison, either the flour extraction rate or flour product ash content needs to be fixed (i.e., kept constant). In this case, the commercial refined flour has longer farinogram dough stability time and similar or slightly lower water absorption than the experimentally milled flour from the same wheat source. (2) For most cases, the commercial refined flour product is milled from a blend of different wheat sources, while each of those wheat elements is milled separately in the lab. Therefore the practical application or solution is to build the relationship pattern under your own set-up for predicting commercial flour product farinograms from the experimental milling product data. For whole wheat flour milling, both experimental and commercial products are very comparable if their mean particle size values are similar.

Another key point is the new crop wheat transition. The best practice is to gradually increase the new crop wheat inclusion into targeted wheat blends or mixes. Under the same principles, the Farinograph is used as one of the essential tools to help with the new crop wheat transition process, especially for hard wheat products.

5.1.2 Using the Farinograph to optimize in-process stream selection

During the milling process, Farinograph testing is an invaluable tool for monitoring mill efficiency and troubleshooting potential quality issues.

One of the highest impact areas where the Farinograph can add value is in the mill stream analysis for mill optimization and stream selection. Comparing the rheological characteristics of a mill's straight grade and patent flours to those of the various clear flour streams can guide a miller on which cuts will maximize the quality and functionality of the final finished flour product while minimizing the percentage of valuable streams going into clear flour product.

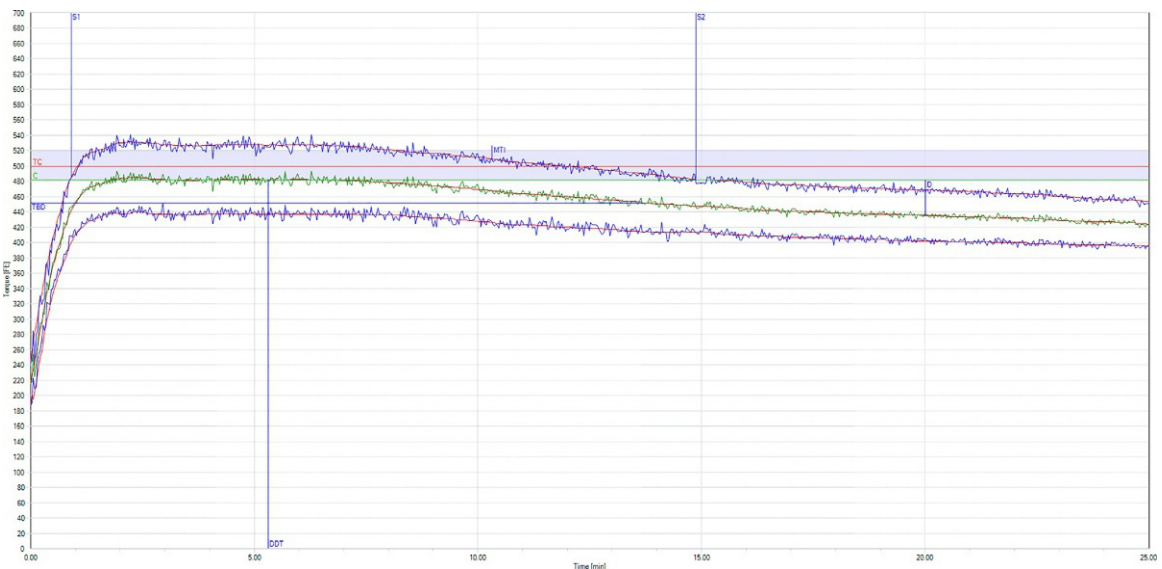
While it may be tempting to simply blend streams for dough stability or flour water absorption based on target ash content and calculation, it is advisable to actually test the samples. Any expected farinogram performance values obtained through linear calculation will likely deviate significantly from the actual results in unpredictable ways. Consider Table 5.2, giving an example of trying to "blend" a patent flour with its corresponding clears to make straight grade (Figs. 5.2 and 5.3).

The calculated stabilities are much higher than the tested value. In general, lower farinogram dough stability streams will have a disproportionately

Table 5.2 Commercial data for straight grade, patent, and clear flour products.^a

	Flour ash (%)	Flour protein (%)	% of straight grade	Water absorption (%)	Dough stability (min)
Patent	0.468	11.3	87.8	60.2	17.6
Clears	1.160	13.3	12.2	66.6	4.9
Calculated straight grade	0.552	11.5	100.0	61.0	16.1
Actual straight grade	0.552	11.5	100.0	60.2	14.0
Actual vs. calculated difference				-0.8	-2.1

^aAll data on 14% moisture basis.



■ FIG. 5.1 Straight grade flour farinogram.

high impact on the final blend's dough stability. Likewise, the calculated absorption is significantly lower than the actual.

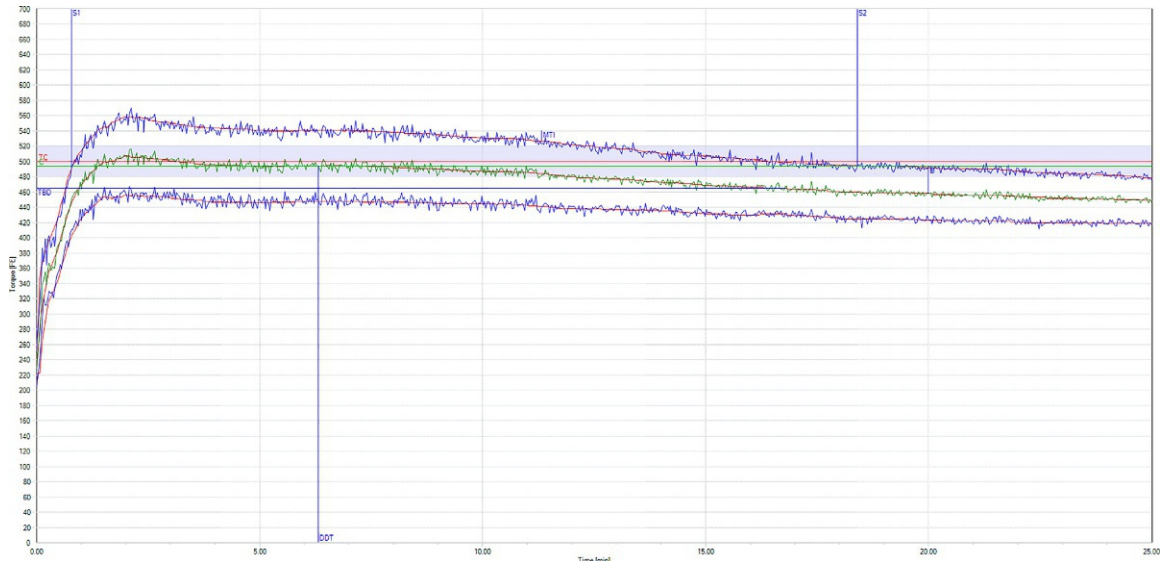
Utilizing the Farinograph in this way, with data from individual streams, works well to raise the dough stability of final patent flour product with minimal loss of flour yield. However, if there is a need to lower stability, it is more cost effective to adjust the starting wheat blend, rather than cutting valuable streams to clear and lowering flour yield.

5.1.3 Using the Farinograph to optimize final product flour blends

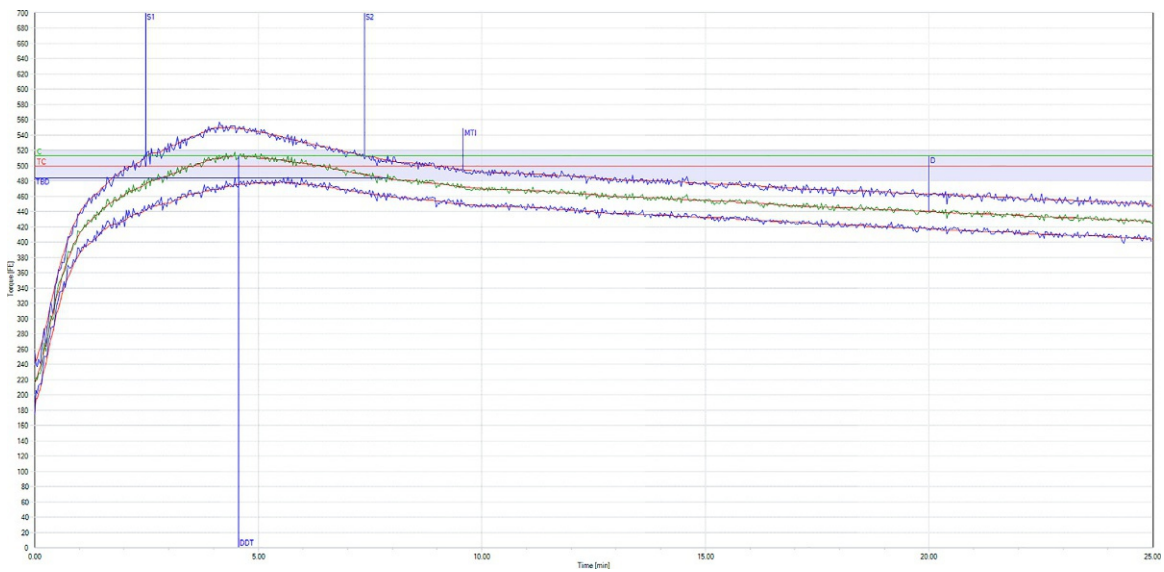
In instances where final flour blending to target and/or reworking is necessary, the Farinograph is a very useful tool for determining correct flour-blend ratios on a small scale before large-scale blending is conducted. However, as with wheat blending, performance does not trend linearly with blend proportions. This can be seen in [Tables 5.3 and 5.4](#). Here, Farinograph data for flour blends of a medium dough-strength flour with a high dough-strength flour can be seen, alongside the expected results.

It can be seen from the data that the farinogram characteristics of the blends vary significantly from what would be expected based on the component flours. This is specifically evident in dough stability.

78 CHAPTER 5 The Farinograph as a tool for wheat-milling operations



■ FIG. 5.2 Patent flour farinogram.



■ FIG. 5.3 Clear flour farinogram.

Table 5.3 Farinogram data of commercial flour products.^a

Sample	Water absorption (%)	Dough stability (min)
100% Medium	59.3	10.4
100% Strong	57.9	51.1

^aAll data on 14% moisture basis.**Table 5.4** Farinogram data of commercial flour blends.^a

Sample	Calculated absorption (%)	Calculated stability (min)	Actual absorption (%)	Actual stability (min)	Absorption difference (%)	Stability difference (min)
90% Medium/ 10% Strong	59.2	14.4	59.1	11.5	-0.1	-2.9
80% Medium/ 20% Strong	59.0	18.5	59.4	12.4	0.4	-6.1
70% Medium/ 30% Strong	58.9	22.5	59.2	15.9	0.3	-6.7

^aAll data on 14% moisture basis.

5.2 LIMITATIONS OF FARINOGRAPH TESTING IN WHEAT MILLING OPERATIONS

Variability in Farinograph test results arises from several sources. It's important to be aware of its impacts on the data interpretation and decision making.

First, the Farinograph mixing bowl is relatively delicate and prone to wear. Over time, this can lead to a drift in results that is not due to changes in actual sample functionality.

The variable nature of wheat itself is another contributor to inconsistent farinogram data. As an agricultural product, the functional characteristics of wheat can vary from origin to origin and crop year to crop year. This, in turn, will show up in Farinograph analysis.

Another source of variability from test to test on a single sample is how the sample is stored. As the sample is aged, flour dough stability can change. If the sample is improperly sealed, the moisture content can change, which will affect water absorption readings.



■ FIG. 5.4 Stream pipes at a commercial flour mill.

However, if the inherent variability of the Farinograph is taken into account, it is a useful tool that aids in decision making throughout the milling process (Fig. 5.4).

5.3 SUMMARY

Within the flour-milling industry, the Farinograph is most widely used in final product quality testing to measure flour quality against customer specifications and predict baking performance. Different attributes can be more or less important, depending on the final product applications. For example, farinogram flour water absorption data can be useful when evaluating cookie and cake flours while the dough stability is of less concern. Both flour water absorption and dough stability are important for bread flours.

Trending this data over time is a valuable aid to monitoring overall mill performance. While testing individual streams is only done once or twice a year, final product testing is done daily. Watching this data allows shifts in mill performance to be caught much sooner than would otherwise be possible.

Overall, the Farinograph has been an essential tool for the wheat flour milling industry since its invention and through each step of operations. Like many other rheology analyses, the challenge of the Farinograph test accuracy and/or precision does exist. Hopefully, with the advancements in technology, we expect forthcoming improvements in the near future.

Using the Farinograph in daily bakery operations

Stanley P. Cauvain

BakeTran, Witney, United Kingdom

CHAPTER OUTLINE

6.1 Key elements of bread production	81
6.2 Dough consistency in bakery practice	82
6.3 Water absorption and recipe water level	83
6.4 Water absorption, recipe water level, and dough processing	84
6.5 Dough development and commercial dough mixing	85
6.6 Dough temperature	87
6.7 Alternate commercial uses for the Farinograph	87
6.8 Conclusion	88
References	89

6.1 KEY ELEMENTS OF BREAD PRODUCTION

To appreciate the practical value of Farinograph data, it is appropriate to first consider a few key elements of bread dough preparation and processing. A critical factor is the development of a gluten network in the dough with the appropriate rheological properties for the product and processing set-up being employed (Cauvain, 2015). In the gluten development process, both gluten-forming proteins and water for their hydration are required. However, it is only when energy is transferred by mixing that the level of gluten development becomes significant. It is the development of the gluten network on which bread quality is built (Cauvain, 2018a). When a fermented dough leaves the mixer (or reaches the end of its bulk fermentation period), the bulk dough is subdivided into unit pieces for subsequent processing. The shape of the individual dough units will be changed and the reaction of the dough to the forces of deformation depend on its rheological character. Key among the rheological characters are what bakers refer to as “consistency”

and “development.” Neither term is well defined but they are related to the ability of the baker to process the dough and achieve the final bread quality sought. While poorly defined, most bakers have an appreciation of the dough qualities required and seek to have the same properties in every dough that they make.

6.2 DOUGH CONSISTENCY IN BAKERY PRACTICE

The evaluation of dough consistency in bakery practice is dominated by the ability to process a given dough product and recipe with minimal effort under a given set of processing conditions. Industrial, mostly automated, breadmaking plants are inevitably more sensitive to changes in dough consistency than smaller-scale bread production units, where the manipulation of dough by hand is carried out, not least because the pressures applied during molding can be readily adjusted; the same is not currently true for machine molding. Despite such differences, all scales of bakery operation aim to make as few changes to daily production as possible and the delivery of wheat flour of a constant quality is considered very important in achieving this aim. In recognition that the quality of wheat flours is unlikely to remain unvarying, the provision of analytical data that can be used to “adjust” dough recipes or processing, or both, is key to the delivery of consistent bread quality.

As noted previously, dough consistency and development are two poorly defined terms that bakers use to describe the rheological properties of dough. Despite the development of analytical methods for the evaluation of dough rheological properties, sensory assessment remains the most commonly practiced method of evaluation of dough consistency in working bakeries. The common sensory method comprises manipulating the dough in the hands, usually combined with various acts of stretching the dough with the fingers. In doing so, bakers are trying to assess the ability of the dough to process through their plant and to “predict” the final bread quality. With both evaluations, experience plays a major role in the strength of their assessment.

The consistency of a given dough is linked with the degree of development, and vice versa, making both the assessment and the prediction complex. [Cauvain \(2015\)](#) considered that four physical properties of dough are key: resistance to deformation, extensibility, elasticity, and stickiness. In a recent unpublished study ([Cato and Cauvain, *pers comm*](#)), it was shown that bakers linked their assessment of dough softness (as an indicator of consistency) and stickiness (as an indicator of suitability for processing) and that the common reaction to doughs that would be considered too soft or

sticky is the reduction of recipe water levels. In the context of this handbook, such studies and other commercial observations bring into sharp focus the value of being able to anticipate and react to variations in flour quality on the basis of suitable analytical data.

6.3 WATER ABSORPTION AND RECIPE WATER LEVEL

The optimization of recipe water levels is a key element in the delivery of a constant dough for processing and for delivering the final quality of bread and other fermented products. The Farinograph provides a means for bakers to assess whether there are variations in the water absorption capacity of the flours entering their processes. As is well known, the water absorption capacity of flours can vary according to differences in flour protein content, level of starch damage, level of pentosans, and moisture content (Cauvain, 2018b). The presence of bran in nonwhite flours has a dramatic effect on the water absorption capacity of a flour, which increases as the level of bran present increases. A key processing requirement for fermented doughs is that they should have a consistency that allows them to be processed following division of the bulk dough into unit pieces through to the moment of entering the prover with no difficulty. In this context, a knowledge of the water absorption capacity of the flour provides valuable insights for practical bakers.

Examination of the water absorption capacity of a flour from the datasheet that may accompany the flour delivery does not in itself tell bakers what the recipe water level should be in their bakery. This is because many product, recipe, and process factors will determine the required consistency of the dough, other than the water absorption capacity of the flour. Thus the value of the water absorption capacity information is that it can alert bakers to the need for potential changes in recipe water level in breadmaking. However, in order to be able to make effective use of such information, bakers must first establish their relationship between the measured Farinograph water absorption capacity of a given flour and the recipe water levels that they will use in practice. Such a relationship can readily be determined by simply checking the analytical data from different batches of flour as they are received and comparing that information with the actual recipe water levels used in production. For example, a simple relationship could be: Farinograph water absorption plus 3% (based on flour weight). Thus if the Farinograph water absorption capacity was 58% (flour weight), the recipe water level would be 61%, and if the Farinograph value fell by 1% to 57%, then the recipe water level would be 60% (flour weight). It is therefore relatively easy to establish a *recipe water absorption factor* that will enable practical

adjustment of recipe water levels to take into account the variations in the water holding capacity of wheat flours.

Product recipe and dough-processing factors will significantly impact on the relationship between the measured Farinograph water absorption capacity of wheat flour and the actual level of recipe water used; process factors are further considered in the following text. Many commonly used ingredients have significant impacts on the *recipe water absorption factor*; they include:

- Salt—in general, lower salt levels lead to lower recipe water levels, though the level of impact of salt is related to choices of breadmaking method and dough processing arrangements. The impact of salt on dough rheology is related to its effect on the partitioning of water between those components in the dough that will absorb water or bond with water. Readers are referred elsewhere for a more detailed discussion on the impacts of salt on breadmaking (e.g., Cauvain, 2007, 2015).
- Sugar—as the level of recipe sugar increases, the level of recipe water required to deliver a standard dough consistency falls. The impact of sugar on water partitioning in the dough is less than that of salt when considered on a weight-for-weight basis, but the level of recipe sugars in some products and in some parts of the world can be significant (e.g., up to 20% in Southeast Asia).
- Milk solids—recipe water levels commonly need to increase when dried milk solids are present.
- Soya and other nonwheat flours—the inclusion of such materials usually requires an increase in recipe water levels.
- Gums—the addition of low levels of gums can significantly increase recipe water levels.
- Fibers—the addition of fibers can significantly increase water levels. However, because the absorption of water by fibers can be slow, the true impact of fiber addition may not be observed until after mixing (see following).
- Nonwheat grains and seeds—while such ingredients will absorb water, their effect may not be observed by the end of the mixing process.

6.4 WATER ABSORPTION, RECIPE WATER LEVEL, AND DOUGH PROCESSING

There are many recipe and process factors that determine the recipe water level used in a given bakery and thus that determine the relationship with the measured Farinograph water absorption capacity of wheat flours. The potential impacts of ingredients on the *recipe water absorption factor* have been

discussed earlier, but among the many other influences are the type of product being manufactured, the breadmaking process employed, and the means by which the bulk dough is processed into unit pieces ready for proving and baking. Some of the key factors include:

- Product type—pan breads and other fermented products baked in molds will commonly have higher recipe water levels than hearth or free-standing breads.
- Choice of breadmaking method—no-time dough production methods usually have higher water levels than those employing fermentation because there is less dough softening.
- Mixing conditions—the mixing conditions used with different dough-making methods deliver differing degrees of dough development that affect dough consistency. In the Chorleywood Bread Process (CBP) the application of partial vacuum during mixing significantly increases water level addition ([Cauvain and Young, 2006](#)).
- Dough temperature—lowering the final dough temperature yields a firmer dough, which may permit the addition of more recipe water (though potentially this has negative effects on final bread quality).
- Dough-processing equipment and methods—different dough-processing equipment and operations will affect the optimum recipe water level.

In some cases, the standard Farinograph method may be adapted to deliver water absorption values closer to those used in commercial practice. For example, in the United Kingdom the practice has been to determine the water level required to reach the 600BU line rather than the standard 500. This alternative method reflects the large-scale use of the CBP, which typically delivers higher energy inputs during dough mixing, which was the key driver to seeking a change to the standard flour-quality assessment method. There can often be sound commercial reasons for employing “nonstandard” options with the Farinograph, especially where the control of recipe water levels and dough consistency are critical to production. In the United Kingdom the significant rise in the manufacture of prepackaged sandwiches based on pan bread ([Young and Cauvain, 2010](#)) imposed more stringent quality requirements on bread manufacturers, which in turn determined the need for greater recipe and process control during manufacture.

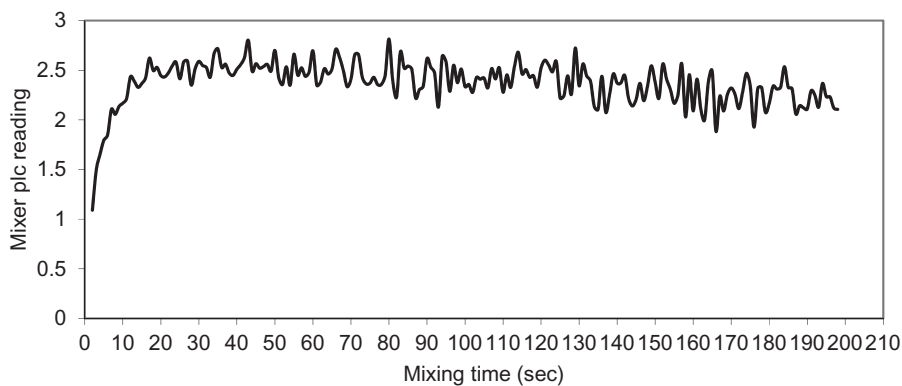
6.5 DOUGH DEVELOPMENT AND COMMERCIAL DOUGH MIXING

Another major use for the Farinograph is for the evaluation of flour “strength” with a focus on understanding potential development of the

gluten network in the context of a given breadmaking process. The common approach has mainly been to evaluate flour properties in a two-component system, flour and optimized water content. This is a perfectly reasonable and acceptable means of comparing flours in a standardized mixing context. For bakers who have access to the relevant equipment on a daily or regular basis, measurement of flour qualities provides a useful quality-control check on incoming raw materials. However, the data from such Farinograph tests have to be interpreted in the context of the expected outcome as far as the final bread quality is concerned. This is a more complex task, since all bakeries are unique with respect to the ingredient-recipe-process combination used to deliver a specified product and the recipe that will be used in a bakery is very different from that used in a standard wheat flour test.

Assessing the likely performance of a given flour with the Farinograph using a “full recipe” formulation is hardly standard practice for bakers on a daily basis, so they mostly rely on the interpretation of standard Farinograph data to adjust their receipt or mixing process using heuristic rules developed through experience in a given bakery. For example, they may adjust the length of mixing time or the level of energy input in the CBP based on the available Farinograph data.

Examination of energy consumption patterns in industrial bakery mixers can open up new possibilities for the use of Farinograph data. Fig. 6.1 illustrates a curve of energy usage derived from a commercial dough mixer exhibiting a remarkable similarity to that from a Farinograph. At the start of commercial dough mixing the energy consumption is low, but as the gluten network begins to develop there is a progressive increase in torque energy shown as increased curve height. Eventually a peak energy value is reached and



■ FIG. 6.1 Energy consumption pattern from commercial CBP dough mixer.

thereafter there is a small decline in torque at given moments in time. This pattern mimics that of the Farinograph, but is based on a full commercial recipe.

The form of the energy trace is related to the torque on the mixer impeller and is not the same as total energy being used (effectively, total energy is given by the area under the curve). The overall shape of the curve is unique to a given type of mixer and is affected, not least, by the speed at which the mixing is carried out. The Farinograph is capable of being operated at different speeds (Cauvain, 2018c) and so offers the opportunity to more closely mimic the behavior of individual commercial mixing equipment. If the testing is carried out with full commercial recipes, then the ability to evaluate in advance the likely performance of a given flour is greatly enhanced. Employed in this manner, the relevance of the standard Farinograph parameters may need to be reevaluated.

6.6 DOUGH TEMPERATURE

It is important to standardize the temperature to which doughs are mixed for evaluating flours in the Farinograph so that meaningful comparisons of flour qualities can be made. However, as with mixing conditions, the actual dough temperatures used in commercial baking environments may differ significantly from that of standard flour tests. It is well known that the sensory “firmness” of a dough is related to its temperature, with lower temperatures delivering firmer doughs—a situation considered favorable by some bakers since they can increase the recipe water content. However, while colder doughs may be considered beneficial in dough recipe water levels terms, such practices may be suboptimal in improver-related dough development terms, since oxidation and enzymic activities will be lessened with lower dough temperatures. The Farinograph has the facility to run dough development assessments at a range of final dough temperatures (Cauvain, 2018c), thus improving its ability to relate flour properties and dough development more closely to commercial mixing practices.

6.7 ALTERNATE COMMERCIAL USES FOR THE FARINOGRAPH

There has been much focus on the application of the Farinograph to identify key flour rheological properties for the manufacture of bakery products but, as noted earlier, there are opportunities for using the Farinograph to provide more commercially applicable data. Some of those relating to the manufacture of bread have been discussed in some detail; [Table 6.1](#) provides

Table 6.1 Alternate uses of the Farinograph with flour-based products.

Bakery product group	Potential uses
Bread and fermented products	<ul style="list-style-type: none"> • Examine impact of fixed energy mixing on dough rheology. • Examine effects of ingredients on dough rheology during mixing (e.g., enzymes). • Determine effects of bran and other materials on water absorption, hydration, and dough rheology. • Understand impact of mixing speed on dough development and rheology.
Short crust pastry dough	<ul style="list-style-type: none"> • Examine effects of ingredients on paste consistency and rheology.
Laminated pastry base dough and cracker doughs	<ul style="list-style-type: none"> • Examine effects of ingredients on paste consistency and rheology. • Understand impact of mixing speed and time on dough rheology.
Cookie dough	<ul style="list-style-type: none"> • Examine impact of paste temperature on paste consistency and rheology. • Examine effects of ingredients on paste consistency and rheology. • Understand impact of mixing speed and time on dough rheology. • Examine impact of paste temperature on paste consistency and rheology.

information on some potential applications to other commercial bakery products. As discussed for bread dough, the application of full commercial recipes remains key to being able to relate data generated with the Farinograph to dough/paste processing and final product quality. When considering alternate commercial uses for the Farinograph, it may be necessary to identify “nonstandard” parameters. For example, the rheological properties recorded at the end of a dough/paste mixing cycle (as defined by the height of the graph when mixing stops) is perhaps a relevant measurement for indicating the likely behavior of the dough/paste when it enters the next processing stage (rather than the peak height achieved during mixing).

6.8 CONCLUSION

While the Farinograph has a long history of being used to evaluate key flour properties such as water absorption capacity, its application in practical commercial environments has been limited to providing information on likely variations in flour qualities on a regular basis. This has provided, and continues to provide, valuable information but as the standard testing methods are somewhat removed by commercial baking operations, a significant degree of data interpretation is required by experts to make best use of the information. The versatility of the modern Farinograph to run at different speeds and with different operating temperatures has significantly increased the relevance of Farinograph data for practicing bakers. However, it is not until full recipe data are gathered that the real potential of the Farinograph can be realized for the commercial baker. Ultimately, more closely mimicking commercial baking operations with Farinograph evaluations will

significantly enhance the potential of the evaluation methods; however, this has yet to be fully realized. In part this is because each bakery operation displays a significant degree of “uniqueness” so that testing becomes highly individualized. At first sight, the scale of the work required to more closely match Farinograph data to daily baking operations may seem daunting but, once established, the value from such an exercise can be significant in commercial terms.

REFERENCES

- Cauvain, S.P., 2007. Reducing salt in bread and other baked products. In: Kilcast, D., Angus, F. (Eds.), *Reducing Salt in Food: Practical Strategies*. Woodhead Publishing, Cambridge, UK, pp. 296–315.
- Cauvain, S.P., 2015. *The Technology of Breadmaking*, third ed. Springer International Publishing AG, Cham, Switzerland.
- Cauvain, S.P., 2018a. Improving the processing of dough to bread. In: *The Future of Baking: Science-Technique-Technology*. Baking+Biscuit International, pp. 36–41.
- Cauvain, S.P., 2018b. The relevance of testing to the manufacture of bread and fermented products. In: Cauvain, S.P. (Ed.), *The ICC Handbook of Cereals, Flour, Dough & Product Testing: Methods and Application*, second ed. DEStech Publications Inc, Lancaster, PA, pp. 143–175.
- Cauvain, S.P., 2018c. Cereals testing equipment—Brabender® GmbH & Co. KG. In: Cauvain, S.P. (Ed.), *The ICC Handbook of Cereals, Flour, Dough & Product Testing: Methods and Application*, second ed. DEStech Publications Inc, Lancaster, PA, pp. 345–371.
- Cauvain, S.P., Young, L.S., 2006. *The Chorleywood Bread Process*. Woodhead Publishing Ltd, Cambridge, UK.
- Young, L.S., Cauvain, S.P., 2010. The rise and rise of the sandwich loaf. *f2m Baking + Biscuit International Review: Bread*, pp. 34–37.

This page intentionally left blank

Using the Farinograph for soft wheat products

Jayne E. Bock

Wheat Marketing Center, Portland, OR, United States

CHAPTER OUTLINE

7.1 Soft wheat and its uses	91
7.2 Cracker processing	92
7.3 Flour-quality requirements for crackers	92
7.4 Making the Farinograph method relevant to cracker applications	94
References	97

7.1 SOFT WHEAT AND ITS USES

Soft wheat is used for a much wider variety of products than hard wheat. Whereas hard wheat flours are predominantly used for breads, soft wheat flours can be used in cakes, pastries, cookies, crackers, some styles of steamed bread, ready-to-eat (RTE) breakfast cereals, batters/breadings, and host of other products, including doughnuts, pretzels, and wafers.

The predominant uses of soft wheat flour are for cakes and cookies. That is an important distinction because these products are primarily dependent on the functionality of sugar and/or fats, meaning flour plays a lesser role in determining processing performance and final product quality (Pareyt et al., 2008, 2009, 2010; Delcour et al., 2012). Additionally, many of these products are batter-based with specific viscosity and flow requirements, so gluten development is not a desired outcome during mixing and processing. As a result, many of these products use flour-quality tests and criteria other than those recorded by the Farinograph (Kweon et al., 2011).

Still, there are soft wheat flour applications that require knowledge of Farinograph flour-quality criteria for proper processing performance and end-product characteristics. The primary focus of this chapter is on using

the Farinograph for cracker applications, but southern-style Chinese steamed breads and cake doughnuts are also examples of soft wheat products that can be dependent on Farinograph characteristics, especially water absorption and dough development time.

7.2 CRACKER PROCESSING

Crackers encompass a broad range of low-moisture products that are characterized by a crisp bite and, in the majority of cases, a lamination step during processing. The range of formulas is vast and frequently overlaps with those of cookies or biscuits, so characterization based on common formulation(s) results in some degree of confusion.

Cracker doughs share a common feature of low formula water levels. Levels of 28%–30% (fwb) are not uncommon. As a result, lean doughs tend to feel dry and exhibit a firm texture. Rich doughs with more fat and/or sugar may exhibit a softer dough texture. However, in all cases, the formula water remains low compared to a bread dough.

Most cracker doughs can be directly mixed and sent on for further processing. However, some cracker doughs require a fermentation step prior to mixing, employing a sponge-and-dough style make-up protocol (e.g., saltine or soda crackers) followed by a 1–2 h bulk fermentation period before processing. In most cases, it is advisable to mix cracker dough until a target temperature is achieved. The target temperature is generally set to avoid activation or loss of gassing power from chemical leavening agents, maintain a desired dough consistency (e.g., Marie biscuits), and/or to preserve enzyme functionality.

Cracker doughs, with the noted earlier exception of fermented versions, proceed to further processing after mixing. The dough is sheeted to an appropriate thickness before cutting and lamination. A four-to-six layer lamination is sufficient for most crackers. After lamination, the dough proceeds through a series of reduction rolls to gradually reduce the dough sheet to the desired thickness before cutting and baking to a final moisture content of $\leq 5\%$.

Interested readers can find a more detailed process description for various types of crackers in *Manley's Technology of Biscuits, Crackers and Cookies* (Manley, 2011).

7.3 FLOUR-QUALITY REQUIREMENTS FOR CRACKERS

The brief, generalized description given here of the cracker-making process should make it apparent to the reader that flours for cracker applications require a unique balance of characteristics:

- The flour can't have excessive water absorption requirements due to the dual needs of achieving an appropriate consistency at low formula water levels as well as the need to bake off moisture to no more than 5% in the final product.
- The flour can't have excessive strength, nor can it have excessive weakness, due to the significant role of sheeting and reduction in the process.
- Excessive strength exacerbates dough snapback (i.e., shrinkage) after cutting, whereas excessive weakness may result in poor gas retention during baking. Both negatively affect final product dimensions.

A generalized “optimal” flour for crackers, therefore, falls in an intermediate strength category coupled with low water absorption. There are two options for achieving this contradiction of intermediate strength with low water absorption values:

- (1) Use of a so-called “strong” soft wheat flour with naturally low water absorption, or
- (2) Use of a soft wheat flour blended with ~10%–20% hard wheat flour to increase strength while preserving lower water absorption.

High protein “strong” soft wheats (i.e., those with 5+10 glutenin subunit combinations) are generally preferred over blends (Kweon et al., 2014). Soft+hard wheat flour blends are less desirable due to the outsized impact a small quantity of hard wheat flour can have on the strength and water absorption characteristics of the blend. However, both options are suitable if the Farinograph characteristics are properly specified in conjunction with other tests (e.g., solvent-retention capacity).

Farinograph water absorption values for a generic cracker flour will tend to fall in the low- to mid-50% range with dough development times and stabilities around ~2–3 min. The shape of the curve should show a moderate amount of breakdown with a mixing tolerance index in the vicinity of ~80–100 BU. Fig. 7.1 is an example of this type of flour. All of these values are based on the constant flour weight method as defined by AACCI Method 54-21.02.

Flours with stronger Farinograph curve characteristics introduce challenges on the processing line. Examples of excessively strong flours are shown in Fig. 7.2. Water absorption requirements are met in both cases. However, other characteristics like dough development time, stability, and mixing tolerance index are either marginally met or entirely out of range. The cracker doughs made from these flours result in significant tearing on the processing line (Fig. 7.3) compared to a more optimal flour (Fig. 7.4), improper dough weights and final product dimensions, and excessively hard final product textures (see Table 7.1).

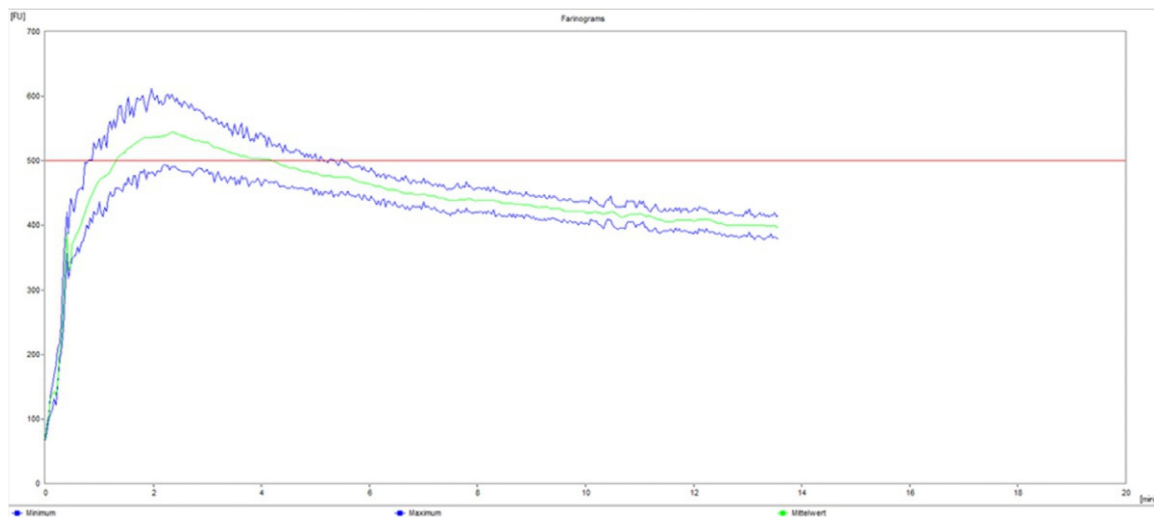


FIG. 7.1 Farinogram from an “optimal” cracker flour.

7.4 MAKING THE FARINOGRAPH METHOD RELEVANT TO CRACKER APPLICATIONS

The Farinograph as described previously is primarily the basis for determining incoming flour quality and suitability for cracker processing using a standardized method. However, better information may be obtained by setting the standardized methods aside and pursuing testing under more realistic conditions.

Mixing a full formula cracker dough at a speed closer to that of an industrial mixer (e.g., 150–200 rpm) at a temperature around 35°C will allow the operator to determine if the flour will allow the dough to achieve optimal consistency for further processing. Additional insights from mixing a full formula dough include identifying the need for small adjustments to formula water, or whether new ingredients (e.g., switching shortening suppliers) alter final dough consistency beyond processing tolerances.

The Farinograph can also be used as a process control tool on the plant floor. Pulling a sample directly from the mixer and running it in the Farinograph can help operators identify problems in dough consistency arising from formulation and/or improper mixing time. Combining freshly mixed and reworked doughs in the Farinograph can also help pinpoint adjustments to the ratio of rework incorporation.

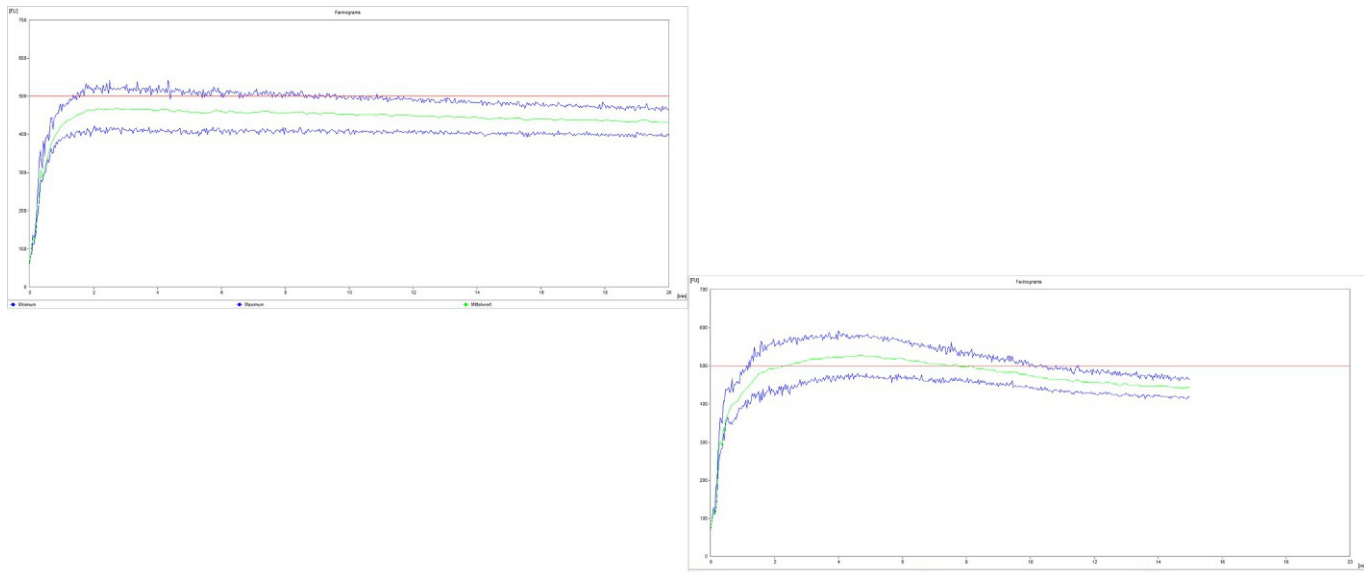


FIG. 7.2 Farinograms from excessively strong flours. (A) Meets water absorption and dough development time requirements, but exhibits excessive stability and low MTI. (B) Meets water absorption requirements, but is slightly out of tolerance for dough development time, stability, and MTI.



FIG. 7.3 Tearing, holes, and uneven hydration observed in a sheeted cracker dough made from excessively strong flour.



FIG. 7.4 Sheeted cracker dough made from a more optimal flour.

Table 7.1 Cracker characteristics from a standard cracker flour compared to two excessively strong flours.

	Length (mm)	Width (mm)	Stack height (mm)	Stack weight (g)	Stack HT:Dough WT	Break force (g)
Control	46.29	47.51	58.74	39.6	1.13	3353
Strong 1	44.08	48.70	63.50	42.6	1.16	4510
Strong 2	45.72	47.80	60.33	40.4	1.14	4110

REFERENCES

- Delcour, J.A., Joye, I.J., Pareyt, B., Wilderjans, E., Brijs, K., Lagrain, B., 2012. Wheat gluten functionality as a quality determinant in cereal-based food products. *Annu. Rev. Food Sci. Technol.* 3, 469–492.
- Kweon, M., Slade, L., Levine, H., 2011. Solvent retention capacity (SRC) testing of wheat flour: principles and value in predicting flour functionality in different wheat-based food processes and in wheat breeding—a review. *Cereal Chem.* 88, 537–552.
- Kweon, M., Slade, L., Levine, H., Gannon, D., 2014. Cookie- versus cracker-baking—what's the difference? Flour functionality requirements explored by SRC and alveography. *Crit. Rev. Food Sci. Nutr.* 54, 115–138.
- Manley, D. (Ed.), 2011. Manley's Technology of Biscuits, Crackers and Cookies, fourth ed. Woodhead Publishing, Cambridge, UK.
- Pareyt, B., Wilderjans, E., Goesaert, H., Brijs, K., Delcour, J.A., 2008. The role of gluten in a sugar-snap cookie system: a model approach based on gluten-starch hybrids. *J. Cereal Sci.* 48, 863–869.
- Pareyt, B., Brijs, K., Delcour, J.A., 2009. Sugar-snap cookie dough setting: the impact of sucrose on gluten functionality. *J. Agric. Food Chem.* 57, 7814–7818.
- Pareyt, B., Brijs, K., Delcour, J.A., 2010. Impact of fat on dough and cookie properties of sugar-snap cookies. *Cereal Chem.* 87, 226–230.

This page intentionally left blank

Farinograph applications for whole wheat flour: Exploring the influence of circulating water temperature and mixing speed on dough mixing properties in the Farnograph

Lingzhu Deng^{a,*} and Gary G. Hou^{a,b}

^a*Wheat Marketing Center, Portland, OR, United States* ^b*SPC Group, Seoul, South Korea*

Whole wheat flour (WWF) is milled whole grain meal that contains all naturally occurring components in the whole kernel. Whole wheat contains 8%–18% protein, 78%–80% carbohydrate, 9%–15% dietary fiber, 1%–2% lipids, and 1%–3% minerals (Miller Jones et al., 2015). Recently, the average production of WWF from 2014 to 2018 in the United States reached 20–23 million cwts, accounting for about 5.0%–5.5% of the total wheat flour production, which was up 3% from 2000 (National Agricultural Statistics Service, 2018). The Dietary Guidelines for Americans recommend whole grains as one of the key items in healthy eating patterns, and consumers recognize the potential health benefits of WW products (Bakken et al., 2016; Ismaiel et al., 2016; Zhu and Sang, 2017). This has led to increased interest from flour millers and food manufacturers to produce a wider range of WW products to meet consumer demands for healthier food items.

The Farnograph is widely used to evaluate flour quality in the flour milling and food industries. It measures several dough mixing properties, including

*Current address: Department of Food Science and Technology, The Ohio State University, Columbus, OH, United States

the amount of water that dough absorbs (i.e., water absorption) to reach a defined consistency; the time in which the dough reaches a maximum consistency (i.e., dough development time); and how long dough remains stable with overmixing (i.e., stability). The water absorption and dough mixing properties from the Farinograph provide information on the overall quality of gluten and its performance potential in baked products (Ktenioudaki et al., 2010). It helps millers and bakers to understand the potential end uses of a flour and make decisions on subsequent processing.

Refined flour is produced from finely ground wheat kernels, often achieved through roller milling, that have been sifted to remove bran and germ from endosperm. Compared with refined flour, WWF contains all the bran and germ fractions.

Bran consists of the outermost layers of wheat kernels including the pericarp, seed coat, nucellar epidermis, aleurone layer, and starchy endosperm (Hoseney and Delcour, 2000). Many studies have shown that wheat bran is particularly high in dietary fiber, constituting about 40%–53% of dry matter in bran (Stevenson et al., 2010; Pavlovich-Abril et al., 2012). WWF contains 3.5–5 times more dietary fiber (14.4%–16.0%, dry basis) than refined flour fiber (3.4%–5.1%) (Seyer and Gélinas, 2009). Of all dietary fibers that are found in bran, arabinoxylans (nonstarch polysaccharides) are the main component, which constitutes 22%–30% of dry matter of wheat bran (Kamal-Eldin et al., 2009). Arabinoxylans possess hydrophilic characteristics. Consequently, when water is added to WWF, arabinoxylans compete with protein for water. The amount of water retained by arabinoxylans, determined by the Farinograph water absorption, is 3.5–9.9 times their weight (Jelaca and Hlynka, 1971; Kim and D'Appolonia, 1977). Other major fiber components of wheat bran are cellulose (25%–33%) and lignin (18%–24%). Similarly, those fibers are also highly related to the water retention of flour (Seyer and Gélinas, 2009).

When the Farinograph is used to test WWF dough rheology, the presence of bran increases the required amount of water that dough absorbs to reach a defined consistency of 500 BU. This implies that less water is available for protein molecules to form gluten, resulting in less gluten or weaker gluten than found in refined flour (Wang et al., 2003). Besides absorbing water, the main components of bran have a fibrous texture that can physically interfere with gluten formation during dough development. Studies have shown that bran particles disrupted and pierced the gluten network, thereby reducing bread volume and negatively affecting crumb texture (Pomeranz et al., 1997; Zhang and Moore, 1999). As a result, the time required for dough to reach a maximum consistency might be shorter, and dough tolerance to overmixing of WWF might be lower than refined flour. Bran particle size

also affects dough rheological properties. WW dough exhibits different strengths with varying bran particle sizes ([Zhang and Moore, 1997](#)).

The AACC International has established an official Farinograph method to test dough mixing properties of refined flour (Method 54-21.02). The Farinograph is equipped with a mixing bowl, for which the operating speed is 63 rpm and the temperature is controlled by a circulating water bath that is set to 30°C. WW farinograms under the standard method show water absorptions between 58%–75% for hard and soft wheats. Farinograms for WWF are prolonged in terms of dough development time and stability, which are about 3–8 min and 8–20 min, respectively. The prolonged mixing process significantly increases the Farinograph testing time and negatively impacts Farinograph applications in WW flour and products.

Many studies have examined the relationship of bread quality to dough properties. Loaf volume could be predicted by Farinograph water absorption, dough development time, and stability along with grain protein content ([Dowell et al., 2008](#)). The prolonged WW dough development time and mixing tolerance under the standard method seems to contradict the weak dough properties of WWF in the presence of bran. As a result, the relationship of WW bread quality to WWF dough mixing properties could be misleading.

In the Farinograph, dough exhibits resistance to the mixing blades during mixing, and a torque is created on the dynamometer that is then transmitted to the lever and scale system, which converts the torque into Brabender units. This is what is used to characterize the dough mixing performance. The resistance of a dough (torque) is measured when subjecting it to mixing action at a constant temperature. Previous research showed that the operating conditions of the Farinograph influence the dough performance. [Bayfield and Stone \(1960\)](#) reported that water absorption changed, and dough development time and stability decreased as the circulating water temperature increased. All the other readings, including mixing tolerance index, arrival time, and valorimeter, were affected accordingly. The influence of mixing speeds and energy inputs on rheological properties of dough were studied by [Chin and Campbell \(2005\)](#), and they found that the aeration and rheological characteristics of dough were dependent on the mixing speed and work input.

We hypothesized that WW dough mixing performance would vary with operating conditions (i.e., circulating water temperature and mixing speed). The bran in the dough might also generate more friction or resistance against the mixing blades during mixing using the standard method, which would increase the dough resistance and extend the time required for dough to depart from the 500 BU line. Varying the circulating water temperature and speed of mixing blades could reduce the physical interaction of bran

particles on dough resistance. This study was undertaken in an attempt to establish a framework for modifying the standard Farinograph method to be more suitable for evaluation of WWF.

Fig. 8.1 shows WW dough water absorption versus circulating water temperature and mixing speed in the Farinograph. As circulating water

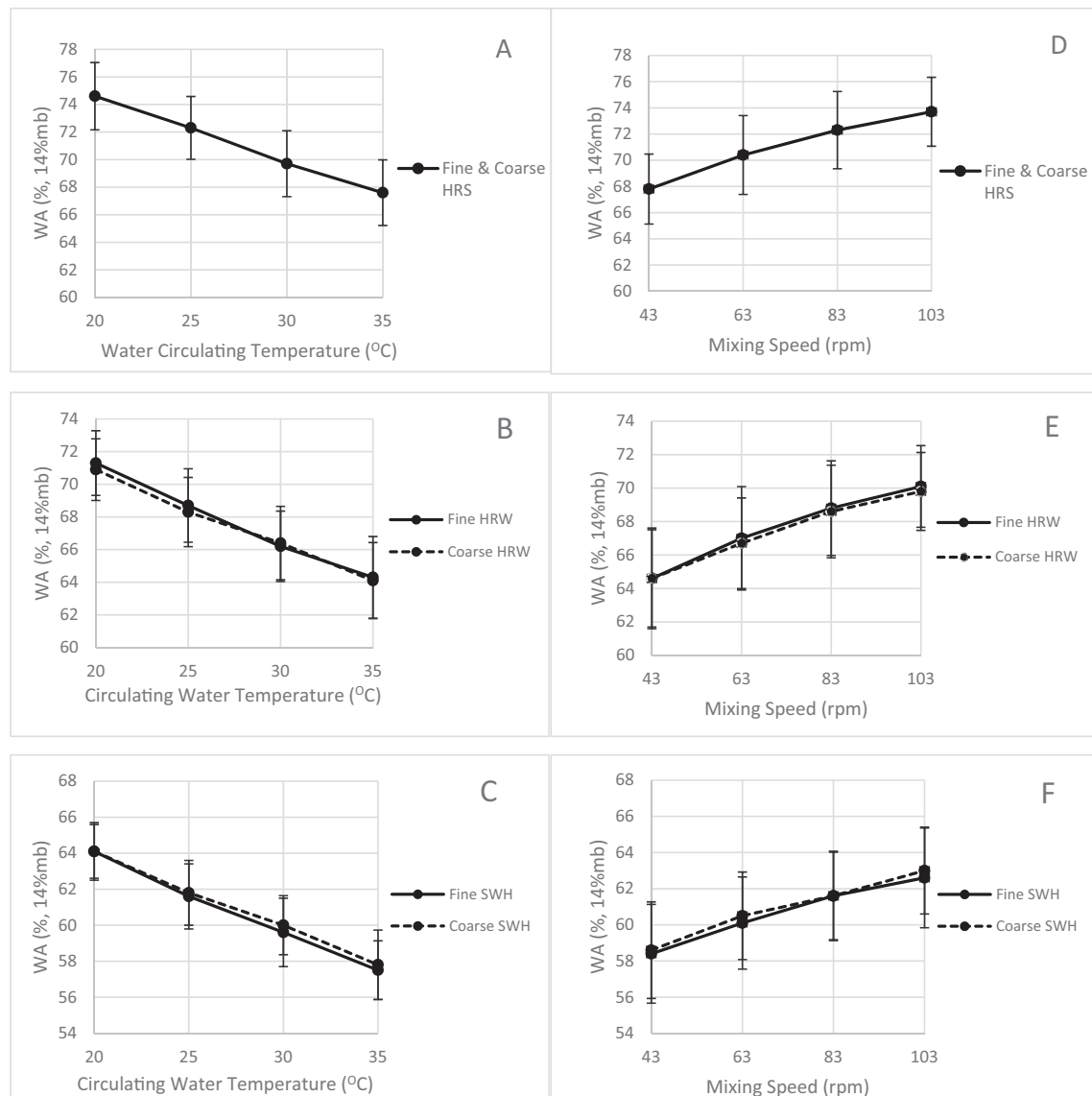


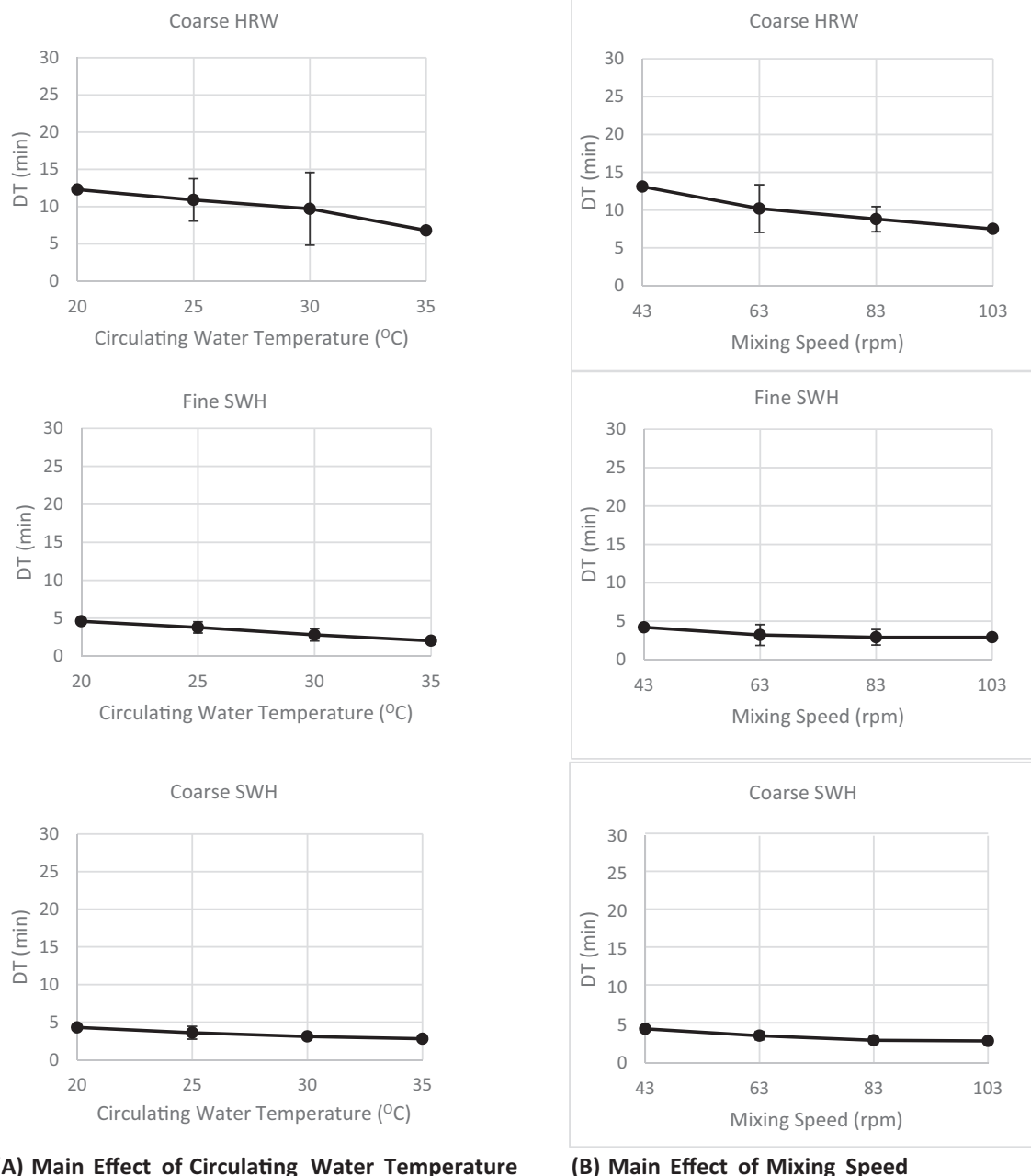
FIG. 8.1 WWF Farinograph mixing water absorption as a function of circulating water temperature (A–C) and mixing speed (D–F) (WWF was made by reconstituting flour, bran and shorts from a Bulher Mill. The bran, germ and shorts were reground one and three times, respectively, using a Perten 3100 Laboratory Mill equipped with a 8-mm mesh for coarse and fine WWF. The median particle sizes of fine and coarse WWFs were 125 and 145 μm , respectively.)

temperature was increased from 20°C to 35°C, water absorption decreased by 7.0% for HRS, 6.8%–7% for HRW, and 6.6% for SWH (Fig. 8.1A–C). The Arrhenius equation describes the temperature dependence of dough viscosity, in that viscosity decreases with the increasing temperature (Bloksma and Nieman, 1975). This explains the decreased water requirement for the dough to reach 500 BU, as the viscosity of the WW dough decreases at a higher temperature. From 43 to 103 rpm mixing speed, water absorption increased by 5.9% for HRS, 5.2%–5.5% for HRW, and 4.2%–4.4% for SWH (Fig. 8.1D–F). Particle size had no effect on water absorption of HRS WWF. However, increased mixing speed and/or higher circulating water temperature tended to show some differences in water absorption between coarse and fine particle sizes of HRW and SWH.

Development time was affected by the main effects of circulating water temperature and mixing speed for coarse particle size HRW and fine/coarse SWH (Fig. 8.2A and B). Development time gradually declined from low to high mixing speed and circulating water temperature. For WWFs of fine HRW and fine/coarse HRS (Fig. 8.2C), development time was affected by the interaction of circulating water temperature and mixing speed. Development time declined from low to high mixing speed at each circulating water temperature, and lower water temperature tended to require a longer development time. The sole exception was the 20°C and 43 rpm combination for the fine particle size HRW. The results showed that WWF takes less time to develop dough at higher mixing speeds and higher circulating water temperatures.

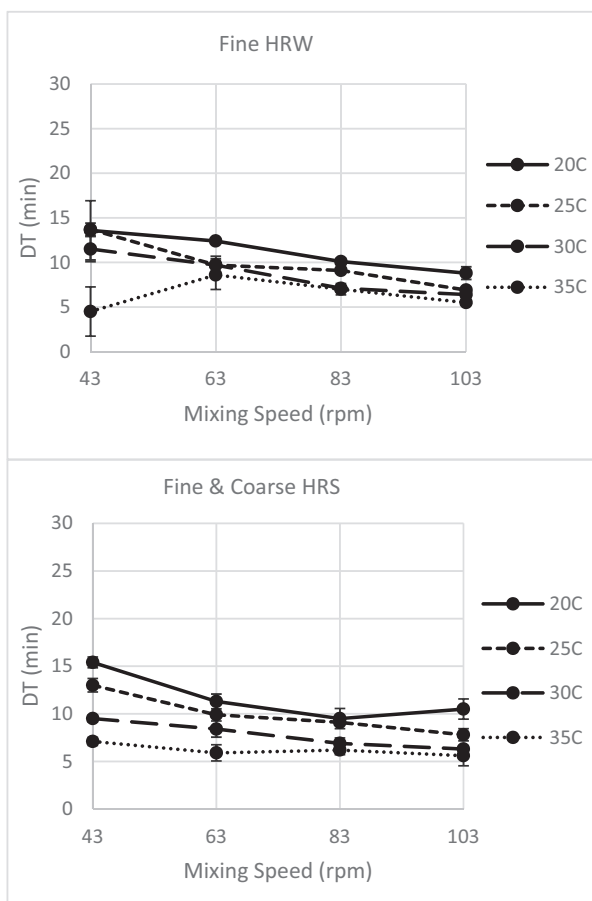
Farinograph stability is a measure of tolerance to overmixing, which is related to the overall quality of the protein. Similar to development time, stability was affected by the main or interaction effects of circulating water temperature and mixing speed for coarse and fine WWFs (Fig. 8.3). Stability showed a larger decline from low to high mixing speed than from the same circulating water temperature (Fig. 8.3A and B), especially for fine HRW and fine/coarse HRS WWFs (Fig. 8.3A).

The total running time of the Farinograph test is influenced by dough development time and mixing tolerance. At 35°C and 103 rpm, the total test times are about 12–14 min for hard wheat and 5.0–5.5 min for soft wheat, both of which are faster than the current standard method. The coefficient of variance of mixing properties for each WW dough characterizes the variability when attempting to replicate Farinograph tests. Different variabilities were observed when the Farinograph test was compared among mixing speed/circulating water temperature combinations. Development time (0%–6.7%) and stability (0%–15.5%) were found to have smaller variabilities at



■ FIG. 8.2 WWF Farinograph develop time (DT) was as a function of circulating water temperature and mixing speed.

(Continued)



(C) Interaction Effects of Circulating Water Temperature and Mixing Speed

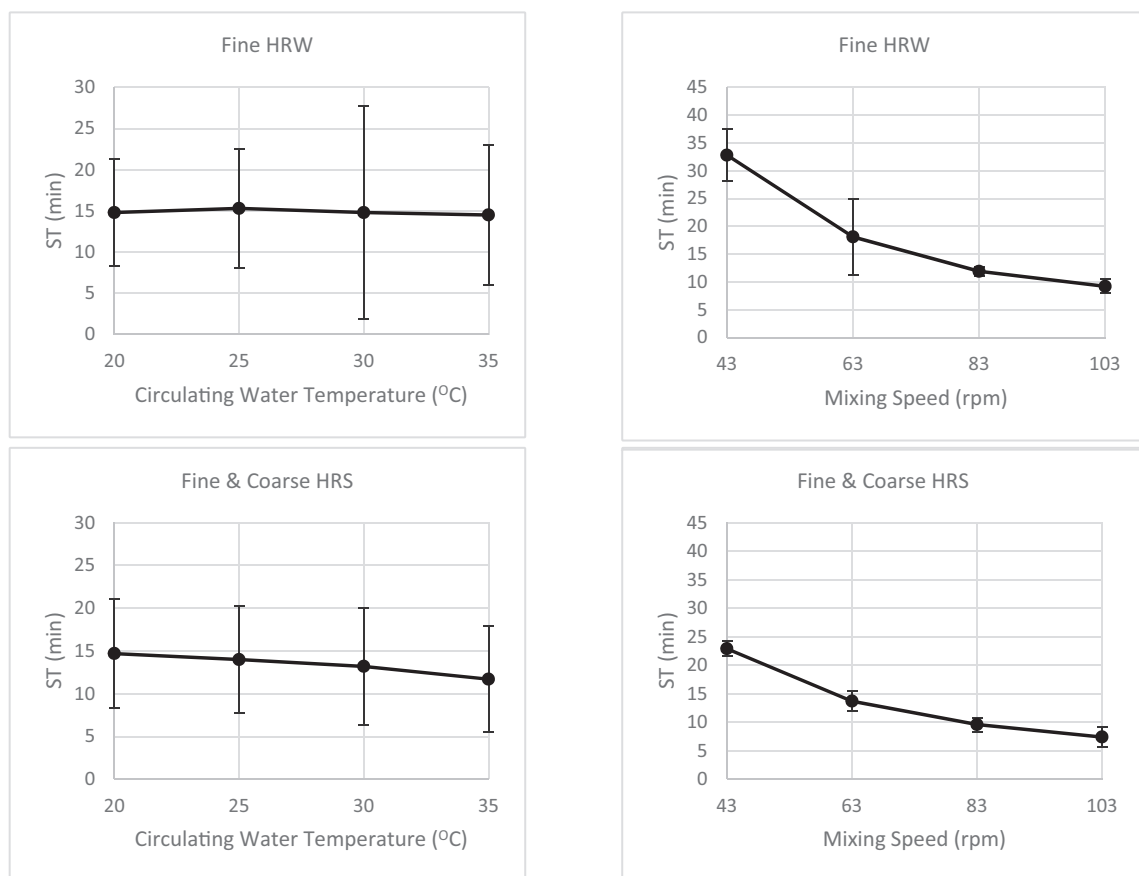
■ FIG. 8.2—CONT'D

35°C and 103 rpm when compared to other speeds and temperatures (0%–61.7% and 0.5%–54.0%). By changing mixing speed and circulating water temperature to 35°C and 103 rpm, a faster test time is achieved while a smaller variation at 35°C and 103 rpm indicates better replicates and more consistent test results.

WW dough mixing properties in the Farinograph vary from those recorded for refined flour and depend on the operating conditions that are used. Higher circulating water temperature improves WW dough mixing. Faster

mixing speeds facilitate more rapid WW dough development and reduce the dough mixing tolerance, probably by eliminating some of the physical interactions of bran particles that influence dough rheological properties. A combination of 35°C circulating water temperature and 103 rpm mixing speed reduced the Farinograph test time and generated more consistent results. This could serve as a starting point for further development of a WWF Farinograph test method.

More tests are needed to verify the modified method by determining the WWF quality differences of different wheat varieties and bran particle sizes. In the last step of the new method development, the relationship of WWF

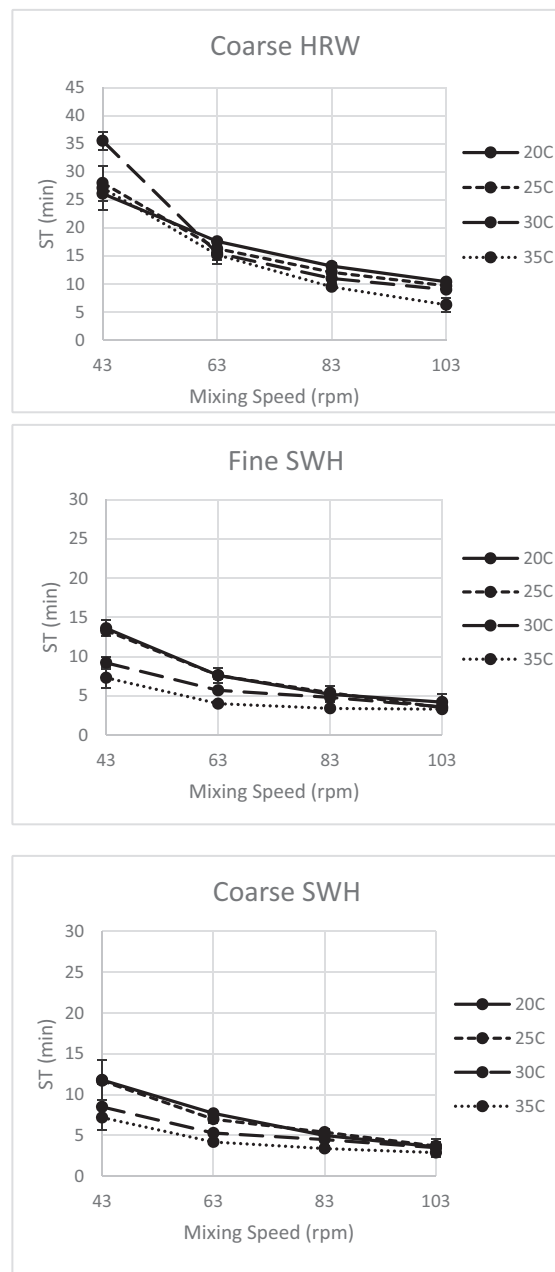


(A) Main Effect of Circulating Water Temperature

(B) Main Effect of Mixing Speed

■ FIG. 8.3 WWF Farinograph dough stability time (ST) as a function of circulating water temperature and mixing speed.

(Continued)



(C) Interactions of Circulating Water Temperature and Mixing Speed

bread quality parameters to the WWF Farinograph water absorption and dough mixing properties at 35°C and 103 rpm will be examined.

REFERENCES

- Bakken, T., Braaten, T., Olsen, A., Kyrø, C., Lund, E., Skeie, G., 2016. Consumption of whole-wheat bread and risk of colorectal cancer among Norwegian women (the NOWAC study). *Nutrients* 8, 40–52.
- Bayfield, E.G., Stone, C.D., 1960. Effects of absorption and temperature upon flour-water farinograms. *Cereal Chem.* 37, 233.
- Bloksma, A.H., Nieman, W., 1975. The effect of temperature on some rheological properties of wheat flour doughs. *J. Texture Stud.* 6, 343–361.
- Chin, N.L., Campbell, G.M., 2005. Dough aeration and rheology: part 2. Effects of flour type, mixing speed and total work input on aeration and rheology of bread dough. *J. Sci. Food Agric.* 85, 2194–2202.
- Dowell, F.E., Maghirang, E.B., Pierce, R.O., Lookhart, G.L., Bean, S.R., Xie, F., Caley, M.S., Wilson, J.D., Seabourn, B.W., Ram, M.S., Park, S.H., Chung, O.K., 2008. Relationship of bread quality to kernel, flour, and dough properties. *Cereal Chem.* 85, 82–91.
- Hoseney, R.C., Delcour, J.A., 2000. Structure of cereals. In: *Principles of Cereal Science and Technology*, third ed. American Association of Cereal Chemists, St. Paul, MN, pp. 1–46.
- Ismaiel, M., Yang, H., Min, C., 2016. Dietary fiber role in type 2 diabetes prevention. *Br. Food J.* 4, 961–975.
- Jelaca, S.L., Hlynka, I., 1971. Water-binding capacity of wheat flour crude pentosans and their relation to mixing characteristics of dough. *Cereal Chem.* 48, 211–222.
- Kamal-Eldin, A., Nygaard-Larke, H., Bach-Knudsen, K.-E., Lampi, A.-M., Piironen, V., Adlercreutz, H., Katina, K., Poutanen, K., Åman, P., 2009. Physical, microscopic and chemical characterization of industrial rye and wheat brans from Nordic countries. *Food Nutr. Res.* 53, 3402–3412.
- Kim, S.K., D'Appolonia, B.L., 1977. Bread staling studies. III. Effect of pentosans on dough, bread, and bread staling rate. *Cereal Chem.* 54, 225–229.
- Ktenioudaki, A., Butler, F., Gallagher, E., 2010. The effect of different mixing processes on dough extensional rheology and baked attributes. *J. Sci. Food Agric.* 90, 2098–2104.
- Miller Jones, J., Adams, J., Harriman, C., Miller, C., Van der Kamp, J.W., 2015. Nutritional impacts of different whole grain milling techniques: a review of milling practices and existing data. *Cereal Foods World* 60, 130–139.
- National Agricultural Statistics Service, 2018. <https://downloads.usda.library.cornell.edu/usda-esmis/files/ws859f64s/4m90f448j/xd07h259d/caflan19.pdf>. (Accessed 22 August 2019).
- Pavlovich-Abril, A., Rouzaud-Sandez, O., Torres, P., Robles-Sanchez, R.M., 2012. Cereal bran and whole grain as a source of dietary fiber: technological and health aspects. *Int. J. Food Sci. Nutr.* 63, 882–889.
- Pomeranz, Y., Shogren, M., Finney, K.F., Bechtel, D.B., 1997. Fiber in bread making—effect on functional properties. *Cereal Chem.* 54, 25–41.

- Seyer, M.-È., Gélinas, P., 2009. Bran characteristics and wheat performance in whole wheat bread. *Int. J. Food Sci. Technol.* 44, 688–693.
- Stevenson, L., Phillipis, F., O'Sullivan, K., Walton, J., 2010. Wheat bran: its composition and benefits to health, a European perspective. *Int. J. Food Sci. Nutr.* 63, 1001–1013.
- Wang, M., Hamer, R.J., Vliet, T.V., Gruppen, H., Marseille, H., Weegels, P.L., 2003. Effect of water unextractable solids on gluten formation and properties: mechanistic considerations. *J. Cereal Sci.* 37, 55–64.
- Zhang, D., Moore, W.R., 1997. Effect of wheat bran particle size on dough rheological properties. *J. Sci. Food Agric.* 74, 490–496.
- Zhang, D., Moore, W.R., 1999. Wheat bran particle size effects on bread baking performance and quality. *J. Sci. Food Agric.* 79, 805–809.
- Zhu, Y., Sang, S., 2017. Phytochemicals in whole grain wheat and their health-promoting effects. *Mol. Nutr. Food Res.* 61, 1–7.

This page intentionally left blank

Use of the Farinograph for gluten-free grains

Andrea Bresciani^a, George Amponsah Annor^b, Mattia Gardella^a, and Alessandra Marti^a

^aDepartment of Food, Environmental and Nutritional Sciences (DeFENS), Università degli Studi di Milano, Milan, Italy

^bDepartment of Food Science and Nutrition, University of Minnesota, Saint Paul, MN, United States

CHAPTER OUTLINE

9.1 Introduction	111
9.2 Use of the Farinograph for GF cereals	113
9.3 Pseudocereals	118
9.4 Pulses	119
9.5 Conclusions	124
Acknowledgment	124
References	125

9.1 INTRODUCTION

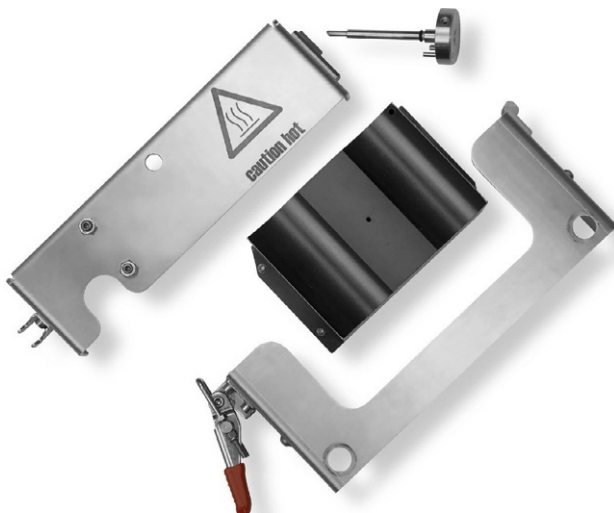
The Farinograph is typically used to measure the mixing behavior of wheat flour-water systems, resulting in the determination of the water absorption, which is the water needed to form a dough with a defined consistency (i.e., 500BU or FU). In addition to the water absorption, the Farinograph also provides information on the mixing stability of the dough, among other factors, such as dough development time. Altogether, the aforementioned indices define the strength of wheat flour and thus its end uses.

Typically, the Farinograph is used in gluten-containing flour-water systems where mixing is done to achieve a 500BU consistency. The growing interest in gluten-free (GF) products and the need to monitor and/or predict the behavior of GF flours during mixing is leading to new applications. Despite its big potential in the GF field, the Farinograph has not yet been fully adapted as a standard piece of equipment for the determination of the water absorption and dough rheology of GF dough systems, particularly due to their sticky

consistency, extreme plasticity, and the fact that GF dough systems are not homogeneous. During the mixing of GF flours in the Farinograph, the doughs tend to push up on the lid of the mixing bowl, which disengages the lid sensor. The Farinograph is designed such that when the lid sensor is disengaged, it causes the mixer to stop mixing. Furthermore, during the mixing of GF flours, the dough material builds up in the center of the mixing bowl and sits above the blades due to the lack of a viscoelastic network like gluten that can engage with the twin sigma blades. This makes it difficult or impossible for the GF dough to be pulled into the active mixing zone, thus resulting in uneven mixing. Another problem with the use of the Farinograph for GF dough systems is that the ranges of the rheological properties of these systems can extend beyond what the Farinograph can measure.

Having said that, the Farinograph has found more successful applications in GF flour-water systems, especially after the development of the FarinoAdd-S300 GF accessory kit, as shown in [Fig. 9.1](#).

According to Brabender GmbH and Co. KG., the FarinoAdd-S300 improves the capabilities of the Farinograph by extending its range of rheological properties that can be measured on GF dough systems. When attached to the Farinograph, the FarinoAdd-S300 secures the lid of the mixing bowl and creates a smaller mixing zone that facilitates better active mixing of GF doughs, thus allowing for an accurate determination of the rheological properties of GF dough systems. Another advantage of the FarinoAdd-S300



■ FIG. 9.1 FarinoAdd-S300 GF accessory kit.

accessory is that it is very easy to mount on the Farinograph mixing bowl without the need for mixer bowl modifications. Despite the benefits of using this accessory kit, it is worth mentioning that it is a relatively new device lacking a standardized method, and thus most of the studies summarized in this chapter either did not use it or used it under differing conditions.

9.2 USE OF THE FARINOGRAPH FOR GF CEREALS

Among cereals, rice and corn are the two most utilized in GF formulations because of their availability and low cost. Moreover, rice is known for its hypoallergenicity and bland taste, which can be an advantage in certain GF products, whereas the color of corn and the functional properties of zein proteins make corn the preferred raw material for many GF products.

One of the first available reports on the use of Farinograph for GF flours goes back to the 1970s when there was little or no market for GF products. The studies of [Ayernor and Steinberg \(1977\)](#) and [Cuevas and Puche \(1986\)](#) laid the groundwork for the use of corn flour in a dough system. They explored using a pregelatinized corn flour in addition to adding a significantly greater amount of water than that required by gluten-containing flours to reach the 500 BU consistency considered optimal for wheat. During mixing, the amount of water added to the flour to obtain a homogeneous mass that has a specific consistency strongly influences the subsequent workability of the dough itself. While some studies considered the 500 BU as the target for the optimum dough consistency, others pointed out that, in the case of GF flours, optimal dough is reached at lower consistency values. As an example, in a fiber-enriched GF formulation, [Cappa et al. \(2013\)](#) showed that more “solid-like” doughs (500 BU) were characterized by reduced development during proofing, likely due to high resistance to deformation, and more “liquid-like” doughs (200 BU) showed better mixing characteristics. Indeed, in the presence of more water, fibers and hydrocolloids can be better dispersed and increase viscosity, thus creating a structure capable of sustaining and developing itself during the leavening process ([Cappa et al., 2013](#)). More recently, [Sahin et al. \(2020\)](#), using the FarinoAdd-S300, determined the optimal amount of water for GF mixtures by the evaluation of bread quality when different water levels were added. Thus, for a recipe containing 98% rice flour and 2% hydroxypropyl methylcellulose (HPMC), the optimal specific volume (2.13 ± 0.05 mL/g) was obtained by preparing a batter with a consistency of 103 BU that was reached by incorporating 100% water. The addition of less than 100% water resulted in greater torque values (i.e., 171 BU and 131 BU for 90% and 95% water addition, respectively) and small specific volumes (1.31 mL/g and

1.46mL/g for 90% and 95% water addition, respectively). On the other hand, the addition of more than 100% water led to a decrease in batter consistency (82BU and 57BU for 105% and 110% water addition, respectively) as well as small specific volume (2.10mL/g and 1.80mL/g for 105% and 110% water addition, respectively) ([Sahin et al., 2020](#)).

Over the years, researchers have focused on the optimization of Farinograph parameters for measuring the dough rheology of GF products. For example, [Cuevas and Puche \(1986\)](#) optimized mixing conditions by testing two hydration levels (35% and 40%), three bowl temperatures (30°C, 50°C, and 70°C) and three mixing speeds (60, 90, and 120 rpm). Regardless of the hydration level, dough consistency increased as the mixing temperature and speed increased, with the greatest effect observed when the speed was changed from 90 to 120 rpm and the temperature increased from 50°C to 70°C. However, as the temperature increased, the dough became stickier and the differences between the hydration levels became less noticeable. It should be noted in interpreting these results that [Cuevas and Puche \(1986\)](#) used the Farinograph to determine the apparent viscosity of corn dough based on the assumption that the apparent viscosity measured was an index of the properties of the dough and not a measure of torque.

With regards to rice, one of the first uses of the Farinograph was reported by [Mossman et al. \(1983\)](#) when they tested the stickiness of cooked milled rice. This was done by kneading precooked rice flour for 20 min in the Farinograph. Based on the Farinograph peak time, the stickiness of different types of rice was differentiated. When the Farinograph was used to test the rheology of rice, it was observed that rice flour had similar water absorption (about 58%) coupled with a longer mixing time compared to wheat flour ([Sivaramakrishnan et al., 2004](#)). Furthermore, the consistency of the rice flour dough increased during mixing, unlike the standard characteristics of wheat flour dough, where it should decrease. This was attributed to rice flour particles becoming trapped in the gap between the back of the mixing blade and the mixing bowl, thus resulting in an increase in torque toward the end of the analysis. It is possible that the use of the FarinoAdd-S300 GF accessory kit and its reduced mixing zone could help with the evaluation of rice flour doughs by improving contact of the overall dough mass with the mixer blades, thereby overcoming the influence of particles trapped behind the blades.

In another study, the effect of storage (up to 3 months) was investigated on the mixing properties of rice flours ([Amin et al., 2020](#)). Interestingly, neither the storage time nor the packaging material (low-density polyethylene vs. metalized polyester) significantly affected Farinograph parameters.

Specifically, water absorption and mixing tolerance index increased slightly with storage while dough development time and dough stability decreased, although nonsignificantly for both.

Treating rice flour with amylolytic enzymes (i.e., α -amylase, glucoamylase, and pullulanase) to create low glycemic index rice flour led to a significant decrease in water absorption capacity, dough development time, dough stability, and mixing tolerance index. These lower values in the treated flour were likely due to starch pregelatinization and its retrogradation while preparing the low glycemic index rice flour (Amin et al., 2020).

In the production of GF baked goods, hydrocolloids are always used to emulate gluten functionality due to their ability to form a gel with water. Hydrocolloids improve both the volume and texture of GF bread, as extensively reviewed by Mir et al. (2016) and Bender and Schönlechner (2020). Among them, hydroxypropyl methylcellulose (HPMC) is the most widely used (Roman et al., 2019). In this frame, most studies that apply the Farinograph in GF systems have focused on the effect of hydrocolloids on dough mixing properties, as summarized in Table 9.1.

Sahin et al. (2020) explored the use of the Farinograph with the FarinoAdd-S300 and a new method to determine how much water could be added to GF bread systems. Rice flour was added to 2% hydrocolloids, specifically HPMC, guar gum, locust bean gum, sodium alginate, and xanthan gum. The best batter stability was observed by adding HPMC. Batter with locust bean gum had the lowest stability. The time required for the development of the batter was the longest when xanthan gum and HPMC were added to the rice batter, whereas the shortest was observed for locust bean gum. All the farinograms from the batters with the added gums looked very much like those from hard wheat flours, suggesting that hydrocolloids have a positive effect in improving the mixing properties of rice flours.

Lazaridou et al. (2007) also investigated the effects of the addition of hydrocolloids on dough rheology and the characteristics of bread made from formulations based on rice flour and corn starch. Hydrocolloids such as pectin, carboxymethyl cellulose (CMC), agarose, xanthan gum, and oat β -glucans were added at levels of 1% and 2%. They observed that pure rice flour showed a water absorption of about 60% and took about 20 min to reach 500 BU. Moreover, the curve was very noisy, and the consistency increased with measuring time, showing it to be a poor dough for baking. The addition of corn starch and milk protein (sodium caseinate) to rice flour improved the rheological properties of the dough. The dough development time for the rice flour was reduced to 4 min when the hydrocolloids were added, and this consistency remained relatively constant throughout the measuring time.

Table 9.1 Effects of hydrocolloids on GF dough mixing properties.

	Water absorption	Dough development time	Dough stability	Degree of softening	Elasticity ^a	Reference
HPMC	+	—	n.a.	+	n.a.	Nour et al. (2017)
Guar gum	+	—	n.a.	+	n.a.	Nour et al. (2017)
Agar gum	+	+	n.a.	+	n.a.	Nour et al. (2017)
Pectin	+	+	n.a.	+	=	Nour et al. (2017) and Lazaridou et al. (2007)
Pectin + guar gum	+	—	n.a.	=	n.a.	Nour et al. (2017)
Pectin + HPMC	+	—	n.a.	+	n.a.	Nour et al. (2017)
Guar gum			n.a.	n.a.	n.a.	Elkhalifa et al. (2007)
Arabic gum			n.a.	n.a.	n.a.	Elkhalifa et al. (2007)
Carboxymethyl cellulose	+	+	n.a.	n.a.	+	Lazaridou et al. (2007)
Agarose	+	+	n.a.	n.a.	—	Lazaridou et al. (2007)
Xanthan	+	—	n.a.	n.a.	+	Lazaridou et al. (2007)
Sodium carboxymethyl cellulose	+	+	+	n.a.	n.a.	Nicolae et al. (2016) and Sahin et al. (2020)

^aBandwidth of the curve at the 500 BU consistency.

n.a. indicates not available; + indicates an increase in the value; — indicates a decrease in the value; = indicates no effect. HPMC, hydroxypropyl methylcellulose.

The addition of the hydrocolloids resulted in an increase in the water absorption of the rice flour blends, partly due to the hydrophilic nature of hydrocolloids. The addition of xanthan gum resulted in the highest water absorption, followed by pectin and agarose. CMC resulted in the lowest water absorption, but also resulted in the most acceptable bread compared to the other hydrocolloids.

Considering the powerful effect of xanthan gum in improving the properties of dough, Hegazy et al. (2009) investigated the addition of 3% xanthan gum on dough made from blends of rice flour, corn starch, defatted soy flour, and chickpea flour. The addition of the xanthan gum to the flour blends increased all the Farinograph properties studied compared to flours without xanthan gum. The dough development time was 10 min for blends made from 50% rice flour, 35% corn starch, 7.5% defatted soy flour, and 7.5% chickpea flour.

Nicolae et al. (2016) used the Farinograph to investigate the addition of sodium carboxymethyl cellulose (NaCMC) on rice flour blends consisting of rice flour, corn starch, sodium caseinate, sugar, and salt. In their study, they looked at the effects of the NaCMC on the water absorption, dough development time, and dough stability. The different percentages of NaCMC (from 0.25% to 2%) added to the GF dough impacted its rheological properties. Water absorption increased with the addition of NaCMC. Moreover, its addition improved the rheological properties of the GF doughs by also increasing the dough development time and the dough stability. These improvements in the dough were translated to the quality of the final product, i.e., bread, especially the volume and texture of the product. They concluded that the addition of 1% NaCMC improved the rheological properties of the GF dough as well as bread quality.

Nour et al. (2017) also used the Farinograph to investigate the dough rheology and properties of rice breads as affected by addition of hydrocolloids and emulsifiers. Control bread was prepared using commercial rice flour, potato starch, fresh yeast, sunflower oil, dry milk, salt, and sugar. Experimental samples were prepared using the following additives at a 2% level, alone or in combination: HPMC, agar gum, guar gum, pectin, citrus fiber, diacetil tartaric acid ester of monoglycerides (DATEM), and glyceryl monostearate. All the additives (both hydrocolloids and emulsifiers) increased the water absorption. The greatest water absorption values were obtained for HPMC-containing dough samples. The addition of hydrocolloids also increased dough consistency due to increases in the viscosity of the doughs (Mudgil et al., 2011). Different behavior was observed for development time according to the type of hydrocolloid. Indeed, pectin, agar gum, and citrus fiber increased this index, whereas guar gum and HPMC (alone or in combination with pectin) decreased the dough development time. Adding hydrocolloids to the control formulation promoted an increase in the degree of softening index, suggesting lower dough capacity to withstand mixing stress.

As a general conclusion, it has been observed that hydrocolloids, when added in the correct amount, improve the mixing properties of GF systems, and that the effects are proportional to the hydrocolloid addition level. These improvements are also observed in the related final products. However, what has been observed for rice is not always true for other grains. In fact, Elkhalifa et al. (2007) investigated the dough mixing properties of sorghum flour and how they are affected by the addition of guar and Arabic gums, alone or in combination. In the Farinograph, the addition of guar gum alone increased the water absorption, dough development time, and stability. But the addition

of Arabic gum, alone or in combination with guar gum, decreased water absorption, dough development time, and stability, suggesting a decrease in dough mixing performance.

9.3 PSEUDOCEREALS

Pseudocereals have become an important ingredient in many food applications over the years. As their uses increase, particularly for baking applications, it is important to investigate their rheological properties. The Farinograph has been used to investigate the dough mixing properties of pseudocereals and their blends. When pea flour, buckwheat flour, and their blends (60% pea flour to 40% buckwheat flour and vice versa) were studied for their rheological properties, the Farinograph showed that the consistency of buckwheat flour and pea-buckwheat flour blends was similar, whereas pea flour demonstrated significantly lower consistency ([Beitane et al., 2015](#)). The addition of buckwheat flour to pea flour increased the consistency of the flour blends but did not increase water absorption. Dough development time was significantly longer for buckwheat flour than for wheat flour, pea flour, and the pea-buckwheat flour blends. Buckwheat flour has a higher stability compared to both wheat and pea flours.

[Sluková et al. \(2017\)](#) also studied the mixing properties of buckwheat flour using the Farinograph. Doughs were prepared using the Farinograph according to the constant flour weight procedure ([AACC Approved Method 54-21.02, 2011](#)) and sampled as mixing progressed. The dough development time for buckwheat flour was 10 min, although it was impossible to achieve a consistency of 500 BU. The maximum torque reached was 300 BU. The authors also observed that the water added to the flour had to be added over a period of 2 min to be able to achieve 300 BU. When the water was added within the first 20 s of the test, as is standard for wheat dough, the buckwheat dough did not achieve the desired consistency, likely due to either the physical nature of the buckwheat proteins (e.g., physical structure of protein bodies) or some aspect of their composition.

The rheological properties of germinated amaranth flour have also been evaluated using the Farinograph ([Paredes-López et al., 1988](#)). In this study, the water absorption of amaranth seeds decreased from 71% to 60% in the first 12 h of germination but increased afterwards with an increase in germination time. A similar observation was made with regards to mixing stability, although the Farinograph arrival time was not affected by germination.

9.4 PULSES

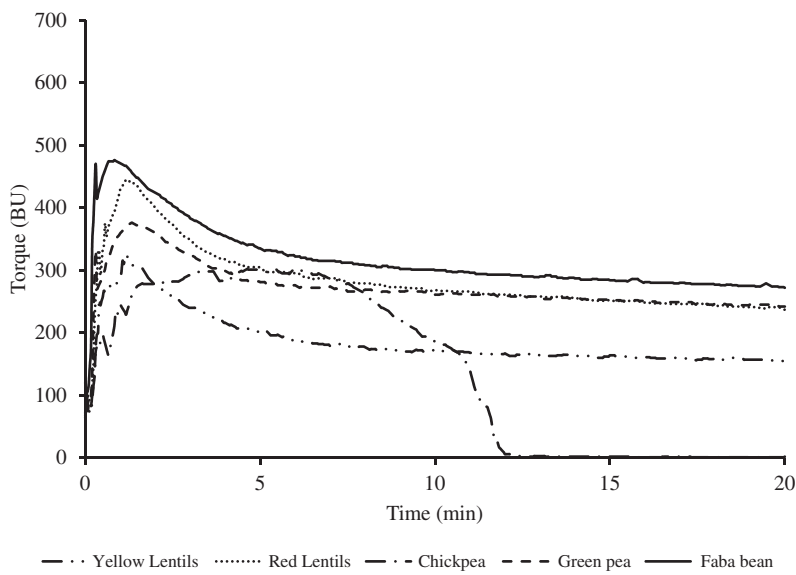
Legumes or pulses are dry edible seeds of plants belonging to the *Fabaceae* (*Leguminosae*) family, which includes field peas, dry beans, lentils, chickpeas, and faba beans. Recently, they have been widely used in food products such as pasta, bread, and other bakery products, thanks to their agronomic and nutritional properties (Bresciani and Marti, 2019). Specifically, pulses are an inexpensive, sustainable source of proteins and other key nutrients, including resistant starch (Hall et al., 2017). Pulses also contain about twice as much protein as cereal grains, with the most abundant storage proteins being globulins and albumins. Although pulse proteins have low levels of sulfur amino acids and do not form gluten, they are interesting from a technological standpoint due to their functional properties, including solubility, water holding capacity, and emulsifying and foaming properties (Foschia et al., 2017).

It is important to efficiently hydrate pulse flours for proper dough development. Figs. 9.2 and 9.3 show the farinograms of different pulse flours hydrated at 50% (Fig. 9.2) and 60% (Fig. 9.3) using the 50g bowl. At 50% hydration, it was observed that none of the pulse flours reached 500 BU. Chickpea and yellow lentil flours achieved maximum torque values around 300 BU, whereas green pea and red lentil flours ranged between approximately 370–450 BU, respectively. Faba bean flour had the greatest torque (approximately 470 BU) at 50% hydration. Interestingly, chickpea doughs did not produce any torque after 12 min of mixing.

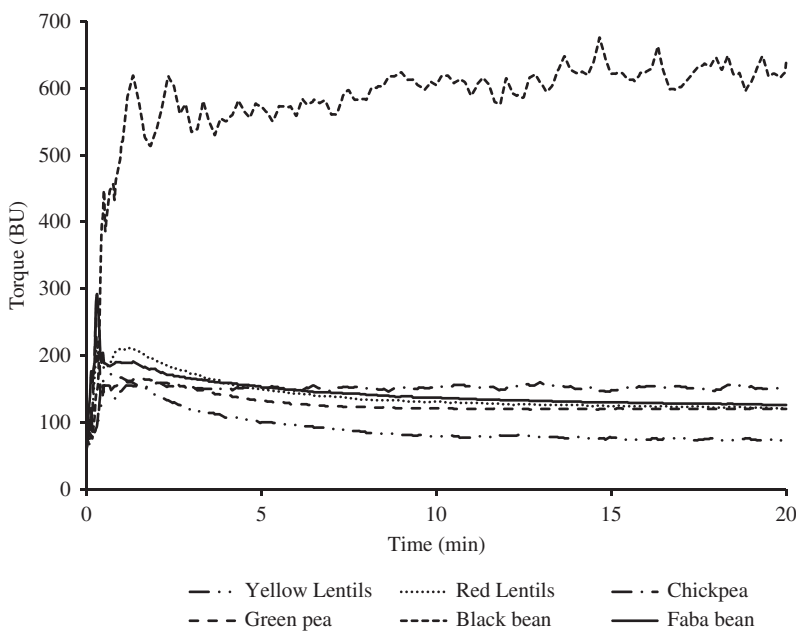
It is important to note that torque for black bean dough at 50% hydration was above the range of the torque specifications for the Farinograph (i.e., it broke the shear pin) and the full run was not completed.

However, when the hydration was increased from 50% to 60%, the torque for all the pulses decreased, as seen in Fig. 9.3. Almost all the pulse samples had maximum torques below 200 BU, while that of black bean dough was about 600 BU. While the torque for all the samples decreased as mixing went on, that of black bean remained mainly constant. In fact, it increased slightly as mixing time increased. It was also observed from Fig. 9.3 that as hydration level increased, the torque differences between the pulses became more subtle. Hence a lower hydration level, probably around 50%, would be recommended to differentiate pulses.

Table 9.2 shows the Farinograph parameters of the samples, specifically dough development time and stability, at both 50% and 60% hydration. The effect of hydration level on mixing properties was relatively similar in all the samples, excluding black bean and chickpea doughs. Specifically,



■ FIG. 9.2 Farinogram of pulses using a 50% hydration level.



■ FIG. 9.3 Farinogram of pulses using a 60% hydration level.

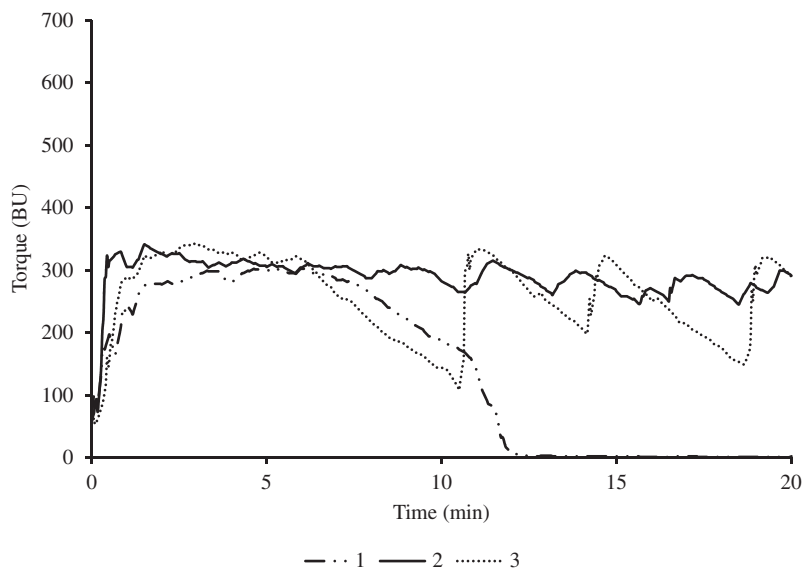
Table 9.2 Farinograph parameters of samples.

Sample	Hydration level (%)	Dough development time (min)	Dough stability (min)
Black bean	50	1.4	1.3
	60	14.7	18.7
Faba bean	50	0.9	1.0
	60	0.3	0.1
Green pea	50	1.4	1.3
	60	0.3	0
Red lentil	50	1.2	0.6
	60	0.3	1.2
Yellow lentil	50	1.2	0.5
	60	0.8	0.9
Pregelatinized yellow lentil	50	1.3	0.8
Chickpea	50	6.2	6.2
	60	13.0	19.5
Pregelatinized chickpeas	50	0.9	0

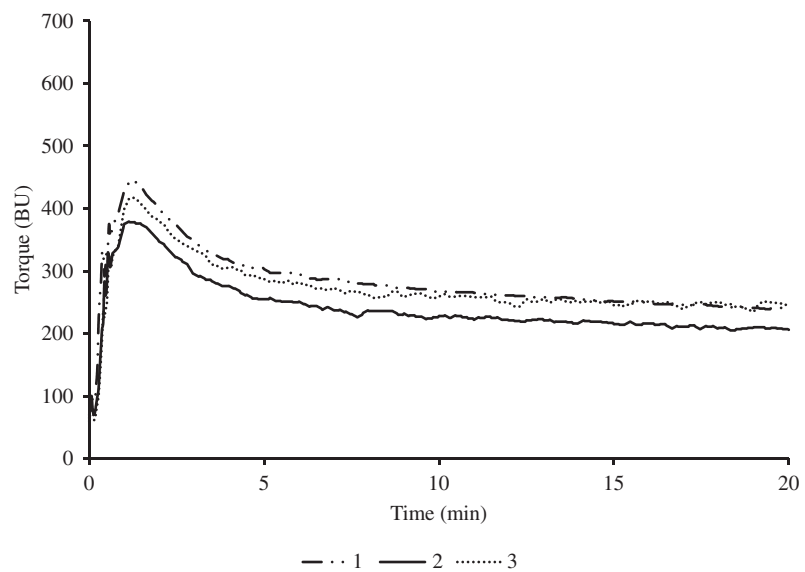
in the case of yellow and red lentils, faba bean, and green pea doughs, both the dough development time and stability decreased as the hydration level increased. The opposite trend was observed in the case of chickpea and black bean doughs (Table 9.2).

Figs. 9.4 and 9.5 show the farinograms of chickpea and red lentil flours from three different suppliers as an example of ingredient variability. It can be seen from these figures that there was significant variability in the dough mixing properties of chickpea flours, even though they were all hydrated at 50% (Fig. 9.4). In the case of red lentil flours, despite all the samples showing a similar curve profile, the maximum consistency ranged from 376BU and 443BU for mill 2 and mill 3, respectively. Because differences in dough consistency would suggest differences in water absorption capacity, it is reasonable to assume that flours from mill 2 and mill 3 will behave differently during processing.

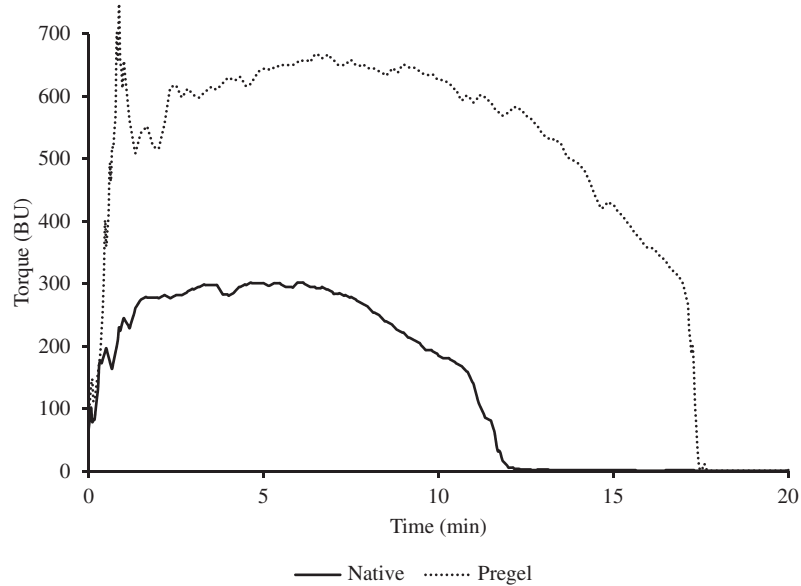
As with cereals, pulses are often used in GF formulations as pregelatinized flours. Pregelatinizing pulse samples can have different effects on the dough mixing properties. Figs. 9.6 and 9.7 show the effects of pregelatinization on the rheological properties of doughs made from chickpea and red lentil flours. All flours were hydrated at 50%. It was observed that



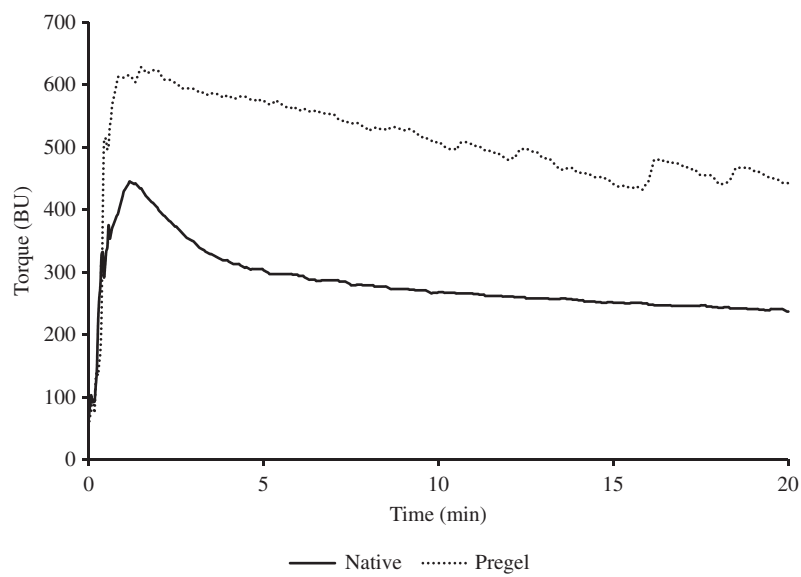
■ FIG. 9.4 Farinograms of chickpea flours from three different mills at a hydration level of 50%.



■ FIG. 9.5 Farinograms of red lentil flours from three different mills at a hydration level of 50%.



■ FIG. 9.6 Farinograms of pregelatinized and raw (native) chickpea flour at a hydration level of 50%.



■ FIG. 9.7 Farinograms of pregelatinized and raw (native) red lentil flour at a hydration level of 50%.

pregelatinization increased the torques of both pulses without affecting the overall mixing profiles. It is well known that thermal treatment carried out to promote starch gelatinization enhances the water absorption and water holding capacity of the related flour.

9.5 CONCLUSIONS

The Farinograph has been demonstrated to be very useful in the determination of the rheological or dough mixing properties of GF products. Though not widely used for GF flours as compared to gluten-containing flours, the Farinograph has been successfully used by researchers to investigate how the addition of hydrocolloids to GF flours or thermal treatments (e.g., pregelatinization) affect their rheology. It has also been used to study the impact of GF flour blends on dough rheology. Some researchers have optimized the hydration level based on a standard torque of 500BU, whereas others have optimized the torque value based on baking trials, making it difficult at times to make comparisons among the results from different studies.

More recently, the increased interest in using pulses in GF formulations—due to their positive agronomic, environmental, and nutritional features—accounts for the need to develop methods for evaluating the mixing properties of pulse flours.

Although the indices assessed by the Farinograph are designed for gluten-containing systems, it is important to note that they provide important and useful information for the study of GF dough. In fact, optimal water absorption, proper mixing time, and good stability are positively correlated to desired characteristics, such as volume and crumb texture, as far as bread quality is concerned. However, as more work is done with the FarinoAdd-S300 to develop and standardize methodology for GF flours and doughs, new opportunities for research, product development, and quality control of GF ingredients will expand on our current understanding of GF systems and their applications.

ACKNOWLEDGMENT

This research is part of the project “MIND FoodS HUB (Milano Innovation District Food System Hub): Innovative concept for the eco-intensification of agricultural production and for the promotion of dietary patterns for human health and longevity through the creation in MIND of a digital Food System Hub”, cofunded by POR FESR 2014-2020_BANDO Call HUB Ricerca e Innovazione, Regione Lombardia.

REFERENCES

- AACC Approved Methods of Analysis, 2011. Method 54-21.02. Rheological Behavior of Flour by Farinograph: Constant Flour Weight Procedure, eleventh ed. Cereals & Grains Association, St. Paul, MN, USA, <https://doi.org/10.1094/AACCIIntMethod-54-21.02>. Approved January 6, 2011.
- Amin, T., Naik, H.R., Hussain, S.Z., Makroo, H.A., Rather, S.A., 2020. Effect of storage materials and duration on the physicochemical, pasting and microstructural properties of low glycemic index rice flour. *Int. J. Biol. Macromol.* 162, 1616–1626.
- Ayernor, G.S., Steinberg, M.P., 1977. Hydration and rheology of soy-fortified pregelled corn flours. *J. Food Sci.* 42 (1), 65–69.
- Beitane, I., Krumina-Zemture, G., Sabovics, M., 2015. Technological properties of pea and buckwheat flours and their blends. *Res. Rural Dev.* 1, 137–142.
- Bender, D., Schönlechner, R., 2020. Innovative approaches towards improved gluten-free bread properties. *J. Cereal Sci.* 91, 102904.
- Bresciani, A., Marti, A., 2019. Using pulses in baked products: lights, shadows, and potential solutions. *Foods* 8 (10), 451.
- Cappa, C., Lucisano, M., Mariotti, M., 2013. Influence of psyllium, sugar beet fibre and water on gluten-free dough properties and bread quality. *Carbohydr. Polym.* 98 (2), 1657–1666.
- Cuevas, R., Puche, C., 1986. Study of the rheological behaviour of corn dough using the Farinograph. *Cereal Chem.* 63 (4), 294–297.
- Elkhalifa, A.E.O., Mohammed, A.M., Mustafa, M.A., Abdullahi, H., E., 2007. Use of guar gum and gum Arabic as bread improvers for the production of bakery products from sorghum flour. *Food Sci. Technol. Res.* 13 (4), 327–331.
- Foschia, M., Horstmann, S.W., Arendt, E.K., Zannini, E., 2017. Legumes as functional ingredients in gluten-free bakery and pasta products. *Annu. Rev. Food Sci. Technol.* 8, 75–96.
- Hall, C., Hillen, C., Garden Robinson, J., 2017. Composition, nutritional value, and health benefits of pulses. *Cereal Chem.* 94 (1), 11–31.
- Hegazy, A.I., Ammar, M.S., Ibrahim, M.I., 2009. Production of Egyptian gluten-free bread. *World J. Dairy Food Sci.* 4 (2), 123–128.
- Lazaridou, A., Duta, D., Papageorgiou, M., Belc, N., Biliaderis, C.G., 2007. Effects of hydrocolloids on dough rheology and bread quality parameters in gluten-free formulations. *J. Food Eng.* 79 (3), 1033–1047.
- Mir, S.A., Shah, M.A., Naik, H.R., Zargar, I.A., 2016. Influence of hydrocolloids on dough handling and technological properties of gluten-free breads. *Trends Food Sci. Technol.* 51, 49–57.
- Mossman, A.P., Fellers, D.A., Suzuki, H., 1983. Rice stickiness. I. Determination of rice stickiness with an Instron tester. *Cereal Chem.* 60 (4), 286–292.
- Mudgil, D., Barak, S., Khatkar, B.S., 2011. Effect of hydrocolloids on the quality characteristics of tomato ketchup. *Carpatian J. Food Sci. Technol.* 3, 39–43.
- Nicolae, A., Radu, G.L., Belc, N., 2016. Effect of sodium carboxymethyl cellulose on gluten-free dough rheology. *J. Food Eng.* 168, 16–19.
- Nour, V., Tuțulescu, F., Ionică, M.E., Corbu, A.R., 2017. Dough rheology and properties of gluten-free rice breads as affected by addition of hydrocolloids and emulsifiers. *Carpatian J. Food Sci. Technol.* 9 (4).

- Paredes-López, O., Cáraez-Trejo, A., Pérez-Herrera, S., González-Castañeda, J., 1988. Influence of germination on physico-chemical properties of amaranth flour and starch microscopic structure. *Starch-Stärke* 40 (8), 290–294.
- Roman, L., Belorio, M., Gomez, M., 2019. Gluten-free breads: the gap between research and commercial reality. *Compr. Rev. Food Sci. Food Saf.* 18 (3), 690–702.
- Sahin, A.W., Wiertz, J., Arendt, E.K., 2020. Evaluation of a new method to determine the water addition level in gluten-free bread systems. *J. Cereal Sci.* 93, 102971.
- Sivaramakrishnan, H.P., Senge, B., Chattopadhyay, P.K., 2004. Rheological properties of rice dough for making rice bread. *J. Food Eng.* 62 (1), 37–45.
- Sluková, M., Levková, J., Michalcová, A., Skřivan, P., 2017. Effect of the dough mixing process on the quality of wheat and buckwheat proteins. *Czech J. Food Sci.* 35 (6), 522–531.

Using the Farinograph and other Brabender torque rheometers to measure the rheological properties of complex biological materials

R.K. Connelly^a, S. Burlawar^a, D.J. Klingenber^b, and C.T. Scott^{b,*}

^a*International Flavors and Fragrances, Inc., St. Louis, MO, United States* ^b*Department of Chemical and Biological Engineering,
University of Wisconsin, Madison, WI, United States*

CHAPTER OUTLINE

10.1 Introduction	128
10.2 Equipment	129
10.2.1 Torque rheometer basics	129
10.2.2 Brabender torque rheometers and accessories in use in the food industry	129
10.2.3 Brabender torque rheometer modifications for high solids biomass research	131
10.3 Procedure	132
10.3.1 Calibration procedure	132
10.3.2 Fitting data with rheological models	133
10.3.3 Data collection	134
10.3.4 Sample results	138
10.4 Representative results from high solids biomass research	143
10.4.1 Rheology of suspensions of acid-hydrolyzed corn stover	143
10.4.2 Effect of rheological modifiers	145
10.4.3 Effect of biomass type	146
10.4.4 Effect of enzymatic hydrolysis	148

*Formerly, U.S. Forest Service Forest Products Lab, 1 Gifford Pinchot Dr., Madison, WI 53706, United States.

10.5 Conclusions 149**Appendices 150**

Appendix I: Instrument calibration 150

Appendix II: Fitting rheological models 155

References 158**10.1 INTRODUCTION**

The Brabender website describes the Farinograph as a double arm torque rheometer. Torque rheometers of the double arm kneading type are ideal for following the rheological changes of very viscous, elastic, or rubbery materials that start out as a semisolid mass with liquid or powder additives during mixing. They work by applying a blending process that combines and keeps the materials in the mixing zone, as well as potentially heating them to create uniform bulk properties ([Green and Southard, 2019](#)). As such, it is possible to use the Farinograph and other double arm torque rheometer tools available from C.W. Brabender with well-established mixer rheometry approaches ([Cullen and Connolly, 2009](#)) to define the rheology of dough revealed in a more fundamental rheological fashion. Mixer rheometry can also be used to study the rheological properties of difficult-to-measure biological materials such as fruit pastes and fillings containing small seeds, fibrous shredded meat fillings and pastes, and lignocellulosic biomass slurries. The goal of this chapter is to lay out how to use mixer rheometer theory with Brabender torque rheometers, mixing bowls, and blades to measure the fundamental rheological properties of difficult-to-measure biological materials including dough, as well as to share how these tools have been used to advance the conversion of lignocellulosic biomass materials to a host of economically valuable products.

Lignocellulosic biomass is a nanoscale assembly of cellulose, hemicellulose, and lignin polymers. The extraction and conversion of these components to fibers, carbohydrates, or other chemicals have significant economic value. The cost of these products from biomass can be reduced by increasing the concentration of insoluble solids in various process operations by reducing the energy requirements associated with water removal. However, increasing solids concentration substantially increases the apparent viscosity of biomass slurries, which makes mixing and conveying operations more challenging. Most biomass conversion processes require several stages of chemical, thermal, and mechanical treatments for particle-size reduction, reaction of treatments, and extraction of products. Each of these unit operations requires an efficient method of conveying and treating

materials. Therefore measures of the rheological properties of biomass slurries throughout various stages of treatments facilitate the design, characterization, and implementation of industrial biorefining operations.

10.2 EQUIPMENT

10.2.1 Torque rheometer basics

Brabender torque rheometers consist of two connected cylindrical chambers that contain blades (impellers) that rotate. The drive shaft rotates one blade directly (blade 1, the driven blade). A gear box is used to rotate the other blade (blade 2, the follower blade). The driven blade rotates with the rotational speed of the drive shaft, while the follower shaft rotates at a different rotational speed, which depends on the gear box. The ratio of the speeds is $b = \Omega_2/\Omega_1$.

Materials are added within the chambers and are mixed or sheared as the blades rotate. The drive shaft torque required to rotate the blades at a given speed can be measured. We describe later how the torque and rotation rate can be used to determine apparent rheological properties.

10.2.2 Brabender torque rheometers and accessories in use in the food industry

The familiar tangential rotating twin sigma blade mixing heads in the 10, 50, and 300 g flour sizes that are the heart of the Farinograph provide a mixing action that shears, stretches, folds, divides, and recombines the dough mass and is well suited for developing dough and understanding its kneading properties. However, by making use of some of the more versatile drive units offered by C.W. Brabender, such as the Do-Corder, Plasti-Corder Lab-station, ATR Plasti-Corder Advanced Torque Rheometer, the Intelli-Torque Plasti-Corder Torque Rheometer, and the MetaStation 4E ([Fig. 10.1A](#)), the Farinograph mixer attachments can be further utilized to become a more general torque rheometer suitable for measuring the rheological properties of a broad range of food and biological materials. In addition, Brabender offers a range of other blade and mixing bowl types, such as the Universal 3 piece mixer with exchangeable cam, Banbury, sigma, triangular lobe, and roller blades ([Fig. 10.1B and C](#)), which can be combined with the previously mentioned drive units to provide different shear and compounding profiles to expand beyond the needs of dough mixing to include difficult-to-measure food and biomass materials that require more intense shear, shredding, or wiping to mix and compound ([Green and Southard](#),



FIG. 10.1 (A) MetaStation 4E with (B) 50 mL Universal 3 piece closed bowl mixer, and (C) the exchangeable roller, cam, Banbury, sigma and triangular lobe blade sets. (Used with permission from C. W. Brabender Instruments, Inc., South Hackensack, NJ USA and Brabender GmbH and Co. Kg, Duisburg, Germany.)

2019). The use of instrument control and data collection software such as the proprietary MixMB from the Brabender-MetaBridge Software for Mixer Material Evaluation allows for easy access to the torque and speed data needed to make use of the theory, which will be described in the rest of the chapter, for evaluating the rheological behavior of what are often difficult-to-measure food and biological materials such as biomass.

10.2.3 Brabender torque rheometer modifications for high solids biomass research

Torque rheometers have been used to measure rheological properties of diverse materials, such as polymer melts (Blyler and Daane, 1967; Bousmina et al., 1999), food pastes (Cullen and Connelly, 2009), and wet granulations of pharmaceutical excipients (Hancock et al., 1994). For our purposes, we redesigned a two-piece Brabender Plasticorder (type six, C.W. Brabender Instruments) to specifically measure the rheological properties of high-solids biomass suspensions with solids content between 20% and 40%. This design incorporates a water-jacketed chamber for temperature control (20–90°C), a thermowell to measure the temperature of the sample within the chamber (indicated as P in Fig. 10.2B), a polycarbonate cover plate to view mixing, and Teflon seals to prevent water leakage. We selected lobed-cam impellers to replicate the intense shear mixing that occurs in the kneading zones of a twin-screw extruder. A small film of vacuum grease was applied to the shafts as an additional water seal and to reduce friction in the mixer head bushings. We further reconfigured the gear head drive system (Fig. 10.2A) to incorporate an in-line torque sensor (e.g., a Futek Model TRS605, 20 Nm capacity), a flex-shaft coupling (Model no. FCR10-4-4-A, MC7 series, Helical Products), and a torque limiter (Dalton Gear). There is a 3:2 differential in rotational speed between the left impeller (driven) and the right impeller (follower), i.e., $b = 2/3$. The capacity of the mixing chamber, when the impellers are installed, is approximately 100 mL.

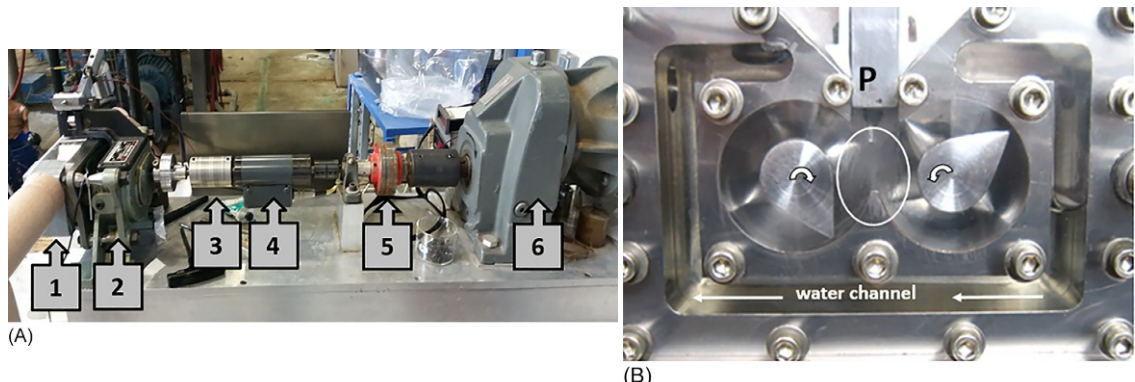


FIG. 10.2 (A) Drive system for the UW/FPL torque rheometer. Significant modifications: (1) Stainless steel mixing chamber shown in (B); (2) Standard 3:2 Plasticorder mixing gear drive; (3) Helical flex-shaft coupling; (4) In-line torque sensor; (5) Torque limiter; (6) 5 hp direct-drive DC motor with 30:1 gear reducer. (B) Front view of the stainless steel torque rheometer with a water channel for heating and cooling. *Rotation arrows* indicate the counter-rotation direction of impellers. The right impeller rotates at two-thirds the speed of the left impeller. The circle indicates location of intense mixing and plug formation. The plunger (P) contains a thermowell to measure the internal chamber temperature and two white Teflon seals to contain the wet biomass.

10.3 PROCEDURE

10.3.1 Calibration procedure

Torque-rotation rate data obtained with a torque rheometer can be converted to conventional rheological quantities using a calibration procedure developed by [Goodrich and Porter \(1967\)](#). The torque rheometer is represented by two sets of concentric cylinders, illustrated in [Fig. 10.3](#). The outer cylinder radius, R_o , is equated with the actual cylindrical bowl radius. The effective inner radius, R_i , is determined by equating the measured torque for a Newtonian fluid with that calculated from the solution of the Navier-Stokes equation ([Ehrhardt, 2008](#)). [Bousmina et al.](#) showed that such a calibration with a Newtonian fluid gives equivalent results to that obtained using a more sophisticated analysis with power-law fluids ([Bousmina et al., 1999](#)). Once the effective inner radius is obtained, the measured drive shaft torque (Γ) and rotation rate (Ω) data can be transformed into apparent shear stress (τ) and apparent shear rate ($\dot{\gamma}$) data for the driven impeller (left impeller for [Fig. 10.3](#)) for a torque rheometer with a speed ratio of $b = \Omega_2/\Omega_1$

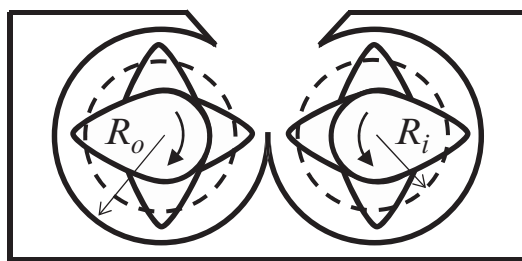
$$\tau = \frac{1}{1 + b^2} \frac{\Gamma}{2\pi R_a^2 h} \quad (10.1)$$

$$\dot{\gamma} = \frac{2R_i R_o \Omega}{\left(\frac{1}{\kappa} - \kappa\right) R_a^2} \quad (10.2)$$

where $R_a \equiv (R_i + R_o)/2$ is the midpoint radius, h is the impeller depth, and $\kappa \equiv R_i/R_o$. The apparent viscosity is then

$$\eta \equiv \frac{\tau}{\dot{\gamma}} \quad (10.3)$$

This approach is consistent with that employed in commercial rheometers. The derivations of Eqs. [\(10.1\)](#), [\(10.2\)](#) are discussed in more detail in [Appendix I](#).



■ FIG. 10.3 Schematic diagram of the torque rheometer shown in [Fig. 10.2B](#).

10.3.2 Fitting data with rheological models

Torque-rotation rate data can also be fit with common rheological models, such as the power-law and Bingham models, to represent the data and to extract the model parameters. The power-law model is commonly used for polymer solutions (Bird et al., 2015). Here, the local shear stress τ_{loc} is related to the local shear rate $\dot{\gamma}_{\text{loc}}$ by

$$\tau_{\text{loc}} = m\dot{\gamma}_{\text{loc}}^n \quad (10.4)$$

where m is the consistency coefficient and n is the flow behavior index. The predicted drive shaft torque for a torque rheometer is $\Gamma = \Gamma_1 + b\Gamma_2$ (Γ_1 and Γ_2 are the torques on the driven and follower impellers), which simplifies to

$$\Gamma = 2\pi R_o^2 L m \left[\frac{2}{n(\alpha^{-2/n} - 1)} \right]^n (1 + b^{n+1}) \Omega^n \quad (10.5)$$

or

$$\ln \Gamma = \ln \left\{ 2\pi R_o^2 L m \left[\frac{2}{n(\alpha^{-2/n} - 1)} \right]^n (1 + b^{n+1}) \right\} + n \ln \Omega \quad (10.6)$$

where $\alpha \equiv R_i/R_o$. Thus by fitting torque-rotation rate data with the preceding equation, the parameters m and n can be extracted. Eq. (10.6) suggests that a plot of $\ln \Gamma$ vs. $\ln \Omega$ will be a straight line for a power-law fluid. The parameter n is obtained directly from the slope; the parameter m can then be determined from the intercept.

For materials with a yield stress, such as concentrated lignocellulosic biomass suspensions, one can employ the Bingham model. Here the local shear stress is related to the local shear rate by

$$\tau_{\text{loc}} = \tau_0 + \eta_{\text{pl}} \dot{\gamma}_{\text{loc}} \quad (10.7)$$

where τ_0 is the yield stress and η_{pl} is the plastic viscosity. The predicted torque is $\Gamma = \Gamma_1 + b\Gamma_2$, where the torque-rotation rate relationship for concentric cylinder geometry k is ($k = 1, 2$)

$$\Gamma_k = 4\pi R_i^2 h \eta_{\text{pl}} \frac{\Omega_k + \frac{\tau_0}{\eta_{\text{pl}}} \ln \left(\frac{r_0}{R_i} \right)}{1 - \left(\frac{R_i}{r_0} \right)^2} \quad (10.8)$$

where r_0 is the location where the velocity goes to zero, which is the minimum of R_o and the solution to the equation

$$\left(\frac{r_0}{R_i} \right)^2 - 1 = \frac{2\eta_{\text{pl}}\Omega_k}{\tau_0} + \ln \left[\left(\frac{r_0}{R_i} \right)^2 \right] \quad (10.9)$$

By fitting the preceding model for the predicted torque to experimental torque-rotation rate data, the yield stress and plastic viscosity can be extracted.

The preceding relationships between the torque and rotation rate for the power-law and Bingham models are derived in more detail in [Appendix II](#).

10.3.3 Data collection

10.3.3.1 Mixing method for measuring rheology of wheat flour dough at peak development

The rheological properties of wheat flour dough are both strain and rate dependent, as well as time dependent during the hydration stage of dough development. Therefore each individual point in a shear stress-shear rate curve must be independently measured using carefully controlled hydration and strain input protocols. [Connelly and McIntier \(2008\)](#) present a well-defined approach that features the nonstandard mixing scheme shown in [Fig. 10.4](#), which allows for consistent, low-speed hydration conditions for all dough samples, followed by dough development to peak torque for a given mixing speed using a constant dough weight. The water additions to the dough formulations were determined based on the water required to reach a torque of 600 Brabender units (BU) at peak consistency on a standard mixing curve as done in AACCI Method #54-22.01 ([AACCI International, 2010](#)). The flour

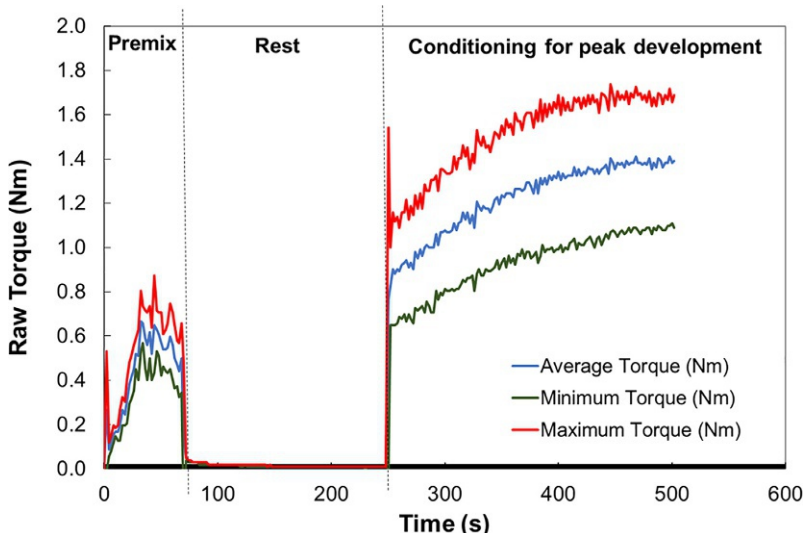


FIG. 10.4 Example torque results for a complete mixing cycle of the flour/water formula dough in the 50 g Farnograph mixing bowl from [Connelly and McIntier \(2008\)](#), including a slow premix for 68 s at a driven blade speed of 20 rpm where the water was quickly added during the first 8 s of the premix, followed by a 3-min rest time before mixing at the standard slow blade speed of 63 rpm for 256.8 s to peak development.

moisture content was monitored, and the formulations adjusted as needed to keep the total moisture and flour solids constant in all tests with a constant total dough weight. The torque at peak development was recorded for each given mixing speed. Alternatively, the torque at a constant energy input or number of revolutions can be used to represent equivalent development (Connelly and McIntier, 2008; Anderssen et al., 1998), which may be easier to use for soft flour doughs that reach peak development quickly or hard flour doughs at lower speeds where the exact peak is difficult to determine. To use this measurement approach for determining the nonlinear rheological properties of wheat flour dough, all mixing speeds used must exceed the critical mixing speed for complete dough development (Connelly and McIntier, 2008; Kilborn and Tipples, 1972).

The measurement approach described previously was applied to both a flour-water dough formulation and a yeasted bread dough formulation variation of that in “Basic Straight-Dough Bread-Baking Method—Long Fermentation” (AACCI Method #10-09.01) (AACC International, 2010) shown in Table 10.1. Bay State Bouncer is a high-protein (13.8%), straight-grade, hard red spring wheat flour from the 2004 crop year that was donated unenriched and untreated by Bay State Milling (Winona, Minnesota, United States). It has a long development time, long stability, and slow rate of breakdown during mixing (Connelly and McIntier, 2008). Table 10.2 includes the rpm and average peak torque results for replicates from Connelly and McIntier (2008) for each formulation at the designated peak development mixing time for each mixing speed using 80 g of dough in a 50 g Farinograph type 5 mixing head with an Intelli-torque drive unit. The minimum critical mixing speed in the Farinograph for this flour was found to be 43 rpm. Below that mixing speed, the energy input to peak

Table 10.1 Dough formulas with water percentage based on 14% flour wet basis moisture content and 600 BU peak torque in the Farinograph at standard mixing speed of 63 rpm following AACCI Method No. 54-22.01 (AACC International, 2010).

Ingredient	Flour/water dough (% of flour)	Basic straight-dough (% of flour)
Bay State Bouncer flour	100	100
Distilled water	59.32	59.97
SAF Instant yeast		2
C and H 100% cane sugar		5
Morton iodized salt		1

Table 10.2 Calculation of apparent viscosity using Farinograph peak development torque data from Connolly and McIntier (2008).

Drive impeller		Flour/water dough @ peak development			Basic straight-dough @ peak development		
Mixing speed (rpm)	Shear rate (s^{-1})	Maximum torque (BU)	Shear stress (Pa)	Apparent viscosity (Pas)	Maximum torque (BU)	Shear stress (Pa)	Apparent viscosity (Pas)
23	16	425	2549	162	363	2180	139
28	19	490	2943	154	417	2504	131
33	23	500	3003	133	451	2708	120
38	26	577	3462	133	523	3138	121
43	29	616	3696	126	530	3183	108
48	33	613	3681	112	557	3342	102
53	36	685	4111	113	557	3342	92
63	43	710	4261	99	601	3609	84
73	50	734	4405	88	655	3930	79
83	57	694	4168	73	682	4096	72
88	60	802	4816	80	670	4021	67
93	64	775	4654	73	694	4168	66
98	67	836	5020	75	665	3994	60
103	70	802	4816	68	699	4198	60
108	74	841	5050	68	712	4273	58
113	77	809	4858	63	734	4405	57
118	81	814	4888	61	702	4213	52
133	91	856	5138	56	748	4492	49
153	105	898	5390	52	800	4801	46
183	125	996	5978	48	751	4507	36
203	139	1072	6435	46	731	4390	32

The duplicate maximum torque results were averaged.

development decreased for both formulations and the loaf weight/volume after baking the yeasted formulation increased due to reduced loaf volume (Connolly and McIntier, 2008).

10.3.3.2 Mixing method for measuring rheology of high solids biomass

Before starting an experiment, the impellers shown in Fig. 10.2B are removed from the rheometer and cleaned. Custom-made Teflon Belleville washers are inserted at the base of the impellers, and a Teflon shim of the same thickness is placed at the back of the chamber housing to prevent water

leakage during a test. A thin film of vacuum grease is applied to the mixer bushings to minimize friction. The mixer is assembled and all seals are then conditioned by operating the torque rheometer empty over the range of test speeds. A no-load average torque and inherent variance are noted. This no-load average torque is subsequently subtracted from the raw test data prior to viscosity calculations. The inherent variance is typically within the resolution of the torque sensor. If the variance is larger, the mixer is disassembled and seals are renewed.

Mixer temperature is maintained by proportioning hot and cold water through the water chamber. Water temperature and chamber interior temperatures are measured with thermocouples, with the interior thermocouple inserted into a thermowell attached to the plunger (P). Torque and driven shaft speeds are measured with a torque transducer coupled directly to the gearbox shaft. A data acquisition system is used to record temperature, torque, and speed, typically at 5 Hz.

In a typical test of high-solids biomass ($> 10\%$), a total sample mass of 100 g is added to the mixer in 10 g increments to prevent the mixer from stalling or the torque transducer from overloading due to excessive initial torque levels. Once the mixing chamber is fully loaded, the plunger is inserted and a 600 s conditioning phase is undertaken at 110 rpm (Fig. 10.5). During the conditioning phase, a steady drop in torque is observed, which can be attributed to a certain degree of particle size reduction.

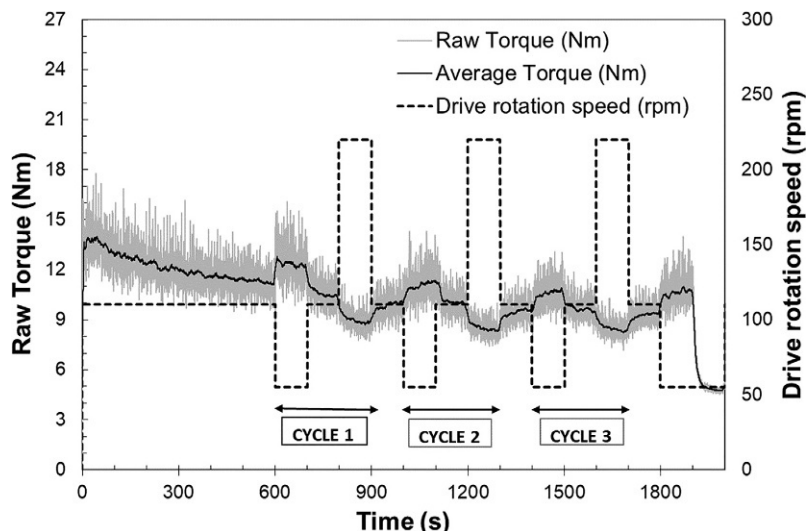


FIG. 10.5 Torque response for hammer-milled corn stover (29 wt.% solids). At 600 s, the drive rotation speed is cycled in three steps (55, 110, and 220 rpm) at 100 s intervals.

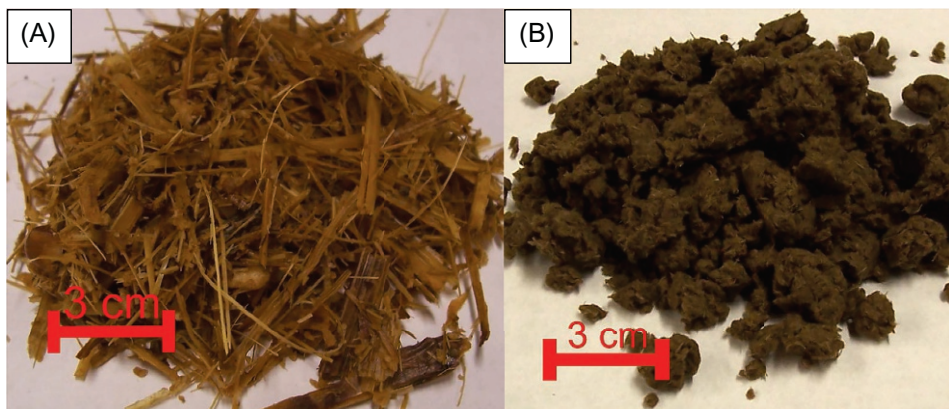


FIG. 10.6 (A) A photograph of hammer-milled corn stover prior to mixing in a torque rheometer; (B) a photograph of corn stover after undergoing the torque rheometry procedure (Samaniuk et al., 2015).

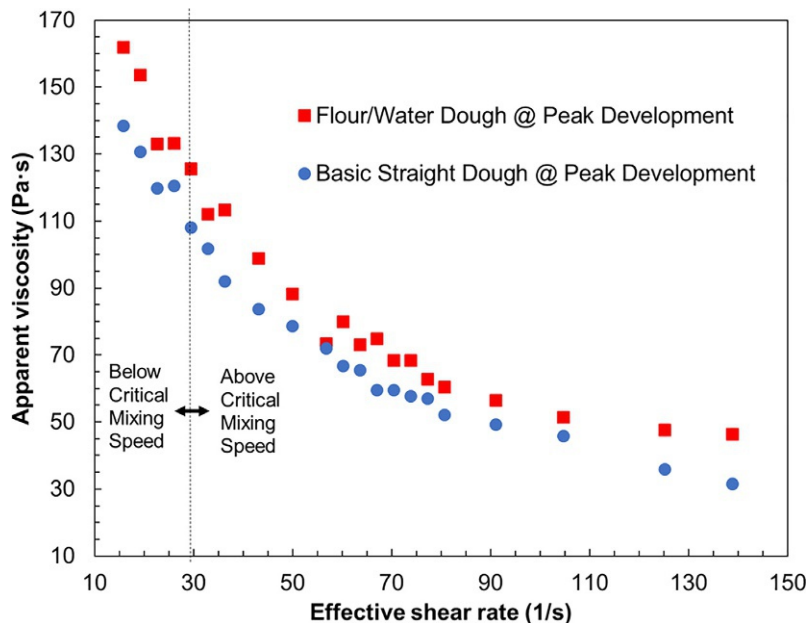
Three speed cycles (55–110–220 rpm) are then imposed on the biomass to elicit the torque/speed behavior at a particular temperature. The speed is held constant for 100 s at each speed level and the plateau torques (Table 10.4) are then used to calculate the apparent rheological properties (e.g., yield stress and plastic viscosity). As a matter of practice, the third speed cycle is used when reporting rheological properties. At the completion of each test, the material is collected (Fig. 10.6), weighed, and saved for further analysis (e.g., composition, moisture content, particle size distribution, etc.). This multispeed, multicycle test protocol can also be used to calculate specific mixing energy and specific mixing intensity as reported by Scott et al. (2011).

10.3.4 Sample results

10.3.4.1 Calculation of rheological properties of wheat flour dough at peak development

Noting that the slow blade is the driven blade in the type 5 Farinograph, the geometric parameters needed for the calculations are the gear ratio ($b = \Omega_2/\Omega_1 = 1.5$), outer cylinder radius ($R_o = 1.99$ cm), blade length ($h = 4.67$ cm), and the BU to Nm conversion factor of 0.00196 Nm/BU (Bloksma, 1984; see Appendix C: Legacy Information, Section III: Theoretical Aspects of the Farinograph). The effective inner radius ($R_i = 1.71$ cm) was taken from Menjivar et al. (1989).

The rheological properties for the flour/water and basic straight-dough formulations at peak development were calculated using the mixer viscometer approach for power-law fluids described in Section 10.3.2 and derived in Appendix II following these steps:



■ FIG. 10.7 Viscosity curves for doughs at peak development from data in Connelly and McIntier (2008). Note that the effective shear rate at the critical mixing speed of 43 rpm is 29 1/s.

1. The local shear stress (τ_{loc}) around the drive blade was calculated using Eq. (10.1), remembering to convert all lengths to meters and the torque from BU to Nm.
2. The effective local shear rate ($\dot{\gamma}_{loc}$) of the drive blade at the midpoint radius was calculated using Eq. (10.2), remembering to convert all lengths to meters and the blade speed to angular velocity using $\Omega = 2\pi(\text{rpm})/60$.
3. The apparent viscosity was calculated using Eq. (10.3). The results are listed in Table 10.2 and the viscosity curve is plotted in Fig. 10.7.
4. Power-law parameters in Eq. (10.4) for the two dough formulations at peak development were also estimated from the natural log of the angular velocity calculated from the rpm and each duplicate torque measurement converted to Nm from BU from Connelly and McIntier (2008) that was above the critical mixing speed of 43 rpm, as plotted in Fig. 10.8. Using Eq. (10.6), the flow behavior index (n) is the slope and the consistency coefficient (m) is calculated from the intercept of the linear fit, remembering to convert all lengths to meters, the torque from BU to Nm, and the blade speed to angular velocity using $\Omega = 2\pi(\text{rpm})/60$. The power-law parameters for the two formulations are shown in Table 10.3.

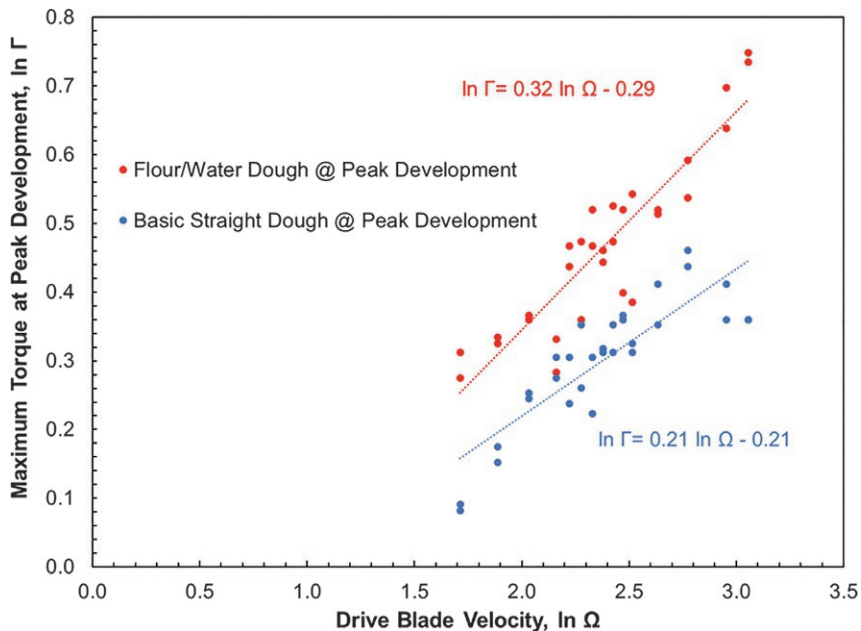


FIG. 10.8 Linearized power-law fits of the angular velocity (in rad/s) and torque (in N m) calculated from results in Connelly and McIntier (2008) for dough at peak development above the critical mixing speed of 43 rpm for complete dough development.

Table 10.3 Power-law model parameter fit results.

Power-law model parameter	Flour/water dough	Basic straight-dough
Consistency coefficient (m , Pa s n)	1535 ± 101	2092 ± 129
Flow behavior index (n)	0.32 ± 0.03	0.21 ± 0.02

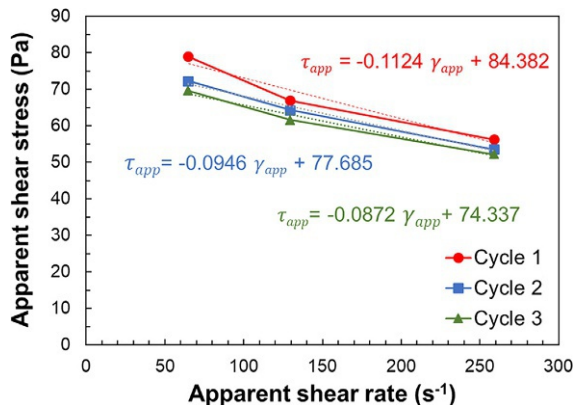
The first thing that becomes obvious in the viscosity curves in Fig. 10.7 is that the basic straight-dough formulation has a lower viscosity than the flour/water formulation, even though the actual wet basis moisture content of the dough is about 2% lower (due to the presence of the other ingredients), and even though the moisture addition levels were chosen to provide equivalent BU at 63 rpm on a standard mixing curve, as done in AACCI Method #54-22.01 (AACC International, 2010). This is likely due to the impact of both additional hydration time binding more of the free water, as seen by the increase in the torque for the flour/water dough at 63 rpm from the 600 BU used to set the water level, as well as the impact of the added ingredients,

including the yeast activity on the dough rheological properties even at these short times. In addition, the flow behavior index shows that the basic straight-dough is more shear thinning while the consistency coefficient is actually higher than the flour/water dough, so at low shear rates the viscosity curves will cross and the fully developed basic straight-dough would be more viscous than the fully developed flour/water dough. Therefore, the basic straight-dough will likely be stiffer than the flour/water dough at the low shear rates of hand kneading, while also being easier to work at the higher shear rates of a mechanical kneading mixer such as the Farinograph. This example shows that using multiple speeds in the Brabender torque rheometer using the Farinograph mixing head can give additional insight into the impact of formulation on dough rheology that can provide an explanation for processability differences of varying formulations.

10.3.4.2 Calculation of rheological properties of high solids biomass suspensions

The experimental data of torque as a function of time at various rotation rates for a 29% hammer-milled corn stover suspension presented in Fig. 10.5 can be converted to apparent rheological properties using the methods described in Section 10.3.1. This data was acquired using the modified torque rheometer illustrated in Fig. 10.2, which has a speed ratio of $b = 2/3$. Rheological properties can be obtained using the following steps (Ehrhardt, 2008; Samaniuk et al., 2011a, 2012, 2015; Ehrhardt et al., 2010; Samaniuk, 2012):

1. When the rotation rate is changed in the speed cycles illustrated in Fig. 10.5, the torque exhibits a transient change to a plateau value. The local shear stress (τ_{loc}) around the driven impeller can be calculated from this plateau torque using Eq. (10.1).
2. The apparent local shear rate ($\dot{\gamma}_{loc}$) for the driven impeller at the mid-point radius can be calculated from the rotation rate using Eq. (10.2). Note that to obtain the apparent shear rate in units of s^{-1} , the rotation rate must be in units of rad/s, i.e., $\Omega = 2\pi(\text{rpm})/60$. The apparent shear stress is plotted as a function of apparent shear rate in Fig. 10.9, for each of the speed cycles illustrated in Fig. 10.5.
3. The apparent viscosity can be calculated using Eq. (10.3).
4. The Bingham model parameters in Eq. (10.7) for the biomass suspension can be obtained from experimental data. If the plateau torque decreases with increasing rotation rate, then the parameters can be obtained by fitting the data for apparent shear stress as a function of apparent shear



■ FIG. 10.9 Apparent shear stress as a function of apparent shear rate for 29% hammer-milled corn stover for each of the speed cycles illustrated in Fig. 10.5. Lines here are the linear fits according to Eq. (10.7).

rate with Eq. (10.7). This is the case for the data presented in Fig. 10.9. If the plateau torque increases with increasing rotation rate, then the parameters can be obtained by fitting the plateau torque-rotation rate data with Eqs. (10.8), (10.9).

The values of plateau torques are tabulated as a function of rotation rate for the three speed cycles in Table 10.4. For all three speed cycles, the torque decreases with increasing speed. Also listed in Table 10.4 are the Bingham model parameters τ_0 (yield stress) and η_{pl} (plastic viscosity) obtained by fitting the data with Eq. (10.7) as described previously. Although the parameters decrease in magnitude from the first to the second speed cycle, both parameters appear to reach steady values in the third speed cycle. For this data, and generally for high solids biomass suspensions without treatments or additives, we note that the plastic viscosity is typically negative (Samaniuk et al., 2012).

Table 10.4 Plateau torque as a function of rotation rate for a 29% hammer-milled corn stover suspension, for each speed cycle illustrated in Fig. 10.5.

Rotation rate (rpm)	Plateau torque (Nm)		
	Cycle 1	Cycle 2	Cycle 3
55	11.8	10.8	10.4
110	10.0	9.6	9.2
220	8.4	8.0	7.8
τ_0 (kPa)	84.4 ± 4.4	77.7 ± 1.7	74.3 ± 2.2
η_{pl} (Pas)	-0.11 ± 0.02	-0.09 ± 0.01	-0.09 ± 0.01
<i>The fitted Bingham parameters for each cycle are listed in the last two rows.</i>			

10.4 REPRESENTATIVE RESULTS FROM HIGH SOLIDS BIOMASS RESEARCH

10.4.1 Rheology of suspensions of acid-hydrolyzed corn stover

Lignocellulosic biomass hydrolyzes in acid at high temperatures. Ehrhardt et al. used the modified torque rheometer to measure the rheological properties of suspensions of screened and washed acid hydrolyzed corn stover for various reaction conditions and solids concentrations (Ehrhardt et al., 2010). The dilute acid (1 wt.% H₂SO₄) hydrolysis reactions were performed in a 2L or a 20L stainless steel, jacket-heated, glass-lined Parr reactor. The dilute-acid hydrolysis procedure was based on the National Renewable Energy Laboratories (NREL) Laboratory Analytical Procedure 007 (LAP-007) (Davis et al., 2013). Temperature profiles were characterized by the effective reaction temperature and H-factor analysis devised by Vroom (1957).

The measured torques were converted to apparent shear stresses (τ_{app}) using Eq. (10.1) and the rotational speeds were converted to apparent shear rates ($\dot{\gamma}_{app}$) using Eq. (10.2). In Fig. 10.10A, the apparent shear stress is plotted as a function of apparent shear rate for various insoluble solids concentrations of suspensions of hammer-milled corn stover acid hydrolyzed at 190°C for 0.5 h. The solid curves are fits of the data with the Bingham model, as

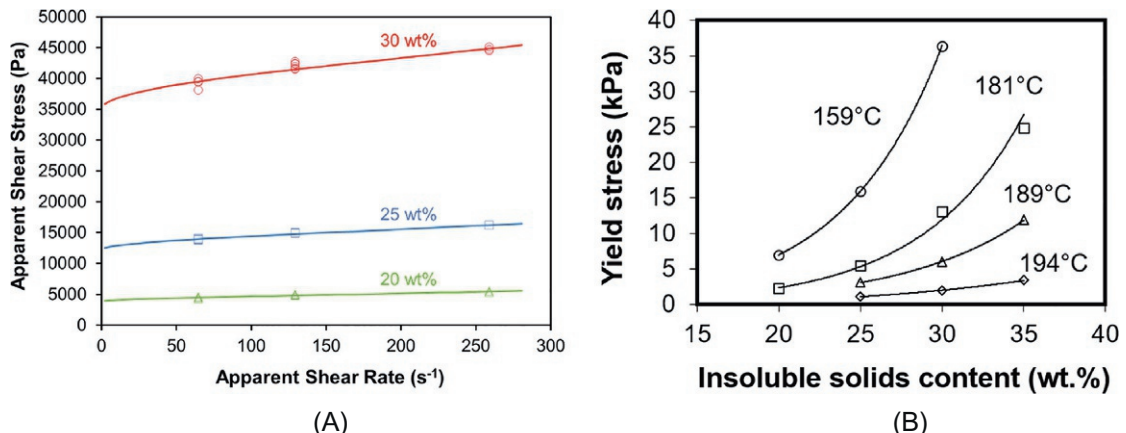


FIG. 10.10 (A) Apparent shear stress as a function of apparent shear rate for suspensions of corn stover hydrolyzed at 190°C for 0.5 h, at various solids concentrations. The symbols represent experimental data, and the curves represent fits with the Bingham model. (B) Yield stress as a function of insoluble solids content for hammer-milled corn stover acid hydrolyzed at different effective reaction temperatures (all torque rheometer measurements were performed at 55°C). The curves are fits of the data with a power-law dependence on concentration (Ehrhardt et al., 2010).

described in [Section 10.3.2](#). The yield stress obtained from such fits is plotted as a function of insoluble solids concentration in [Fig. 10.10B](#), for various effective reaction temperatures. The concentration dependence of the yield stress for such suspensions is commonly represented by

$$\tau_0 = aC^b \quad (10.10)$$

where the parameters a and b are fit to the experimental data. The curves in [Fig. 10.10B](#) are the fits with this power-law expression. The parameter a decreases as the effective reaction temperature is increased, but the parameter b is similar for all effective reaction temperatures ($3.7 < b < 4.4$).

In a separate study, the rheological properties of suspensions of dilute-acid hydrolyzed corn stover were measured using a variety of different rheometers, geometries, and techniques ([Stickel et al., 2009](#)). The different equipment included conventional rheometers with parallel plate, cone and plate, and vane geometries (in oscillatory shear mode), and the modified torque rheometer (in unidirectional rotational flow). The material tested was ground corn stover sieved with a 2-in. screen, which was hydrolyzed with 0.048 g H₂SO₄ per g dry biomass at 190°C for 1 min.

In [Fig. 10.11B](#), the yield stress is plotted as a function of insoluble solids concentration, including data obtained from all of the rheometers and measurement techniques. The yield stress increases rapidly with solids

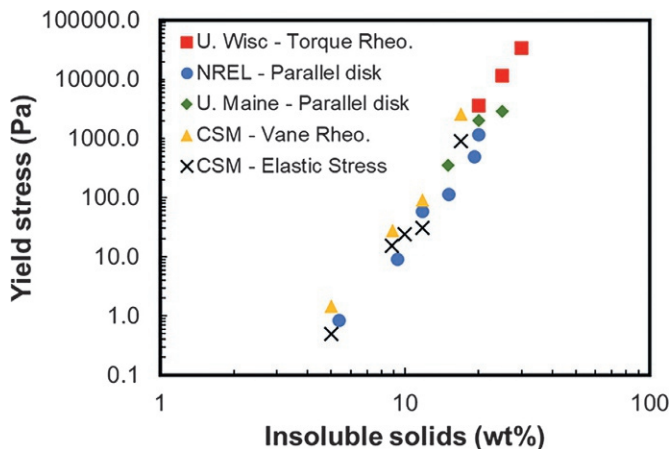
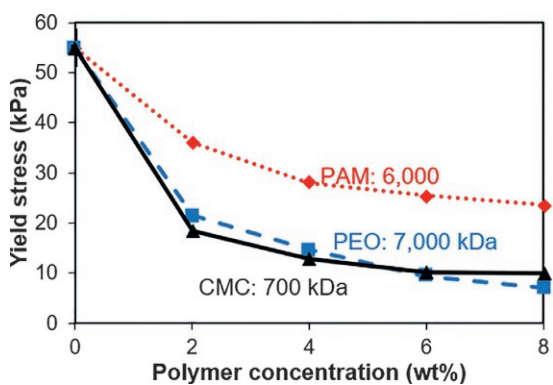


FIG. 10.11 Yield stress as a function of insoluble solids concentration. NREL and the University of Maine (U. Maine) used an elastic stress method with parallel plates. The two data sets from the Colorado School of Mines (CSM) are from a unidirectional vane method and from the elastic stress method. The data from the University of Wisconsin (U. Wisc) were obtained with the modified torque rheometer ([Stickel et al., 2009](#)).

concentration, following the power-law dependence of Eq. (10.10) with a power-law exponent of $b=5.7\pm0.5$. There is generally good agreement among the results obtained with the different methods, especially with regard to the change in yield stress with concentration. The data also illustrate that torque rheometry is the only technique capable of measuring the yield stress at large concentrations (>20 wt.% insoluble solids).

10.4.2 Effect of rheological modifiers

Rheological modifiers, such as water soluble polymers (WSPs), surfactants, and particles, can be used to reduce the yield stress of lignocellulosic biomass suspensions. Water soluble polymers are the most effective rheological modifiers, reducing the yield stress of highly concentrated biomass suspensions by 50%–80% with addition concentrations of 1%–3% (based on the dry weight of the biomass solids). This is illustrated in Fig. 10.12 where the yield stress, measured using the modified torque rheometer, is plotted as a function of WSP concentration (based on the dry weight to the biomass) for a 25 wt.% suspension of hammer-milled corn stover (Samaniuk et al., 2012; Samaniuk, 2012). Results are shown for three different WSPs: cationic poly(acrylamide) (PAM), anionic carboxymethyl cellulose (CMC), and nonionic poly(ethylene oxide) (PEO). For all three WSPs, the yield stress decreases with increasing polymer concentration. The WSPs are believed to reduce the yield stress by adsorbing to the biomass fiber surfaces and reducing interfiber friction (Samaniuk et al., 2017; Zauscher and Klingenberg, 2001).



■ FIG. 10.12 Yield stress of hammer-milled corn stover at 25 wt.% solids as a function of WSP concentration for various WSPs (Samaniuk et al., 2012).

The rate at which rheological modifiers reduce the apparent viscosity of a biomass suspension can provide insight into how quickly WSPs hydrate and disperse in the initial kneading zone of a twin-screw extruder, or other shear intense mixing devices, to form a homogeneous paste. Torque rheometry can be used to investigate this phenomenon (Samaniuk et al., 2012). To evaluate this transient effect, and to reduce the testing time required, a rapid screening method was developed. Two changes in the previously mentioned experimental procedure were introduced. First, the torque rheometer was only half filled with biomass (50g). Second, a fixed rotation rate was employed (55 rpm, no speed cycles). The effect of the modifiers on the transient torque response was quantified by the torque reduction and drop time, defined as follows and illustrated in Fig. 10.13A:

- 1. Torque reduction, TR :** This is defined as the percent decrease in the torque upon addition of modifier. Referring to Fig. 10.13A, the torque prior to the modifier addition is Γ_A , and the torque reached at steady state is Γ_C . The torque reduction, expressed as a percent, is defined as

$$TR = 100 \frac{\Gamma_A - \Gamma_C}{\Gamma_A} \quad (10.11)$$

- 2. Drop time, t_d :** This is defined as the time required for the torque to decrease to 80% of the total torque reduction. Referring to Fig. 10.13A, Γ_B is defined

$$0.8 = (\Gamma_A - \Gamma_B) / (\Gamma_A - \Gamma_C) \quad (10.12)$$

The time required to reach $\Gamma = \Gamma_B$, after the modifier addition, is the drop time.

The torque reduction and drop times after the addition of various WSPs (1 wt.%) to 25 wt.% hammer-milled corn stover suspensions are shown in Fig. 10.13B. For all WSPs investigated, the drop times are on the order of seconds to tens of seconds. This information is valuable for screening various modifiers when large, rapid changes in rheological properties are desirable, as in extrusion operations.

10.4.3 Effect of biomass type

The rheological properties of the lignocellulosic biomass depend on the biomass type. This can be due to variations in the physical and chemical structure of the biomass, which arise from anatomical differences and different relative amounts of cellulose, hemicellulose, and lignin. Samaniuk et al. (2015) used torque rheometry to measure the yield stress of suspensions of three different types of biomass—corn stover, newsprint,

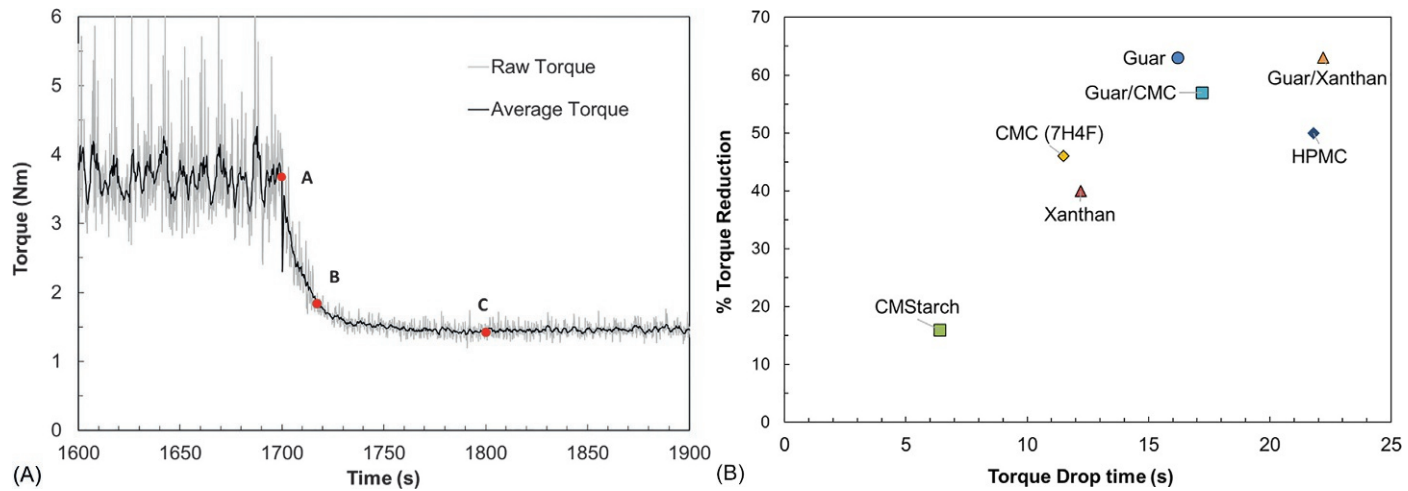


FIG. 10.13 (A) Torque as a function of time for WSP addition (1 wt.% Guar) to a 25 wt.% hammer-milled corn stover suspension. Point A indicates when the WSP is added to the torque rheometer. Point C indicates the steady-state torque achieved after WSP addition. Point B indicates the point at which 80% of the total torque reduction is achieved. Note the dramatic reduction in torque fluctuations after a stable torque is achieved. (B) Torque reduction vs. drop time following the addition of various rheological modifiers (1 wt.% based on the dry weight of the biomass) to 25 wt.% hammer-milled corn stover suspensions (Samaniuk et al., 2012).

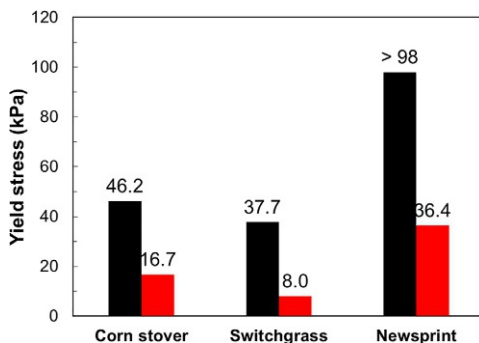


FIG. 10.14 Yield stress of 25 wt.% suspensions of corn stover, switchgrass, and newsprint without and with 2 wt.% rheological modifier (CMC; based on the dry weight of the biomass) (Samaniuk et al., 2015).

and switchgrass—without and with CMC (700kDa) as a rheological modifier. Suspensions with insoluble solids concentrations of 25 wt.% were prepared. The CMC concentration was 2wt.% based on the dry weight of the biomass.

Torque rheometry results are presented in Fig. 10.14 where the yield stress of the different biomass suspensions (25 wt.%) are plotted without and with added CMC. The yield stress could not be measured for the newsprint suspension without CMC; the torque response exceeded the capacity of the modified torque rheometer, which corresponds to a yield stress of 98 kPa. The addition of 2 wt.% CMC decreased the yield stress of all three materials by at least 60%. The larger decrease in yield stress of the switchgrass suspension (79%) relative to the corn stover and newsprint (63%) suggests that the physical chemistry of the biomass influences the rheological properties of the CMC-modified biomass.

10.4.4 Effect of enzymatic hydrolysis

The effect of enzymes on biomass rheology can also be evaluated using a torque rheometer. Samaniuk et al. (2011b) investigated the effect of enzymes on the torque response of 20 wt.% cotton fiber suspensions. Results are presented in Fig. 10.15 where the torque at 55 rpm and 55°C is plotted as a function of time for suspensions without and with enzymes. The torque is smaller for the suspensions containing enzymes, presumably because the enzymes hydrolyze the cotton fibers. The authors also showed that the weight average fiber length changes as a function of time for all suspensions. In the presence of enzymes, the final particle size was 60% smaller than in

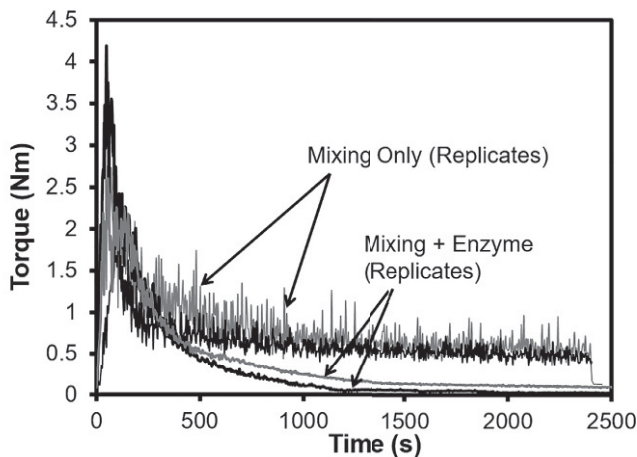


FIG. 10.15 The torque required for mixing concentrated cotton fiber suspensions (20 wt.% solids) as a function of time for replicate experiments without and with enzymes. Mixing speed: 55 rpm ([Samaniuk et al., 2011b](#)).

the absence of enzymes after the completion of the experiment. In addition, there is a synergistic effect of mixing and enzymatic hydrolysis; mixing increases the rate of cellulose conversion while the increased conversion facilitates mixing. This synergy was hypothesized to be partially due to particle size reduction.

10.5 CONCLUSIONS

Torque rheometers can be used to evaluate rheological properties of a variety of complex biological materials that are difficult to analyze in more conventional rheometers. Torque rheometry experiments can be used to obtain apparent rheological properties, or to fit data with rheological models. Understanding rheological properties can facilitate development of processing methods and probe effects of composition.

Methods for carrying out experiments with dough and lignocellulosic biomass suspensions were described. We showed that torque rheometry was useful for determining rheological behavior at peak dough development and to explore effects of composition on that behavior. In lignocellulosic biomass suspensions, we showed how torque rheometry can be used to measure rheological properties, examine effects of rheological modifiers and biomass type, and determine effects of enzymes.

APPENDICES

Appendix I: Instrument calibration

The modified torque rheometer was calibrated in order to convert torque and rotation speed data to apparent shear stress and apparent shear rate data, and to obtain rheological parameters from experimental data. The approach is to represent the torque rheometer bowl as two equivalent concentric cylinder geometries. The calibration corresponds to determining the effective radius of the inner cylinder. Once this radius is obtained, torque-rotation rate data can be converted to apparent shear stress-apparent shear rate data. The calibration analysis presented in this section follows that described by Goodrich and Porter (1967).

The torque rheometer gear box and shafts are illustrated in Fig. I.1. The input drive shaft is driven by the motor at speed Ω . The torque on the drive shaft, Γ , is measured. There are two output shafts. The driven shaft rotates with speed $\Omega_1 = \Omega$, and the follower shaft rotates with speed $\Omega_2 = b\Omega$. The torques exerted by the output shafts on the material within the bowl (not shown in Fig. I.1), Γ_1 and Γ_2 , are not measured.

Conservation of energy requires that (neglecting energy dissipated within the gear box)

$$\Gamma\Omega = \Gamma_1\Omega_1 + \Gamma_2\Omega_2 \quad (\text{I.1})$$

Using $\Omega_1 = \Omega$ and $\Omega_2 = b\Omega$, we obtain

$$\Gamma = \Gamma_1 + b\Gamma_2 \quad (\text{I.2})$$

This result is independent of the rheological properties of the material within the bowl.

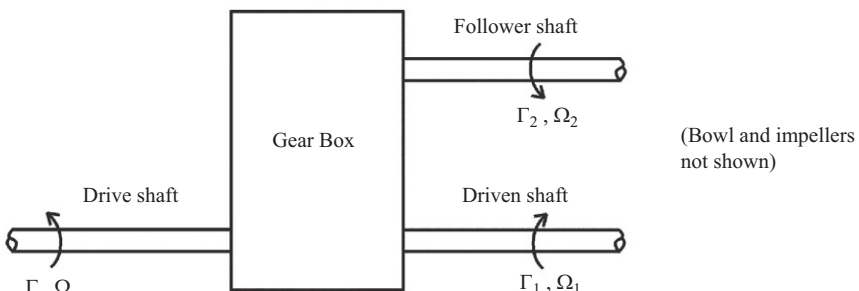
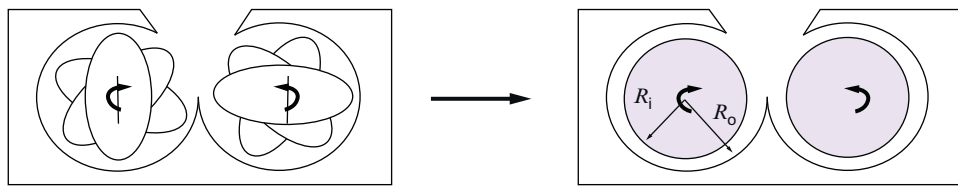


FIG. I.1 Schematic diagram of the torque rheometer shafts and gear box.



■ FIG. I.2 Illustration of the representation of the torque rheometer bowl as two sets of concentric cylinders.

To obtain apparent rheological properties of the material within the bowl, we assume that the average shear stress exerted on each impeller τ_k ($k = 1, 2$) can be related to the torque on the shaft by

$$\tau_k = K_\tau \Gamma_k \quad (\text{I.3})$$

and that the average shear rate on each impeller $\dot{\gamma}_k$ is related to the shaft speed by

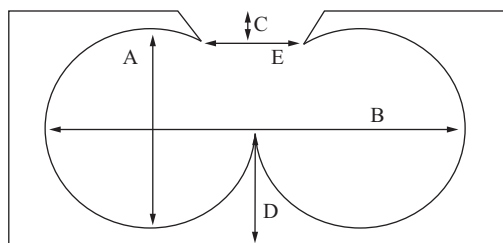
$$\dot{\gamma}_k = K_{\dot{\gamma}} \Omega_k \quad (\text{I.4})$$

We further assume that the bowl can be represented as two concentric cylinder geometries, with identical inner and outer radii (R_i and R_o , respectively) and depth h , as illustrated in Fig. I.2. For R_o and h , we use the measured chamber radius and depth, respectively. The bowl dimensions are illustrated in Fig. I.3 and tabulated in Table I.1. Following Goodrich and Porter (1967), the coefficient K_τ is related to the dimensions by

$$K_\tau = \frac{1}{2\pi R_i^2 h} \quad (\text{I.5})$$

This result is independent of the rheological properties of the material within the bowl.

The coefficient $K_{\dot{\gamma}}$, however, does depend on the rheological behavior of the material within the bowl. For calibration, we consider Newtonian fluids. The relationship between shear rate and shaft speed is determined by solving



■ FIG. I.3 Schematic diagram of the torque rheometer bowl with dimensions labeled.

Table I.1 Torque rheometer bowl dimensions.

Dimension	Value	Value
A	1.54 in.	3.91 cm
B	3.15 in.	8.00 cm
C	1.325 in.	3.37 cm
D	1.735 in.	4.41 cm
E	0.475 in.	1.21 cm
Depth (h)	1.875 in.	4.76 cm
Volume (w/o impellers)		150 mL
Volume (w/ impellers)		90 mL

the equation of motion (Bird et al., 2015), which yields the dependence of the coefficient $K_{\dot{\gamma}}$ on the bowl dimensions,

$$K_{\dot{\gamma}} = \frac{2}{1 - (R_i/R_o)^2} \quad (\text{I.6})$$

For Newtonian fluids in laminar flow, the torque is proportional to the rotation rate ($\Gamma_k \propto \Omega_k$ in each chamber). Using $\Omega_2 = b\Omega_1$, this gives $\Gamma_2 = b\Gamma_1$. Substituting this into Eq. (I.2) yields

$$\Gamma = (1 + b^2)\Gamma_1 \quad (\text{I.7})$$

or

$$\Gamma_1 = \frac{\Gamma}{1 + b^2} \quad (\text{I.8})$$

Eq. (I.8) relates the torque on shaft 1 to the measured input torque. Combining Eq. (I.8) with Eqs. (I.3), (I.4), along with the Newtonian constitutive law, $\tau = \eta\dot{\gamma}$, one can obtain the relationship between the viscosity of the fluid in chamber 1, η , and the input torque and rotation rate,

$$\eta\Omega = K\Gamma \quad (\text{I.9})$$

where

$$K = \frac{1}{1 + b^2} \frac{K_{\tau}}{K_{\dot{\gamma}}} = \frac{1}{1 + b^2} \left(\frac{1}{R_i^2} - \frac{1}{R_o^2} \right) \frac{1}{4\pi h} \quad (\text{I.10})$$

Thus by plotting the product $\eta\Omega$ as a function of Γ for a Newtonian liquid of known viscosity, one can obtain from the slope K and the effective inner cylinder radius R_i .

For the calibration, we used a Newtonian oil (Cannon N190000). The manufacturer supplies viscosity values at various temperatures, which are listed

Table I.2 Viscosity as a function of temperature for the calibration fluid (Cannon N190000; data provided by supplier).

T (°C)	η (Pas)
20	860.3
25	532.2
40	146.5
60	33.78

in Table I.2. The viscosity-temperature data are well-represented by the function

$$\eta = A \exp\left(\frac{B}{T}\right) \quad (\text{I.11})$$

where $A = 1.696 \times 10^{-9}$ Pas and $B = 7895$ K, as illustrated in Fig. I.4.

The torque was measured as a function of rotation rate at various temperatures for this fluid in the modified torque rheometer with $b = 2/3$. The viscosity was evaluated using Eq. (I.11) and the measured temperature. The product $\eta\Omega$ is plotted as a function of Γ (after subtracting the baseline torque) in Fig. I.5. A least-squares fit of the data with a straight line yields a slope of 648 ± 9 Pas rpm/in. lb. Using Eq. (I.9), we obtain an effective inner radius of 17.89 mm. This value is slightly smaller than the impeller radius (18.80 mm), and is consistent with those obtained by Goodrich and Porter (1967) and Bousmina et al. (1999) in similar torque rheometers.

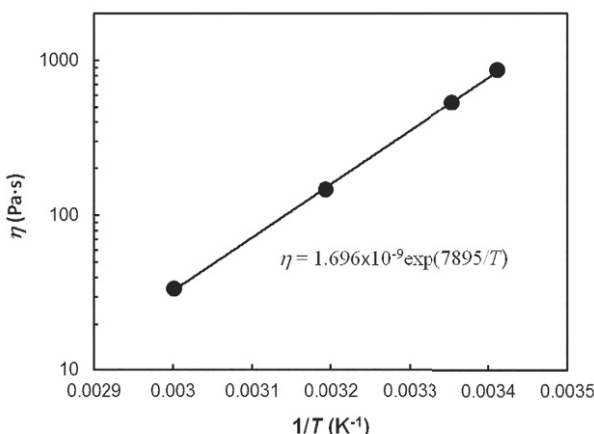
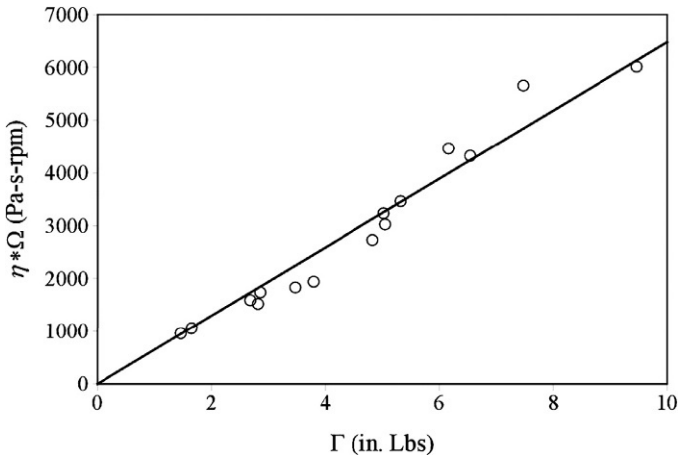


FIG. I.4 Viscosity as a function of inverse temperature for the calibration fluid (Cannon N190000). The symbols represent the values listed in Table I.2. The solid line is a least-squares fit of the data with Eq. (I.11).



■ FIG. I.5 Calibration plot of $\eta\Omega$ as a function of Γ for measurements with a Newtonian fluid (Cannon N190000) at various temperatures in the torque rheometer. The solid line is a least-squares fit of the data with a straight line.

With the effective inner cylinder radius determined, one can now convert torque-rotation rate data to apparent shear stress-apparent shear rate data. For concentric cylinder k , the stress at radial position r is related to the torque by

$$\tau_k = \frac{\Gamma_k}{2\pi r^2 h} \quad (\text{I.12})$$

This expression is independent of the constitutive behavior of the material. The relationship between the rotation rate and the shear rate at some position, however, depends on the constitutive behavior. For a Newtonian fluid, the shear rate at radial position r can be obtained from the solution of the equation of motion (Bird et al., 2015),

$$\dot{\gamma}_k = \frac{2R_i R_o \Omega_k}{\left(\frac{1}{\kappa} - \kappa\right) r^2} \quad (\text{I.13})$$

where $\kappa = R_i/R_o$. Following Bousmina et al. (1999), we choose to evaluate the stress and shear rate in the middle of the gap, where

$$r = R_a = \frac{1}{2}(R_i + R_o) \quad (\text{I.14})$$

This choice is consistent with that employed in commercial rheometers. Combining the previous three equations with Eq. (I.8) and $\Omega_1 = \Omega$, and inserting the values of the geometric parameters and $b = 2/3$, we obtain

$$\tau_1 = K_\tau \Gamma \quad (\text{I.15})$$

$$\dot{\gamma}_1 = K_{\dot{\gamma}} \Omega \quad (\text{I.16})$$

with $K_\tau = 6.697 \times 10^3 \text{ Pa/Nm}$ and $K_{\dot{\gamma}} = 1.1233 \times 10^1 \text{ s}^{-1}/(\text{rad/s})$. We refer to the stress and shear rate values obtained using Eqs. (I.15), (I.16) as “apparent” because (1) the concentric cylinder geometry is an idealization, and (2) Eq. (I.16) is only strictly valid for Newtonian fluids. One may also interpret the apparent stress and apparent shear rate as linearly transformed torque and rotation rate, respectively.

Appendix II: Fitting rheological models

It is tempting to simply fit a rheological model to experimental data for apparent shear stress as a function of the apparent shear rate to extract the parameters of a non-Newtonian rheological model (e.g., the power-law or Bingham model). However, this is not appropriate, as the apparent shear rate (i.e., Eq. I.16) is obtained from a Newtonian model. Instead, we fit the torque-rotation rate relationship predicted by the rheological model to the torque-rotation rate data obtained from the torque rheometer. This approach captures the velocity profile behavior observed for non-Newtonian fluids, which can be quite different from that for a Newtonian fluid.

As with the torque rheometer calibration, the torque rheometer is represented as a pair of identical concentric cylinder geometries (see Fig. I.2). Values for the outer cylinder radius R_o and depth h are obtained from the measured values (Fig. I.3 and Table I.1). For the inner cylinder radius, we use the value obtained by the calibration with a Newtonian fluid. [Bousmina et al. \(1999\)](#) analyzed the behavior of power-law fluids in a torque rheometer. They concluded that the effective inner radius obtained from calibration is insensitive to the constitutive behavior of the fluid, and thus the value of the inner radius obtained from calibration with one fluid can be employed in the analysis of the behavior of a fluid with different constitutive behavior. Although their analysis considered only power-law and Newtonian fluids, we employ the value of effective inner radius obtained by calibration with a Newtonian fluid in our analysis of the behavior of non-Newtonian fluids in the torque rheometer.

Consider first a single concentric cylinder geometry, where the inner cylinder is rotated with angular velocity Ω and the outer cylinder is stationary. Assuming steady, laminar, and isothermal flow in the annular gap, and neglecting end effects, the momentum balance reduces ([Bird et al., 2015](#)) to an ordinary differential equation for the shear stress $\tau_{r\theta}$,

$$\frac{d}{dr}(r^2\tau_{r\theta})=0 \quad (\text{II.1})$$

This equation can be integrated to determine the shear stress distribution in the annular gap,

$$\tau_{r\theta}(r)=\frac{C_1}{r^2} \quad (\text{II.2})$$

where C_1 is a constant of integration. This result is valid for Newtonian and non-Newtonian fluids. To make further progress, specific rheological models need to be employed. Here we will show how to get the relationship between torques and rotation rates for the power-law and Bingham models.

In cylindrical coordinates, the power-law model for the geometry described previously is

$$\tau_{r\theta}=m\left[-r\frac{d}{dr}\left(\frac{v_\theta}{r}\right)\right]^n \quad (\text{II.3})$$

where v_θ is the tangential velocity and $-rd/dr(v_\theta/r)$ is the shear rate. Insertion of this equation into Eq. (II.2) and integration subject to the boundary conditions $v_\theta(R_i)=\Omega R_i$ and $v_\theta(R_o)=0$ gives the velocity profile

$$v_\theta(r)=\frac{\Omega}{\alpha^{-2/n}-1}r\left[\left(\frac{R_o}{r}\right)^{2/n}-1\right] \quad (\text{II.4})$$

shear rate distribution

$$\dot{\gamma}(r)=\frac{2}{n\alpha^{-2/n}-1}\left(\frac{R_o}{r}\right)^{2/n} \quad (\text{II.5})$$

and shear stress distribution

$$\tau_{r\theta}(r)=mR_o^2\left[\frac{2}{n(\alpha^{-2/n}-1)}\right]^n\frac{\Omega^n}{r^2} \quad (\text{II.6})$$

The torque exerted by the fluid on the inner cylinder is

$$\Gamma=2\pi R_i^2 h \tau_{r\theta}|_{r=R_i}=2\pi R_o^2 hm\left[\frac{2}{n(\alpha^{-2/n}-1)}\right]^n\frac{\Omega^n}{r^2} \quad (\text{II.7})$$

This is the torque for a single set of concentric cylinders. As described previously, the torque rheometer is modeled as two such sets of concentric cylinders, one rotating with angular velocity $\Omega_1=\Omega$, and the other rotating with angular velocity $\Omega_2=b\Omega$. The torque exerted by the biomass on the cylinders is related to the torque on the input shaft by Eq. (I.2). Thus the torque on the input shaft is

$$\Gamma = 2\pi R_o^2 hm \left[\frac{2}{n(\alpha^{-2/n} - 1)} \right]^n [1 + b^{n+1}] \Omega^n \quad (\text{II.8})$$

Torque-rotation rate data can be fit with this equation to obtain the parameters m and n .

Finally, we show a similar analysis for the Bingham model. In cylindrical coordinates, the Bingham model is expressed as

$$\tau_{r\theta}(r) = \tau_0 - \eta_{pl} r \frac{d}{dr} \left(\frac{v_\theta}{r} \right) \quad (\text{II.9})$$

where v_θ is the tangential velocity and $-rd/dr(v_\theta/r)$ is the shear rate.

The existence of a yield stress makes it necessary to differentiate between two different flow regimes in tangential flow between concentric cylinders. The first flow regime appears at small stresses, where the inner cylinder rotates at Ω , and the material is sheared near the inner cylinder but remains an unsheared solid at larger radii. The radius at the boundary between the sheared and unsheared regions is r_0 . As the rotation rate is increased, the sheared region increases (r_0 increases). For sufficiently large rotation rates, the sheared region fills the entire gap between the cylinders (second flow regime).

Consider the first case where an unsheared region exists between the cylinders (i.e., $R_i < r_0 < R_o$). Integration of the equation of motion gives $\tau_{r\theta} = C_1/r^2$. Insertion of the Bingham model (Eq. II.9), and integrating again using the boundary conditions $v_\theta(R_i) = R_i \Omega$ and $v_\theta(r_0) = 0$ gives the velocity profile in the sheared region ($R_i < r < r_0$)

$$\frac{v_\theta}{r} = \left[\frac{\Omega + \frac{\tau_0}{\eta_{pl}} \ln \left(\frac{r_0}{R_i} \right)}{\frac{1}{R_i^2} - \frac{1}{r^2}} \right] \left(\frac{1}{r^2} - \frac{1}{r_0^2} \right) + \frac{\tau_0}{\eta_{pl}} \ln \left(\frac{r_0}{r} \right) \quad (\text{II.10})$$

with $v_\theta = 0$ in the unsheared region ($r_0 < r < R_o$). The shear rate in the sheared region is

$$\dot{\gamma} = -r \frac{d}{dr} \left(\frac{v_\theta}{r} \right) = -\frac{\tau_0}{\eta_{pl}} + 2 \left[\frac{\Omega + \frac{\tau_0}{\eta_{pl}} \ln \left(\frac{r_0}{R_i} \right)}{\frac{1}{R_i^2} - \frac{1}{r^2}} \right] \frac{1}{r^2} \quad (\text{II.11})$$

The torque exerted by the inner cylinder on the fluid is

$$\Gamma = \int_0^h \int_0^{2\pi} \tau_{r\theta} \Big|_{r=R_i} R_i^2 d\theta dz = 4\pi R_i^2 h \eta_{pl} \left[\frac{\Omega + \frac{\tau_0}{\eta_{pl}} \ln \left(\frac{r_0}{R_i} \right)}{1 - \frac{R_i^2}{r_0^2}} \right] \quad (\text{II.12})$$

Again, this is valid when $R_i < r_0 < R_o$. The value of r_o can be determined by noting that the torque can also be expressed as

$$\Gamma = 2\pi r_o^2 \tau_0 h \quad (\text{II.13})$$

By equating the left sides of Eqs. (II.12), (II.13), we obtain the following equation that can be solved numerically for r_o ,

$$\left(\frac{r_0}{R_i}\right)^2 - 1 = \frac{2\eta_{pl}\Omega}{\tau_0} + \ln \left[\left(\frac{r_0}{R_i}\right)^2 \right] \quad (\text{II.14})$$

If $r_0 > R_o$ (i.e., when all the material is sheared), the velocity, shear rate, and torque can still be obtained using Eqs. (II.10), (II.11), and (II.12), respectively, by replacing r_0 with R_o .

As described earlier, the torque rheometer is modeled as two such sets of concentric cylinders, one rotating with angular velocity $\Omega_1 = \Omega$, and the other rotating with angular velocity $\Omega_2 = b\Omega$. The torque exerted by the biomass on the cylinders is related to the torque on the input shaft by Eq. (I.2). Thus, to fit the Bingham model to experimental data, the torque predicted by Eq. (II.12) must be computed twice, once for each value of Ω , and combined via Eq. (I.2) to obtain the predicted input shaft torque. These calculations are repeated using an appropriate fitting algorithm to obtain “best” values of parameters τ_0 and η_{pl} .

REFERENCES

- AACC International, 2010. AACC Approved Methods of Analysis, eleventh ed. Cereals & Grains Association, St. Paul, MN, USA. ISBN 978-1-891127-68-2.
- Anderssen, R.S., Gras, P.W., MacRitchie, F., 1998. The rate-independence of the mixing of wheat flour dough to peak dough development. *J. Cereal Sci.* 27, 167–177.
- Bird, R., Stewart, W., Lightfoot, E., Klingenberg, D.J., 2015. *Introductory Transport Phenomena*. Wiley, New York, NY.
- Bloksma, A.H., 1984. Theoretical aspects of the Farinograph. In: D'Appolonia, B.L., Kunerth, W.H. (Eds.), *The Farinograph Handbook*, third ed. American Association of Cereal Chemists International, St. Paul, MN, pp. 7–12.
- Blyler, J.L.L., Daane, J.H., 1967. An analysis of Brabender torque data. *Polym. Eng. Sci.* 1–4.
- Bousmina, M., Ait-Kadi, A., Faisant, J.B., 1999. Determination of shear rate and viscosity from batch mixer data. *J. Rheol.* 43 (2), 415–433.
- Connelly, R., McIntier, R.L., 2008. Rheological properties of yeasted and nonyeasted wheat doughs developed under different mixing conditions. *J. Sci. Food Agric.* 88 (13), 2309–2323.
- Cullen, P.J., Connelly, R.K., 2009. Rheology and mixing. In: *Food Mixing: Principles and Applications*. Blackwell Publ. Ltd, Oxford, UK, pp. 50–72 (Chapter 4).

- Davis, R., Tao, L., Tan, E.C.D., Biddy, M.J., Beckham, G.T., Scarlata, C., Ross, J., Lukas, J., Knorr, D., Schoen, P., 2013. NREL report: Process Design and Economics for the Conversion of Lignocellulosic Biomass to Hydrocarbons: Dilute-Acid and Enzymatic Deconstruction of Biomass to Sugars and Catalytic Conversion of Sugars to Hydrocarbons. Tech. Rep. October 2013, NREL/TP-5100-62498..
- Ehrhardt M.R., 2008. Master's thesis. University of Wisconsin-Madison.
- Ehrhardt, M.R., Monz, T.O., Root, T.W., Connelly, R.K., Scott, C.T., Klingenber, D.J., 2010. Rheology of dilute acid hydrolyzed corn stover at high solids concentration. *Appl. Biochem. Biotechnol.* 160 (4), 1102–1115.
- Goodrich, J.E., Porter, R.S., 1967. A rheological interpretation of torque-rheometer data. *Polym. Eng. Sci.* 7 (1), 45–51.
- Green, D.W., Southard, M.Z., 2019. Mixing of viscous fluids, pastes, and doughs. In: Perry's Chemical Engineers' Handbook, ninth ed. McGraw-Hill Education, New York, Chicago, San Francisco, Athens, London, Madrid, Mexico City, Milan, New Delhi, Singapore, Sydney, Toronto (Chapter 18.2).
- Hancock, B., York, P., Rowe, R., 1994. An assessment of substrate-binder interactions in model wet masses. 1: Mixer torque rheometry. *Int. J. Pharm.* 102 (1), 167–176.
- Kilborn, R.H., Tipples, K.H., 1972. Factors affecting mechanical dough development. I. Effect of mixing intensity and work input. *Cereal Chem.* 49, 34–47.
- Menjivar, J., Connelly, R.K., Hsu, K., 1989. Application of a mixing recorder to determine fundamental rheological properties of food materials. In: Proceedings of the 5th International Congress on Engineering & Food, Cologne, FRG, May 28–June 3, pp. 49–58.
- Samaniuk, J.R., 2012. Ph.D. thesis. University of Wisconsin-Madison.
- Samaniuk, J.R., Wang, J., Root, T.W., Scott, C.T., Klingenber, D.J., 2011a. Rheology of concentrated biomass. *Korea Aust. Rheol. J.* 23 (4), 237–245.
- Samaniuk, J.R., Scott, C.T., Root, T.W., Klingenber, D.J., 2011b. The effect of high intensity mixing on the enzymatic hydrolysis of concentrated cellulose fiber suspensions. *Bioresour. Technol.* 102, 4489–4494.
- Samaniuk, J.R., Scott, C.T., Root, T.W., Klingenber, D.J., 2012. Rheological modification of corn stover biomass at high solids concentrations. *J. Rheol.* 56 (3), 649–665.
- Samaniuk, J.R., Scott, C.T., Root, T.W., Klingenber, D.J., 2015. Effects of process variables on the yield stress of rheologically modified biomass. *Rheol. Acta* 54 (11–12), 941–949.
- Samaniuk, J.R., Scott, C.T., Root, T.W., Klingenber, D.J., 2017. The influence of polymer adsorption, and fiber composition, on the rheology of aqueous suspensions of aspen, cotton, and corn stover pulps. *Biomass Bioenergy* 103, 47–54.
- Scott, C.T., Samaniuk, J.R., Klingenber, D.J., 2011. Rheology and extrusion of high-solids biomass. *Tappi J.* 10 (5), 47–53.
- Stickel, J.J., Knutsen, J.S., Liberatore, M.W., Luu, W., Bousfield, D.W., Klingenber, D.J., Scott, C.T., Root, T.W., Ehrhardt, M.R., Monz, T.O., 2009. Rheology measurements of a biomass slurry: an inter-laboratory study. *Rheol. Acta* 48 (9), 1005–1015.
- Vroom, K., 1957. The H-factor: a means of expressing cooking times and temperatures as a single variable. *Pulp Pap. Mag. Canada* 58, 228–231.
- Zauscher, S., Klingenber, D.J., 2001. Friction between cellulose surfaces measured with colloidal probe microscopy. *Coll. Surf. A* 178, 213–229.

This page intentionally left blank

Advanced research applications

Jose C. Bonilla, Neslihan Bozdogan, and Jozef L. Kokini

Department of Food Science, Purdue University, West Lafayette, IN, United States

CHAPTER OUTLINE

11.1 Gluten and gluten subfraction contributions in dough development during mixing 163

- 11.1.1 Gluten protein classification and impact in wheat flour and dough 163
- 11.1.2 Gliadin and glutenin classification and contribution to mixing 164
- 11.1.3 Glutenin macropolymer behavior during mixing 165

11.2 Visualization of gluten proteins during dough mixing/development 166

- 11.2.1 Gluten and starch visualization at different mixing regimes through fluorescence fingerprint 166
- 11.2.2 Visualization of gluten with nano-fluorescent quantum dots 166

11.3 Visualization of gliadin during dough mixing using fluorescent nanoparticles 168

- 11.3.1 Quantum dots as tracers for cereal proteins with confocal laser scanning microscopy as a detection system 168
- 11.3.2 Imaging of gliadin subfraction during mixing and in baked bread 169

11.4 Current research in visualization of gluten subfractions during dough mixing 170

- 11.4.1 Immunofluorescent imaging of HMW and LMW glutenins through specifically developed antibodies 170
- 11.4.2 Detection of gliadins, HMW glutenins, and LMW glutenins in wheat dough with autofluorescence and nongluten controls 172

11.5 Distribution of extension rate and shear rate and prediction of maximum stable bubble size inside the C.W. Brabender Farinograph 184

References 188

The method of mixing, including energy input, mixing time, and mixing speed, has significant effects on the quality of wheat dough. Dough is a matrix formed by blending water and wheat flour while mechanical force is introduced by the mixing blades and transferred to the mixture. During mixing, the dough forms a three-dimensional gluten phase and aqueous phase consisting of water soluble compounds and starch (Autio and Laurikainen, 1997; Migliori and Correra, 2013). The official method from the Cereals and Grains Association (former AACC International) to determine the rheological behavior and quality parameters of wheat flour doughs requires the use of a Brabender Farinograph (Method 54-22.01). The Farinograph is used as a mixing instrument that measures the mechanical resistance of dough to mixing, which depends on the rheological properties of the dough (Lee et al., 2001). The dough development time is the time elapsed from the beginning of mixing to the peak of the farinogram (point of greatest strength). Flours with short development times are known as weak flours, while flours with long development times are known as strong flours (Fig. 11.1). The strength of the dough is related to protein content and gluten composition, so weak flours contain lower amounts of protein (8%–9%), while strong wheat flours contain higher amounts of protein (12%–14%). From a compositional standpoint, flours with greater glutenin:gliadin ratios have greater dough strength and stability than flours with lower glutenin:gliadin ratios at a similar protein content.

This chapter introduces the use of newly available *in situ* techniques to visualize and study the distribution of the different gluten subunits during wheat dough development. Quantum dots conjugated to specific antibodies can be used for detection of gliadins, LMW, and HMW glutenins in the dough matrix. Images from the wheat dough are then collected using a confocal laser scanning microscopy. Quantitative data is obtained from the collected images using newly available software for image processing. Also, studies of the distribution of the extension rate and shear rate, and prediction of maximum stable bubble size inside the C.W. Brabender Farinograph are discussed.

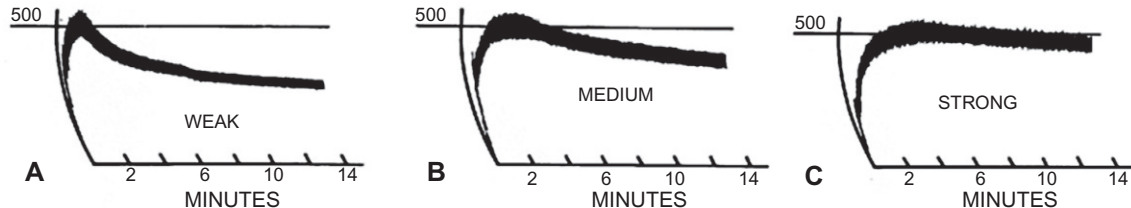


FIG. 11.1 Farinograms from flours of different strengths. (A) Weak flour: dough development time (DDT), 1.25 min; (B) medium strength flour: DDT, 2.75 min; and (C) strong flour: DDT, 5 min. (Reproduced from D'Appolonia, B.L., Kunerth, W.H. (eds.), 1984. *The Farinograph Handbook*, third ed. (Editorial). American Association of Cereal Chemists. ISBN: 0913250376, 9780913250372, 64 pp.)

11.1 GLUTEN AND GLUTEN SUBFRACTION CONTRIBUTIONS IN DOUGH DEVELOPMENT DURING MIXING

Dough is a complex system, which consists of a hydrated gluten matrix with embedded starch particles (Tronsmo et al., 2003). The hydrated gluten proteins, the starch matrix, and starch-protein interactions give rise to unique viscoelastic properties during dough mixing and development. These properties are then lost with addition of extra mixing energy for prolonged periods. Dough viscoelastic properties are the result of interactions that occur among the gluten proteins (Shewry et al., 2002). It has been shown that the continuous and elastic gluten network is formed by disulfide bonds between gluten subunits, and also hydrogen bonds, entanglements, and ionic and hydrophobic interactions (Tronsmo et al., 2003). The baking quality of different flours has been correlated to protein content and gluten composition (Magnus et al., 2000).

11.1.1 Gluten protein classification and impact in wheat flour and dough

Cereal proteins have been traditionally classified into four classes based on their solubility, known as the Osborne classification. The Osborne classification divides the cereal proteins into albumins, soluble in water; globulins, soluble in dilute salt solutions; prolamins, soluble in water-alcohol mixtures; and glutelins, soluble in diluted acids (Osborne, 1907). The prolamins and glutelins of wheat are gliadins and glutenins, respectively. It is now well accepted that wheat storage proteins (gliadins and glutenins) are closely related to dough quality. The current understanding indicates that the gluten content and the ratio of gliadin to glutenin are the main factors responsible for the gluten properties, which influence the mixing behavior of the doughs and final product quality (Hoseney et al., 1970; Kokini et al., 1994; Micard and Guilbert, 2000; Shewry and Tatham, 1990; Wrigley et al., 1982, 2006).

The strength of the gluten complex depends on the rheological properties and extensibility of its subunits, glutenins, and gliadins (Wrigley et al., 2006). Glutenin subunits give stiffness/elasticity to the gluten network. They are built as polymeric proteins through intermolecular and intramolecular disulfide bonds (Loussert et al., 2008). Gliadins are monomeric proteins, soluble in aqueous alcohols, and generally contribute more to flowability and mobility. The quality of a baked bread product depends on the properties of the dough given by the gluten proteins during mixing. Fig. 11.2 shows how the gluten network entraps the starch in wheat flour

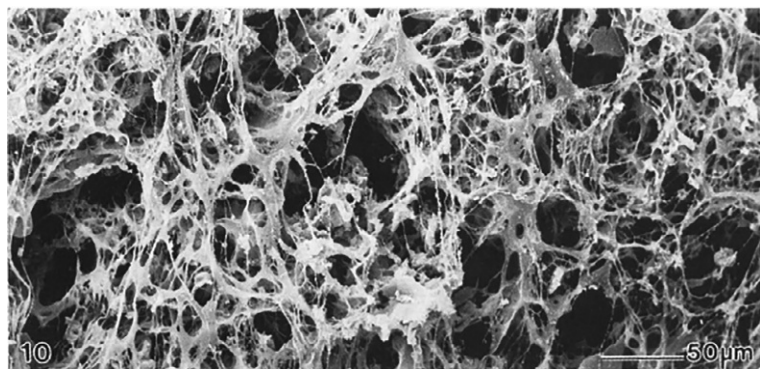


FIG. 11.2 Scanning electron micrograph of gluten network after enzymatic removal of starch. (Reproduced from Amend, T., Belitz, H.-D., 1991. Microstructural studies of gluten and a hypothesis on dough formation. *Food Struct.* 10 (4), Article 1. Available at: <https://digitalcommons.usu.edu/foodmicrostructure/vol10/iss4/1/>.)

dough. In Fig. 11.2, the starch has been removed by enzymatic digestion, giving us a clear visualization of the gluten network.

11.1.2 Gliadin and glutenin classification and contribution to mixing

Gliadins are classified into four different groups: α -, β -, γ -, and ω -gliadins, based on their differences in molecular mobility (Jones et al., 1959). They are usually differentiated using electrophoresis in polyacrylamide gels at low pH. The amino acid composition of the different gliadin groups does not show significant variations. The most notable change is that the ω -gliadins are classified as sulfur-poor prolamins due to their lack of sulfur-containing amino acids (cysteine and methionine), whereas the other fractions are classified as sulfur-rich prolamins (Shewry et al., 1986). In addition to the few variations on the amino acid composition, the amino acid sequence length changes, giving the different fractions different molecular weights in electrophoresis. Specific contributions of gliadin subfractions have not been strongly correlated to dough quality aspects.

On the contrary, based on their functionality and their mobility vis-à-vis SDS-PAGE, glutenins can be divided into low molecular weight glutenins (LMW) and high molecular weight glutenins (HMW) (Delcour and Hosney, 2010). During bread making, increases in mixing time, peak time, resistance to extension, and loaf volume have been seen with increasing glutenin levels up to a maximum dough strength (Uthayakumaran et al., 1999). LMW glutenins show a similar behavior to gliadins in terms of their

contribution to the viscosity of the gluten network and loaf volume (Clarke et al., 2003; Singh and Shepherd, 1988). Dough strength is mostly influenced by the presence of HMW glutenins, as they have a greater elasticity impact when compared to LMW glutenins and gliadins (Gupta and MacRitchie, 1994; Nieto-Taladriz et al., 1994; Tatham et al., 1985). Dough development times and bread-loaf volumes decrease significantly when HMW glutenins are extracted (MacRitchie, 1987).

11.1.3 Glutenin macropolymer behavior during mixing

The aggregation of glutenin proteins in wheat flour and undermixed wheat dough is known as a glutenin macropolymer. A glutenin macropolymer (GMP) is defined as the gluten protein aggregates insoluble in 1.5% SDS and it consists of HMW glutenins and LMW glutenins (Graveland et al., 1982). The amount of GMP extracted from wheat dough depends on the dough's mixing time. It has been shown that proper mixing disrupts the GMP aggregates (Don et al., 2005), as shown in Fig. 11.3. We can observe how GMP is still present in undermixed dough, but disappears by the peak or dough development time, and is not present in overmixed dough.

It has been shown that mixing changes the physicochemical properties of GMP (Weegels et al., 1997). The GMP aggregates play an important role in dough viscoelasticity, as they are composed of high and low molecular weight glutenins (Don et al., 2005; Kieffer and Stein, 1999; Lee et al., 2001). It has been proposed that gluten network disruption when more mechanical force is applied over time is due to the physical disruption of the disulfide bonds between HMW glutenins and LMW glutenins. However, the loss of dough elastic properties cannot be explained by glutenin disulfide bond disruption alone.

The study of the effects of the individual gluten subunits in dough rheology during the mixing process has been performed using fractionation and reconstitution techniques (Finney, 1943). During extraction processes, the

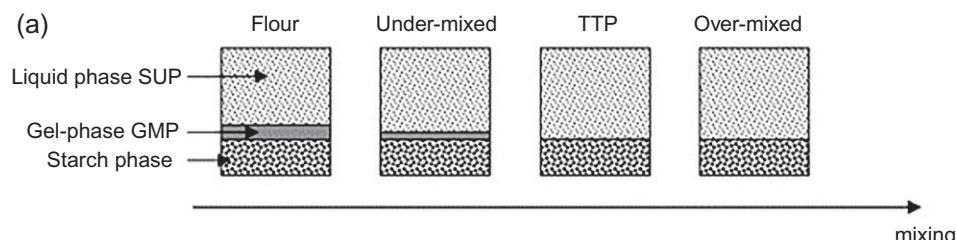


FIG. 11.3 Solubilization of gluten macropolymer vs. mixing energy input. (Reproduced from Don, C., Lichtendonk, W.J., Plijter, J.J., van Vliet, T., Hamer, R.J., 2005. The effect of mixing on glutenin particle properties: aggregation factors that affect gluten function in dough. *J. Cereal Sci.* 41, 69–83. <https://doi.org/10.1016/j.jcs.2004.09.009>.)

proteins are solubilized, so their structural conformation is modified. A significant amount of valuable information about gliadins and glutenins has been gained by studying extracted proteins; however, it is not possible to guarantee that the extracted proteins show the same rheological behaviors or present the exact same properties in the dough matrix, where they are interacting with starch and lipids. The use of visualization techniques aid in studying gluten proteins and their subfractions *in situ* without the need for fractionation or extraction.

11.2 VISUALIZATION OF GLUTEN PROTEINS DURING DOUGH MIXING/DEVELOPMENT

11.2.1 Gluten and starch visualization at different mixing regimes through fluorescence fingerprint

Different techniques have been used to visualize gluten during the mixing process. A method called fluorescence fingerprint (FF) has been used to visualize the distributions of gluten and starch in wheat dough under different mixing conditions. The fluorescence fingerprint method consists of a set of fluorescent spectra acquired at consecutive excitation wavelengths for each specific constituent, in this case proteins (gluten) and carbohydrates (starch). The detection of characteristic emissions after multiple excitations of the sample makes possible the detection of gluten and starch within the matrix (Tsuta et al., 2007). This technique has been used to collect fluorescent images of dough at different mixing points: an undermixed dough, an optimally mixed dough, and an overmixed dough. In Fig. 11.4, the red color (dark gray color in print version) represents gluten while the green color (light gray color in print version) represents starch. Black areas are representations of air bubbles (Kokawa et al., 2012). As expected, it was found that the undermixed dough shows a less heterogeneous distribution of gluten within the starch matrix due to lack of time for the components to mix after hydration. The optimally and overmixed doughs show a more homogeneous distribution (Kokawa et al., 2013).

11.2.2 Visualization of gluten with nano-fluorescent quantum dots

The use of nanofluorescent quantum dots (QDs) with a detailed fluorescent imaging protocol for detecting the gluten network in flat bread was first introduced by Sozer and Kokini (2014). Water-soluble quantum dots made from cadmium selenide capped with zinc sulfide (CdSe/ZnS QDs) and functionalized with carboxyl terminated groups were used in this new approach.

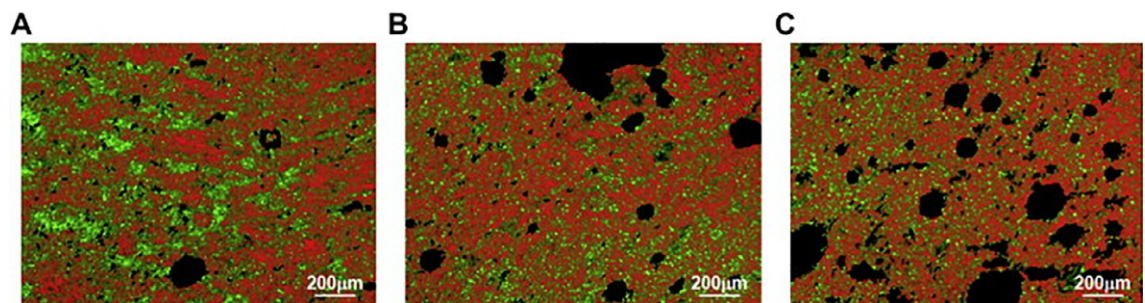


FIG. 11.4 Pseudocolored images of dough in undermixing stage (A), optimum-mixing stage (B), and overmixing stage (C). The red (dark gray in print version) and green areas (light gray areas in print version) are the pixels whose FFs show a high value of cosine similarity to the FFs of gluten and starch, respectively. The black areas are the pixels masked as bubble areas. (Reproduced from Kokawa, M., Sugiyama, J., Tsuta, M., Yoshimura, M., Fujita, K., Shibata, M., Araki, T., Nabetani, H., 2013. Development of a quantitative visualization technique for gluten in dough using fluorescence fingerprint imaging. *Food Bioprocess Technol.* 6, 3113–3123. <https://doi.org/10.1007/s11947-012-0982-7>.)

The top, center, and bottom layers of freshly made flat bread were sectioned to a thickness of 20 μm and then stained with QDs. The staining procedure conjugates the QDs to amino groups of gluten proteins in the dough. Samples were then analyzed under a confocal laser scanning microscope (CLSM). These results showed that QDs provide stable long-term fluorescent imaging capability for wheat gluten with negligible quenching after prolonged laser excitation (Sozer and Kokini, 2014). Samples stained with organic dyes, in this case, rhodamine B, were used as a control, and it was demonstrated that quantum dots are more suitable than dyes in wheat doughs since their images show brighter and more distinguishable fluorescent detection than the rhodamine B-stained samples. Fig. 11.5 shows fluorescent images of

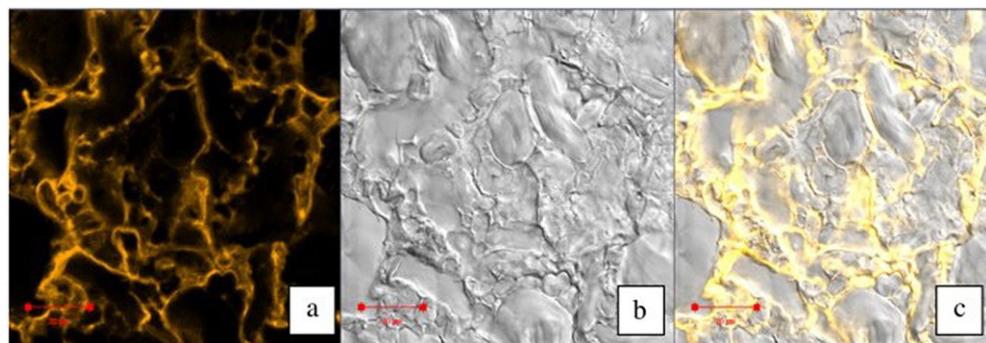


FIG. 11.5 Gluten network distribution in bread. Cross-section of bread labeled with QDs. (A) Fluorescence image; (B) Differential interference contrast (DIC) image; (C) merged fluorescence-DIC image. Scale bar 20 μm. (Reproduced from Sozer, N., Kokini, J.L., 2014. Use of quantum nanodot crystals as imaging probes for cereal proteins. *Food Res. Int.* 57, 142–151. <https://doi.org/10.1016/j.foodres.2013.12.031>.)

QD-labeled gluten proteins in bread samples. With this study a deeper understanding of the movement of gluten during baking was achieved. There were notable differences in the way gluten distributes and interacts around either ungelatinized or gelatinized starch. The brighter yellow color areas (light gray color areas in print version) in Fig. 11.5 indicate that parts of the gluten were more concentrated. This concentration can be attributed to water loss and crust formation during baking, which increases the gelatinization temperature and delays the conversion of native starch into gelatinized starch (Primo-Martín et al., 2009; Sozer and Kokini, 2014).

11.3 VISUALIZATION OF GLIADIN DURING DOUGH MIXING USING FLUORESCENT NANOPARTICLES

11.3.1 Quantum dots as tracers for cereal proteins with confocal laser scanning microscopy as a detection system

The study of gluten in dough matrices during the mixing process with fluorescent fingerprint or with amine-reactive dyes is not specific enough to show how the singular protein subfractions contribute to the gluten agglomeration or network formation and disruption that we see at different stages of mixing. To investigate this, a more specific method is needed. With the study from Sozer and Kokini (2014), the use of inorganic nanofluorescent quantum dots to tag cereal proteins was introduced in cereal science research. This study proved that quantum dots are suitable for detection of protein in cereal matrices. Different size QDs emit different colors, so different color QDs are available to tag different protein subfractions using the same technique. QDs do not have a specific excitation range; instead it is very broad, and this makes them easy to excite when compared to organic dyes, which have narrow excitation ranges. QDs are also easier to differentiate from each other because their emission spectra are very narrow; thus emissions from green QDs do not mix with the emissions of red QDs. All these characteristics make QDs suitable for simultaneous detection of different protein subfractions (Bonilla et al., 2016).

Immunofluorescence is a widely used method for detection of proteins in biological tissues in which a fluorescent dye, in this case QDs, is attached to specific antibodies. In this method, the antibodies work as the recognition element for specific proteins. The antibodies recognize their target proteins through noncovalent protein-protein interactions. Thus the fluorescent detection of the QDs is a visual representation of the target proteins. One of the most useful detection techniques for the recognition of immunofluorescence in biological tissues in the use of confocal laser scanning

microscopy (CLSM). CLSM excites the samples with a high-energy laser focusing on a specific spot in the sample and the equipment does a pattern scanning procedure in a defined area. Once the laser hits a specific spot in the sample, the excited dyes/compounds (QDs in this case) emit fluorescence in all directions. The equipment is equipped with a pinhole located before the detector, which collects the photons emitted by the samples. This pinhole blocks emissions of different sections from the Z-axis of the samples, thus differentiating emission at different depths in the same spot. The images are collected from different Z-stacks and the microscope software generates 3D representations of the fluorescent emission in the samples, and then combines all the different X-Y spots scanned. Another important feature of CLSM is that with the multiple sets of filters and detectors in it, it can differentiate the emissions from QDs emitting at different wavelengths at the same spot. This feature is very useful when trying to detect different protein subfractions in the same sample.

11.3.2 Imaging of gliadin subfraction during mixing and in baked bread

Immunofluorescence was used by Bozkurt et al. (2014) to detect gliadins in wheat dough. In this approach, they used QDs conjugated to gliadin antibodies. Dough samples from wheat flour and water were prepared and the water absorption of the wheat flour was recorded. The flour was then mixed with their known water absorption level and small dough samples were taken at arrival time (AT), peak time (PT), and departure time (DT). AT, PT, and DT are illustrated in Fig. 11.6.

Bozkurt's study investigated the location and distribution of gliadins as a function of wheat flour mixing time in a Brabender Farinograph. Gliadin

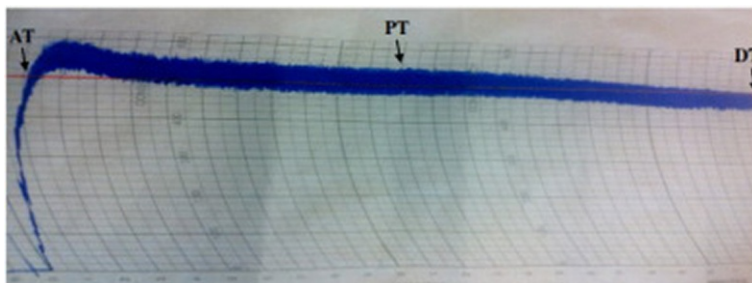


FIG. 11.6 A Farinogram of wheat flour dough showing arrival time (AT), peak time (PT), and departure (DT) time was indicated with arrows. (Reproduced from Bozkurt, F., Ansari, S., Yau, P., Yazar, G., Ryan, V., Kokini, J., 2014. Distribution and location of ethanol soluble proteins (Osborne gliadin) as a function of mixing time in strong wheat flour dough using quantum dots as a labeling tool with confocal laser scanning microscopy. *Food Res. Int.* 66, 279–288. <https://doi.org/10.1016/j.foodres.2014.09.028>.)

antibodies were conjugated with QDs using dithiothreitol (DTT) to disrupt disulfide bonds in the antibodies, then the carboxyl modified QDs were cross-linked to the now free and available sulfur groups through a succinimidyl 4-(*N*-maleimidomethyl)cyclohexane-1-carboxylate (SMCC). The samples collected at arrival time, peak time, departure time, and breakdown time were treated with the antibody-QD solutions. The images collected from CLSM allowed for the easy identification of gliadin proteins. By analyzing the collected images at different mixing times, it was found that mixing led to significant changes in the spatial distribution of gliadin in the dough structure. High intensities indicated that gliadins preferentially located themselves around the air cells, but they were also found in the bulk areas of the dough. Starch gelatinization, which is dependent on the moisture mobility in the samples, seems to affect variability in the distribution of gliadins (Fig. 11.7).

Fig. 11.8 shows the distribution and the fluorescence intensity of gliadin surrounding the gas cell walls. The dark spots observed in Fig. 11.8 correspond to gas cells formed by air inclusion during mixing. The high peaks around the cell represent the intensity of QDs detected, where higher intensity represents a greater presence of gliadin. This is consistent with the work of Li et al. (2004), who observed that gliadin was not only found in the strands of dough, but was also seen associated with the gas cell walls.

11.4 CURRENT RESEARCH IN VISUALIZATION OF GLUTEN SUBFRACTIONS DURING DOUGH MIXING

11.4.1 Immunofluorescent imaging of HMW and LMW glutenins through specifically developed antibodies

New antibodies for HMW and LMW glutenins have recently been developed and conjugated with different color QDs (Bonilla et al., 2018). These antibodies were developed using comparative proteomics, with unique and frequent peptides identified for each glutenin subunit (HMW and LMW). The peptides were synthetized and injected into rabbits. The rabbits' immune system developed antibodies against the peptides, which were then collected and purified. The antibodies were conjugated with QDs using a site-click chemistry method. In this new site-click method, the QDs are cross-linked to sugar groups located in the tails of the antibodies. Thus with this method the use of reducing agents that could potentially disrupt antibody integrity is avoided (Bonilla et al., 2016; Zeglis et al., 2013). In this study, HMW and LMW glutenins were detected in a sample wheat dough, and their distribution overlapped in many areas of the gluten network (Fig. 11.9) (Bonilla et al., 2018).

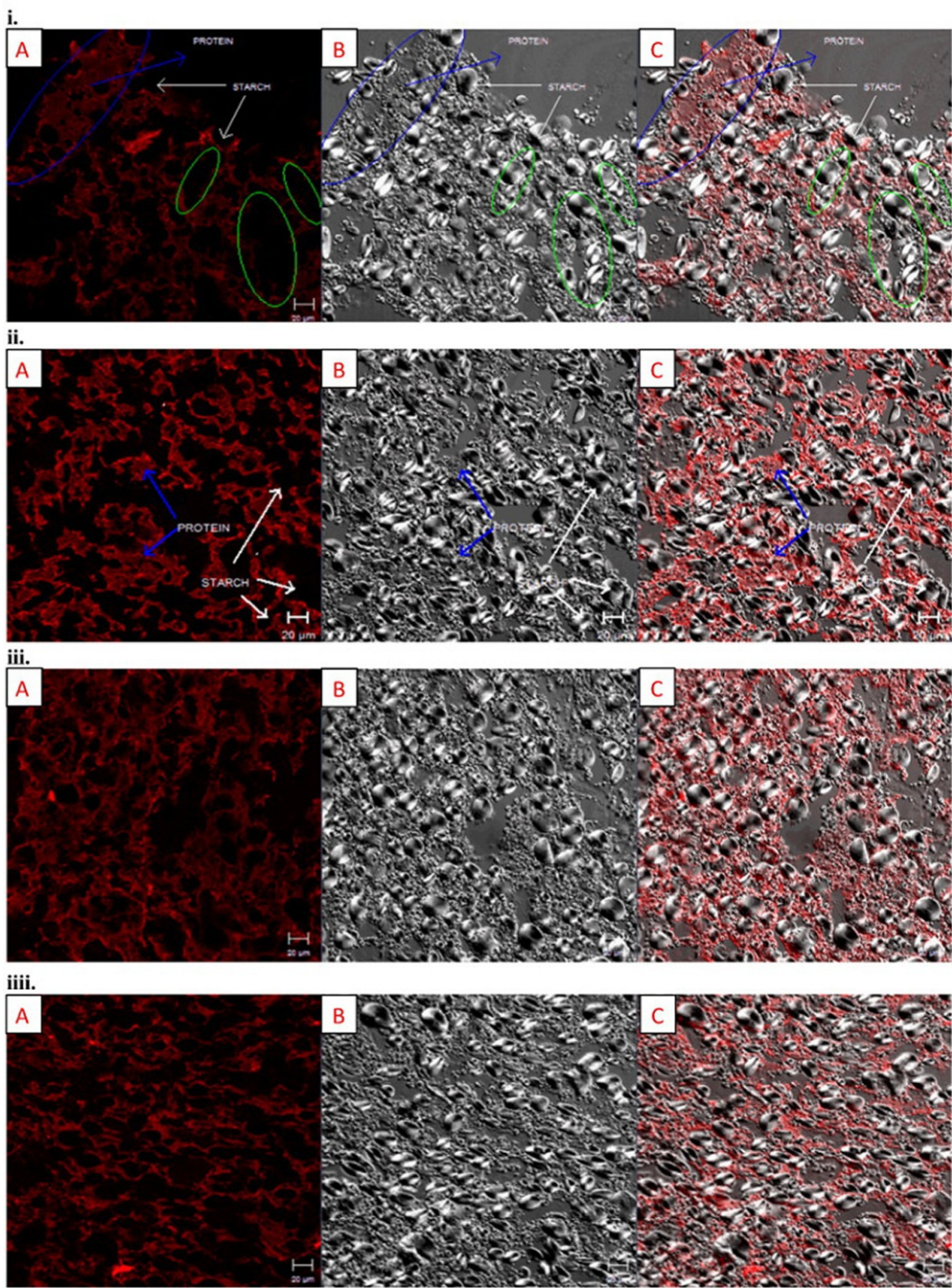


FIG. 11.7 Microstructure of dough sections at different times. (i) Arrival time, (ii) peak time, (iii) departure time, and (iv) 10 min after departure time. (A) (left) Gliadin molecules bound to QDs; the red zones (light gray zones in print version) are antigliadin bound to QDs representing gliadin and the black zones are nongliadin zones; (B) (middle) starch granules under polarized light; the bright shapes represent starch and the gray zones represent largely the protein. (C) (right) Overlay of (A) and (B) showing the distribution of gliadin (red (light gray in print version)) in the dough matrix and around starch (gray). Blue indicator (gray indicator in print version) shows a region where gliadin strands were aggregated and green ellipsoids (gray ellipsoids in print version) illustrated the gliadin free region. (Reproduced from Bozkurt, F., Ansari, S., Yau, P., Yazar, G., Ryan, V., Kokini, J., 2014. Distribution and location of ethanol soluble proteins (Osborne gliadin) as a function of mixing time in strong wheat flour dough using quantum dots as a labeling tool with confocal laser scanning microscopy. *Food Res. Int.* 66, 279–288. <https://doi.org/10.1016/j.foodres.2014.09.028>.)

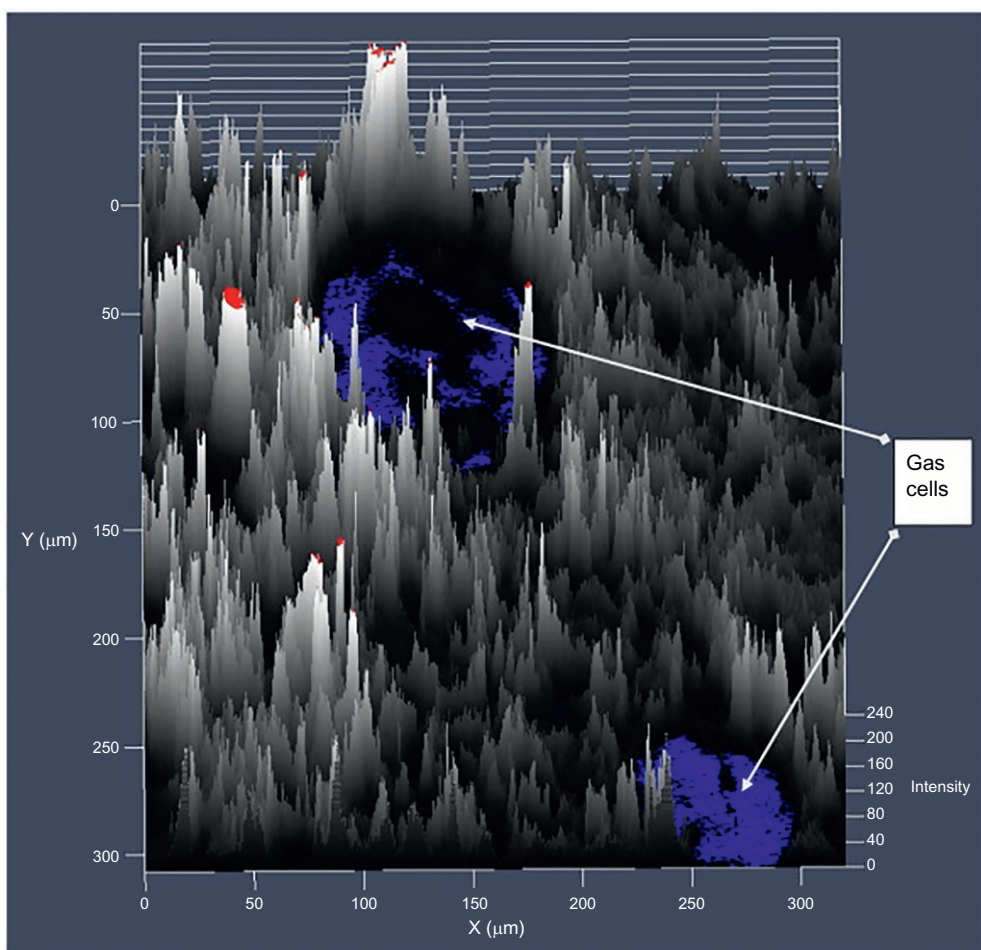
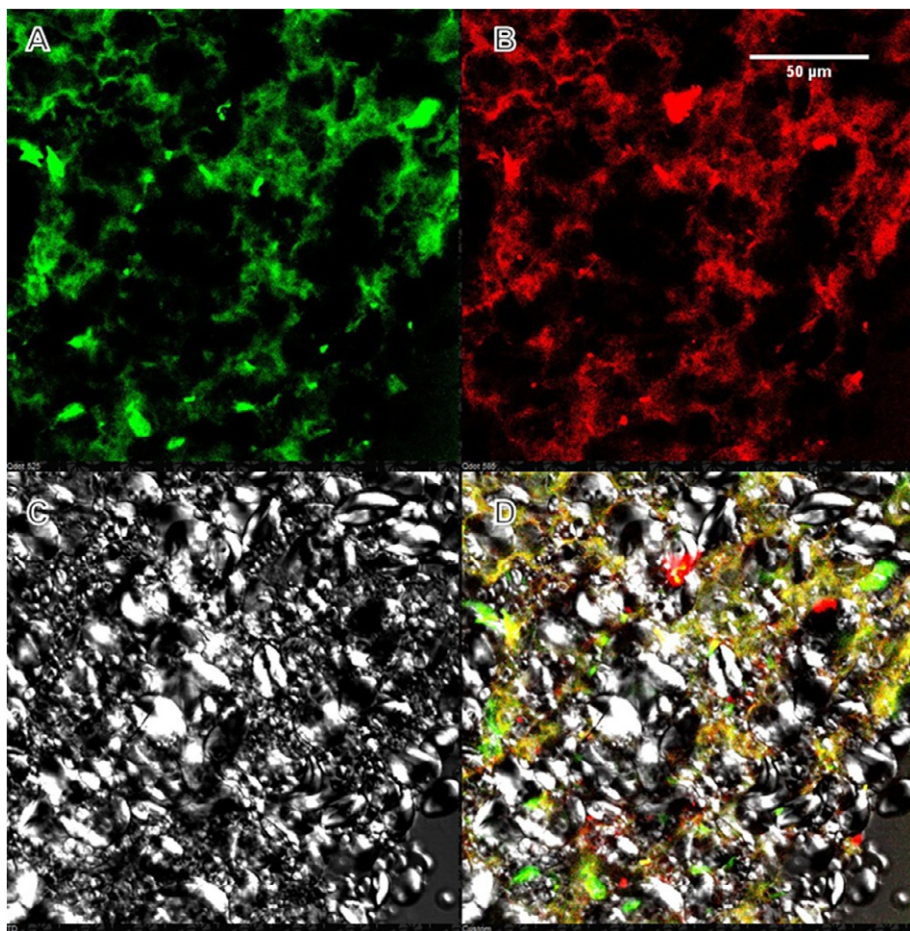


FIG. 11.8 Distribution of gliadin around gas cells where the fluorescence intensity is highest relative to bulk dough. The image represents a dough section $300 \mu\text{m} \times 300 \mu\text{m}$ and the peaks represent the fluorescence intensity of quantum dots conjugated with antigliadin. Fluorescence intensity is proportional to the height of the observed peaks and the whiteness of the peak. (Reproduced from Bozkurt, F., Ansari, S., Yau, P., Yazar, G., Ryan, V., Kokini, J., 2014. Distribution and location of ethanol soluble proteins (Osborne gliadin) as a function of mixing time in strong wheat flour dough using quantum dots as a labeling tool with confocal laser scanning microscopy. *Food Res. Int.* 66, 279–288. <https://doi.org/10.1016/j.foodres.2014.09.028>.)

11.4.2 Detection of gliadins, HMW glutenins, and LMW glutenins in wheat dough with autofluorescence and nongluten controls

Simultaneous detection of gliadin, HMW, and LMW glutenins at different stages of dough mixing was achieved using the newly developed antibodies for high and low molecular glutenins along with the commercial antigliadin



■ FIG. 11.9 (A) Localization of LMW glutenins in wheat dough stained with the anti-LMW conjugated with 525 nm QDs. (B) Localization of HMW glutenins in wheat dough stained with the anti-HMW conjugated with 585 nm QDs. (C) Starch matrix detection on wheat dough with polarized light. (D) Merged image of glutenins detection within the starch matrix in wheat dough. (Reproduced from Bonilla, J.C., Ryan, V., Yazar, G., Kokini, J.L., Bhunia, A.K., 2018. Conjugation of specifically developed antibodies for high- and low-molecular-weight glutenins with fluorescent quantum dots as a tool for their detection in wheat flour dough. *J. Agric. Food Chem.* 66, 4259–4266. <https://doi.org/10.1021/acs.jafc.7b05711>.)

antibodies (Bonilla et al., 2019b). Each of the three antibodies was conjugated with different color QDs; more specifically, 525 nm, 585 nm, and 655 nm QDs were used for gliadins, LMW glutenins, and HMW glutenins, respectively, using the site-click technique. The distribution of the three proteins and their interactions were measured at peak time, arrival time, departure time, and 10 min after departure, as shown in Fig. 11.10.

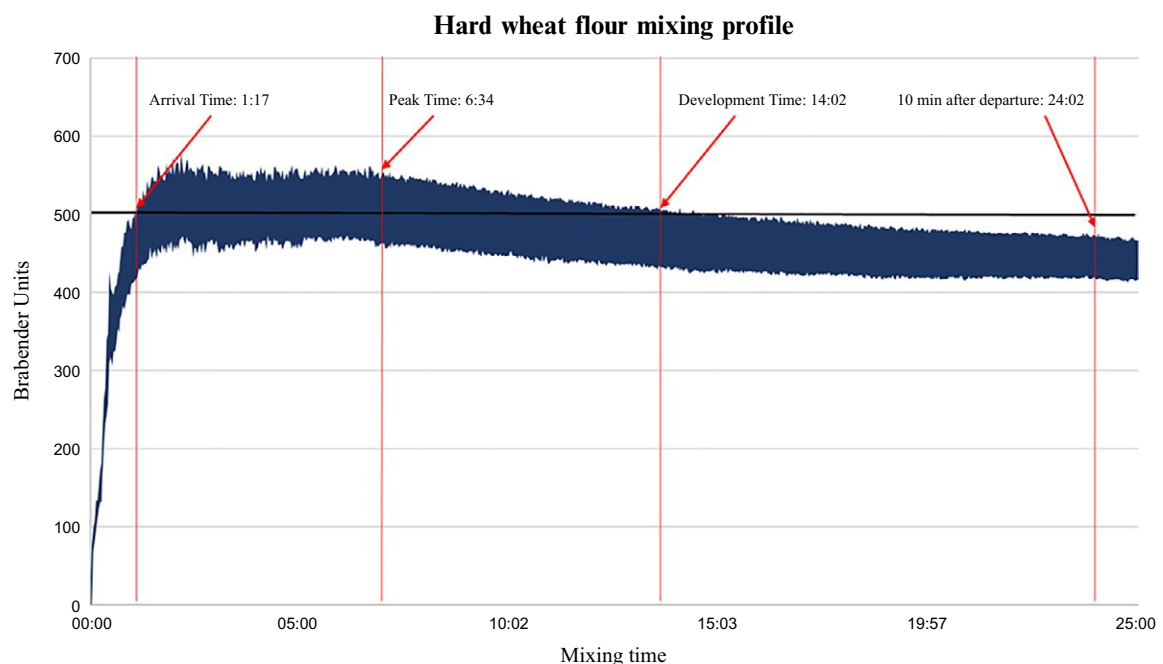


FIG. 11.10 Hard wheat flour farinogram at 58.8% added water.

Dough samples collected at these mixing points were frozen immediately and cryosectioned onto microscope slides (Bonilla et al., 2019a). The dough samples on the slides were stained with the three antibody-QDs in solution, and any unbound antibody-QDs were washed away with phosphate-buffered saline solution. The samples were examined under confocal microscopy and the images analyzed with protein network analysis (Bernklau et al., 2016) and colocalization coefficients (Bonilla et al., 2019b). The changes have been reported from arrival to peak, from peak to departure, and from departure to 10 min after departure. Quantitative imaging analyses with two different image-processing software packages provided proportionated quantitative description of the changes occurring between the different mixing times.

Colocalization analysis has been used to study how one gluten subunit distributes in comparison with a different gluten subunit. The colocalization tool is available in the analysis software from many confocal microscopes. The colocalization coefficient indicates the “degree” of colocalization between two different detection channels in the microscope. In this case, each different

QD color is detected in a different channel of the microscope. The “Manders” colocalization coefficient is a measure of the coexistence and possible interactions between two different gluten subunits. The colocalization coefficient measures the fraction of pixels with positive emission values from both channels in the same area (Manders et al., 1993). A value of “1” indicates 100% colocalization between the two channels being analyzed, meaning that the pixels displaying emission from “channel A” are the same pixels displaying emission from “channel B.” A value of “0” indicates that none of the pixels showing emission in “channel A” match in location with the pixels showing emission in “channel B.” Understanding the location of different gluten subunits gives a deeper understanding of structural associations/interactions between the gluten subunits at different mixing times.

The protein network analysis technique has been used to quantify the amount of network formation by each protein subunit (Bernklau et al., 2016). The protein network analysis method quantifies the protein network, measuring total protein area, protein percentage area, number of protein junctions, number of protein end points, and mean lacunarity. Lacunarity is a measure of the shape, uniformity, and structural variance of the gluten network. Fig. 11.11 shows how a fluorescent image from gluten is converted into a measurable network.

Fig. 11.12 shows the distribution of LMW glutenins, HMW glutenins, and gliadins during arrival and peak time. At arrival time, the LMW glutenins and HMW glutenins (channel A and channel B) are found in a few spots with high intensities, and then they become more evenly distributed within the sample at the peak time. Gliadins appear dispersed in the images at both times, with more homogeneous distribution at peak time. This has been

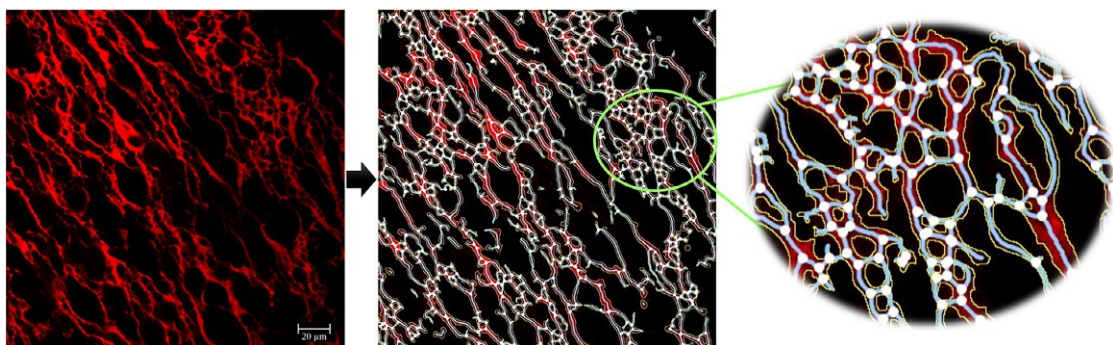


FIG. 11.11 Protein network analysis of a wheat dough sample. Middle and Right: picture after image processing with AngioTool (white = junctions, blue (light gray in print version) = protein skeleton, yellow (dark gray in print version) = protein outline/area). (Reproduced from Bernklau, I., Lucas, L., Jekle, M., Becker, T., 2016. Protein network analysis—a new approach for quantifying wheat dough microstructure. *Food Res. Int.* 89, 812–819. <https://doi.org/10.1016/j.foodres.2016.10.012>.)

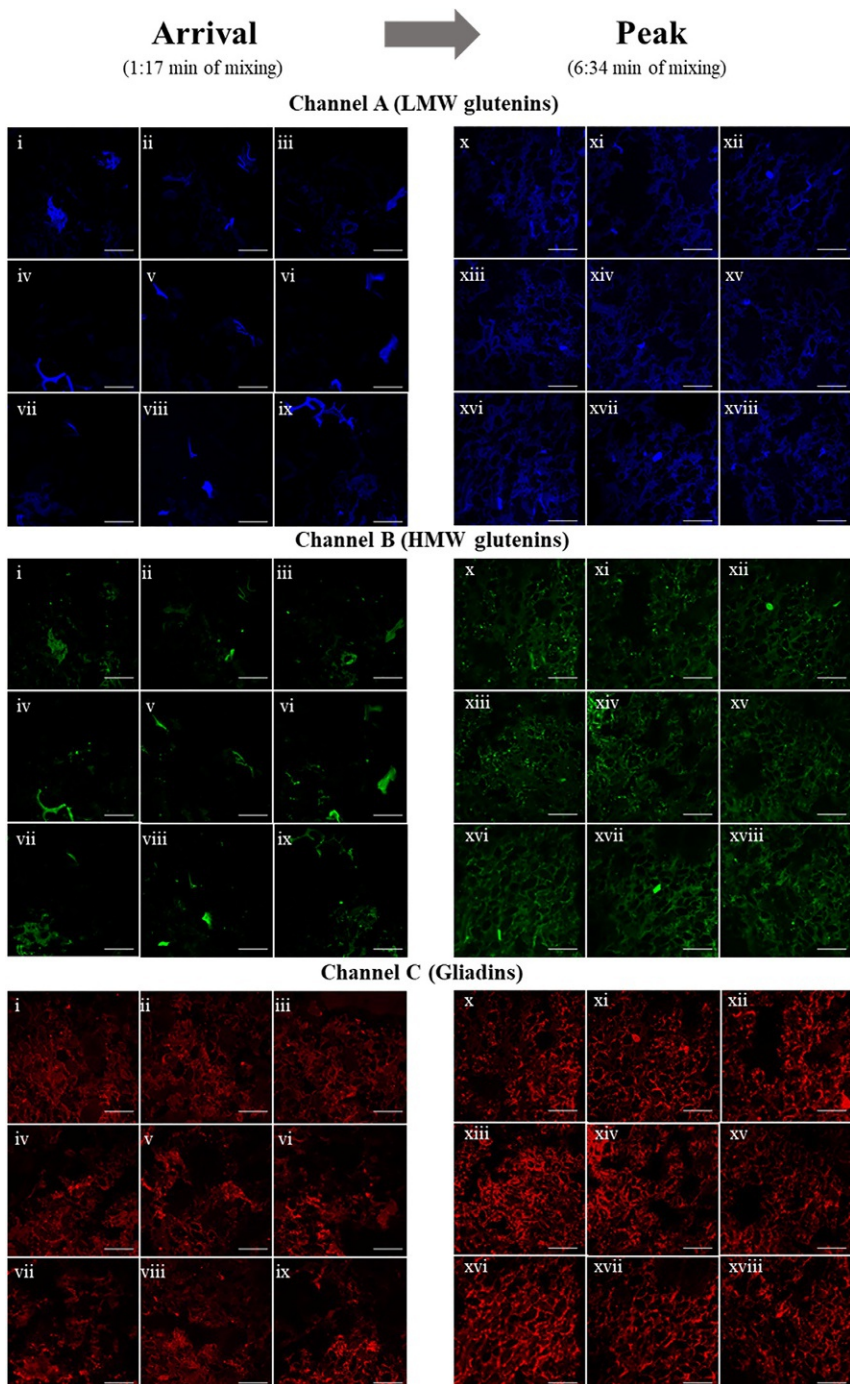


FIG. 11.12 Distribution of LMW glutenins (Channel A), HMW glutenins (Channel B), and gliadins (Channel C) from nine different areas of wheat dough at arrival time (i–ix) and peak time (x–xviii) in the Farinograph. Bar 50 µm. (Reproduced from Bonilla, J.C., Schaber, J.A., Bhunia, A.K., Kokini, J.L., 2019b. Mixing dynamics and molecular interactions of HMW glutenins, LMW glutenins, and gliadins analyzed by fluorescent co-localization and protein network quantification. *J. Cereal Sci.* 89, 102792. <https://doi.org/10.1016/j.cjs.2019.102792>.)

corroborated by the colocalization factors and proteins analysis network, as shown in [Table 11.1](#).

The protein analysis parameters, including protein area, protein percentage area, network junctions, and network endpoints, are significantly higher for gliadin compared to LMW and HMW glutenins at arrival time, as shown in [Table 11.1](#). Also, gliadins present a lower lacunarity, with lacunarity being a measure of the variance of the gaps in the network. A lower lacunarity means a more uniform network formation. This is attributed to the greater molecular mobility of gliadins compared to glutenins. More importantly, all three protein subunits increase their protein network characteristics from arrival to peak and decrease their lacunarity. On the other hand, at arrival time, the colocalization coefficients of LMW glutenins with gliadins and HMW glutenins with gliadins are statistically lower than the colocalization of LMW glutenins with HMW glutenins. These colocalization coefficients show a significant increase from arrival to peak, corroborating the results from the protein network analysis. These increases in protein network characteristics and colocalization coefficients are correlated with an increase of 45 Brabender units (BU) in the Farinograph, from 465 BU at arrival time to 510 BU at peak time. These images and the quantitative data serve as a proof of the gluten network formation by all the different gluten subunits during dough mixing.

Analysis of the distribution of LMW glutenins, HMW glutenins, and gliadins from peak time to departure time.

[Fig. 11.13](#) shows the changes in distribution between peak and departure time in the Farinograph. LMW glutenins behave differently than HMW glutenins. LMW glutenins transition from a homogeneous distribution among the samples at peak time to a more agglomerated state at departure time. HMW glutenins and gliadins seem more distributed at departure time when compared to LMW glutenins. This is proven by the protein network analysis data, in that LMW glutenins present a much greater reduction in protein network characteristics (protein area, area percentage, network junctions, end points), and a higher increase in lacunarity from peak to arrival when compared to HMW glutenins and gliadins. [Table 11.2](#) also shows that the colocalization between LMW glutenins-gliadins decreases significantly from peak to departure, corroborating the observational and protein network analysis results. The colocalization coefficient between HMW glutenins-gliadins and the LMW glutenins with HMW glutenins do not show a significant decrease.

The changes in gluten subunit distribution from peak to departure suggest that the initial breakdown of the gluten network and decrease in dough strength are attributed to the dissociation of the LMW glutenins from the

Table 11.1 Network analysis and colocalization analysis on the fluorescent detection of HMW glutenins, LMW glutenins, and gliadins at arrival and peak times in the Farinograph.

Protein subunit	Protein area		Protein percentage area		Network junctions		Network end points		Mean Lacunarity		Colocalization coefficients		
	Arrival	Peak	Arrival	Peak	Arrival	Peak	Arrival	Peak	Arrival	Peak	Protein subunits	Arrival	Peak
LMW	7778 ^{b,y}	50,954 ^{a,y}	4.40 ^{b,y}	20.32 ^{a,y}	45.00 ^{b,y}	468.33 ^{a,y}	168 ^{b,y}	541 ^{a,y}	2.275 ^{a,x}	0.263 ^{b,x}	LMW-Gliadin	0.42 ^{b,z}	0.62 ^{a,y}
HMW	6104 ^{b,y}	36,979 ^{a,z}	3.43 ^{b,y}	14.64 ^{a,z}	27.22 ^{b,y}	258.33 ^{a,z}	184 ^{b,y}	739 ^{a,x}	2.232 ^{a,x}	0.270 ^{b,x}	HMW-Gliadin	0.53 ^{b,y}	0.84 ^{a,x}
Gliadin	44,055 ^{b,x}	79,981 ^{a,x}	17.55 ^{b,x}	30.93 ^{a,x}	367.6 ^{b,x}	675.33 ^{a,x}	689 ^{a,x}	693 ^{a,x}	0.363 ^{a,y}	0.105 ^{b,y}	LMW-HMW	0.81 ^{a,x}	0.79 ^{a,x}

^{a,b} Numbers with different letters show significant difference between the mixing times (arrival time and peak time) ($P < .05$). Statistical analyses were conducted separately for each protein and for each parameter; for instance, the protein area of HMW glutenins at arrival time was statistically compared to the protein area of HMW glutenins at peak time only.

^{x,y} Numbers with different letters show significant differences between the three different protein subunits (LMW, HMW, and gliadin) ($P < .05$). Statistical analyses were conducted separately for each mixing time and for each parameter; for instance the protein area of HMW glutenins at arrival time was statistically compared to the protein area of LMW glutenins and gliadins at arrival time only.

Reproduced from Bonilla, J.C., Schaber, J.A., Bhunia, A.K., Kokini, J.L., 2019b. Mixing dynamics and molecular interactions of HMW glutenins, LMW glutenins, and gliadins analyzed by fluorescent co-localization and protein network quantification. *J. Cereal Sci.* 89, 102792. <https://doi.org/10.1016/j.cjs.2019.102792>.

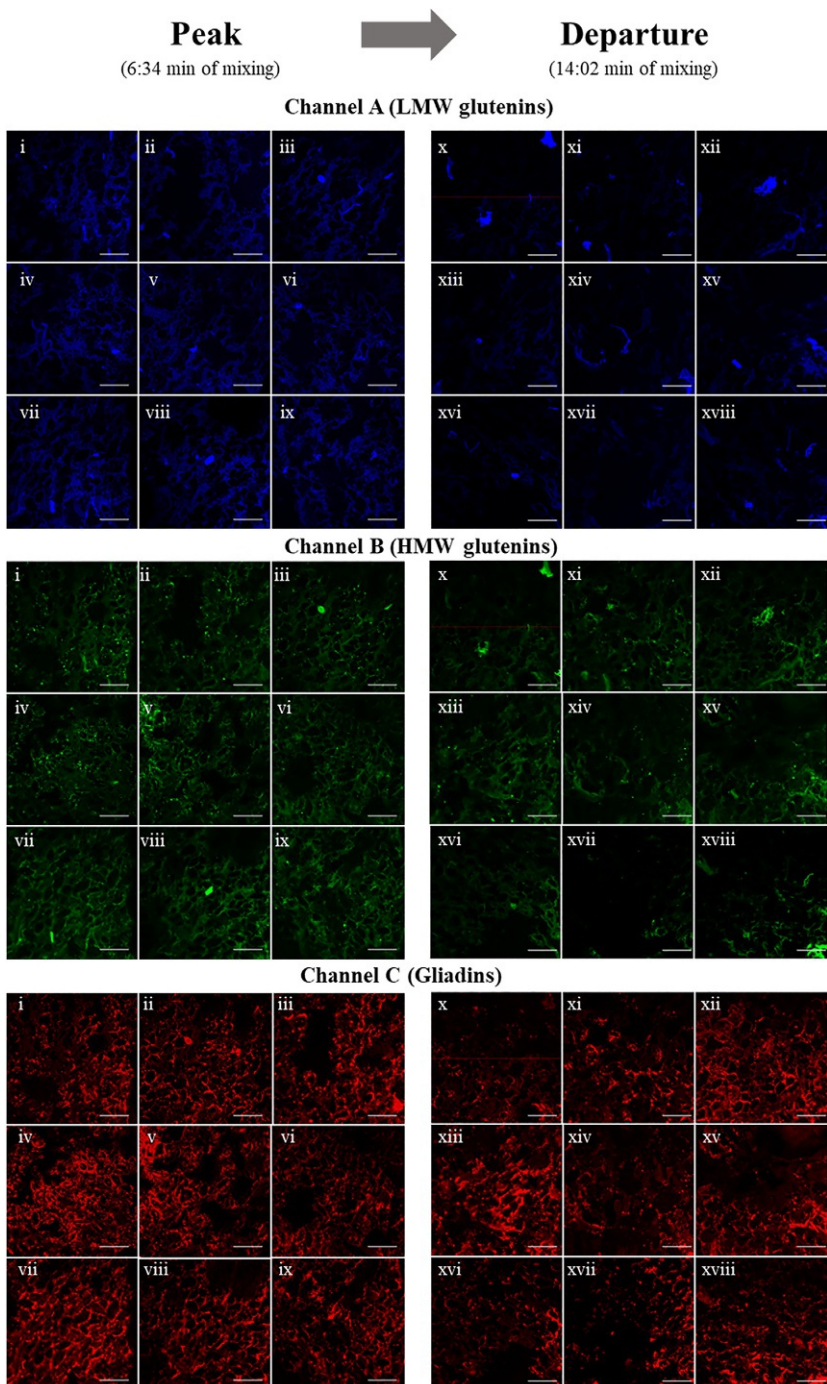


FIG. 11.13 Distribution of LMW glutenins (Channel A), HMW glutenins (Channel B), and gliadins (Channel C) from nine different areas of wheat dough at peak (i–ix) and departure time (x–xviii) in the Farinograph. Bar 50 µm. (Reproduced from Bonilla, J.C., Schaber, J.A., Bhunia, A.K., Kokini, J.L., 2019b. Mixing dynamics and molecular interactions of HMW glutenins, LMW glutenins, and gliadins analyzed by fluorescent co-localization and protein network quantification. *J. Cereal Sci.* 89, 102792. <https://doi.org/10.1016/j.jcs.2019.102792>.)

Table 11.2 Network analysis and colocalization analysis on the fluorescent detection HMW glutenins, LMW glutenins, and gliadins at peak and departure times in the Farinograph.

Protein subunit	Protein area		Protein percentage area		Network junctions		Network end points		Mean Lacunarity		Colocalization coefficients		
	Peak	Depart.	Peak	Depart.	Peak	Depart.	Peak	Depart.	Peak	Depart.	Protein subunits	Peak	Depart.
LMW	50,954 ^{a,y}	16,988 ^{b,y}	20.3 ^{a,y}	7.3 ^{b,y}	468 ^{a,y}	99 ^{b,y}	541 ^{a,y}	367 ^{b,y}	0.26 ^{b,x}	0.99 ^{a,x}	LMW-Gliadin	0.62 ^{a,y}	0.53 ^{b,y}
HMW	36,978 ^{a,z}	2229 ^{b,y}	14.6 ^{a,z}	9.1 ^{b,y}	258 ^{a,z}	130 ^{b,xy}	738 ^{a,x}	522 ^{b,z}	0.27 ^{b,x}	0.77 ^{a,x}	HMW-Gliadin	0.84 ^{a,x}	0.80 ^{a,x}
Gliadin	79,981 ^{a,x}	46,664 ^{b,x}	30.9 ^{a,x}	18.1 ^{b,x}	675 ^{a,x}	333 ^{b,x}	693 ^{a,x}	770 ^{a,x}	0.10 ^{b,y}	0.28 ^{a,y}	LMW-HMW	0.79 ^{a,x}	0.79 ^{a,x}

^{a,b} Numbers with different letters show significant difference between the mixing times (peak time and departure time) ($P < .05$). Statistical analyses were conducted separately for each protein and for each parameter, for instance the protein area of HMW glutenins at peak time was statistically compared to the protein area of HMW glutenins at departure time only.

^{xy} Numbers with different letters show significant differences between the three different protein subunits (LMW, HMW, and gliadin) ($P < .05$). Statistical analyses were conducted separately for each mixing time and for each parameter; for instance, the protein area of HMW glutenins at peak time was statistically compared to the protein area of LMW glutenins and gliadins at peak time only.

gluten network formed by the three different gluten subunits at peak time. At departure time the dough still has high strength, close to 500 Brabender units, confirming that the HMW glutenin subunits play a major role in dough and gluten strength.

Fig. 11.14 shows the changes in distribution of the three different gluten subunits from departure to 10 min after departure time. In this later stage of mixing, the HMW glutenin subunits show a similar behavior to the LMW glutenin subunits from peak to departure time, agglomerating in a few spots. **Table 11.3** shows how the network characteristics (protein area, percentage area, network junctions, and network endpoints) are drastically reduced. Also, the lacunarity is increased. These indicators show how the network characteristics of the HMW glutenin subunits are lost 10 min after the departure time in the Farinograph. The colocalization of HMW glutenins with gliadins is significantly decreased, proving that the gluten network is completely disintegrated.

A more recent study has shown how the three different gluten subunits distribute differently in wheat doughs from soft wheat, hard wheat, and semolina (Bonilla et al., 2020a). The different interactions between HMW glutenins, LMW glutenins, and gliadins were studied at different stages of dough mixing. The three different doughs were all mixed with 55% added water; therefore they all have different Farinograph peak torque values due to their different protein contents and water absorption requirements. Dough samples were taken at peak or dough development time and 10 min after dough development time. It was found that HMW glutenins are relatively immobile because of their reduced molecular mobility and do not redistribute themselves for stronger doughs, such as those from hard wheat flour. On the other hand, a greater stability of strong doughs is possible due to the network formed by the redistribution of LMW glutenins and gliadins. In weaker doughs, such as those from soft wheat, the decay in dough strength involves the breakdown of each individual protein subunit. The constant redistribution of LMW glutenins in the semolina samples was found to be responsible for the stable farinogram seen in the mixing of semolina. The large amount of LMW glutenins found in semolina allows the constant interaction (detaching and reattaching) of HMW glutenins and LMW glutenins. Overall, the use of these quantitative analysis techniques and in situ detection of gluten subunits were found to be more sensitive to the changes occurring in the gluten network than oscillatory rheological analysis. Following studies have looked at how these gluten proteins behave during rheological measurements (Bonilla et al., 2020b). The understanding of how gluten proteins behave inside the C. W. Brabender mixing bowl has led to further studies on how these proteins influence the behavior of dough in large amplitude deformations (Turksoy et al., 2020).

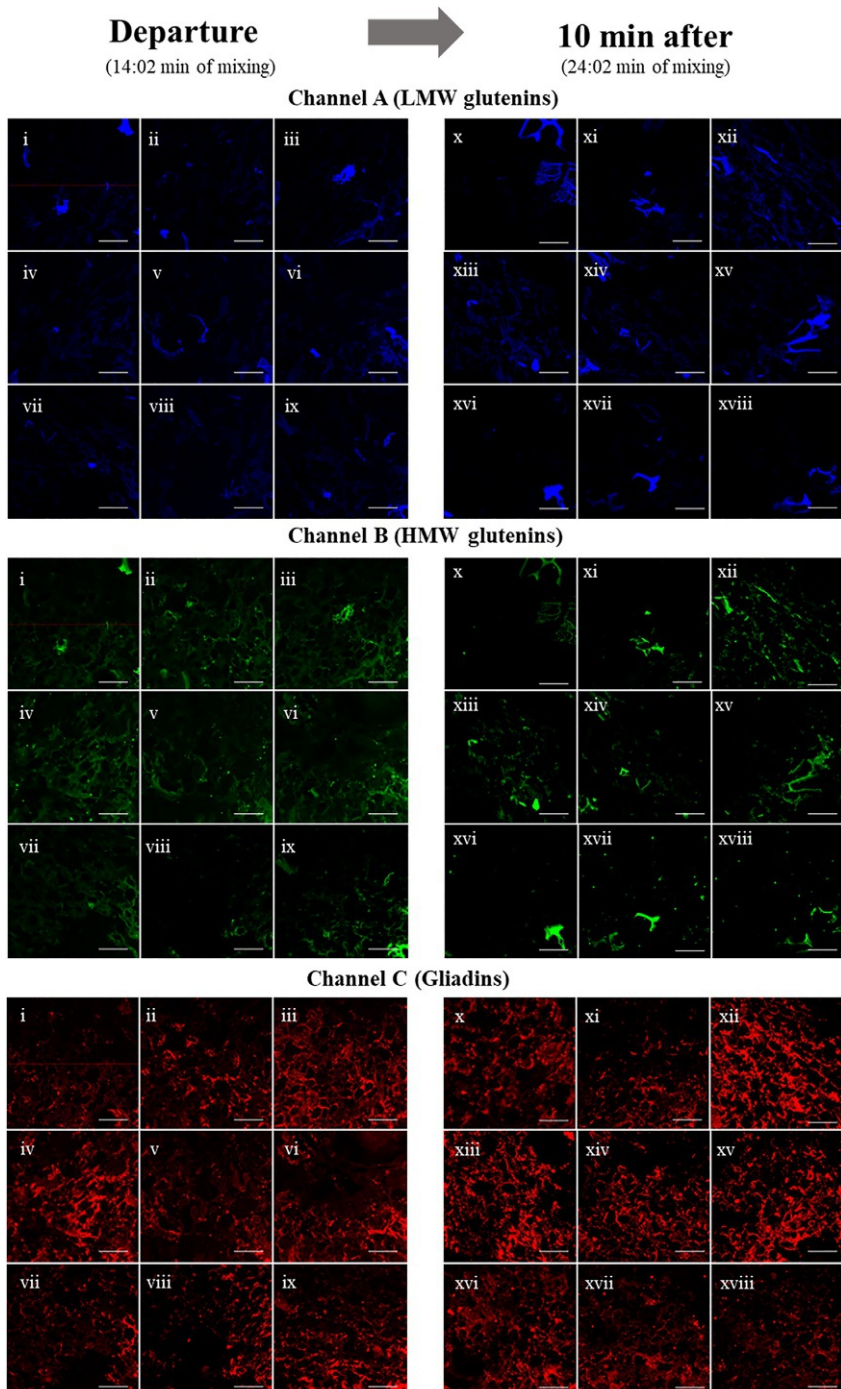


FIG. 11.14 Distribution of LMW glutenins (Channel A), HMW glutenins (Channel B), and gliadins (Channel C) from nine different areas of wheat dough at departure time (i–ix) and 10 min after departure time (x–xvii) in the Farinograph. Bar 50 µm. (Reproduced from Bonilla, J.C., Schaber, J.A., Bhunia, A.K., Kokini, J.L., 2019b. Mixing dynamics and molecular interactions of HMW glutenins, LMW glutenins, and gliadins analyzed by fluorescent co-localization and protein network quantification. *J. Cereal Sci.* 89, 102792. <https://doi.org/10.1016/j.jcs.2019.102792>.)

Table 11.3 Network analysis on the fluorescent detection HMW glutenins, LMW glutenins, and gliadins at peak and departure times in the Farinograph.

Protein subunit	Protein area		Protein percentage area		Network junctions		Network end points		Mean Lacunarity		Colocalization coefficients		
	Depart.	10 min	Depart.	10 min	Depart.	10 min	Depart.	10 min	Depart.	10 min	Protein subunits	Depart.	10 min
LMW	16,988 ^{a,y}	16,035 ^{a,x}	7.3 ^{a,y}	7.78 ^{a,y}	99 ^{a,y}	98 ^{a,y}	367 ^{a,y}	270 ^{a,y}	0.99 ^{a,x}	1.87 ^{a,x}	LMW-Gliadin	0.53 ^{a,y}	0.42 ^{b,y}
HMW	22,294 ^{a,y}	11,995 ^{b,x}	9.1 ^{a,y}	5.64 ^{b,y}	130 ^{a,xy}	57 ^{b,y}	522 ^{a,z}	207 ^{b,y}	0.77 ^{b,x}	2.11 ^{a,x}	HMW-Gliadin	0.80 ^{a,x}	0.41 ^{b,y}
Gliadin	46,664 ^{b,x}	71,008 ^{a,x}	18.1 ^{b,x}	27.7 ^{a,x}	333 ^{b,x}	587 ^{a,x}	770 ^{a,x}	617 ^{b,x}	0.28 ^{a,y}	0.17 ^{a,y}	LMW-HMW	0.79 ^{a,x}	0.79 ^{a,x}

^{a,b} Numbers with different letters show significant difference between the mixing times (departure time and 10 min after departure) ($P < .05$). Statistical analyses were conducted separately for each protein and for each parameter; for instance, the protein area of HMW glutenins at arrival time was statistically compared to the protein area of HMW glutenins at peak time only.

^{x,y} Numbers with different letters show significant differences between the three different protein subunits (LMW, HMW, and gliadin) ($P < .05$). Statistical analyses were conducted separately for each mixing time and for each parameter; for instance, the protein area of HMW glutenins at departure time was statistically compared to the protein area of LMW glutenins and gliadins at departure time only.

11.5 DISTRIBUTION OF EXTENSION RATE AND SHEAR RATE AND PREDICTION OF MAXIMUM STABLE BUBBLE SIZE INSIDE THE C.W. BRABENDER FARINOGRAPH

In a recent study using the Brabender Farinograph, mixing and development of hard wheat dough was simulated ([Bozdogan et al., n.d.](#)). Finite element method (FEM) codes provided by the ANSYS Polyflow company with the mesh superposition technique were used to calculate the distribution of extension rates, shear rates and the effects of the distribution of extension rate and shear rate on bubble size distribution inside the mixer. Three components of the local velocity (v_x, v_y, v_z), extension rate magnitudes, shear rate magnitudes, and maximum stable bubble sizes as a function of time and location were determined inside the Brabender Farinograph using 3D finite element simulation. The same mesh structures shown in [Fig. 11.15A](#) and [B](#) that were used in the studies of [Connelly and Kokini \(2006a,b\)](#) were also used here. The Bird-Carreau constitutive model, which successfully predicted steady and oscillatory shear viscoelastic properties of wheat flour doughs ([Dhanasekharan et al., 1999; Dus and Kokini, 1990](#)), was used to simulate the shear rate dependence of viscosity of hard wheat flour dough. Extension rate ($\dot{\epsilon}$) (Eq. 11.1) was calculated using the second and third invariants of strain rate tensor using the exact derivations of [Debbaut and Crochet \(1988\)](#). Flow type parameter (α) (Eq. 11.2) was defined to quantify the deformation and rotation of the flow ([Bentley and Leal, 1986](#)).

$$\dot{\epsilon} = 3III_D / II_D \quad (11.1)$$

$$\frac{\text{Magnitude of strain rate}}{\text{Magnitude of vorticity}} = \frac{1 + \alpha}{1 - \alpha} \quad (11.2)$$

Critical capillary number, Ca_{cr} , was calculated to determine the maximum stable bubble diameter in the fluid. All bubble sizes would have to be smaller than this critical bubble diameter in the flow field defined by the local flow strength. The relationship between the flow type parameter and the critical capillary number and maximum stable bubble size diameter was determined by the equations developed by [Bentley and Leal \(1986\)](#) given in Eqs. (11.3), (11.4).

$$Ca_{cr} = \frac{0.145 p^{-1/6}}{\alpha^{1/2}} \quad (11.3)$$

$$Ca_{cr} = 2^{1/3} \frac{\mu_c G}{\sigma} r \quad (11.4)$$

where σ is the surface tension of the dough, μ_c is the viscosity of the hard wheat flour dough, G is the strength of the external flow, and r is the radius of the bubble.

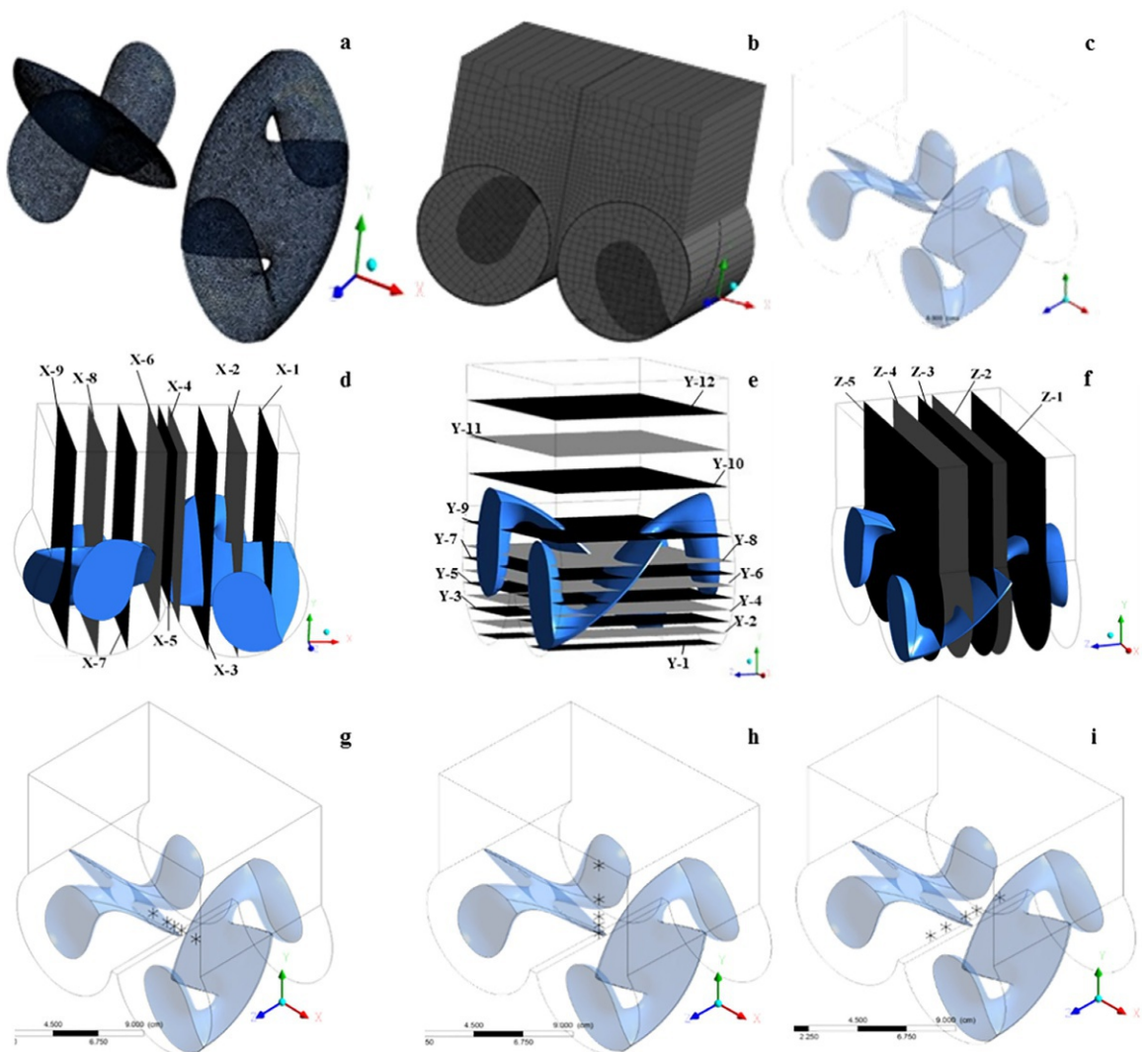


FIG. 11.15 Meshes for the Farinograph, and location of measurement planes and points; (A) blades, (B) barrel, (C) beginning positions of the paddles, (D) Plane X-1, Plane X-2, Plane X-3, Plane X-4, Plane X-5, Plane X-6, Plane X-7, Plane X-8, and Plane X-9, (E) Plane Y-1, Plane Y-2, Plane Y-3, Plane Y-4, Plane Y-5, Plane Y-6, Plane Y-7, Plane Y-8, Plane Y-9, Plane Y-10, Plane Y-11, and Plane Y-12, (F) Plane Z-1, Plane Z-2, Plane Z-3, Plane Z-4, and Plane Z-5, (G) Points on X axis (Point 1, Point 2, Point 3, Point 4, and Point 5), (H) Points on Y axis (Point 1, Point 6, Point 7, Point 8, and Point 9), and (I) Points on Z axis (Point 1, Point 10, Point 11, Point 12, and Point 13).

In order to measure the extension rate, shear rate, and maximum stable bubble size inside the mixer, measurement planes and points were created (Fig. 11.15D and E).

Determination of the extension rate inside the Farinograph was conducted for the first time and it was used to calculate the maximum stable

size distribution inside the mixer. Three different flow patterns were observed during the mixing process, and the results showed that both extension rate and shear rate are time and location dependent. The magnitudes of extension rate and shear rate varied with the rotation rate of each paddle, local layout of the paddles, and interaction between the paddles. The largest extension and shear rates were found to exist inside the mixing chambers, especially in the center of the mixer, which is affected by both paddles, and on the locations that were swept by the blades (Fig. 11.16). These locations are the places where the larger bubbles are broken down into much smaller bubbles under the impact of the strong flows that exist.

Because of large extension and shear rate magnitudes, especially in the center of the mixer, we observe high dispersive and distributive mixing. In the upper locations of the mixer, the dough was shown to experience much smaller flow strengths.

Critical capillary number, which is the critical ratio of the viscous forces to interfacial forces, was calculated as a function of flow strength and it was found that in smaller flow strengths, bubbles need a higher critical capillary

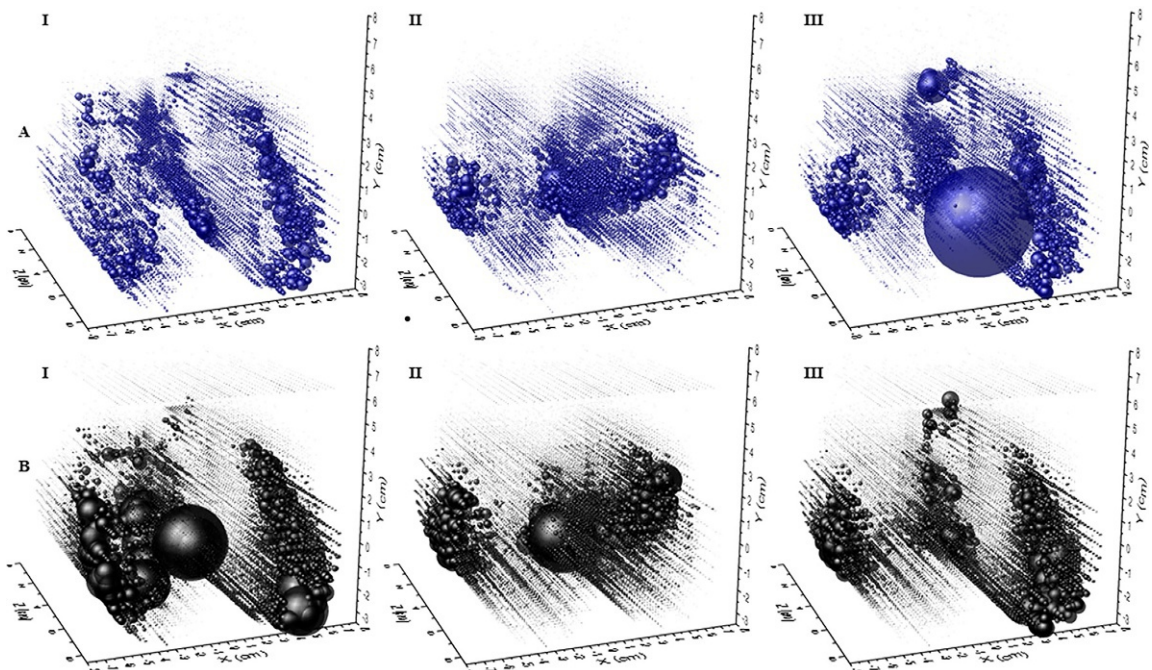


FIG. 11.16 Distribution of (A) Extension rate magnitude, and (B) Local shear rate magnitude at (I) 0.645168 s; (II) 0.967752 s; (III) 1.902862 s inside the mixer. Scaling factors were used to represent the magnitudes. For extension rate magnitudes, 0.5 used as scaling factor, and for local shear rate magnitudes, 0.1 used as scaling factor.

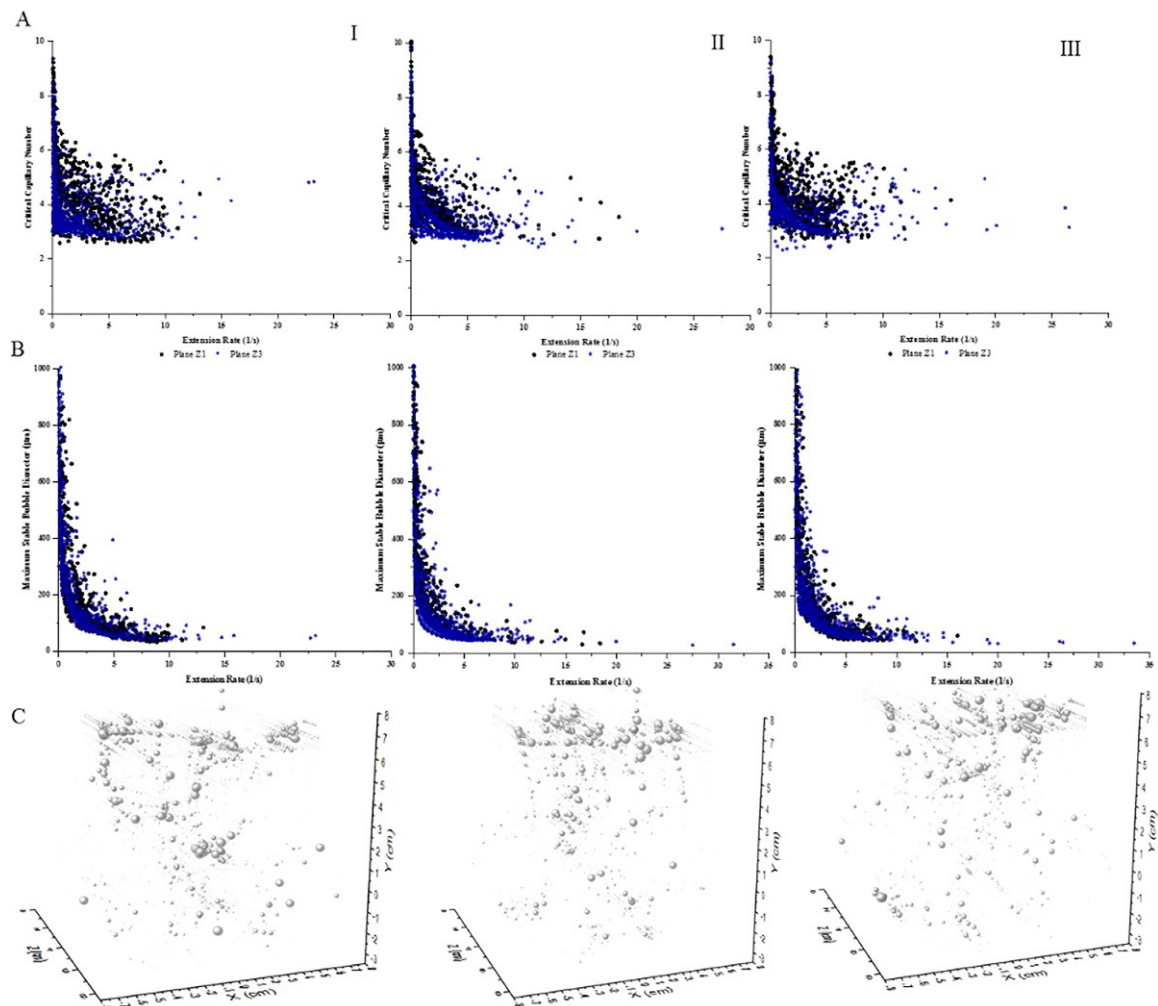


FIG. 11.17 (A) Extension rate dependency of critical capillary number, (B) Extension rate dependency of maximum stable bubble diameter, (C) Bubble size distribution inside the mixer (scaling factor is 5) at (I) 0.645168 s, (II) 0.967752 s, (III) 1.90862 s.

number to break, which can be obtained with high viscous forces (Fig. 11.17). However, since the shear rate and extension rates are small in these regions, the resulting viscous forces are also small, and any bubbles that form here need to migrate toward the center of the mixer in order to break down into smaller bubbles. In addition, it was determined that different planes show different flow strengths to break up the bubbles to different degrees. The development of the dough was observed using maximum stable bubble sizes at different simulation times. Maximum stable bubble sizes

were smaller and more homogeneous inside the mixing chambers, especially in the center of the mixer compared with the upper parts of the mixer. Smaller and more homogeneous bubble sizes were induced by larger flow strengths during mixing. It was found that increase in the extension rate caused a more pronounced decrease in bubble diameter than shear rate. In addition, variation in the flow types between the planes creates both small and big bubbles. However, flow patterns that create the movement of the fluid inside the mixer helps the fluid to experience different flow types and creates smaller and more homogeneously distributed bubble sizes. Clearly, numerical simulations can help design a mixer and process conditions that can help create bubble size distribution for optimal dough quality and characteristics for optimal expansion of bread. These studies also show that numerical simulation can help in scale-up of mixers for optimal operation of the mixer.

In conclusion, the use of individual labeling of gluten subunit proteins allowed their tracking in a Farinograph bowl during mixing. The mechanical forces transferred from the Farinograph mixing blades to the dough have a different impact on the HMW glutenins, LMW glutenins, and gliadins depending on the gluten characteristics of the flour and the mixing conditions. HMW glutenins tend to redistribute and mix less at high dough strengths. LMW glutenins are the first gluten subunit to break down when the dough is overmixed. The greater LMW:HMW glutenins ratio in semolina is responsible for the prolonged stability during semolina mixing. Gliadins are the most molecularly mobile protein subunit in dough, and they flow and redistribute more evenly than the other subunits during all stages of mixing. These studies are nicely complemented with mixing simulations of how the bubbles redistribute in Farinograph bowls during mixing since gluten proteins are also surface proteins. Further studies could potentially help identify the function of each gluten subunit at the surface of the dough bubbles and indicate how the protein subunits contribute to bubble stability and therefore dough mixing stability.

REFERENCES

- Autio, K., Laurikainen, T., 1997. Relationships between flour/dough microstructure and dough handling and baking properties. *Trends Food Sci. Technol.* 8, 181–185.
[https://doi.org/10.1016/S0924-2244\(97\)01039-X](https://doi.org/10.1016/S0924-2244(97)01039-X).
- Bentley, B.J., Leal, L.G., 1986. An experimental investigation of drop deformation and breakup in steady, two-dimensional linear flows. *J. Fluid Mech.* 167, 241–283.
<https://doi.org/10.1017/S0022112086002811>.
- Bernklau, I., Lucas, L., Jekle, M., Becker, T., 2016. Protein network analysis—a new approach for quantifying wheat dough microstructure. *Food Res. Int.* 89, 812–819.
<https://doi.org/10.1016/j.foodres.2016.10.012>.

- Bonilla, J.C., Bozkurt, F., Ansari, S., Sozer, N., Kokini, J.L., 2016. Applications of quantum dots in food science and biology. *Trends Food Sci. Technol.* 53, 75–89. <https://doi.org/10.1016/j.tifs.2016.04.006>.
- Bonilla, J.C., Ryan, V., Yazar, G., Kokini, J.L., Bhunia, A.K., 2018. Conjugation of specifically developed antibodies for high- and low-molecular-weight glutenins with fluorescent quantum dots as a tool for their detection in wheat flour dough. *J. Agric. Food Chem.* 66, 4259–4266. <https://doi.org/10.1021/acs.jafc.7b05711>.
- Bonilla, J.C., Bernal-Crespo, V., Schaber, J.A., Bhunia, A.K., Kokini, J.L., 2019a. Simultaneous immunofluorescent imaging of gliadins, low molecular weight glutenins, and high molecular weight glutenins in wheat flour dough with antibody-quantum dot complexes. *Food Res. Int.* 120, 776–783. <https://doi.org/10.1016/j.foodres.2018.11.038>.
- Bonilla, J.C., Schaber, J.A., Bhunia, A.K., Kokini, J.L., 2019b. Mixing dynamics and molecular interactions of HMW glutenins, LMW glutenins, and gliadins analyzed by fluorescent co-localization and protein network quantification. *J. Cereal Sci.* 89. <https://doi.org/10.1016/j.jcs.2019.102792>, 102792.
- Bonilla, J.C., Erturk, M.Y., Kokini, J.L., 2020a. Understanding the role of gluten subunits (LMW, HMW glutenins and gliadin) in the networking behavior of a weak soft wheat dough and a strong semolina wheat flour dough and the relationship with linear and non-linear rheology. *Food Hydrocoll.* 108, 106002. <https://doi.org/10.1016/j.foodhyd.2020.106002>.
- Bonilla, J.C., Erturk, M.Y., Schaber, J.A., Kokini, J.L., 2020b. Distribution and function of LMW glutenins, HMW glutenins, and gliadins in wheat doughs analyzed with ‘in situ’ detection and quantitative imaging techniques. *J. Cereal Sci.* 93. <https://doi.org/10.1016/j.jcs.2020.102931>, 102931.
- Bozdogan, N., Tayman, S., Kumcuoglu, S., Kokini, J.L., n.d. Comparison of the Behavior and Distribution of Shear and Extension Rates in a Model Sigma Blade Mixer for a Bird-Carreau Type Non-Newtonian Fluid. Unpubl. Data.
- Bozkurt, F., Ansari, S., Yau, P., Yazar, G., Ryan, V., Kokini, J., 2014. Distribution and location of ethanol soluble proteins (Osborne gliadin) as a function of mixing time in strong wheat flour dough using quantum dots as a labeling tool with confocal laser scanning microscopy. *Food Res. Int.* 66, 279–288. <https://doi.org/10.1016/j.foodres.2014.09.028>.
- Clarke, B.C., Phongkham, T., Gianibelli, M., Beasley, H., Bekes, F., 2003. The characterisation and mapping of a family of LMW-gliadin genes: effects on dough properties and bread volume. *Theor. Appl. Genet.* 106, 629–635. <https://doi.org/10.1007/s00122-002-1091-1>.
- Connelly, R.K., Kokini, J.L., 2006a. 3D numerical simulation of the flow of viscous Newtonian and shear thinning fluids in a twin sigma blade mixer. *Adv. Polym. Technol.* 25, 182–194. <https://doi.org/10.1002/adv.20071>.
- Connelly, R.K., Kokini, J.L., 2006b. Mixing simulation of a viscous Newtonian liquid in a twin sigma blade mixer. *AICHE J.* 52, 3383–3393. <https://doi.org/10.1002/aic.10960>.
- Debbaut, B., Crochet, M.J., 1988. Extensional effects in complex flows. *J. Non-Newton. Fluid Mech.* 30, 169–184. [https://doi.org/10.1016/0377-0257\(88\)85023-7](https://doi.org/10.1016/0377-0257(88)85023-7).
- Delcour, J.A., Hoseney, R.C., 2010. Principles of cereal science and technology authors provide insight into the current state of cereal processing. *Cereal Foods World* 55(1), 21–22.
- Dhanasekharan, M., Huang, H., Kokini, J.L., 1999. Comparison of observed rheological properties of hard wheat flour dough with predictions of the Giesekus-Leonov, White-Metzner and Phan-thien tanner models. *J. Texture Stud.* 30, 603–623. <https://doi.org/10.1111/j.1745-4603.1999.tb00233.x>.

- Don, C., Lichtendonk, W.J., Plijter, J.J., van Vliet, T., Hamer, R.J., 2005. The effect of mixing on glutenin particle properties: aggregation factors that affect gluten function in dough. *J. Cereal Sci.* 41, 69–83. <https://doi.org/10.1016/j.jcs.2004.09.009>.
- Dus, S.J., Kokini, J.L., 1990. Prediction of the nonlinear viscoelastic properties of a hard wheat flour dough using the Bird-Carreau constitutive model. *J. Rheol.* 34, 1069–1084. <https://doi.org/10.1122/1.550110>.
- Finney, K.F., 1943. Fractionating and reconstituting techniques as tools in wheat flour research. *Cereal Chem.* 20, 381–396.
- Graveland, A., Bosveld, P., Lichtendonk, W.J., Moonen, H.E.H., Scheepstra, A., 1982. Extraction and fractionation of wheat flour proteins. *J. Sci. Food Agric.* 33, 1117–1128. <https://doi.org/10.1002/jsfa.2740331109>.
- Gupta, R.B., MacRitchie, F., 1994. Allelic variation at glutenin subunit and gliadin loci, Glu-1, Glu-3 and Gli-1 of common wheats. II. Biochemical basis of the allelic effects on dough properties. *J. Cereal Sci.* 19, 19–29. <https://doi.org/10.1006/jcrs.1994.1004>.
- Hoseney, R.C., Pomeranz, Y., Finney, K.F., 1970. Functional (breadmaking) and biochemical properties of wheat flour components. VII. Petroleum ether-soluble lipoproteins of wheat flour. *Cereal Chem.* 47, 135–140.
- Jones, R.W., Taylor, N.W., Senti, F.R., 1959. Electrophoresis and fractionation of wheat gluten. *Arch. Biochem. Biophys.* 84, 363–376. [https://doi.org/10.1016/0003-9861\(59\)90599-5](https://doi.org/10.1016/0003-9861(59)90599-5).
- Kieffer, R., Stein, N., 1999. Demixing in wheat doughs—its influence on dough and gluten rheology. *Cereal Chem.* 76, 688–693. <https://doi.org/10.1094/CCHEM.1999.76.5.688>.
- Kokawa, M., Fujita, K., Sugiyama, J., Tsuta, M., Shibata, M., Araki, T., Nabatani, H., 2012. Quantification of the distributions of gluten, starch and air bubbles in dough at different mixing stages by fluorescence fingerprint imaging. *J. Cereal Sci.* 55, 15–21. <https://doi.org/10.1016/j.jcs.2011.09.002>.
- Kokawa, M., Sugiyama, J., Tsuta, M., Yoshimura, M., Fujita, K., Shibata, M., Araki, T., Nabatani, H., 2013. Development of a quantitative visualization technique for gluten in dough using fluorescence fingerprint imaging. *Food Bioprocess Technol.* 6, 3113–3123. <https://doi.org/10.1007/s11947-012-0982-7>.
- Kokini, J.L., Cocero, A.M., Madeka, H., de Graaf, E., 1994. The development of state diagrams for cereal proteins. *Trends Food Sci. Technol.* 5, 281–288. [https://doi.org/10.1016/0924-2244\(94\)90136-8](https://doi.org/10.1016/0924-2244(94)90136-8).
- Lee, L., Ng, P.K.W., Whallon, J.H., Steffe, J.F., 2001. Relationship between rheological properties and microstructural characteristics of nondeveloped, partially developed, and developed doughs. *Cereal Chem.* 78, 447–452. <https://doi.org/10.1094/CCHEM.2001.78.4.447>.
- Li, W., Dobraszczyk, B.J., Wilde, P.J., 2004. Surface properties and locations of gluten proteins and lipids revealed using confocal scanning laser microscopy in bread dough. *J. Cereal Sci.* 39 (3), 403–411. <https://doi.org/10.1016/j.jcs.2004.02.004>.
- Loussert, C., Popineau, Y., Mangavel, C., 2008. Protein bodies ontogeny and localization of prolamin components in the developing endosperm of wheat caryopses. *J. Cereal Sci.* 47, 445–456. <https://doi.org/10.1016/j.jcs.2007.05.012>.
- MacRitchie, F., 1987. Evaluation of contributions from wheat protein fractions to dough mixing and breadmaking. *J. Cereal Sci.* 6, 259–268. [https://doi.org/10.1016/S0733-5210\(87\)80063-2](https://doi.org/10.1016/S0733-5210(87)80063-2).
- Magnus, E.M., Bråthen, E., Sahlstrøm, S., Vogt, G., Færgestad, E.M., 2000. Effects of flour composition, physical dough properties and baking process on hearth loaf

- properties studied by multivariate statistical methods. *J. Cereal Sci.* 32, 199–212. <https://doi.org/10.1006/jcrs.2000.0325>.
- Manders, E.M.M., Verbeek, F.J., Aten, J.A., 1993. Measurement of co-localization of objects in dual-colour confocal images. *J. Microsc.* 169, 375–382. <https://doi.org/10.1111/j.1365-2818.1993.tb03313.x>.
- Micard, V., Guillet, S., 2000. Thermal behavior of native and hydrophobized wheat gluten, gliadin and glutenin-rich fractions by modulated DSC. *Int. J. Biol. Macromol.* 27, 229–236. [https://doi.org/10.1016/S0141-8130\(00\)00122-7](https://doi.org/10.1016/S0141-8130(00)00122-7).
- Migliori, M., Correra, S., 2013. Modelling of dough formation process and structure evolution during farinograph test. *Int. J. Food Sci. Technol.* 48, 121–127. <https://doi.org/10.1111/j.1365-2621.2012.03167.x>.
- Nieto-Taladriz, M.T., Perretant, M.R., Rousset, M., 1994. Effect of gliadins and HMW and LMW subunits of glutenin on dough properties in the F6 recombinant inbred lines from a bread wheat cross. *Theor. Appl. Genet.* 88, 81–88. <https://doi.org/10.1007/BF00222398>.
- Osborne, T.B., 1907. *The Proteins of the Wheat Kernel*. Carnegie institution of Washington.
- Primo-Martín, C., Sözer, N., Hamer, R.J., Van Vliet, T., 2009. Effect of water activity on fracture and acoustic characteristics of a crust model. *J. Food Eng.* 90, 277–284. <https://doi.org/10.1016/j.jfoodeng.2008.06.039>.
- Shewry, P.R., Tatham, A.S., 1990. The prolamin storage proteins of cereal seeds: structure and evolution. *Biochem. J.* 267, 1–12.
- Shewry, P.R., Tatham, A.S., Forde, J., Kreis, M., Miflin, B.J., 1986. The classification and nomenclature of wheat gluten proteins: a reassessment. *J. Cereal Sci.* 4, 97–106. [https://doi.org/10.1016/S0733-5210\(86\)80012-1](https://doi.org/10.1016/S0733-5210(86)80012-1).
- Shewry, P.R., Halford, N.G., Belton, P.S., Tatham, A.S., 2002. The structure and properties of gluten: an elastic protein from wheat grain. *Philos. Trans. R. Soc. B Biol. Sci.* 357, 133–142. <https://doi.org/10.1098/rstb.2001.1024>.
- Singh, N.K., Shepherd, K.W., 1988. Linkage mapping of genes controlling endosperm storage proteins in wheat. *Theor. Appl. Genet.* 75, 628–641. <https://doi.org/10.1007/BF00289132>.
- Sozer, N., Kokini, J.L., 2014. Use of quantum nanodot crystals as imaging probes for cereal proteins. *Food Res. Int.* 57, 142–151. <https://doi.org/10.1016/j.foodres.2013.12.031>.
- Tatham, A.S., Miflin, B.J., Shewry, P.R., 1985. The beta-turn conformation in wheat gluten proteins: relationship to gluten elasticity. *Cereal Chem.* 62, 405–412.
- Tronsmo, K.M., Magnus, E.M., Baardseth, P., Schofield, J.D., Aamodt, A., Færgestad, E.M., 2003. Comparison of small and large deformation rheological properties of wheat dough and gluten. *Cereal Chem.* 80, 587–595. <https://doi.org/10.1094/CHEM.2003.80.5.587>.
- Tsuta, M., Miyashita, K., Suzuki, T., Nakauchi, S., Sagara, Y., Sugiyama, J., 2007. Three-dimensional visualization of internal structural changes in soybean seeds during germination by excitation-emission matrix imaging. *Trans. ASABE* 50, 2127–2136. <https://doi.org/10.13031/2013.24072>.
- Turksoy, S., Erturk, M.Y., Bonilla, J.C., Turasan, H., Kokini, J., 2020. Effect of aging at different temperatures on LAOS properties and secondary protein structure of hard wheat flour dough. *J. Cereal Sci.* 92. <https://doi.org/10.1016/j.jcs.2020.102926>. In this issue.

- Uthayakumaran, S., Gras, P.W., Stoddard, F.L., Bekes, F., 1999. Effect of varying protein content and glutenin-to-gliadin ratio on the functional properties of wheat dough. Cereal Chem. 76, 389–394. <https://doi.org/10.1094/CHEM.1999.76.3.389>.
- Weegels, P.L., Hamer, R.J., Schofield, J.D., 1997. Depolymerisation and re-polymerisation of wheat glutenin during dough processing. II. Changes in composition. J. Cereal Sci. 25, 155–163. <https://doi.org/10.1006/jcrs.1996.0082>.
- Wrigley, C.W., Lawrence, G.J., Shepherd, K.W., 1982. Protein mapping by combined gel electrofocusing and electrophoresis: application to study of genotypic variation in wheat gliadins. J. Plant Physiol. 9, 15–30.
- Wrigley, C., Bekes, F., Bushuk, W., 2006. Gliadin and glutenin the unique balance of wheat quality. In: Presented at the AACC International, St. Paul, Minnesota.
- Zeglis, B.M., Davis, C.B., Aggeler, R., Kang, H.C., Chen, A., Agnew, B.J., Lewis, J.S., 2013. Enzyme-mediated methodology for the site-specific radiolabeling of antibodies based on catalyst-free click chemistry. Bioconjug. Chem. 24, 1057–1067. <https://doi.org/10.1021/bc400122c>.

Section C

Appendices

This page intentionally left blank

Appendix



Bowl cleaning and maintenance

Every Farinograph test necessitates cleaning of the bowl afterwards to remove dough and/or sample residue. Proper cleaning can extend the life of the bowl and prevent unnecessary down-time due to maintenance or repair needs. However, many common mistakes made during cleaning can result in damage to the mixer and/or drifting of results over time. This section is designed to provide general cleaning instructions as well as key points that indicate repairs are needed to bring the bowl back into good operating condition.

CLEANING

Proper cleaning starts with appropriate cleaning materials, which include:

- Cleaning flour
- Soft cloths
- Brushes with soft bristles
- Floss or other small string
- Water

METAL OBJECTS, SCOURING AGENTS, CHEMICALS, AND/OR DETERGENTS SHOULD NEVER BE USED TO CLEAN A FARINOGRAPH MIXER.

The first step of cleaning is to add cleaning flour to the dough or sample in the mixer. Cleaning flour is usually a mixture of regular wheat flour (1000g) with bran (100g) and fine salt (150g) for gentle abrasive action. Adding an appropriate amount (determined by mixer bowl size and sample) of this cleaning flour to the mixer bowl makes the dough easier to remove, as it absorbs excess water and gently abrades dough or sample residue from the mixer blades and walls.

After all the cleaning flour is fully incorporated into the dough, the mixer should be stopped, disassembled, and the dough mass removed. The mixer should be fully unscrewed from the base of the unit and the coupling separated from the clutch halves to allow free turning of the mixer blades. If the mixer blades are removable, the blades should be removed and cleaned separately with a wet cloth.

Next, a wet cloth should be used to remove all dough or sample residue from the mixer bowl, walls, lid, and blades. It is often easier to do this if a small container of water is available nearby.

Alternatively, the removable portion of the mixer bowl can be placed in a container of water and scrubbed with a cloth or a brush with soft bristles. Blades can also be placed in a container of water and scrubbed similarly, although not at the same time as the mixer bowl, to minimize the potential for damage. The bowl and blades should be dried separately with a soft cloth after cleaning.

The body of nonremovable mixer blades can be cleaned with a wet cloth or brush. However, cleaning behind the blades is essential and requires the use of water and floss or other small string to flush and remove debris stuck between the mixer blade and back wall. The blade and wall should be dried afterwards with a soft cloth.

The mixer bowl should be reassembled once all components have been thoroughly cleaned and dried. All removable blades should be lubricated with a thin layer of silicone gel lubricant on their respective bronze bushings as per manufacturer instructions before reassembly. The coupling can then be rejoined to the clutch halves and the mixer screwed down to the unit base again for further use.

MAINTENANCE

Mixers should ideally be sent in for maintenance and calibration every 2 years. It is recommended to do this sooner if the mixer accrues a high number of operating hours. However, some warning signs may indicate that a mixer needs to be sent in immediately for maintenance and repairs:

- Leakage of dough behind the blades—Indicates that the mixing blade bushings are worn and require replacement.
- Rough or irregular farinograms—A sign of worn or damaged mixing blades or bearings. Repairs to the blades and/or replacement of the bearings are required.
- Excessively high water absorption values—Caused by bowl surface damage. This is not typically repairable and may require the purchase of a new mixer bowl.
- Excessive smearing of dough on bowl walls—Signifies a clearance issue between the blades and the bowl. This may not be repairable as blades and bowls are manufactured as a set and are not typically interchangeable. Resolving the issue may require the purchase of a new mixer bowl.

Troubleshooting

The following is a noncomprehensive list of possible errors, causes, and troubleshooting solutions that are commonly encountered with the Farinograph unit.

Error	Cause	Solution
Mixer overload	<ul style="list-style-type: none"> • Broken shear pin 	<ul style="list-style-type: none"> • Replace shear pin per guidance in the instrument instruction manual
Torque rises steeply at the beginning of the test without flattening	<ul style="list-style-type: none"> • Insufficient cleaning, leading to hardened residue on the blade bushings or mixer bowl • Lack of clearance between the coupling disk and clutch halves • Blades are bent or damaged • Defective load cell 	<ul style="list-style-type: none"> • Disassemble the bowl and thoroughly clean all mixer components • Loosen the screws holding the mixer to the unit base, pull the mixer forward to create space, and replace the screws • Check mixer blades for damage. Damaged blades will require replacement • Repair and calibration of the Farinograph unit is required
Diagram shows wrong values	<ul style="list-style-type: none"> • Lid was not placed on the mixer after water addition • Wrong test parameters entered in a user-defined method • Wrong flour weight loaded • Distilled water not used for the test • Wrong temperature for dosing water • Wrong circulating water temperature • Low flow rate at the circulator • Dough pushing past the blade bushings and rear mixer wall • Lack of clearance between the coupling disk and clutch halves 	<ul style="list-style-type: none"> • Ensure mixer lid is replaced after water addition • Verify test parameters • Check precision of the balance • Ensure that only distilled water is used for tests • Check temperature and temperature setting of dosing water • Check circulator temperature and temperature setting • Check circulator flow rate • Repair blade bushings and calibration of the mixing bowl required • Check the coupling to ensure it has clearance

Error	Cause	Solution
Water dosing system defective	<ul style="list-style-type: none"> • Insufficient cleaning of the mixer • Mixer or blades are damaged • Load cell defective • Fault in the electronics 	<ul style="list-style-type: none"> • Disassemble the bowl and thoroughly clean all mixer components • Check mixer blades for damage. Damaged blades will require replacement • Water dosing system will require repair and calibration. Use external burette for water dosing • Farinograph unit will require repair and calibration
Instrument not communicating with software	<ul style="list-style-type: none"> • Improper setting of COM ports • Driver update required 	<ul style="list-style-type: none"> • Ensure proper COM ports are identified for each device parameter in the Tools → Options → Device menu • Driver updates usually occur automatically. Contact your Brabender service agent for assistance with driver updates if resetting the COM ports does not resolve the issue



Legacy information

I PREFACES TO PRIOR EDITIONS

PREFACE TO THE THIRD EDITION

The original *Farinograph Handbook* came about as a direct result of the topics and lectures covered during the AACC's Farinograph Workshop. Those individuals who assisted in the preparation of the first two editions by devoting their time and effort have been recognized in the preface to each of these editions.

The farinograph is a dough-testing tool widely used to gain information about the unique mixing characteristics of a wheat flour. To obtain maximum benefit from such an instrument, however, the operator must be thoroughly familiar with the operation of the instrument, the type of information it can provide, its limitations, and the sources of error.

The third edition of *The Farinograph Handbook* has been prepared to update it and expand it to include various studies conducted with this instrument. New chapters include topics covering: theoretical aspects, special uses and techniques, dough rheology, precautions, and modifications and new developments. Chapters from the previous editions have been retained but in many instances revised where necessary. The topics of these include: a discussion of the farinograph instrument, the types of farinograph curves and factors affecting them, and the interpretation of the farinogram.

To those individuals who have contributed subject matter to this third revised version of *The Farinograph Handbook*, a sincere thank you is extended. The names of these individuals are given at the beginnings of the chapters they have contributed.

Others who have helped make the revision possible include John Herman, C.W. Brabender Instruments, Inc; Dr. Don Lilllard, A.E. Staley Mfg. Co; R.J. Tarleton, and members of the AACC staff. In addition, secretarial assistance provided by the Department of Cereal Chemistry and Technology and the USDA Hard Red Spring and Durum Wheat Quality Laboratory, North Dakota State University, is appreciated.

Bert L. D'Appolonia
Wallace H. Kunerth

PREFACE TO THE SECOND EDITION

The original purpose of compiling the information in the first edition of *The Farinograph Handbook* was to enable those who attended the AACC's Farinograph Workshop to have a bound copy of the topics and lectures covered. The unexpected popularity of the *Handbook* necessitated several printings of the first edition. Because of this popularity, the Association and the Physical Testing Methods Committee revised and expanded the *Handbook* with a second edition.

To be effective and proficient, the operator of any instrument must have a thorough knowledge of the function of the various parts of the instrument as well as a technical knowledge of the measurements of the test. It is the purpose of this *Handbook* to explain the functions of the various parts of the farinograph, their importance, and their effect on the farinogram.

It must be pointed out that the farinograph results do not always check the baking results or those of other tests. It is difficult at times to interpret farinograms, and disagreements as to interpretations of various curve characteristics exist between different operators. However, two similar types of flour which give different farinograms will respond differently during baking under varying shop conditions.

The farinograph has proved to be a useful tool and gives the cereal chemist a permanent record of changes in dough characteristics during mixing. But, as yet, not enough about farinography is known so that an operator can be completely dogmatic about his findings. A thorough knowledge of the farinograph and its limitations are necessary to interpret a farinogram judiciously.

Those devoted committee members who have assisted in the revision of the *Handbook* and deserve a vote of thanks for their advice and suggestions are: Donald Colpitts, General Mills, Inc.; Jean Croteau, The Pillsbury Company; John Giertz, Kansas Milling Company; I. Hlynka, Canadian Grain Research Laboratory; Robert Laster, Retired; P. N. Leverentz, International Multifoods; Dale K. Mecham, USDA Western Utilization Research and Development Division. Others who are not members of the Committee but helped to make revision of the *Handbook* possible were: August O. Schmitz, C.W. Brabender Instruments, Inc.; R.J. Tarleton and members of the AACC staff, and especially, Mr. Joel Dick of the USDA Hard Red Spring and Durum Wheat Quality Laboratory.

William C. Shuey
Physical Testing Methods Committee

PREFACE TO THE FIRST EDITION

It is customary that written work in particular should have a prologue or foreword, but the special circumstances leading to the Farinograph Workshop and *The Farinograph Handbook* set up a mandatory situation. The obligation of the author of this preface is to document and to recall the uncommon and noteworthy route which led the "teachers" and "students" here. Simply

stated, this course was created from need and reared by the efforts of those who, recognizing an obligation, took action.

The span between idea and reality was large. Between the two were the deterrents, called problems, such as help, publicity, limited book knowledge of fundamentals, and the necessity of the authors to produce for their employers at the same time. Several members stayed with their belief that it should be done and did it.

The result is that three men of industrial firms and three members of nonprofit groups, by setting aside competitive interests and academic arguments, put their knowledge to work to bring into reality the first school of farinograph usage in this country. Time will judge their contribution to the AACC, but their initiative can be recognized today. As chairman of the committee sponsoring the school, I am proud to present those who brought this book and school into being. They are: William C. Shuey, General Mills, Inc., Minneapolis, Minnesota; Lawrence Locken, Russell-Miller Milling Co., Minneapolis, Minnesota; Robert Laster, Joe Lowe Corp., New York, New York; I. Hlynka, Grain Research Laboratory, Winnipeg, Canada; Dale K. Mecham, Western Regional Research Laboratory, Albany, California; Max Milner, United Nations Children's Fund, United Nations, New York.

Less directly charged with the school formation, but adding immeasurably to it, were: R.J. Tarleton of the AACC; and the manufacturers, C.W. Brabender and Arthur Hartkopf. The American Institute of Baking and William B. Bradley kindly arranged for and provided the facilities for the school.

Stephen J. Loska Jr.
Physical Testing Methods Committee

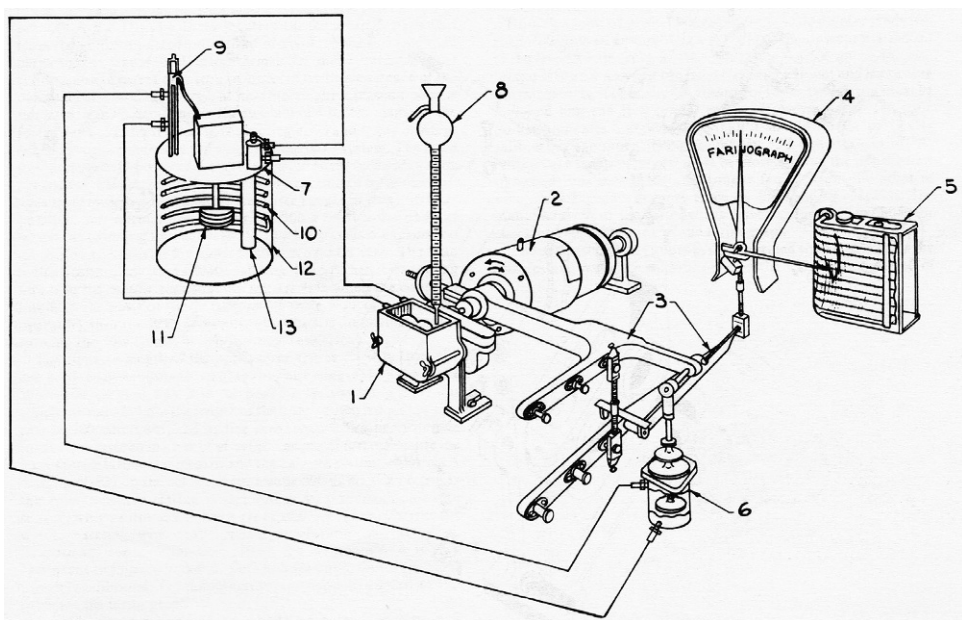
II THE FARINOGRAPH

W.C. Shuey

*Federal Grain Inspection Service, United States Department of Agriculture, Washington, DC,
United States*

The farinograph is a dynamic, physical dough-testing instrument. It is essentially a torque-measuring, recording dough mixer. The plasticity and mobility of a dough subjected to prolonged, relatively gentle mixing action at a constant temperature are measured. The resistance the dough offers to the mixing blades during mixing is transmitted to a dynamometer, which is connected to a lever and scale system, and to a pen, which traces a curve on a kymograph chart.

This instrument has eight basic parts: mixing bowl, dynamometer, lever system, scale system, recording mechanism, dashpot, thermostat, and buret, as shown in Fig. C.1. The mixing bowl is driven by a coupling; the freely swinging dynamometer is mounted on ball bearings so that changes in dough mobility during mixing are transmitted back to the dynamometer, which

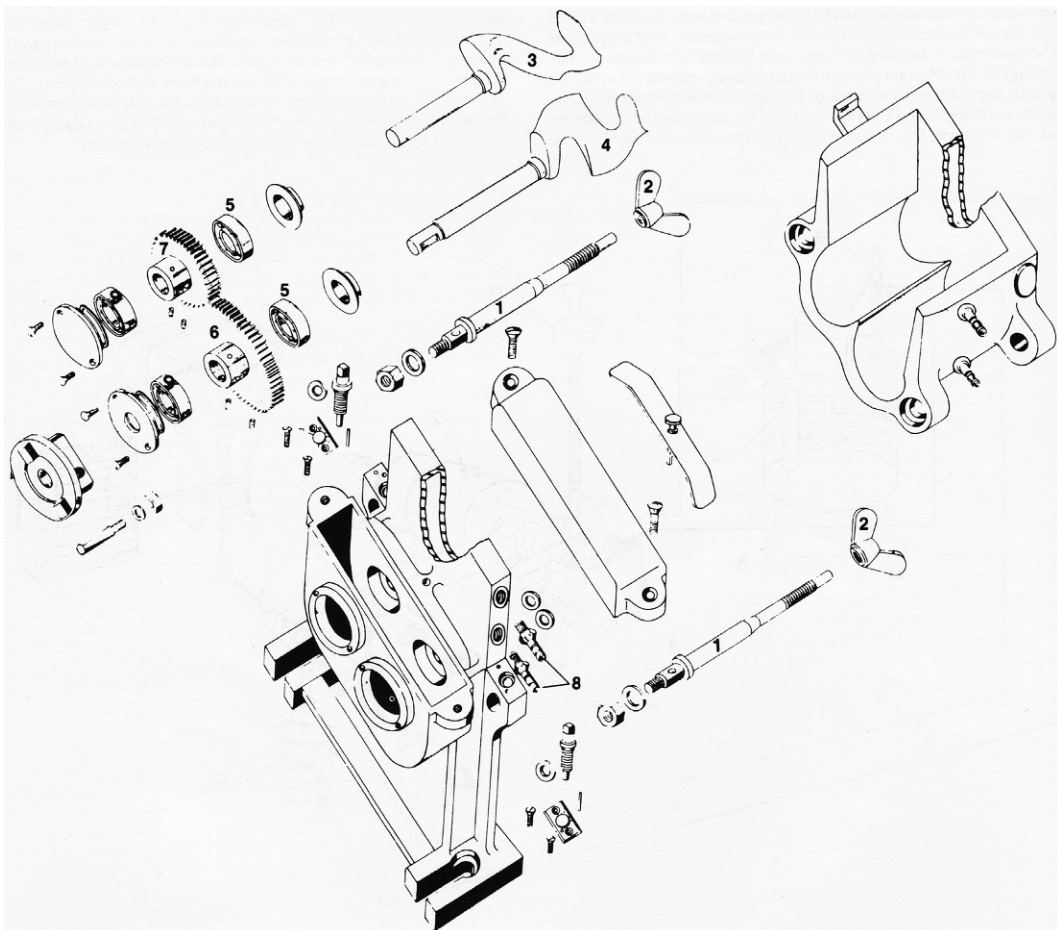


■ FIG. C.1 The basic parts of a farinograph: Mixing bowl (1), dynamometer (2), lever system (3), scale system (4), recording mechanism (5), dashpot (6), thermostat (7), buret (8), thermoregulator (9), cooling coils (10), circulating pump (11), reservoir tank (12), heating element (13). (Diagram adapted from figure supplied by C.W. Brabender Instruments, Inc.)

equals these changes by turning the housing in the opposite direction. The change in the resistance of the dough is mechanically recorded on graph paper through a series of linkages connecting the housing, the lever system, and the scale system. To minimize the oscillation of the lever system, a dashpot is inserted into the circuit. The temperature of the mixing bowl and the dashpot is kept constant by water circulating from the thermostat. Water is added to the dough from the buret, which is mounted directly over the bowl.

MIXING BOWL

Dough is developed in the farinograph mixing bowl (Fig. C.2). As the cutaway drawing shows, the bowl and the back wall of the bowl are hollow to allow water from the thermostat to circulate; the water is introduced and drawn off through the two inlets-outlets. The upper paddle is the fast paddle; the lower one is the slow paddle. These paddles run at a differential speed of 3:2. The slow paddle operates at the same speed as the shaft from the dynamometer, with a range between 59 and 63 rpm. The fast paddle operates between 88.5 and 94.5 rpm. This differential is obtained by the gears in the gear housing behind the back wall of the bowl. The shafts of the mixing paddles, or sigma blades, ride in ball bearings that are aligned in the casting. The bowl is held in place against the back wall by aligning bolts and is secured by wing nuts.



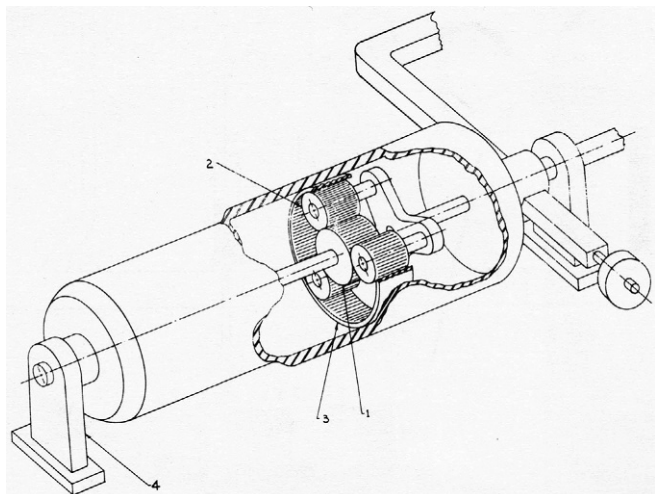
■ FIG. C.2 Phantom diagram of a farinograph bowl: Aligning bolts (1), wing nuts (2), fast paddle (3), slow paddle (4), ball bearings (5), gears (6 and 7), inlets-outlets (8). (Courtesy C.W. Brabender Instruments, Inc.)

The adjustment and condition of the mixing bowl have a critical effect on the results obtained by the farinograph (see Chapter 4).

DYNAMOMETER

The driving mechanism and force for the mixing bowl are furnished by a dynamometer (Fig. C.3). There are three working parts of the dynamometer:

1. The motor and motor shaft with a driving gear;
2. The counter-rotating reduction planetary gears connected to a concentric shaft that extends past the end of the dynamometer housing. The mixing bowl is coupled to the end of this shaft, which furnishes the power that drives the mixing paddles;



■ FIG. C.3 Cutaway view of a dynamometer: Motor drive gear (1), planetary gears (2), ring gear (3), ball-bearing mounting (4).

3. The ring gear, which supplies a track for the driving gears and furnishes the counter-rotating force. The entire dynamometer housing is mounted on ball bearings at each end so that it is free to rotate about the axis of the ball bearing in either direction.

Most farinographs are now equipped to operate at two speeds. Farinograms are normally run at the fast speeds, 62 rpm on the slow paddle and 93 rpm on the fast paddle. However, for very weak flours that break down very rapidly, the slow speeds, 31 rpm on the slow paddle and 46.5 rpm on the fast paddle, are used to slow the rate of dough breakdown. When the switch is in the slow position, the motor operates at half the regular speed. Many operators run soft wheat flours at this speed. When the farinograph is run at the slow speed, the damping setting of the dashpot must be readjusted.

The principle of a dynamometer is that the action and reaction are both equal and opposite. As a dough offers resistance to the mixing blades, a torque is created that forces the housing of the dynamometer in the direction opposite to that of the driving force. This action equalizes the amount of torque applied to the concentric shaft of the dynamometer. In other words, the dynamometer reacts much as a hand does when operating a handheld electric drill. That is, when soft wood is drilled, little or no force is necessary to keep the drill from turning; however, when hard metal is drilled, considerable force is needed to keep the drill from turning. The rotation of the planetary gears around the motor drive gear is similar to the action imparted by the drill; the ring gear attached to the housing assembly causes a reaction similar to the one a hand exerts when it holds the drill.

The parts of the dynamometer that can affect farinograms are the ball-bearing mountings at each end of the dynamometer, the gears in the dynamometer housing, and the motor or motor switch.

The ball-bearing mountings at each end of the dynamometer support the housing. If they are damaged in any way, or if they are not properly lubricated, the housing assembly cannot swing freely and the curve characteristics are affected. These bearings should not need lubrication unless the grease becomes contaminated with water or acid. Should that happen, the bearings must be cleaned thoroughly and repacked with a good ball-bearing grease free of both acid and resin. If the bearings become damaged, they must be replaced.

The gears in the dynamometer housing can also affect farinograms. If any of these gears are damaged, they must be replaced. To keep the gears in good condition, the oil in the dynamometer (30 W) should be changed about once a year. Instruments manufactured since 1956 use 180g of STP.

The motor and its switch must be kept in good working order so that the motor will operate at the proper speed. Since dough mixing and rate of development are closely correlated with the speed of the mixer, it is imperative that the mixer speed be constant.

The role of the dynamometer in the operation of the farinograph is very important. If the dynamometer does not function properly, meaningful results cannot be obtained.

LEVER SYSTEM

A lever system (Fig. C.1) is attached directly to the dynamometer housing to magnify the movements of the housing at a definite ratio. When a dough offers resistance to the mixing blades, it produces a torque on the dynamometer housing; this torque activates the lever system. The moment of force, or torque (T), is the rotary effect of a force about a pivot and is equal to the product of the force (F) applied on an arm at a distance (D) from the pivot point ($T = F \times D$). The distance (D) of the force arm is measured from the concentric shaft, the point of pivot, to the link coupling between the upper and lower arms. To make sure that the farinograph registers only torque afforded by the resistance of the dough during mixing, a large, adjustable weight is placed opposite the lever arm to compensate for two outside forces, namely, the forces derived from friction in the mixing bowl and in the bearings of the dynamometer, and the weight of the lever system. The main function of the lower lever arm is to transmit to the balance or scale system the movement of the upper lever arm caused by the torque. This lever system is designed so that three ranges in sensitivity are possible. The normal position for the 300-g bowl is the point at which the coupling link between the two lever arms is engaged on the knife edges nearest the upper lever arm or scale head. The ratio in this position, the least sensitive setting, is 1:5. When the coupling link is in the middle position, the ratio is 1:3. When the coupling link is in the position farthest from the scale head (closest to the operator), the ratio is 1:1. This position, which is the normal one for running the 50-g bowls, is also the most sensitive.

The effective length of the upper lever arm is 200mm from the center of the dynamometer shaft to the knife edge of the upper arm. When the coupling link is in the position for the

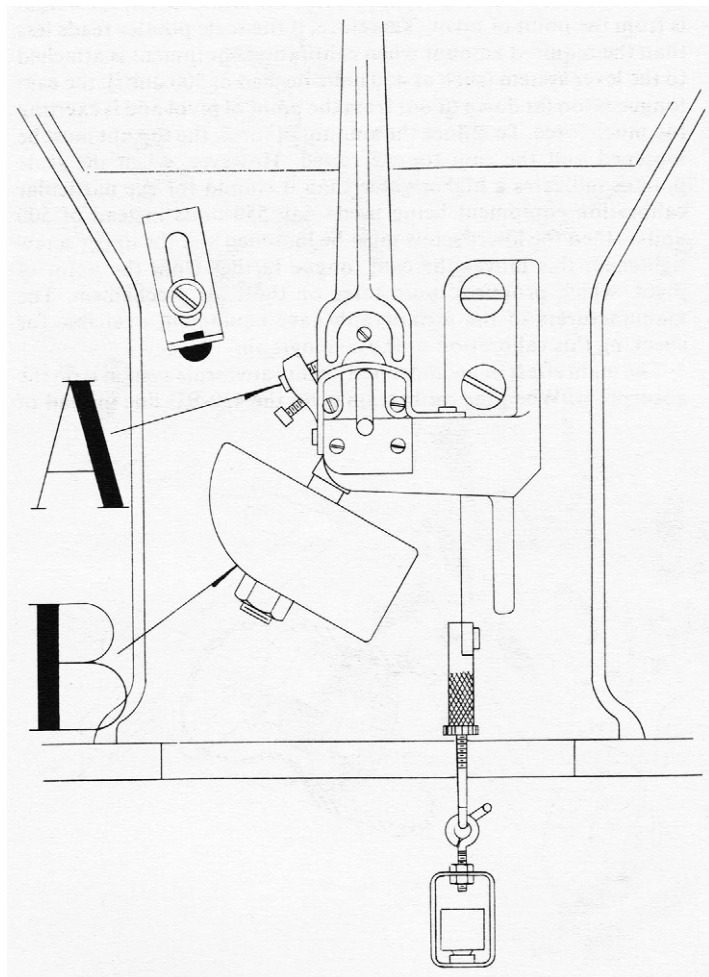
300-g bowl—at which the ratio is 1:5—the length of the lever system is equal to 1 m; that is, 200 mm multiplied by five is equal to 1 m. Therefore, the torque is measured in units of gfm (gf = grams of force) because the lever system is in meter lengths and the balance system in grams. A reading of 500 on the scale system means 500 gfm. The range for the least sensitive setting is 0–1000 gfm. The medium-range setting, with a ratio of 1:3, has a range of 0–333 gfm, whereas the sensitive setting, with a ratio of 1:1, gives a range of 0–200 gfm. Because improper calibration affects the farinogram, it is very important to know whether or not the lever and balance system is properly calibrated. The manufacturer can explain in detail how to calibrate the farinograph.

In addition to calibrating the lever and balance system, it is important to watch the knife edges of the coupling links. Precautions should be taken to make sure that they are not damaged and do not bind when the scale system is activated through the range of the scale head. When a farinograph is set up or when the bowl is changed, the counterweights must be adjusted to cancel out any friction caused by the bowl, and the pen and the pointer of the scale head must ride on zero of the graph paper and of the scale head, respectively. Halfway between the dashpot and the dynamometer on the base plate of the farinograph are two adjustment screws or bolts that arrest the movement of the lower lever arm. These bolts should be adjusted so that the pointer on the scale head travels only a short distance past the 0- and 1000-unit marks on the scale. This limits the movement of the lever system and prevents it from damaging the balance system by too much movement. When the proper precautions are taken, the lever system should function properly in the operation of the farinograph.

SCALE HEAD (BALANCE SYSTEM)

The balance system is the mechanism in the scale head (Fig. C.4). This part of the equipment is like an ordinary scale, except that the scale is attached to the lower lever arm, rather than to a pan, through a special linkage. The function of the balance mechanism is to give dimension to the torque that is applied at the concentric shaft of the dynamometer by converting it to gfm. Each unit on the scale is considered one Brabender unit (BU). When the 300-g bowl is used, 1 BU corresponds to 1 gfm of torque; for the 50-g bowl, 1 BU corresponds to 0.2 gfm.

Two adjustable weights in the scale mechanism calibrate the scale system. The set of adjusting nuts is for making fine adjustments to the forces in the balance system or mechanism. The heavy cam tongue counterweight is used to calibrate the lever and scale mechanism of the farinograph. In its normal position, the cam tongue is held at an angle to the vertical position of the axis of the knife edges in the scale head. This weight exerts a continuous downward force that is proportional to the distance that the weight is from the point of pivot. Therefore if the scale pointer reads less than the required amount when calibration equipment is attached to the lever system (such as 450 units instead of 500 units), the cam tongue is too far down or out from the point of pivot and is exerting too much force. To reduce the amount of force, the top nut must be loosened and the cam tongue raised. However, when the scale pointer indicates a higher value than it



■ FIG. C.4 Balance weights in the scale head. A = adjusting nuts used for fine adjustments in the balance system; B = heavy cam tongue.

should for the particular calibration equipment being used—say 550 units instead of 500 units—then the lower screw must be loosened and the upper screw tightened; this moves the cam tongue farther from the point of pivot, which produces more force on the scale mechanism. The manufacturers of the farinograph have equipment available for checking this calibration of the farinograph.

The main effect of an improperly calibrated scale system is on the absorption. When the calibration is on the 450-BU line instead of on the 500-BU line, the dough must be made more stiff by approximately 1.5%–2.0% to center the curve on the 500-BU line. This amount of absorption would have a definite effect on the farinogram (see Chapter 4). If the calibration

reads, for example, 550 instead of 500, the dough would have to be made softer by approximately 1.5% more absorption than is normally required for centering the curve on the 500-BU line. This would also affect the farinogram. Therefore it is important that the balance mechanism be calibrated if the results of different farinograms are to be compared.

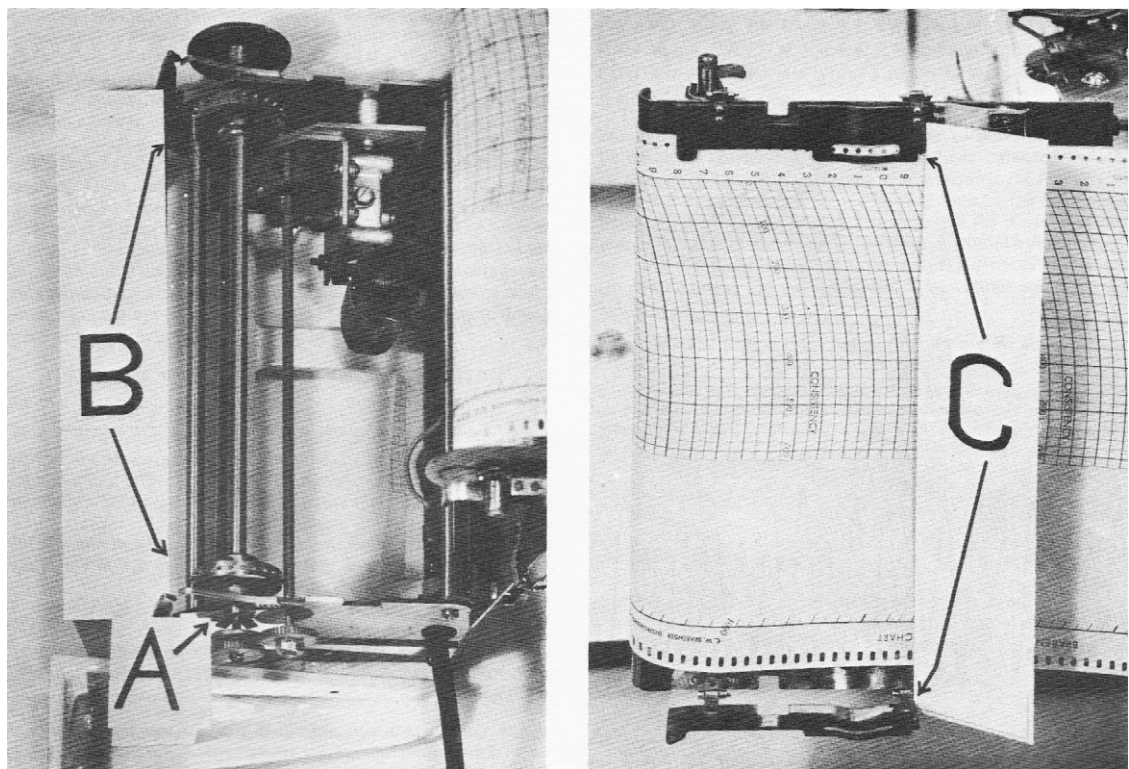
The knife edges of the scale assembly must also be watched. If these are damaged in any way, they will not function properly. Of course, it is imperative for the entire system to be able to move freely when activated. There also should be no outside friction, such as the rubbing of the pointer on the scale, that would impair the movement of the balance mechanism.

RECORDING MECHANISM (KYMOGRAPH)

The kymograph, or recording mechanism ([Fig. C.1](#)), consists of two main parts. These are the pen arm, which holds a pen, and the mechanism that drives the chart paper.

In front of the scale head is an extended shaft that is attached to the scale mechanism. The pen arm is also attached to this shaft, which rotates around the point of pivot of the knife edges in the scale mechanism. The pen arm has two adjustments, fine and coarse, for adjusting the pen so that the reading on the graph paper corresponds to the reading of the pointer on the scale head. The coarse adjustment is made first, when the farinograph is assembled. The pen arm is placed on the shaft so that the pen will correspond approximately to the same reading on the chart as the reading on the scale head. When the pen is in the writing position on the chart paper, there should be just enough contact with the paper for a line to be drawn. It is important that the pressure the pen exerts on the paper not impair the free movement of the balance or scale-head system. The amount of force the pen exerts is adjusted by moving the pen arm in or out from the scale head on the extended shaft. When the pen arm has been so attached to the shaft, it is secured by tightening the bolt with an allen wrench. This is the coarse adjustment. The pen is secured on the end of the pen arm so that when the lever mechanism is activated, the pen draws an arc identical to the lines on the chart paper. After the pen has been secured, the fine adjustment can be made. Using the knurled bolt on the pen arm, the pen is adjusted to read exactly the same as the scale-head pointer. These readings should be checked on the 500-BU line by raising the lever arm until the pointer reads 500 on the scale head and the pen reaches the 500-BU line on the chart paper. When setting the distance of the pen arm and the pen head, it is important for the chart paper to run horizontally on the kymograph or recording-mechanism table.

[Fig. C.5](#) (left) shows the mechanism of the kymograph. For this part to operate properly, the paper should travel at a rate of 1 cm/min. The main problem arising from this equipment is the speed at which the paper travels. Occasionally, the chart paper travels more slowly than the recommended speed. This is usually caused by slippage in the clutch mechanism through a gradual weakening of the clutch spring. To correct this, the tension the spring exerts on the clutch face must be increased. Of course, if the motor that drives the mechanism will not operate at the proper speed, the motor should be replaced.



■ FIG. C.5 Recording mechanism assembly and recording table. A = clutch spring, B = sprockets, C = hold-down plates on the recording table.

The sprockets should be matched so that the paper runs horizontally and is square with the edge of the table of the recording mechanism. If the sprockets are not adjusted properly, the chart paper runs at a slight angle and may tear. To correct this, the set screws that secure one sprocket on the drive shaft are loosened, and the drive shaft is turned slightly in the direction necessary to align the two sprockets. The hold-down plates (Fig. C.5 right) keep the chart paper smooth on the table of the recording mechanism and feed it over the drive sprockets. The teeth of the sprockets must be engaged in the holes on the graph paper, and the paper must lie flat on the table.

DAMPING MECHANISM

The dashpot (Fig. C.1), a damping device, is added to the lever system to minimize the amount of oscillation during mixing. This device is essentially a piston operating in a cylinder full of oil. The amount of damping is regulated by the height of the piston in the cylinder and by the oil head over the piston. It has generally been recommended that the time required for the lever system to recover from a reading of 1000 to a reading of 100 on the scale head should be between 0.6 and 0.8 s. A medium-strength flour is often used to set the damper so that it will give a curve

80 BU wide. The center of a curve 80 BU wide is easy to determine. To widen the band width of the curve, the adjusting knob is turned counterclockwise; to narrow it, the adjusting knob is turned clockwise. The band width of the curve does have some influence on the farinograph readings and appears to affect the top of the curve more than the bottom. Therefore, readings such as arrival time, stability, and mixing tolerance index, which rely on the top of the curve for their measurements, are affected most.

The important thing to remember about the damping system is that the oil in the dashpot should be clean. If dirt or foreign materials get into the oil, they can impair the movement of the piston by becoming wedged between the side of the piston and the cylinder wall. Impaired movement affects the curve and can cause incorrect interpretations of the farinograms. The oil in the dashpot should be checked periodically and changed about once a year. A good grade of 10W oil should be used.

THERMOSTAT

The thermostat (Fig. C.1), like the bowl, is one of the most important parts of the farinograph. The studies of many investigators show that the temperature of the circulating water in the bowl has a very pronounced effect on the farinograms (see Chapter 4). The function of the thermostat is to circulate water at a constant temperature through the mixing bowl and the dashpot. In the dashpot, the thermostat keeps the temperature of the oil constant so that its viscosity remains the same. In the mixing bowl, the thermostat dissipates the heat that develops while the dough is mixed in the bowl.

Fig. C.1 shows the parts of the thermostat: the thermoregulator, the cooling coils, the circulating pump, the reservoir tank, and the heating element.

THERMOREGULATOR

The thermoregulator keeps the circulating water at a constant temperature. The predetermined temperature of the circulating water is set with this part of the thermostat. Complete instructions for setting this regulator are furnished by the manufacturer.

COOLING COILS

Inside the tank is a series of cooling coils through which cold water is circulated. This water is used to dissipate the heat collected from the mixing bowl and/or from the room on hot days. The rate at which water is circulated to these coils depends on two factors: the temperature of the water being circulated in the cooling coils and the amount of heat being collected by the circulating water. The flow rate of the cooling-coil water should be adjusted so that the pilot light will come on for short intervals every 2 or 3 min.

CIRCULATING PUMP

The circulating pump is attached to the outlet side of the thermostat and affords the pressure for the circulating water. The pump should operate at such efficiency that the water from the bowl is

maintained at the proper operating temperature. The rate of flow necessary for the pump to maintain this temperature depends on the length and size of tubing, the cavities in the casting of the bowl, and the temperature of the air surrounding the farinograph. For most conditions, a flow rate of 3L/min is satisfactory. One precaution should be taken in hooking up the thermostat: A minimum amount of tubing should be used for connecting the thermostat to the mixing bowl and dashpot. Excessive tubing may increase the difficulty of maintaining the proper temperature.

RESERVOIR TANK

The reservoir tank is a large tank for holding the circulating water. The volume of water in this tank should be sufficient to maintain the temperature desired for the circulating water and to operate the functional parts of the thermostat properly. This level of water is indicated by a float on the reservoir cover. The tank should be filled with distilled water that should be replaced approximately once a year. When the water in the reservoir is replaced, all the parts of the thermostat should be cleaned by removing all the scale and other matter that may have accumulated. Also, any parts that show wear should be replaced, and spots where the paint has chipped should be repainted.

HEATING ELEMENT

The heating element is placed in the water of the reservoir and is controlled automatically by a relay connected to the thermoregulator. The purpose of this heating element is to maintain a balance in the temperature of the circulating water between the temperature of the water in the cooling coil and the heat generated in the bowl by the dough during mixing. This element is also in the circuit with the pilot light, which comes on when the heating element is functioning. When this unit does not operate properly, the cause may be a broken thermoregulator, bad points in the relay system, burnt solenoids in the relay system, or a burned-out element in the heating unit.

The best way to check whether or not the thermostat is operating properly is to insert a thermometer to measure the temperature of the circulating water. There are several ways of doing this. One of the easiest is to insert a glass tee containing a thermometer in the outlet hose from the mixing bowl. This provides an opportunity to continually observe the temperature of the water leaving the bowl.

In another method, a jar equipped with inlet and outlet hose connections and containing a thermometer is inserted between the thermostat and the return outlet of the mixing bowl. With this arrangement, the temperature of the water returning to the reservoir of the thermostat can be determined.

BURET

The buret ([Fig. C.1](#)) measures the water that is incorporated into a dough in the mixing bowl. The most important thing about the operation of the buret is the rate at which the water is delivered.

This should be such that the buret empties itself in less than half a minute; for normal farinograms, the water should be added within the first 30 s that the farinogram is run. Two sizes of titrating burets are furnished with the farinograph. A buret with a capacity of 225 mL is furnished for the large bowl, and one with a capacity of 50 mL is furnished for the small bowl.

The titrating burets should be cleaned periodically with a solution of 10 parts concentrated sulfuric acid to one part saturated potassium dichromate solution. This solution is extremely corrosive and should be handled with caution. The buret should be filled with the solution and allowed to stand overnight. After the buret is drained, it must be rinsed repeatedly with tap water and given a final rinse with distilled water. The buret should be kept full when not in use.

The height of the buret tip should be adjusted in the holder so that it will swing clear of the top of the mixing bowl when the bowl is covered with a cover plate. It should not be so far from the mixing bowl that the water will splash out or be difficult to introduce into the mixing bowl. The buret holder should be oiled occasionally at the mounting post, which is attached to the base plate of the farinograph, so that the arm that carries the buret can swing freely and can be moved out of the way after the water has been added to the mixing bowl.

III THEORETICAL ASPECTS OF THE FARINOGRAPH

A.H. Bloksma

Institute for Cereals, Flour and Bread TNO, Wageningen, The Netherlands

The farinograph mixer serves two purposes. It mixes flour and water into a dough, develops it, and finally overmixes it. At the same time, it acts as a sensing element that measures the dough's resistance to mixing during successive stages of its development. Dough resistance is determined by the rheological properties of the dough, particularly viscosity. Surface properties of the dough, particularly its sticking to the bowl walls and blades, also contribute to the resistance measured.

By definition, the (apparent) viscosity of a material is the ratio of shear stress and the corresponding rate of shear. Therefore instruments for the measurement of viscosity are designed to derive (1) the shear stress in the test sample from a measured force, torque, or pressure, and (2) the rate of shear in the test sample from the velocity of a moving surface or a rotating shaft. These derivations are possible only if the geometry of the test sample and its deformation are simple. For measurements on nonlinear materials, other factors should be considered. With nonlinear materials, the shear stress is not proportional to the rate of shear; as a result, the apparent viscosity depends on the rate of shear. Therefore, for measurements on these materials, it is advantageous for the shear to be homogeneous, i.e., the same throughout the test sample. Viscometers consisting either of two coaxial cylinders with a narrow gap between them or of a cone

and plate with a small angle between them meet these requirements; the farinograph bowl does not. Visual inspection of the dough being mixed shows that the rate of shear differs among its various parts and that the rate of shear of a single element varies with time.

Nevertheless, attempts have been made to use two coupled coaxial cylinder viscometers as a model for the Brabender Plasti-Corder, which is similar to the farinograph (Goodrich and Porter, 1967; Blyler and Daane, 1967).^a The parameters of the model can be derived from measurements on materials whose rheological properties have been determined with other viscometers. The most important of these parameters is the diameter of the inner cylinders, which, in the model, are substituted for the irregularly shaped mixer blades. This approach allows an estimate of the average rate of shear of the material in the bowl. This estimate can also be made, with fewer assumptions, on the basis of measurements with dough only in the farinograph and in various viscometers.

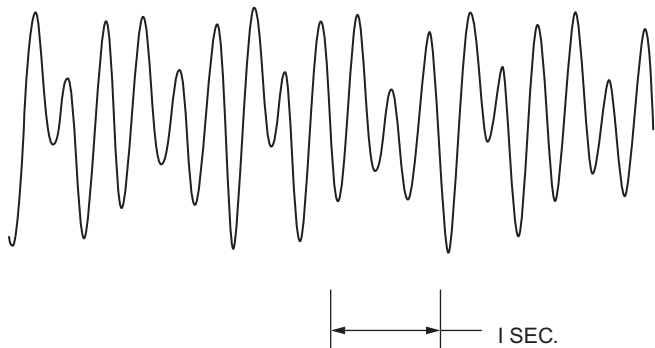
PERIODIC VARIATIONS OF THE DEFLECTION

One can easily observe that the deflection of the farinograph varies with time, even under conditions in which the dough properties are constant or vary only slightly as a result of dough development or breakdown. The frequency of the variation of the deflection is so high that, with the usual speed of the kymograph paper transport and the usual thickness of the recorder pen, the instrument records a band with a certain width. This width is restricted by the inertia of the system and by the adjustable oil damper.

The periodicity of the variations can be made more visible by increasing the speed of the kymograph paper transport (Muller, 1968) or by electronically recording the torque on the driving shaft (Voisey et al., 1966, 1971). Fig. C.6, which was obtained by electronic recording, shows a main frequency of 3.1 s^{-1} . In addition, the distance between the lower peaks has a frequency of 1.03 s^{-1} . Because these lower peaks are alternately followed by a low minimum and a higher one, the basic frequency is 0.51 s^{-1} .

The periodic variations in the deflection are explained as follows. Since the mixer blades are not cylindric but are irregularly shaped, the resistance of the dough to mixing depends upon the relative positions of the two mixer blades. The fast mixer blade rotates at a speed that is $3/2$ times that of the slow blade. Their speeds in revolutions per unit time are called $(3/2)\cdot n$ and n , respectively. In a time interval of $2/n$, the slow blade makes two revolutions and the fast one three; after this time interval, the relative positions of the blades are the same as at the beginning of it. Consequently, the relative positions of the blades vary periodically with a frequency

^aIn the derivation of their Eq. (C.10), Blyler and Daane (1967) apparently added the torques on the two inner cylinders. However, the torque on the fast-rotating cylinder should be multiplied by its relative speed, i.e., $3/2$; compare Eq. (C.14) of Goodrich and Porter (1967). As a consequence, $(3/2)^n$ in Eq. (C.10) of Blyler and Daane should be replaced by $(3/2)^{n+1}$.



■ FIG. C.6 Periodically varying torque obtained by electronic recording. (Reprinted, by permission, from Voisey, P.W., Miller, H., Kloek, M., 1966. An electronic recording dough bowl. IV. Applications in farinography. *Cereal Chem.* 43, 438.)

of $n/2$. The speed of the slow blade of modern farinographs is 63 rpm (ISO, 1980)^b; consequently, $n/2 = 0.52 \text{ s}^{-1}$, which agrees well with the observed value of 0.51 s^{-1} for the basic frequency. The main frequency of 3.1 s^{-1} is twice the rotational speed of the fast mixer blade; this might be explained by the symmetry of the blade itself.

MECHANICS OF THE LEVER SYSTEM

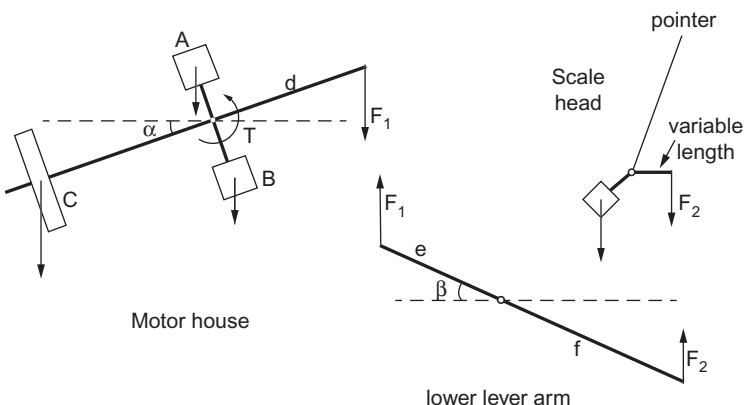
The motor, gear box, dynamometer, and a lever arm are rigidly connected to one another; they are referred to in this section as the “motor house.” Suppose that the motor house exerts a torque T on the driving shaft. This torque is in a clockwise direction if observed from the position of the operator. Consequently, the driving shaft exerts a counterclockwise torque T on the motor house; this torque is shown in Fig. C.7.

The motor house can rotate on two ball bearings. The counterclockwise torque T would cause rotation of the motor house at an accelerated speed if it were not balanced by other torques on it. The main balancing torque is due to the force F_1 that is exerted by the link to a second lever arm under the farinograph base, i.e., the lower lever arm. The torque of the counterweight C acts in the same direction as T . The torques caused by the weight A on top of the motor house and by the weight B of the oil basin under the motor house are less important. The various torques are in equilibrium, if:

$$-T + F_1 d \cdot \cos \alpha - C \cdot \cos \alpha - A \cdot \sin \alpha + B \cdot \sin \alpha = 0. \quad (\text{C.1})$$

The meanings of the symbols are explained in Table C.1.

^bIn older farinographs, the speed of the slow mixer blade is 60 rpm. This is the speed specified in the ICC standard (1972). It corresponds with a basic frequency of 0.50 s^{-1} .



■ FIG. C.7 Forces that act on the motor house, the lower lever arm, and the scale head. Symbols are explained in Table C.1.

Table C.1 Symbols used in description of mechanics of lever system.^a

Symbol	Definition
A	Product of the gravity force on the weight on top of the motor house and its distance to the axis; $19,000 \text{ gf cm} = 1.8 \text{ N m}$
a	Torque at zero deflection; zero
B	Product of the weight of the oil basin under the motor house and its distance to the axis. Value unknown; it should be approximately equal to A. A liquid in a vessel exerts a smaller torque than the same solid mass, because the liquid can flow inside the vessel.
b	Change in the torque on the motor house per unit deflection. With the 300-g bowl setting, $100 \text{ gf cm/BU} = 9.8 \cdot 10^{-3} \text{ N m/BU}$; with the 50-g bowl setting, $20 \text{ gf cm/BU} = 2.0 \cdot 10^{-3} \text{ N m/BU}$.
c	Product of the gravity force on the counterweight and its distance to the axis minus the torque exerted by the parts at the right-hand side of the motor house. With the 300-g bowl setting, $10,000 \text{ gf cm} = 0.98 \text{ N m}$; with the 50-g bowl setting, $2000 \text{ gf cm} = 0.20 \text{ N m}$.
D	Deflection of scale
d	Length of the right-hand part of the motor house lever arm: 200 mm
e	Length of the front part of the lower lever arm. With the 300-g bowl setting, 54 mm; with the 50-g bowl setting, 270 mm
F_1	Force on the right-hand end of the motor house lever arm and on the front end of the lower lever arm
F_2	Force on the rear end of the lower lever arm and on the scale head
f	Length of the rear part of the lower lever arm: 270 mm
P	Force on the scale head at zero deflection: $100 \text{ gf} = 0.98 \text{ N}$
q	Change in the force on the scale head per unit deflection: $1 \text{ gf/BU} = 9.8 \cdot 10^{-3} \text{ N/BU}$
r	Displacement of the rear end of the lower lever arm at zero deflection: -11 mm
s	Change in the position of the rear end of the lower lever arm per unit deflection: 0.022 mm/BU
T	Torque on the motor house
α	Rotation of the motor house; with a horizontal lever arm, $\alpha = 0$
β	Rotation of the lower lever arm; with a horizontal arm, $\beta = 0$

^aNumerical values are based on measurements on an arbitrary instrument and should not be considered standards.

The lever arm that forms part of the motor house is linked to the front end of the lower lever arm, which can rotate around a horizontal axis perpendicular to the driving shaft; although the two arms rotate in mutually perpendicular planes, in Fig. C.7 they are depicted as being in the same plane. Because the length of the link is constant,

$$d \cdot \sin \alpha = e \cdot \sin \beta. \quad (\text{C.2})$$

The link exerts equal forces F_1 on the ends of both lever arms, one upward and one downward. Equilibrium of torques on the lower lever arm exists, if:

$$F_1 e \cdot \cos \beta - F_2 f \cdot \cos \beta = 0. \quad (\text{C.3})$$

The rear end of the lower lever arm is linked to a scale by a flexible steel band. The scale head is a third balance, although a complicated one. As a result of the particular shape of the body over which the steel band is drawn, the length of one of its arms depends on its position. If the scale head is correctly adjusted, the force F_2 on the rear end of the lower lever arm is rectilinearly related to the deflection:

$$F_2 = p + qD. \quad (\text{C.4})$$

The same is approximately true for the displacement of the rear end of the lower lever arm:

$$f \cdot \sin \beta = r + sD. \quad (\text{C.5})$$

The angles over which the lever arms rotate are small (Table C.2). Therefore, the following approximations are possible (if the angles are expressed in radians):

$$\sin \alpha \approx \alpha; \sin \beta \approx \beta, \quad (\text{C.6})$$

$$\cos \alpha \approx \cos \beta \approx 1. \quad (\text{C.7})$$

Combining Eqs. (C.1)–(C.7) leads to:

$$T = a + bD, \quad (\text{C.8})$$

$$\text{with } a \equiv \frac{dfp}{e} - \frac{er}{df} \cdot (A - B) - C, \quad (\text{C.9})$$

Table C.2 Maximum deflections of lever arms.^a

	Radians	Degrees and minutes
Motor house lever arm (α)		
300-g Bowl setting	0.011 ^b	0° 38'
50-g Bowl setting	0.054	3° 4'
Lower lever arm (β)		
Both settings	0.041	2° 18'

^aThe deflections listed correspond with a deflection on the scale of 1000 BU (full scale deflection). With zero deflection on the scale, the lever arm deflections have the same absolute values with the negative sign. With a 500-BU deflection on the scale, the deflections of the arms are zero.

^bIf $\alpha = 0.054 \text{ rad}$, $(\sin \alpha)/\alpha = 0.9995$ and $\cos \alpha = 0.9985$.

$$b \equiv \frac{dfq}{e} - \frac{es}{df} \cdot (A - B). \quad (\text{C.10})$$

The following conclusions can be drawn from Eqs. (C.8)–(C.10).

If the behavior of the scale is linear (Eqs. C.4 and C.5), the relationship between torque and deflection is also linear. If calibration of the instrument shows that the latter relationship is nonlinear, the cause must be sought primarily in the scale head.

On the basis of measurements on various parts of the instrument, one can conclude that the second term of the right-hand side of Eq. (C.10) is small in comparison with the first term. Therefore, the sensitivity of the instrument, $1/b$, is mainly determined by the ratio e/dfq . If the farinograph is to be used with a bowl for 50g of flour, the link between the motor house and the lower lever arm is shifted, which makes length e five times larger. Consequently, b is reduced by a factor of 5, namely from 100gfcm/BU to 20gfcm/BU (Table C.3 shows the values in newton meters per Brabender unit, Nm/BU). However, if $A - B$ is different from zero, the ratio between the sensitivities will deviate from exactly 5.

If the weight on top of the motor house is adjusted so as to be further from the axis, A becomes larger and b consequently decreases; the instrument becomes more sensitive. Conversely, adding oil to the dynamometer increases B and makes the instrument less sensitive. However, these measures are not recommended for adjusting incorrect sensitivities; adjustment of the scale head and/or of the position of the link between the lever arms is a better approach.

In a correctly adjusted farinograph, zero deflection corresponds with zero torque on the driving shaft: $a=0$. Eq. (C.9) shows that this can be attained by adjusting C , that is, by adjusting the position of the counterweight. Eq. (C.9) also explains why, in the setting for a 50-g bowl ($e=\text{larger}$), the counterweight must be placed close to the axis ($C=\text{smaller}$).

Table C.3 Calculation of the power per unit mass of dough.

Symbol	Units	300-g bowl	50-g bowl
b	gfcm/BU N/m/BU	100 $9.8 \cdot 10^{-3}$	20 $1.96 \cdot 10^{-3}$
$\dot{\Omega}$	rpm rad/s	63 6.60	63 6.60
M^a	kg	0.480	0.080
$b\dot{\Omega}/M$	W/(kg BU)	0.135	0.162

^aWater addition is assumed to be 60g per 100g of flour.

ENERGY AND POWER

If a torque T acts on a body that rotates over an angle Ω (in radians) in a direction corresponding with the torque, the work E done by the torque equals:

$$E = T \Omega. \quad (\text{C.11})$$

This can be proven as follows. The torque corresponds with a force T/r that acts upon a point at a distance r from the axis of rotation. The displacement of this point by the rotation equals Ωr . The work is defined as the product of force and displacement: $E = (T/r) \cdot \Omega r = T\Omega..$

Consequently, the power W (that is, the work done per unit time) equals:

$$W = T \dot{\Omega}, \quad (\text{C.12})$$

in which $\dot{\Omega}$ is the rate of rotation. This equation allows one to calculate the relation between the farinograph deflection and the power per unit mass of dough. Therefore, we use Eq. (C.8) with $a=0$, in which M is the mass of the dough.

$$\frac{W}{M} = \frac{b\dot{\Omega}}{M} \cdot D \quad (\text{C.13})$$

In Table C.3, the factor $b\dot{\Omega}/M$ is calculated for bowls holding 300 and 50 g of flour. The factor for the two bowls is different because the dough masses differ by a factor of 6, whereas the torques per unit deflection differ by a factor of 5. This apparent anomaly will later be used to estimate the relative contribution of surface properties of the dough to the farinograph deflection.

The preceding paragraph has shown that a farinogram can be read as a curve of power versus time. The area A under such a curve is proportional to the energy consumed in a certain time interval. This is useful if one wants to characterize the mixing action on a dough by a single figure, e.g., if the mixing energy of the farinograph is to be compared with that of some other bowl. Generally, the work per unit mass of dough can be calculated by the equation:

$$\frac{E}{M} = \frac{b\dot{\Omega}}{Mhv} A, \quad (\text{C.14})$$

in which

h = the width of the kymograph paper per unit deflection and

v = the speed of the kymograph paper transport.

This equation is equally applicable to curves recorded by a Do-Corder with deviating sensitivity, speed of rotation, and/or speed of paper transport. In the preceding form, it can only be applied if the various quantities are expressed in corresponding units. If, for example, conventional units are used:

b' = scale value in gf cm/BU (1 gf cm/BU = $9.81 \cdot 10^{-5}$ N m/BU),

$\dot{\Omega}'$ = speed of rotation in revolutions per minute (1 rpm = $2\pi/60$ rad/s),

v' = speed of kymograph paper transport in centimeters per minute ($1 \text{ cm/min} = 1/60 \text{ cm/s}$),

A' = surface area in square centimeters,

M = mass of dough in kilograms, and

E/M = energy in joules per kilogram of dough,

then a numerical factor must be added, resulting in

$$\begin{aligned}\frac{E}{M} &= 9.81 \cdot 10^{-5} \cdot \frac{2\pi}{60} \cdot 60 \cdot \frac{b' \dot{\Omega}'}{M h v'} \cdot A' \\ &= 6.16 \cdot 10^{-4} \cdot \frac{b' \dot{\Omega}'}{M h v'} \cdot A'\end{aligned}\quad (\text{C.15})$$

For a farinogram recorded using a normal farinograph equipped with a 300-g bowl ($b' = 100 \text{ gf cm/BU}$, $\dot{\Omega}' = 63 \text{ rpm}$, $M = 0.48 \text{ kg}$ [Table C.3], $h = 0.0178 \text{ cm/BU}$, $v' = 1 \text{ cm/min}$), 1 cm^2 of surface area corresponds to 454 J/kg.

The equations derived in this section can also be used to calculate the rate of flow of thermostat water required to properly control the bowl temperature. If changes in dough and bowl temperatures are negligible, then the power that is consumed in mixing results in an increase of the temperature of the water that is pumped through the walls of the bowl. This is described by the equation:

$$Qc \cdot \Delta\Theta = T\dot{\Omega} = bD\dot{\Omega}, \quad (\text{C.16})$$

in which:

Q = the mass of water that flows through the bowl walls per unit time,

c = the specific heat of water,

$\Delta\Theta$ = the temperature difference between the water flowing out and the water flowing in, and

T , $\dot{\Omega}$, b , and D have the same meaning as used earlier.

All known standards specify that the bowl temperature shall be maintained at $30 \pm 0.2^\circ\text{C}$ (AACC, 1983; ICC, 1972; ISO, 1983); a temperature difference of 0.2 K causes a shift in consistency at 500 BU of approximately 3 BU (Bloksma, 1971). This precision can be attained only if the temperature difference between outflowing and inflowing water is smaller than 0.2 K. (It is possible to meet the conditions with a temperature difference of 0.4 K if the temperature of the inflowing water is 29.8°C and absolutely constant. Since the latter condition is impossible to meet, a maximum temperature difference of 0.2 K is more realistic.) Substituting into Eq. (C.16) $\Delta\Theta = 0.2 \text{ K}$, $c = 4180 \text{ J kg}^{-1} \text{ K}^{-1}$, $b = 9.81 \cdot 10^{-4} \text{ N m/BU}$, $D = 700 \text{ BU}$ (temperature control must also be sufficient with stiff doughs), and $\dot{\Omega} = 6.6 \text{ rad/s}$, one finds that $Q = 0.054 \text{ kg/s}$ or 3.3 L/min. For a proper temperature control, the actual flow rate under these conditions must be well above this value. If the sensitivity of the instrument is set at a lower value (i.e., if b is larger), or if the rate of rotation is more rapid, as may occur in the Do-Corder, the rate of flow must be accordingly larger.

TIME EFFECTS IN TEMPERATURE CONTROL

To control temperature, thermostat water maintained at a constant temperature is pumped through the walls of the farinograph bowl. Generally, the temperatures of flour and water, and consequently the initial dough temperature, differ from that of the bowl walls. An important problem is how rapidly the dough temperature will approach the wall temperature.

Because of the mixing action, dough temperature can be considered homogeneous. It changes as a result of two factors: (1) heat exchange with the bowl walls (the rate of heat exchange is assumed to be proportional to the temperature difference) and (2) conversion of mechanical energy into heat (for simplicity, dough development and the effect of the actual dough temperature on heat production are neglected; the recorded consistency is assumed to be constant).

These processes are described by the differential equation:

$$Me \cdot d\Theta = [k \cdot (\Theta_w - \Theta) + W] \cdot dt, \quad (C.17)$$

in which

M =mass of dough,

c =specific heat of dough,

Θ =temperature of dough,

Θ_w =temperature of bowl wall,

k =heat transfer coefficient between bowl wall and dough,

W =mixing power, and

t =time.

If at $t=0$, $\Theta=\Theta_i$, its solution is:

$$\Theta = \Theta_w + \frac{W}{k} + \left(\Theta_i - \Theta_w - \frac{W}{k} \right) \cdot \exp \left(-\frac{kt}{Mc} \right) \quad (C.18)$$

The predicted change of dough temperature with time is shown in Fig. C.8. After very long times ($t \gg Mc/k$), Eq. (C.18) can be simplified to:

$$\Theta \approx \Theta_w + \frac{W}{k}. \quad (C.19)$$

Dough temperature has become constant; the system is in a steady state. The dough temperature is then higher than the temperature of the bowl walls. In the steady state, the temperature difference between bowl walls and dough causes a flow of heat from the dough to the walls that is equal to the heat produced in the dough by mixing.

The time required to attain the steady state depends on the ratio Mc/k , which has the dimension of time. The specific heat c of dough is calculated in Table C.4 from its composition and the specific heats of its constituents. The heat transfer coefficients k are estimated on the basis of measurements of dough temperatures after very long mixing times during which the steady

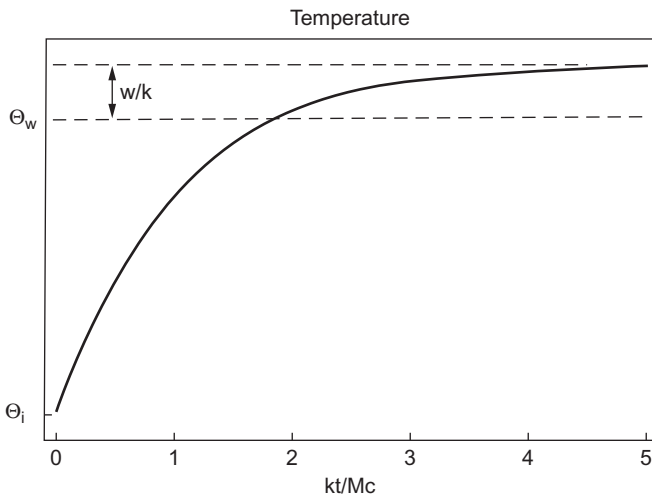


FIG. C.8 Dough temperature as a function of time. Time is expressed in dimensionless units, kt/Mc . c = specific heat of dough, k = heat transfer coefficient between bowl wall and dough, M = mass of dough, t = time, W = mixing power, Θ_i = initial dough temperature, Θ_w = bowl wall temperature.

Table C.4 Calculation of the specific heat of a flour-water dough.

	Mass ^a (kg)	Specific heat ^b (J kg ⁻¹ K ⁻¹)	Heat capacity (J K ⁻¹)
Flour			
Carbohydrates	0.72	1220	880
Protein and fat	0.14	1900	270
Water	0.14	4180	590
Added water	0.60	4180	2510
Total	1.60	2650 ^c	4240

^aPer kilogram of flour.

^bSpecific heats of constituents are taken from Van Beek and Veerkamp (1982).

^cCalculated as 4240 J K^{-1} ; $1.60 \text{ kg} = 2650 \text{ J kg}^{-1} \text{ K}^{-1}$.

state had been attained. These estimates and the resulting values of the ratio Mc/k are shown in Table C.5.

The steady-state temperature is approached asymptotically. Therefore, asking how much time is required for the dough temperature to reach this temperature is impractical; the answer is always infinite time. However, by means of Eq. (C.18) and the values of Mc/k in Table C.5, one can calculate how much time is required for the dough temperature to reach a level that is a small but finite amount lower than the steady-state temperature. Results of such calculations are shown in Fig. C.9.

Table C.5 Calculation of rate at which dough temperature approaches steady-state value.

	Units	Bowl for	
		300 g of flour	50 g of flour
Power, ^a W	W	32.4	6.5
Temperature difference, ^b $\Theta - \Theta_W$	K	1.4	1.2
Heat transfer coefficient, ^c k	WK^{-1}	23	5.4
Mass of dough, M	kg	0.48	0.080
Specific heat of dough, c	$Jkg^{-1} K^{-1}$	2650	2650
Ratio Mc/k	s	55	39

^aAt a deflection of 500 BU.
^bAfter a long mixing time.
^cThe heat transfer coefficient should be proportional to the surface area. Therefore a ratio between the two bowls of $(300/50)^{2/3} = 3.3$ would be expected. The ratio between the experimental values is 4.3. This suggests that one of the values for k in this table, or both, may differ from the real values by 30%.

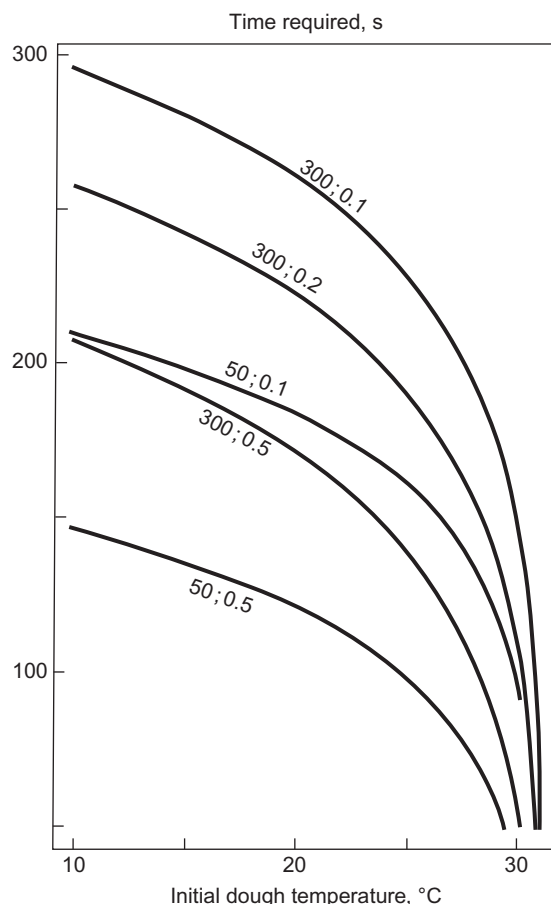


FIG. C.9 Time required for dough temperature to reach a level that is a small amount lower than the steady-state temperature, as a function of initial dough temperature. Steady-state temperatures: for a bowl for 300 g of flour, 31.4°C; for 50 g of flour, 31.2°C. Labels indicate size of bowl (grams of flour) and difference (in Kelvin) between the steady-state temperature and the actual dough temperature.

This figure shows that, under normal conditions, the steady-state temperature is closely approached after 2–4 min of mixing. Only when dough development times are very short will the dough reach maximum consistency before its temperature has closely approached the steady-state level. Fig. C.9 confirms that temperature control in a bowl for 50 g of flour is more rapid than in one for 300 g of flour. It also shows that more time is required if the initial dough temperature is lower; for rapid temperature control, an initial dough temperature above 20°C, preferably above 25°C, is required. This is why the temperatures of the flour and water must be brought sufficiently close to the standard temperature of 30°C before a farinogram can be made. International standards specify the limits given in Table C.6. The lower limits correspond to a dough temperature of 23°C. In practice, the initial dough temperature is higher because, before water is added, the dry flour is mixed for 1 min in the bowl at a temperature of 30°C.

In the valorigraph, a similar instrument made in Hungary, the temperature is controlled by air that circulates around the bowl. The temperature course in the valorigraph can also be described by Eq. (C.18) if the heat capacity of the bowl is included in Mc . The large mass of the bowl increases Mc by a factor of 6. In addition, the heat transfer coefficient k is considerably smaller. Consequently, Mc/k is much larger: temperature control is very much slower than in the farinograph.

CONTRIBUTION OF DOUGH SURFACE PROPERTIES TO THE DEFLECTION

The incorporation of common salt in a dough reduces its consistency as measured by the farinograph (Hlynka, 1962). However, measurements with the extensigraph or a similar instrument and with the Simon research water absorption meter demonstrate that the addition of salt increases the resistance of dough to deformation. It is also known that doughs with salt stick less to metal surfaces than do doughs without it. Bennett and Coppock (1953) suggested that, in the farinograph, the increase in resistance of the interior of the dough as a result of the addition of salt is more than offset by a reduction in dough stickiness. This suggestion was confirmed by experiments in which the walls and blades were coated with liquid paraffin to eliminate the adhesion of the dough to them; this resulted in a decrease of deflection (Muller, 1968).

Table C.6 International specifications for temperature, °C.

Organization	Temperature limits of				
	Flour		Water		
	Lower	Upper	Lower	Upper	
ICC (1972) ^a	20	40	25	35	
ISO (1983) ^b	20	30	25	35	

^aInternational Association for Cereal Science and Technology ICC.
^bInternational Organization for Standardization.

The difference in power per unit mass of dough at the same farinograph deflection between a bowl for 300 g of flour and one for 50 g of flour allows an estimate of how much the adhesion of dough to the walls and blades contributes to the deflection. The adhesion is a surface property. The total power consumption W is composed of an internal dissipation of power, due to viscous flow, and a dissipation of power at the dough-metal interface. These two components are assumed to be proportional to the volume and to the surface area of the dough, that is to L^3 and L^2 , respectively, if L is a length that characterizes the size of the dough. This is equivalent to the assumption that the internal dissipation per unit volume I and the surface dissipation per unit surface area S are independent of the size of the bowl. Then one can write for two bowls a and b:

$$W_a = L_a^3 \cdot I + L_a^2 \cdot S \quad (\text{C.20a})$$

$$W_b = L_b^3 \cdot I + L_b^2 \cdot S. \quad (\text{C.20b})$$

If the index a refers to a bowl for 300 g of flour and b to one for 50 g of flour, then $W_a/W_b=5$ and $L_a^3/L_b^3=6$. With this additional information, the relative magnitudes of the two terms at the right-hand sides of Eqs. (C.20a) and (C.20b) can be calculated; the results are listed in Table C.7.

Table C.7 shows that, if the preceding assumptions are correct, surface properties of the dough contribute about 1/4 and 1/3 to the total deflection with bowls for 300 and 50 g of flour, respectively; these contributions are not negligible. On the basis of experiments with a paraffin-coated bowl, [Muller \(1968\)](#) estimated the contribution of surface properties in a bowl for 300 g of flour to be 1/5 of the total deflection.

The surface dissipation of power is relatively more important in the smaller bowl, in which the surface-to-volume ratio is larger. The fact that the absolute value of the internal dissipation per unit mass of dough is the same for both bowls is also a direct consequence of the assumptions made.

Differences in stickiness between doughs is a possible explanation for the observation that doughs with identical farinograph consistencies may behave quite differently in other rheological tests in which surface properties play another role or no role at all. The extensigraph test is an example. In the extensigraph, when doughs having identical farinograph consistencies are stretched, the resistance to stretching can vary greatly. [Bloksma and Meppelink \(1973\)](#) observed

Table C.7 Contributions of internal and surface dissipation of energy to the farinograph deflection.

Size of bowl (g of flour)	Relative contributions		Absolute contributions W/(kg BU)		
	Internal	Surface	Internal	Surface	Total^a
300	0.76	0.24	0.102	0.033	0.135
50	0.63	0.37	0.102	0.060	0.162

^aIn accordance with Table C.3.

that sensory assessment of the stiffness of doughs having identical farinograph consistencies varied; it depended on both cultivar and crop year. Although the sensory assessment did not correlate with the farinograph consistency, it did correlate with the extensigraph resistance and with measurements with a cone-and-plate viscometer.

AVERAGE RATE OF SHEAR

Having calculated the internal dissipation of energy in the farinograph bowl, one can estimate the average rate of shear and the average shear stress in the bowl. The argument by which the estimate is derived is as follows:

On the one hand, the relation between the rate of shear of dough and the shear stress on it has been established by means of various viscometers referred to earlier. Fig. C.10 shows results of such measurements over a wide range of shear rates. At a given rate of shear, the experimental values for the shear stress vary by a factor of 3. This is good agreement because the experiments have been conducted with doughs prepared from various flours, with and without salt and with various farinograph consistencies. With an increasing rate of shear, the shear stress also increases, although much less than proportionally. At a rate of shear of 10^{-3} s^{-1} , the apparent

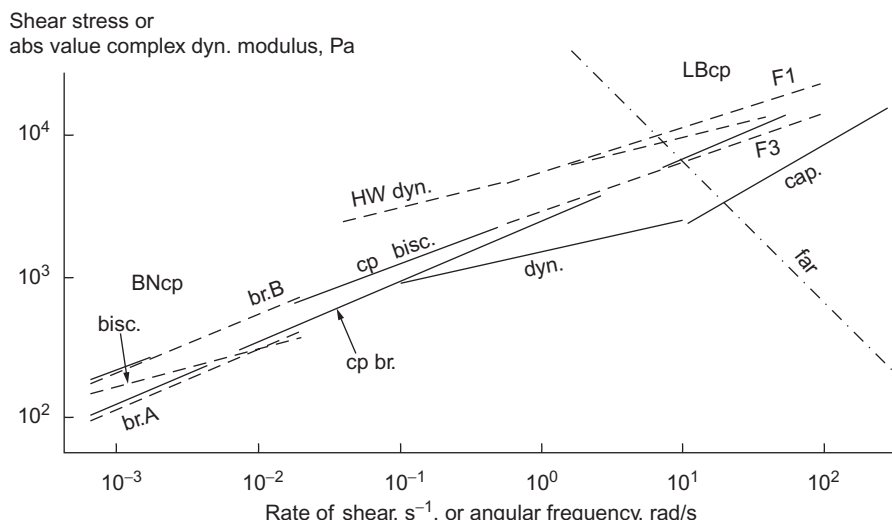


FIG. C.10 Various measurements of the shear stress in dough as a function of rate of shear. The figure includes results of oscillatory measurements, namely, the absolute value of the complex dynamic modulus versus the angular frequency; such plots generally agree well with those of shear stress versus shear rate (Cox and Merz, 1958). cap = constant rate of shear in capillaries; cp = constant rate of shear between cone and plate; dyn = dynamic (oscillatory) measurements, br = bread flour, bisc. = biscuit flour. Solid lines are based on unpublished observations (1980) of A. H. Bloksma and J. A. Duijzer. Dashed lines represent literature data: HW = Hibberd and Wallace (1966); LB = Launay and Buré (1973) (for simplicity, only the lowest and highest of a series of seven flours examined by these authors are shown); BN = Bloksma and Nieman (1975). Dash-dot line marked "far" corresponds with the internal dissipation of power in a farinograph bowl.

viscosity (shear stress divided by rate of shear) is $1.7 \cdot 10^5 \text{ Pa s}$; at a rate of shear of 10^2 s^{-1} , it is only $1.6 \cdot 10^2 \text{ Pas}$.

On the other hand, in viscous flow, the product of shear stress and rate of shear equals the rate of dissipation of energy per unit volume, which, in a farinograph bowl, is proportional to the measured consistency. Although the farinograph consistencies of the doughs used for the measurements in Fig. C.10 are not always known, they will be about 500 BU. At this consistency, the internal dissipation of energy in a farinograph bowl is 51 W/kg (Table C.7); as the specific mass of dough is 1250 kg/m^3 (Bloksma, 1963), this corresponds to an internal dissipation of energy of $51 \times 1250 = 6.4 \cdot 10^4 \text{ W/m}^3$. In Fig. C.10, the line marked “far” corresponds with a product of shear stress and rate of shear equal to this value.

The intersection of this line with the experimental relation between rate of shear and shear stress represents the average conditions in a farinograph bowl, if the consistency is 500 BU. The rate of shear is about 10 s^{-1} , and the shear stress $6 \cdot 10^3 \text{ Pa}$. These figures do not have more precision than an estimate of the order of magnitude for several reasons. First, the shearing action in a farinograph bowl is very nonhomogeneous. Second, the experimental values for the shear stress at a given rate of shear vary by a factor of 3 (corresponding with a factor of 2 in the estimated rate of shear). Third, there is an uncertainty by a factor of 1.3 as to the farinograph consistencies of the doughs used for the various experiments (corresponding with a factor of 1.2 in the estimated rate of shear).

Launay (1979) estimated the mean rate of shear in a farinograph bowl to be very much higher, namely 10^4 s^{-1} , but he did not explain this figure. Such a high rate of shear could occur in the narrow gap between the blades and the bowl wall, if there were any dough in this gap.

IV AACC PHYSICAL TESTING METHODS COMMITTEE FARINOGRAPH COLLABORATIVE STUDY

Three years of work culminated in an announcement by the Physical Testing Methods Committee in the February 1961 issue of *Cereal Science Today* (Shuey, 1961) of a farinograph mixer calibration program. The committee members believed that this program would fill the needs of cereal chemist farinograph users. The program was officially dropped in July 1967, primarily because of the lack of interest by the association members.

During the winter of 1963–64, the Physical Testing Methods Committee conducted a collaborative study with 10 laboratories that had certified farinograph bowls. This study revealed that collaborators do not follow explicit instruction. Although the standard deviations had been reduced by approximately one-half for the data obtained from the certified bowls as opposed to the overall National Check Sample Service data, it was decided that a more intensified study should be conducted. The Physical Testing Methods Committee solicited volunteers from the National Check Sample Service collaborators to determine sources of error in farinograph

readings by the inclusion of specific studies. Thirty collaborators offered to participate in the study—9 had certified bowls and 21 had noncertified bowls.

The objectives of the study were to determine:

1. The error introduced by individuals reading their own farinograms that were run on their own farinograph,
2. The error introduced by one person reading the farinograms that have been run by various individuals on their own farinographs,
3. The error introduced by individuals reading the same farinograms, and
4. The effectiveness of the AACC bowl certificate program.

A questionnaire sent to the Check Sample Service collaborators disclosed that three different procedures were used, even though specific instructions had been given. Not only were different procedures used, but the band width of curves varied from 20 to 120 BU, which in itself has a pronounced effect on the readings.

READING THE FARINOGRAM

The first study utilized the HL-4, HL-5, and HL-6 series from the 1964 National Check Samples. Each participating collaborator read his own curve, which he had produced on his farinograph. These same farinograms were also read by one individual. Average data are compiled in [Table C.8](#).

The data show better agreement between the certified bowls than between the noncertified bowls. The overall average results also show an improvement in the agreement among bowls when one individual read the farinograms as opposed to collaborators reading their own farinograms.

The second study employed copies of 10 curves from the 1964 series of the National Check Sample. Each participating collaborator was sent a set of 15 curves, 5 of which were duplicates. The average data are given in [Table C.9](#).

A comparison of the data in [Table C.9](#) with that in [Table C.8](#) shows a decrease in coefficient of variation of approximately one-half to one-third, indicating that the variability could be reduced by this amount if all farinographs could reproduce exactly the same curve. However, average standard deviations between differences in pairs given in [Table C.10](#) indicate that this is about the best improvement that could be obtained, as individuals reading the same curve are not consistent.

The third study combined a flour storage experiment with the regular study of comparing certified and noncertified bowls. This study utilized the HL-4, HL-5, and HL-6 series of the 1965 Farinograph Check Samples. In June of 1965, a sufficient quantity of flour for the three collaborative check samples was secured and placed in cold storage at 10°F. The flour used was milled from a blend of 90% hard red winter and 10% hard red spring wheats. The HL-4 sample was sent

Table C.8 Average readings for 1964 National Check Sample farinograms HL-4, HL-5, and HL-6 series.

Reading ^a	Bowls	1964 collaborators			One individual		
		Mean	Range	Coef. of var.	Mean	Range	Coef. of var.
ABS	Noncertified	60.1	5.27	2.0	—	—	—
	Certified	60.1	2.97	1.7	—	—	—
ARR	Noncertified	2.17	2.8	32.2	2.10	2.7	31.0
	Certified	2.27	1.8	25.5	2.23	1.7	23.8
MIX	Noncertified	7.97	4.2	12.0	7.70	3.7	11.7
	Certified	7.90	1.7	7.1	7.63	1.7	7.2
STA	Noncertified	12.30	6.8	13.7	12.13	5.8	11.9
	Certified	12.00	4.4	11.2	11.97	3.9	10.9
DEP	Noncertified	14.40	6.3	10.8	14.23	5.3	9.6
	Certified	14.23	4.8	10.8	14.23	4.7	10.9
MTI	Noncertified	33.00	33	26.4	30.33	28	24.2
	Certified	34.00	25	25.6	31.33	27	27.7
TMD	Noncertified	62.00	50	20.2	59.66	57	23.1
	Certified	54.00	37	26.7	52.67	35	21.8
VAL	Noncertified	69.00	22	7.5	69.33	12	4.7
	Certified	69.67	6	5.3	69.33	6	3.0

^aABS = absorption, ARR = arrival time, MIX = mixing time, STA = stability, DEP = departure time, MTI = mixing tolerance index, TMD = twenty-minute drop, VAL = valorimeter value.

Table C.9 Average readings from copies of 1964 check sample farinograms.

Reading ^a	Mean	Range	Coef. of var.
ARR	2.3866	0.5801	8.1
MIX	8.0333	1.400	5.0
STA	12.353	2.3066	4.3
DEP	14.720	1.8000	3.0
MTI	33.29	17.60	13.6
TMD	54.66	24.33	11.9
VAL	70.00	9.40	2.8

^aARR = arrival time, MIX = mixing time, STA = stability, DEP = departure time, MTI = mixing tolerance index, TMD = twenty-minute drop, VAL = valorimeter value.

out in July 1965, the HL-5 sample in September 1965, and the HL-6 sample in November 1965, thus covering a period of over 5 months.

From the original group of 30 collaborators, only 18 reported the results on all 3 of the previously mentioned National Check Sample reports. Therefore, 12 of the original 30 collaborators, those who did not submit results on all 3 samples, were excluded from the data compiled for this study. Of the remaining 18 collaborators, 7 had AACC-certified bowls and 11 had noncertified

Table C.10 Average standard deviations of differences between paired curves (by collaborators) from 1964 check sample farinograms.

Reading ^a	Curves 2 and 8	Curves 3 and 13	Curves 5 and 11	Curves 7 and 15	Curves 9 and 12	Average
ARR	0.301	0.215	0.108	0.143	0.151	0.184
MIX	0.318	0.175	0.310	0.234	0.580	0.323
STA	0.551	0.443	0.469	0.841	1.00	0.661
DEP	0.491	0.337	0.343	0.819	1.06	0.610
MTI	1.98	5.36	3.61	2.26	8.48	4.338
TMD	2.53	3.56	4.92	3.78	8.27	4.612
VAL	1.25	1.08	1.80	0.94	1.17	1.248

^aARR = arrival time, MIX = mixing time, STA = stability, DEP = departure time, MTI = mixing tolerance index, TMD = twenty-minute drop, VAL = valorimeter value.

bowls. The data were gleaned from the regular 1965 National Check Sample Service reports and divided into two categories: AACC-certified bowls and noncertified bowls.

The average results are given in Table C.11 for the 1965 set. Since the farinograms were not available for one individual to read, as was the case in the 1964 study, only the collaborators' readings were analyzed. Therefore only the average results of the collaborators' readings for 1964 and 1965 were tabulated in Table C.12, which gives an overall picture of the 2-year study.

The data for 1965 are similar to the 1964 series, although fewer collaborators participated in the study. With the exception of the tolerance index, the farinograms produced with the certified bowls show smaller coefficients of variation than the noncertified bowls. The average decrease in the range of the certified versus the noncertified bowls was very evident, showing a percent decrease in the range of 33.5% for absorption, 36.7% for arrival time, 55.4% for mixing time, 40.0% for stability, 21.2% for departure time, 35.2% for tolerance index, and 62.5% for valorimeter value.

FLOUR STORAGE

Since a storage study was incorporated in the 1965 series, paired comparison analyses were made to determine if there was any difference in the respective readings between the HL-4 and HL-5 and the HL-4 and HL-6 series. No significant differences were found, and it could be assumed that the farinogram of a flour stored under these conditions would not change.

CERTIFIED BOWLS

The fourth study conducted involved six certified mixers located in the immediate Minneapolis area. One bowl was the AACC Standard or Reference Bowl of the Association. These six mixers were tested on the collaborator's farinograph and on a standardized farinograph, using two

Table C.11 Average collaborators' readings for 1965 check sample farinograms for HL-4, HL-5, and HL-6 series.

Reading^a	Bowls	Mean	Range	Coef. of var.
ABS	Noncertified	61.2	4.0	1.9
	Certified	61.4	3.2	2.2
ARR	Noncertified	2.67	3.2	39.0
	Certified	2.30	1.3	20.4
MIX	Noncertified	8.30	2.3	8.1
	Certified	7.83	1.2	6.3
STA	Noncertified	12.77	7.2	17.3
	Certified	12.77	4.0	11.2
DEP	Noncertified	15.43	5.5	10.9
	Certified	15.07	4.5	10.4
MTI	Noncertified	30.67	20	18.7
	Certified	31.33	18	23.1
TMD	Noncertified	50.33	38	26.7
	Certified	45.33	20	16.6
VAL	Noncertified	71.00	10	3.8
	Certified	70.33	6	3.0

^aABS = absorption, ARR = arrival time, MIX = mixing time, STA = stability, DEP = departure time, MTI = mixing tolerance index, TMD = twenty-minute drop, VAL = valorimeter value.

Table C.12 Average collaborators' readings for 1964 and 1965 check sample farinograms for HL-4, HL-5, and HL-6 series.

Reading^a	Bowls	Mean	Range	Coef. of var.
ABS	Noncertified	60.7	4.65	2.0
	Certified	60.8	3.09	1.9
ARR	Noncertified	2.42	3.00	36.0
	Certified	2.29	1.90	23.1
MIX	Noncertified	8.14	3.25	10.1
	Certified	7.87	1.45	6.7
STA	Noncertified	12.54	7.00	15.6
	Certified	12.39	4.20	11.2
DEP	Noncertified	14.94	5.90	10.8
	Certified	14.65	4.65	10.6
MTI	Noncertified	31.84	26.5	22.7
	Certified	32.67	20.0	24.4
TMD	Noncertified	56.17	44.0	23.1
	Certified	49.67	28.5	22.1
VAL	Noncertified	70.00	16.0	5.6
	Certified	70.00	6.0,	4.1

^aABS = absorption, ARR = arrival time, MIX = mixing time, STA = stability, DEP = departure time, MTI = mixing tolerance index, TMD = twenty-minute drop, VAL = valorimeter value.

flours and two samples of each. Besides the regular sample, one sample was accurately preweighed and the absorption given. Both samples were run by the constant dough-weight method.

Table C.13 contains the standard deviation data for the AACC-certified bowls located in the immediate Minneapolis area. Also given are the standard deviations for these same bowls from data obtained when they were officially certified prior to being shipped to their respective laboratories.

The results show smaller standard deviations for the various readings when the bowls were used on one farinograph. However, the magnitude varied with the type of flour and was not consistent. The preweighed samples did not appear to offer any advantage and, in fact, on the average gave larger deviations than the regular samples. Comparison of the average standard deviations of "standardized" and "certified" results indicates that the arrival time, departure time, and tolerance index were approximately half again as large as when the bowls were originally certified and the mix time was five times larger. The data show that the certified bowls have not maintained as close a tolerance in readings after shipment and use as when they were first certified. The farinograph on which the bowl was placed influenced the results, and the number of farinographs caused an apparent increase in the variability between bowls.

Table C.13 Standard deviations of certified bowls located in Minneapolis area.

Farinograph	Absorption or height	Reading^a					
		ARR	MIX	DEP	MTI	TMD	VAL
Spring Wheat Flour	Regular Sample						
	Collaborator's	0.966	0.505	1.069	0.675	7.379	—
	Standardized	0.626	0.139	0.814	0.492	4.964	—
	Certified	0.671	0.139	0.159	0.335	3.162	5.456
	Preeweighed Sample						
	Collaborator's	19.21	0.22	1.73	3.20	8.37	5.92
Winter Wheat Flour	Standardized	16.25	0.397	0.55	1.77	7.42	8.68
	Regular Sample						
	Collaborator's	0.818	0.192	0.894	0.595	4.964	—
	Standardized	0.492	0.165	0.304	0.340	4.964	—
	Certified	0.425	0.045	0.045	0.259	4.472	8.050
	Preeweighed Sample						
	Collaborator's	27.40	0.275	0.792	1.17	6.32	11.62
	Standardized	19.65	0.021	0.484	0.865	8.66	11.18

^aARR = arrival time, MIX = mixing time, DEP = departure time, MTI = mixing tolerance index, TMD = twenty-minute drop, VAL = valorimeter value.

CONCLUSIONS

The studies showed that differences in mixing bowls, in farinographs, in operators, and in reading the curves all contribute to lack of agreement in farinogram data obtained on the same flour. However, use of certified bowls from the certification program did effectively improve the agreement between collaborators.

V FARINOGRAPH PROCEDURES OF THE AACC, ICC, AND RACI

The official procedures of the American Association of Cereal Chemists (AACC), the International Association for Cereal Chemistry (ICC), and the Royal Australian Chemical Institute (RACI) are given in this appendix.

AMERICAN ASSOCIATION OF CEREAL CHEMISTS

PROCEDURE

ADJUSTMENT OF FARINOGRAPH

1. Adjust farinograph thermostat to maintain temp. of $30^{\circ}\text{C} \pm 0.2^{\circ}\text{C}$ at entrance to mixing bowl. Check temp. of circulating water as indicated by thermoregulator against high-grade thermometer. Make sure that thermostat water is circulating freely through hose and bowl jackets.
2. With help of spirit level mounted on base plate, adjust position of latter to horizontal by means of four footscrews. Then fix footscrews by means of their locknuts.
3. Make certain that chart paper runs exactly horizontal. Two small plates on spring-loaded hinges at front of recording device operate as guides for paper and may be swung open to make this adjustment.

USE OF LARGE AND SMALL MIXING BOWLS

In changing from one bowl to another, the following adjustments are involved:

1. Sensitivity. Three sensitivities are provided by alternative positions for linkage between dynamometer lever arm at top of machine, and scale-head lever arm below base plate. Position toward back of machine provides least sensitivity and is used with large mixing bowl. Middle position is not ordinarily used with flour dough. Most sensitive position at front of lever arm is always used with small mixing bowl. Connecting linkage between upper and lower lever arms is moved from one setting to the other by pushing lever arms toward each other, disengaging both linkage ends from lever knife edges, and sliding them to desired position.
2. Zero position of scale-head pointer. Adjust scale-head pointer to zero position of dial by changing position of threaded balance weights when instrument is running at fast speed with mixer empty. Smaller of the two weights should be removed entirely when small bowl is

used. Make final writing-arm adjustment with knurled screw on left side of scale-head shaft so that scale-head pointer and writing pen give identical readings.

3. Adjustment of band width. Damping device should be adjusted only after oil in damping chamber has been at operating temp. at least 1 h and after damping piston has been moved up and down several times. To make adjustment: raise dynamometer lever arm until scale-head pointer indicates 1000. Release lever arm and measure with stopwatch the time required for pointer to go from 1000 to 100 on scale head (should be between 0.6 and 0.8 s). Damping adjustment controls band width of farinogram. To obtain wider damper opening and quicker movement of scale-head pointer and thus wider curve, turn adjustment screw counterclockwise. Opposite adjustment produces narrower band. Band width at peak of curve of 70–80 BU is recommended. It may be advantageous to mark damper adjustment screw at correct setting.
4. Cleaning. At completion of each test and while machine is running, add dry flour to bowl to make stiff dough with consistency of 800–900 BU within 1 min of mixing with test dough. Then stop machine, unscrew bowl wing nuts, take off front section of mixing bowl, and discard dough. Remove any adhering particles quickly before they dry, using small plastic spatula for scraping blades and side walls of bowl. (Spatula should be of softer material than mixing bowl in order not to damage the latter.) Finally, clean bowl with dampened cloth and wipe all parts dry, including space behind paddles. (*Caution:* Never use chemical agents such as borax, or any dough stiffeners other than flour, since traces of chemicals can affect subsequent curves and may even react with metal surfaces of bowl.)

For bronze bowls, put cleaning dough through mixing bowl every morning, or after machine has stood for several hours, to rub off thin film of oxidation on surface. If preliminary titration of flour sample is conducted (as explained in following text), this may be regarded as cleaning dough. A stainless-steel bowl does not require cleaning dough. Also, after standing, small particles of dough may harden between shafts and blades at back of mixing bowl and cause resistance to turning. Correct this by placing a few drops of water on inside back wall of bowl directly over shafts, with blades turning to soften dough particles. Then use strong jet of water or blast of air or CO₂ to remove dough. Return of scale-head pointer to zero position indicates that these dough particles have been softened and removed.

Clean titrating buret periodically with solution made of 10 parts concentrated H₂SO₄ to 1 part saturated potassium dichromate solution. Fill buret with this solution and let stand overnight. *This solution is extremely corrosive and should be handled with caution.* After draining buret, rinse repeatedly with tap water and finally with distilled water. After recording each titration, and when not in use, keep buret, including tip, filled with water at all times.

Place chart writing pen in water at end of each day to prevent drying of ink, or wash pen thoroughly before it dries.

A. Constant Flour Weight (Variable Dough Weight) Procedure

LARGE BOWL

Specify procedure used.

1. Turn on thermostat and circulating pump at least 1 h prior to using instrument.
2. Determine moisture content of flour as directed in any oven method for flour (Methods 44–15 ff).^c (Keep flour samples in moisture-proof containers. Accurate moisture values are very important.)
3. Place in bowl 300 ± 0.1 g flour (14% mb; Note 1; Table 82–83).^c
4. Fill large buret with water at room temp., making sure that tip is full and automatic zero adjustment of buret is functioning properly.
5. Put a few drops of ink in pen and place in contact with 9-min position on chart. Turn on machine to high-speed setting and run for 1 min until zero-minute line is reached. At this instant begin adding water to right front corner of bowl from large buret to volume nearly that of expected absorption of flour. When dough begins to form, scrape down sides of bowl with plastic scraper, starting on right side, front, and working counterclockwise. Cover with glass plate. If it appears that mixing curve will level off at value larger than 500 BU, cautiously add more water. After water is added, again cover bowl with glass plate to prevent evaporation.
6. The first titration attempt rarely produces a curve that has maximum resistance centered on 500-BU line; therefore, in a subsequent titration, adjust absorption either up or down until this is achieved to within 20 BU. A titration producing wider variation affects scoring of curve. As a guide to correcting preliminary titration values, it can be reckoned that difference between each horizontal line (20 BU) corresponds approximately to 0.6%–0.8% absorption (1.8–2.4 mL water), depending on flour. When correct absorption is achieved, curve at maximum dough development is centered on 500-BU line.
7. For final titration, add all water within 25 s after opening buret stopcock. Permit machine to run until adequate curve is available for evaluation as desired (see [Interpretation](#)), i.e., absorption, slightly beyond peak; stability, until top of curve recrosses 500-BU line after peak; valorimeter, 12 min beyond peak. At this point lift pen from paper by means of small locking knob on pen arm, add dry flour to bowl, and proceed with cleaning of bowl.
8. Report absorption values to nearest 0.1%. Calculate absorption on 14% mb determined with large bowl, by means of following equation: Absorption % = $(x+y - 300)/3$, where x = milliliters of water to produce curve with maximum consistency centered on 500-BU line, and y = grams of flour used, equivalent to 300 g, 14% mb.

SMALL BOWL

Same principle as for large bowl, except 50 ± 0.1 g flour (14% mb; Note 2; Table 82–83) is used. Titration is conducted with *small* buret. In this case, each interval between horizontal lines of chart (20 BU) corresponds to about 0.4 mL water.

^cAll methods and tables referred to in the AACC farinograph procedure can be found in the Approved Methods of the American Association of Cereal Chemists, 8th ed. 1983. The Association: St. Paul, MN.

Calculate absorption on 14% mb, determined with small bowl, using equation: Absorption % = $2(x+y - 50)$, where x = milliliters of water to produce curve with maximum consistency centered on 500-BU line, and y = grams of flour used, equivalent to 50 g, 14% mb.

B. Constant Dough Weight Procedure

LARGE BOWL

Specify procedure used.

1. Turn on thermostat and circulating pump at least 1 h prior to using instrument.
2. Determine moisture content of flour as directed in any oven method for flour (Methods 44–15 ff). (Keep flour samples in moisture-proof containers. Accurate moisture values are very important.) Correction of absorption to 14% mb under this procedure may be postponed until as-is farinograph absorption is determined.
3. Make estimate of as-is absorption to produce curve centered on 500-BU line. From Table 54-28A, determine weights of flour and water that correspond to estimated as-is absorption. Add flour, weighed to ± 0.1 g, to bowl. Set pen point at 9-min mark on chart.
4. Start mixer and run at high speed with dry flour 1 min until zero-min line is reached. At this instant, begin adding water from large buret at right front corner of mixing bowl. All water must be added within 25 s. Scrape down sides of bowl with plastic spatula. Cover with glass plate to prevent evaporation.
5. Since first attempt rarely produces a curve centered on 500-BU line at maximum consistency, reestimate absorption according to approx. Relationship: $20\text{BU} = 0.6\%$ absorption, determine corresponding flour and water weights from Table 54-28A, and conduct second run. When curve is obtained with maximum consistency centered at $500 \pm 20\text{BU}$, continue mixing until adequate curve is available for evaluation as desired (see *Interpretation*).
6. At this point, lift pen from paper by means of small locking knob on pen arm, add dry flour to bowl, and proceed with cleaning of bowl.

Flour absorption corrected to 14% mb, reported to nearest 0.1%, is obtained by calculation as illustrated in Note 2, from Table 54-29, or preferably from Table 82-21.

SMALL BOWL

Principle is same as for large bowl.

1. Use dough weight of 80 g (Table 54-28A) and make water addition with *small* buret. Weigh flour to ± 0.1 g.
2. Obtain absorptions on 14% mb (a) by calculations as illustrated in Note 2, (b) from Table 54-29, or preferably (c) from Table 82-21.

INTERPRETATION

Values other than absorption are frequently derived from farinograph curves. Among those that have been proposed are the following:

1. Dough development time. This is interval, to nearest 0.5 min, from first addition of water to that point in maximum consistency range immediately before first indication of weakening. This value has also been referred to as "peak" or "peak time." For flours having a curve that is nearly flat for several min, peak time may be determined by taking mean between midpoint of flat portion of top of curve and highest point of arc of bottom of curve. Occasionally two peaks may be observed; the second should be taken for determination of dough development time.
2. Valorimeter value. This is empirical single-figure quality score based on dough development time and tolerance to mixing that is derived from farinogram by means of special template supplied by manufacturers of farinograph equipment.
3. Tolerance index. This value is difference in BU from top of curve at peak to top of curve measured at 5 min after peak is reached. A related measurement called "drop-off" refers to difference in BU from 500-BU line to center of curve measured at 20 min from addition of water.
4. Stability. This is defined as time difference, to closest 0.5 min, between point where top of curve first intersects 500-BU line (arrival time) and point where top of curve leaves 500-BU line (departure time). If curve is not centered exactly on 500 line at maximum resistance but rather, for example, at 490 or 510 level, a line must be drawn at 490 or 510 level parallel to 500 line. This new line is then used in place of 500 line to determine arrival time, departure time, and stability.
5. Time to breakdown. This is time from start of mixing until there has been a decrease of 30 units from peak point. It is determined by drawing horizontal line through center of curve at its highest point and then drawing another parallel line at 30-unit lower level. Time from start of mixing until center of descending curve crosses this lower line is "time to breakdown."

NOTES

1. Farinograms of various flours are affected differently with addition of malt supplement. In general, addition of malt shortens dough development time and lowers absorption. Practical evaluation of a flour may require addition of malt in amount required for proper diastatic activity.
2. Example: If flour sample contains 12.5% moisture, amount of flour required for 300-g test would be: $(86.0/87.5) \times 300 = 294.9$ g. For the 50-g test this would be: $(86.0/87.5) \times 50 = 49.1$ g.
3. The following equation may be used to convert as-is absorption determined by Constant Dough Weight procedure to absorption at 14% moisture content.

$$A = 86 \frac{(A + B)}{(100 - M)} - 14$$

where A = absorption, 14% mb; B = absorption, as-is mb; M = flour moisture, as-is basis. This equation is derived from the following considerations: One may equate two doughs of equal weight, of same consistency in farinograph, made from same flour but at different moisture contents. Total water in each dough is same. Then

$$\frac{\text{water added} + \text{water in flour}}{\text{dry wt of flour}} = \frac{\text{water added} + \text{water in flour}}{\text{dry wt of flour}}$$

For example, to calculate absorption (A) at 14% moisture equivalent to 70% absorption (B) at 11.1% moisture (M),

$$\frac{A + 14}{100 - 14} = \frac{70 + 11.1}{100 - 11.1}, \text{ or}$$

$$A = 86 \frac{B + M}{100 + M} - 14 = \frac{81.1}{88.9} - 14 = 64.5\%$$

INTERNATIONAL ASSOCIATION FOR CEREAL CHEMISTRY METHOD FOR USING THE BRABENDER FARINOGRAPH PROCEDURE

1. Determine the moisture content of the flour by the I.C.C. Standard Method.
2. If necessary bring the flour to $30^{\circ}\text{C} \pm 10^{\circ}\text{C}$. Turn on the thermostat and circulate the water for at least 1 h prior to using the instrument. During use check the temperature of the circulating water and of the mixing bowl, the latter in the hole provided. Both temperatures should be $30^{\circ}\text{C} \pm 0.2^{\circ}\text{C}$.
3. Lubricate the mixing bowl with a drop of water between its back wall and each of the blades. Adjust the position of the balance weight(s) so as to obtain zero deflection of the pointer with the blades rotating at fast speed in the empty, clean bowl. Adjust the arm of the pen so as to obtain identical readings from the pointer and the recording pen. Adjust the damper so that, with the motor running, the time required for the pointer to go from 1000 to 100 BU is 1.0 ± 0.2 s.
4. Place in the bowl the equivalent of 300 ± 0.1 g flour at 14% moisture. Cover the bowl.
5. Fill buret, including the tip, with water at $30^{\circ}\text{C} \pm 5^{\circ}\text{C}$.
6. Set the chart paper so that the pen is in contact with a 9 min line. Mix at fast speed for 1 min. Start adding water from the buret to the right-hand front corner of the bowl when the pen crosses the zero-min line. Add a volume of water close to that expected to bring the curve to the 500-BU line. When the dough forms, scrape down the sides of the bowl with the plastic spatula. Cover the bowl. If the consistency is too high, add a little more water to center the curve on 500 ± 20 BU at its peak. Stop mixing and clean the bowl.
7. Make a second and further mixings if necessary until the correct water addition is made within 25 s and continue mixing until 12 min past the peak or until the desired features of the curve are revealed.

PRESENTATION OF RESULTS

1. Water absorption

Calculate the water absorption on a 14% moisture basis as follows:

$$\text{Water absorption, \%} = \frac{(x + y - 300)}{3}$$

where x = milliliters of water added to produce curve with maximum consistency of 500 BU at the center and y = grams of flour used, equivalent to 300 g at 14% moisture. Report absorption to nearest 0.1%.

2. Development time

This is the time to that point on the curve immediately before the first signs of weakening. Report development time to the nearest 0.5 min. In the relatively infrequent case where two peaks are observed, the second peak should be used to measure development time.

3. Degree of softening

This is the difference between the center of the curve at the peak and the center of the curve 12 min after the peak. Report the degree of softening to the nearest 5 BU.

REMARKS

1. Reproducibility

The collaborative tests carried out by the Study Group in 1966–67 gave the following values for the coefficient of variation for a single determination in a single farinograph:

Water absorption	0.55%
Dough development time	8.9%
Degree of softening	7.5%

THE ROYAL AUSTRALIAN CHEMICAL INSTITUTE OPERATIONAL PROCEDURES

1. Preparation

Allow the flour to equilibrate with a room temperature of 21–24°C, avoiding change in moisture content.

Sieve the flour at least once through approximately 16 mesh sieve, thus mixing thoroughly and ensuring uniformity and even moisture distribution.

Prepare and standardize the instrument, especially zero check and 500 paper test.

Wash out the bowl thoroughly, including a stream of warm water directed behind the blades while the motor is running. Dry the bowl and blades with a soft cloth. When clamping the bowl front in place, ensure that the final turn of the two wing nuts is made simultaneously to give even tension.

Run a cleaning dough using a test flour or one similar to it. Clean and dry as before. For bronze bowls run a cleaning dough at 600–650 BU consistency for 15 min, unless the bowl

has been idle for more than 1 h, when two such doughs are required. Wash and dry the bowl after each cleaning dough.

2. Test Method

Weigh exactly 300 g of the sifted blended sample. Transfer to the bowl. Start the pen writing on the chart. Use the knife edge carrier bar to work the pen up and down to start it writing, if necessary, NEVER the pen arm. Describe a reference arc from 0 to 1000 units.

Mix dry for 1 min with the perspex plate cover in place. Use "fast" speed, 60 rpm, unless otherwise directed.

As the pen reaches a minute-line on the chart, drain into the right front corner of the bowl the estimated amount of distilled water at 30°C at maximum buret speed. Under no circumstances "titrate" water into the flour during any test where results are to be used or reported. At once scrape down the upper walls with a soft spatula, causing any particles removed to be reincorporated in the dough. Cover the bowl with a perspex plate and observe development. Should the mean consistency at maximum development not be 500 (or other prescribed value) within plus or minus 20 units, release the nib, clean bowl as described, and repeat the test with a suitably corrected amount of water.

To clean, add fine semolina to assist in drying out the dough for removal. The amount used should be such that the consistency registered is not above 750 units and should be mixed in for the least possible time.

Remove the dough and wash the bowl and blades thoroughly.

A large coarse cloth is useful for this purpose.

Where the consistency at development is satisfactory, allow mixing to continue for sufficient time to reveal the rate of breakdown.

LITERATURE CITED

- American Association of Cereal Chemists, 1983. Farinograph method for flour. In: Approved Methods, eighth ed. The Association, St. Paul, MN. Method 54-21.
- Bennett, R., Coppock, J.B.M., 1953. Dough consistency and measurement of water absorption on the Brabender farinograph and Simon "Research" water absorption meter. Trans. Am. Assoc. Cereal Chem. 11, 172.
- Bloksma, A.H., 1963. Oxidation by molecular oxygen of thiol groups in unleavened doughs from normal and defatted wheat flours. J. Sci. Food Agric. 14, 529.
- Bloksma, A.H., 1971. Rheology and chemistry of dough. In: Pomeranz, Y. (Ed.), Wheat, Chemistry and Technology, second ed. American Association of Cereal Chemists, St. Paul, MN, p. 523.
- Bloksma, A.H., Meppelink, E.K., 1973. Sensory assessment of stiffness and rheological measurements on doughs of identical farinograph consistencies. J. Texture Stud. 4, 145.
- Bloksma, A.H., Nieman, W., 1975. The effect of temperature on some rheological properties of wheat flour doughs. J. Texture Stud. 6, 343.
- Blyler, L.L., Daane, J.H., 1967. An analysis of Brabender torque rheometer data. Polym. Eng. Sci. 7, 178.
- Cox, W.P., Merz, E.H., 1958. Correlation of dynamic and steady flow viscosities. J. Polym. Sci. 28, 619.
- Goodrich, J.E., Porter, R.S., 1967. A rheological interpretation of torque-rheometer data. Polym. Eng. Sci. 7, 45.
- Hibberd, G.E., Wallace, W.J., 1966. Dynamic viscoelastic behaviour of wheat flour doughs. I. Linear aspects. Rheol. Acta 5, 193.

- Hlynka, I., 1962. Influence of temperature, speed of mixing, and salt on some rheological properties of dough in the farinograph. *Cereal Chem.* 39, 286.
- International Association for Cereal Science and Technology ICC, 1972. Standard No. 115, Method for Using the Brabender Farinograph. The Association, Vienna.
- International Organization for Standardization, 1983. Draft International Standard 5530/1, Wheat Flour—Physical Characteristics of Doughs. Part I: Determination of Water Absorption and Rheological Properties Using a Farinograph. The Organization, Geneva.
- Launay, B., 1979. Propriétés rhéologiques des pâtes de farine: Quelques progrès récents. *Ind. Aliment. Agric.* 96, 617.
- Launay, B., Buré, J., 1973. Application of a viscometric method to the study of wheat-flour doughs. *J. Texture Stud.* 4, 82.
- Muller, H.G., 1968. Aspects of dough rheology. In: *Rheology and Texture of Foodstuffs. Monograph 27*. Society of Chemical Industry, London, p. 181.
- Shuey, W.C., 1961. Farinograph curve characteristics. *Cereal Sci. Today* 6, 41.
- Van Beek, G., Veerkamp, C.H., 1982. Een programma voor het berekenen van de thermische eigenschappen van voedingsmiddelen. *Voedingsmiddelentechnologie* 15 (19), 63.
- Voisey, P.W., Miller, H., Kloek, M., 1966. An electronic recording dough bowl. IV. Applications in farinography. *Cereal Chem.* 43, 438.
- Voisey, P.W., Miller, H., Byrne, P.L., 1971. The Ottawa electronic recording farinograph. *Cereal Sci. Today* 16, 124.

VI SELECTED REFERENCES CONCERNING THE FARINOGRAPH THAT HAVE APPEARED IN CEREAL CHEMISTRY AND CEREAL FOODS WORLD

Cereal foods world

- Al-Suaidy, M.A., Johnson, J.A., Ward, A.B., 1973a. Effects of premilling, soaking, and freezing on milling, physical dough properties, and baking of hard red winter wheat. *Cereal Sci. Today* 18, 160.
- Al-Suaidy, M.A., Johnson, J.A., Ward, A.B., 1973b. Effects of certain biochemical treatments on milling and baking properties of hard red winter wheat. *Cereal Sci. Today* 18, 174.
- Blokksma, A.H., 1972. Flour composition, dough rheology, and baking quality. *Cereal Sci. Today* 17, 380.
- Blokksma, A.H., Francis, B., Zaat, J.C.A., 1962. The alveograph, farinograph, and extensigraph. *Cereal Sci. Today* 7, 308, 312, 336.
- Brabender, M., 1973. Resistography. A dynamic quick method to classify wheat and flour quality. *Cereal Sci. Today* 18, 206.
- Crabtree, J., Dendy, D.A.V., 1979. Comilling of flour species of millet with wheat to produce composite flours. *Cereal Foods World* 24, 103.
- D'Appolonia, B.L., Shuey, W.C., Sibbitt, L.D., Gilles, K.A., 1971. Relations between mixing requirements of flour using a continuous baking unit and conventional lab mixers. *Cereal Sci. Today* 16, 206.
- Editorial, 1960. The farinograph mixing bowl. *Cereal Sci. Today* 5, 106.
- Finney, P.L., Bains, G.S., Hoseney, R.C., Lineback, D.R., 1973. Quality of Indian wheats. *Cereal Sci. Today* 18, 392.
- Gracza, R., 1964. The rate of energy consumption in mixing air classified flour fractions into doughs. *Cereal Sci. Today* 9, 274, 276, 281.
- Gross, H., Bell, R.L., Fischer, F., Redfern, S., 1967. Further studies on use of fungal enzymes with flour brew. *Cereal Sci. Today* 12, 394, 414.

- Gross, H., Bell, R.L., Redfern, S., 1966. Use of fungal enzymes with flour brews. *Cereal Sci. Today* 11. 419, 422.
- Guy, E.J., Vettel, H.E., Pallansch, M.J., 1967. Farinograph characteristics of milk-flour dough. *Cereal Sci. Today* 12, 200.
- Guy, E.J., Vettel, H.E., Pallansch, M.J., 1974. Effect of cheese whey protein concentrates on the baking quality and Theological characteristics of sponge doughs made from hard red spring wheat flour. *Cereal Sci. Today* 19, 551.
- Henika, R.G., 1965. Cysteine, whey and oxidant reactions in continuous mix. *Cereal Sci. Today* 10. 420, 424.
- Hyldon, R., 1964. Farinograph studies on evaluating vital wheat gluten. *Cereal Sci. Today* 9. 4, 6, 12.
- Ikezoe, K., Tipples, K.H., 1968. Farinograph studies on the effect of various oxidizing agents in the sponge and-dough system. *Cereal Sci. Today* 13. 327, 330, 358, 360.
- ISO, Wheat flour—Physical characteristics of doughs—Part 1: Determination of water absorption and rheological properties using a farinograph. International standard 5530/1, International Organization for Standardization, Geneva, Switzerland, 1980.
- Johnson, J.A., Khan, M.N.A., Sanchez, C.R.S., 1972. Wheat cultivars, environment and bread baking quality. *Cereal Sci. Today* 17, 323.
- Kulp, K., Volpe, T., Barrett, F.F., Jonsson, K., 1980. Low protein wheat flour utilized in soy fortified bread. *Cereal Foods World* 25, 609.
- Lorenz, K., Johnson, J.A., 1970. Flour starch damage by ballmilling: effect on physical dough properties and quality of continuous-mix bread. *Cereal Sci. Today* 15. 46, 51.
- MacArthur, L.A., D'Appolonia, B.L., 1982. Microwave and gamma radiation of wheat. *Cereal Foods World* 27, 58.
- Mullen, J.D., Smith, D.E., 1968. Protein composition and solubility. *Cereal Sci. Today* 13. 398, 425.
- Paulsen, T.M., Horan, F.E., 1965. Functional characteristics of edible soya flours. *Cereal Sci. Today* 10, 14.
- Redfern, S., Brachfeld, B.A., Maselli, J.A., 1964. Laboratory studies of processing temperatures in continuous breadmaking. *Cereal Sci. Today* 9, 190.
- Satin, M., McKeown, B., Findlay, C., 1978. Design of a commercial natural fiber white bread. *Cereal Foods World* 23, 676.
- Shuey, W.C., 1958. Effect of malt supplement on farinograms. *Cereal Sci. Today* 3. 280, 281.
- Shuey, W.C., 1959. Farinograph technology. *Cereal Sci. Today* 4, 309.
- Shuey, W.C., 1961. Farinograph curve characteristics. *Cereal Sci. Today* 6, 41.
- Sietz, W., 1978. Advances in ingredient testing equipment. *Cereal Foods World* 23, 187.
- Tanaka, K., Tipples, K.H., 1969. Relation between farinograph mixing curves and mixing requirements. *Cereal Sci. Today* 14. 296, 310.
- Trum, G.W., Rose, L.C., 1964. Practical dough rheology in continuous dough processing. *Cereal Sci. Today* 9. 156, 158, 186.
- Tsen, C.C., 1976. Regular and protein fortified cookies from composite flours. *Cereal Foods World* 21, 633.
- Tsen, C.C., Farrell, E.P., Hoover, W.J., Crowley, P.R., 1975. Extruded soy products from whole and dehulled soybeans cooked at various temperatures for bread and cookie fortifications. *Cereal Foods World* 20, 413.
- Vidal, F.D., Flanders, T.E., Joiner, R.R., 1965. Baking characteristics versus physical tests with matured flour. *Cereal Sci. Today* 10. 32, 26, 40.
- Voisey, P.W., Miller, H., Byrne, P.L., 1971. The Ottawa electronic recording farinograph. *Cereal Sci. Today* 16. 124, 130.
- Watson, C.A., McNeal, F.H., Berg, M.A., Hartman, G.P., 1967. Weathering of mature wheat by rain and snow and their influence on grain quality. *Cereal Sci. Today* 12. 86, 142.
- Watson, C.A., Welsh, J.R., 1966. Monosomics. *Cereal Sci. Today* 11, 286.

Cereal chemistry

- Aitken, T.R., Fisher, M.H., 1945. Mixing tolerances of varieties of hard red spring wheat. *Cereal Chem.* 22, 392.
- Aitken, T.R., Fisher, M.H., Anderson, J.A., 1944. Effect of protein content and grade on farinograms, extensograms, and alveograms. *Cereal Chem.* 21, 465.
- Aitken, T.R., Geddes, W.F., 1938. The effect on flour strength of increasing the protein content by addition of dried gluten. *Cereal Chem.* 15, 181.
- Aitken, T.R., Geddes, W.F., 1939. The relation between protein content and strength of gluten-enriched flours. *Cereal Chem.* 16, 223.
- Allgauer, A.J., Hill, G., Spotts, E.K., Dalby, G., 1954. The flour factor in the farinograph test for evaluating the baking properties of milk solids. *Cereal Chem.* 31, 311.
- Bailey, R.S., 1940. A method for the formulation of farinograph curves. *Cereal Chem.* 17, 701.
- Bailey, C.H., Munz, E., 1938. The march of expansion and temperature in baking bread. *Cereal Chem.* 15, 413.
- Bayfield, E.G., Stone, C.D., 1960. Effects of absorption and temperature upon flour-water farinograms. *Cereal Chem.* 37, 233.
- Bean, M.M., Erman, E., Mecham, D.K., 1969. Baking characteristics of high-protein fractions from air-classified Kansas hard red winter wheats. *Cereal Chem.* 46, 27.
- Bice, C.W., Geddes, W.F., 1949. Studies on bread staling. IV. Evaluation of methods for the measurement of changes which occur during bread staling. *Cereal Chem.* 26, 440.
- Bohn, L.J., Bailey, C.H., 1936. Effect of mixing on the physical properties of dough. *Cereal Chem.* 13, 560.
- Bohn, L.J., Bailey, C.H., 1937. Effect of fermentation, certain dough ingredients, and proteases upon the physical properties of flour doughs. *Cereal Chem.* 14, 335.
- Bowlby, C., Tucker, H., Miller, B.S., Johnson, J.A., 1953. A comparison of methods for determining proteolytic activity. *Cereal Chem.* 30, 480.
- Brabender, C.W., 1932. Studies with the farinograph for predicting the most suitable types of American export wheats and flours for mixing with European soft wheats and flours. *Cereal Chem.* 9, 617.
- Brabender, C.W., 1934. Six years of farinography. *Cereal Chem.* 11, 586.
- Bushuk, W., 1963. A farinograph technique for studying gluten. *Cereal Chem.* 40, 430.
- Calderon, M., Navarro, S., Linder, Z., 1970. Effect of common fumigants on the baking qualities of wheat. *Cereal Chem.* 47, 422.
- D'Appolonia, B.L., Gilles, K.A., Medcalf, D.G., 1970. Effect of water-soluble pentosans on gluten-starch loaves. *Cereal Chem.* 47, 194.
- Dahle, L.K., Hinz, R.S., 1966. The weakening action of thioctic acid in unyeasted and yeasted doughs. *Cereal Chem.* 43, 682.
- Dahle, L.K., Murthy, P.R., 1970. Some effects of antioxidants in dough systems. *Cereal Chem.* 47, 296.
- Dahle, L.K., Pinke, P.A., 1968. A note comparing effects of dough mixing of thioctic acid (lipoic acid) and yeast-fermented flour extracts. *Cereal Chem.* 45, 287.
- Doguchi, M., Hlynka, I., 1967. Some rheological properties of crude gluten mixed in the farinograph. *Cereal Chem.* 44, 561.
- Favor, H.H., Johnson, N.F., 1947. Effect of poly-oxyethylene stearate on the crumb softness of bread. *Cereal Chem.* 24, 346.
- Freilich, J., 1948. Studies on bread staling. III. Influence of fermentation variables on bread staling as measured by compressibility and farinograph procedures. *Cereal Chem.* 25, 87.
- Freilich, J., Frey, C.N., 1944. Dough oxidation and mixing studies. VI. Effects of oxidizing agents in the presence of reducing matter. *Cereal Chem.* 21, 241.
- Freilich, J., Frey, C.N., 1947. Dough oxidation and mixing studies. VII. The role of oxygen in dough mixing. *Cereal Chem.* 24, 436.

- Freilich, J., McHugh, S., Frey, C.N., 1935. Correlation of experimental and commercial baking tests. *Cereal Chem.* 12, 668.
- Frey, C.N., Freilich, J., Ekstedt, H., 1937. Correlation of experimental and commercial baking tests when using sponge doughs. II. *Cereal Chem.* 14, 629.
- Geddes, W.F., Aitken, T.R., 1937. The comparative quality of flours from corresponding wheats milled on an Allis Chalmers experimental mill and a Brabender automatic laboratory mill. *Cereal Chem.* 14, 511.
- Geddes, W.F., Aitken, T.R., Fisher, M.H., 1940. The relation between the normal farinogram and the baking strength of western Canadian wheat. *Cereal Chem.* 17, 528.
- Gracza, R., 1959. The subsieve-size fractions of a soft wheat flour produced by air classification. *Cereal Chem.* 36, 465.
- Gracza, R., 1960. The subsieve-size fractions of a hard red spring wheat flour produced by air classification. *Cereal Chem.* 37, 579.
- Grogg, B., Caldwell, E.F., 1958. Gelatinization of starch materials in the farinograph. *Cereal Chem.* 35, 196.
- Henika, R.G., Rodgers, N.E., 1965. Reactions of cysteine, bromate, and whey in a rapid breadmaking process. *Cereal Chem.* 42, 397.
- Hermitté, R.J.J., Shellenberger, J.A., 1947. Effect of excessive methyl bromide fumigation on flour. *Cereal Chem.* 24, 449.
- Hlynka, I., 1949. Effect of bisulfite, acetaldehyde, and similar reagents on the physical properties of dough and gluten. *Cereal Chem.* 26, 307.
- Hlynka, I., 1959. Dough mobility and absorption. *Cereal Chem.* 36, 378.
- Hlynka, I., 1960. Intercomparison of farinograph absorption obtained with different instruments and bowls. *Cereal Chem.* 37, 67.
- Hlynka, I., 1962. Influence of temperature, speed of mixing, and salt on some rheological properties of dough in the farinograph. *Cereal Chem.* 39, 286.
- Hlynka, I., Anderson, J.A., 1946. A machine for measuring the extensibility and resistance to extension of gluten. *Cereal Chem.* 23, 115.
- Hlynka, I., Kuzina, F.D., Shuey, W.C., 1961. Conversion of constant-flour farinograph absorption to constant-dough basics. *Cereal Chem.* 38, 386.
- Hoffman, C., Schweitzer, T.R., Spotts, E.K., Dalby, G., 1948. Evaluation of the baking properties of roller process nonfat dry milk solids by a farinograph procedure. *Cereal Chem.* 25, 385.
- Howe, M., 1946. Further studies on the mechanism of the action of oxidation and reduction on flour. *Cereal Chem.* 23, 84.
- Irvine, G.N., Bradley, J.W., Martin, G.C., 1961. A farinograph technique for macaroni doughs. *Cereal Chem.* 38, 153.
- Jankiewicz, M., Pomeranz, Y., 1965. Comparison of the effects of N-ethylmaleimide and urea on rheological properties of dough. *Cereal Chem.* 42, 37.
- Jaska, E.J., 1961. Effect of bleaching on flour as measured by structural relaxation of dough. *Cereal Chem.* 38, 369.
- Johnson, J.A., Miller, B.S., 1953. The relationship between dough consistency and proteolytic activity. *Cereal Chem.* 30, 471.
- Johnson, J.A., Shellenberger, J.A., Swanson, C.O., 1946a. Farinograms and mixograms as a means of evaluating flours for specific uses. *Cereal Chem.* 23, 388.
- Johnson, J.A., Shellenberger, J.A., Swanson, C.O., 1946b. Extensograph studies of commercial flours and their relation to certain other physical dough tests. *Cereal Chem.* 23, 400.
- Jongh, G., 1961. The formation of dough and bread structures. I. The ability of starch to form structures, and the improving effect of glyceryl monostearate. *Cereal Chem.* 38, 140.

- Jørgensen, H., 1936. On the existence of powerful but latent proteolytic enzymes in wheat flour. *Cereal Chem.* 13, 346.
- Kent-Jones, D.W., Geddes, W.F., 1936. A cooperative study of the utility of different methods for evaluating flour strength. *Cereal Chem.* 13, 239.
- Kulp, K., Bechtel, W.G., 1963. Effect of water-insoluble pentosan fraction of wheat endosperm on the quality of white bread. *Cereal Chem.* 40, 493.
- Lai, S.-P., Finney, K.F., Milner, M., 1959. Treatment of wheat with ionizing radiations. IV. Oxidative, physical, and biochemical changes. *Cereal Chem.* 36, 401.
- Lancaster, E.B., Anderson, R.A., 1959. Consistency measurements on batters, doughs and pastes. *Cereal Chem.* 36, 420.
- Landis, Q., 1935. An index of proteolytic activity by the use of the farinograph. *Cereal Chem.* 12, 25.
- Landis, Q., Freilich, J., 1935. Studies on test dough mixer calibration. *Cereal Chem.* 12, 665.
- Larsen, R.A., Jenness, R., Geddes, W.F., 1949. Effect of heat treatment of separated milk on the physical and baking properties of doughs enriched with dry milk solids. *Cereal Chem.* 26, 189.
- Larson, B.L., Jenness, R., Geddes, W.F., Coulter, S.T., 1951. An evaluation of the methods used for determining the baking quality of nonfat dry milk solids. *Cereal Chem.* 28, 351.
- Louw, J.B., Krynaud, G.N., 1961. The relationship between farinograph mobility and absorption. *Cereal Chem.* 38, 1.
- Markley, M.C., 1937. The colloidal behavior of flour doughs. I. The thixotropic nature of starch-water systems. *Cereal Chem.* 14, 434.
- Markley, M.C., 1938. The colloidal behavior of flour doughs. III. Studies upon the properties of flour-starch-water systems. *Cereal Chem.* 15, 438.
- Markley, M.C., Bailey, C.H., 1938. The colloidal behavior of flour doughs. II. A study of the effects of varying the flour-water ratio. *Cereal Chem.* 15, 317.
- Markley, M.C., Bailey, C.H., 1939. The colloidal behavior of flour doughs. V. Comparison of the increase in mobility of doughs upon either prolonged mixing or fermentation with the effects of varied mixing times upon loaf characteristics. *Cereal Chem.* 16, 265.
- Markley, M.C., Bailey, C.H., Harrington, F.L., 1939. The colloidal behavior of flour doughs. VI. Dough formation from flours of diverse types. *Cereal Chem.* 16, 271.
- Matsuamoto, H., Oshima, I., Hlynka, I., 1960. Effect of bisulfite and acetaldehyde on the disulfide linkage in wheat protein. *Cereal Chem.* 37, 710.
- Matsuo, R.R., Irvine, G.N., 1970. Effect of gluten on the cooking quality of spaghetti. *Cereal Chem.* 47, 173.
- Mattern, P.J., Sandstedt, R.M., 1957. The influence of the water-soluble constituents of wheat flour on its mixing and baking characteristics. *Cereal Chem.* 34, 252.
- Matthews, R.H., Sharpe, E.J., Clark, W.M., 1970. The use of some oilseed flours in bread. *Cereal Chem.* 47, 181.
- Mecham, D.K., 1959. Effects of sulphydryl-blocking reagents on the mixing characteristics of doughs. *Cereal Chem.* 36, 134.
- Mecham, D.K., Cole, E.G., Pence, J.W., 1965. Dough-mixing properties of crude and purified glutens. *Cereal Chem.* 42, 409.
- Mecham, D.K., Knapp, C., 1966. The sulphydryl content of doughs mixed under nitrogen. *Cereal Chem.* 43, 226.
- Meredith, P., Hlynka, I., 1964. The action of reducing agents on dough. *Cereal Chem.* 41, 286.
- Merritt, P.P., Ausemus, E.R., 1944. Effect of scab on the quality of hard red spring wheat. *Cereal Chem.* 21, 199.
- Merritt, P.P., Stamberg, O.E., 1941. Some studies on flour absorption. *Cereal Chem.* 18, 632.
- Miller, B.S., Hays, B., Johnson, J.A., 1956. Correlation of farinograph, mixograph, sedimentation, and baking data for hard red winter wheat flour samples varying widely in quality. *Cereal Chem.* 33, 277.
- Milner, M., Johnson, J.A., 1950. The influence of drying temperature and dry ice treatment on the quality of immature wheat. *Cereal Chem.* 27, 358.

- Milner, M., Shellenberger, J.A., 1953. Physical properties of weathered wheat in relation to internal fissuring detected radiographically. *Cereal Chem.* 30, 202.
- Moore, C.L., Herman, R.S., 1942. The effect of certain ingredients and variations in manipulations on the farinograph curve. *Cereal Chem.* 19, 568.
- Munz, E., Bailey, C.H., 1936. Relation of amylase activity to gassing rate. *Cereal Chem.* 13, 346.
- Munz, E., Bailey, C.H., 1937. Effect of the enzymes of malted wheat flour upon certain properties of flour and dough. *Cereal Chem.* 14, 445.
- Munz, E., Brabender, C.W., 1940a. Prediction of baking value from measurements of plasticity and extensibility of dough. I. Influence of mixing and molding treatments upon physical dough properties of typical American wheat varieties. *Cereal Chem.* 17, 78.
- Munz, E., Brabender, C.W., 1940b. Extensograms as a basis of predicting baking quality and reaction to oxidizing agents. *Cereal Chem.* 17, 313.
- Munz, E., Brabender, C.W., 1941. American wheat types and varieties as distinguished by farinograms and extensograms. *Cereal Chem.* 18, 316.
- Murthy, P.R., Dahle, L.K., 1969. Studies on a simplified dough system composed of gliadin, glutenin and starch. *Cereal Chem.* 46, 463.
- Near, C., Sullivan, B., 1935. The use of the farinograph as an accurate measure of absorption. *Cereal Chem.* 12, 527.
- Pelshenke, P., 1933. A short method for the determination of gluten quality of wheat. *Cereal Chem.* 10, 90.
- Pfeifer, V.F., Vojnovich, C., Anderson, R.A., 1958. Vital wheat gluten by drum-drying. *Cereal Chem.* 35, 458.
- Pinckney, A.J., Greenaway, W.T., Zeleny, L., 1957. Further developments in the sedimentation test for wheat quality. *Cereal Chem.* 34, 16.
- Skovholt, O., Bailey, C.H., 1932. The effect of temperature and of the inclusion of dry skimmilk upon the properties of doughs as measured with the farinograph. *Cereal Chem.* 9, 523.
- Skovholt, O., Bailey, C.H., 1935a. The effect of mixing and fermentation upon the protein structure and colloidal properties of doughs. *Cereal Chem.* 12, 307.
- Skovholt, O., Bailey, C.H., 1935b. Free and bound water in bread doughs. *Cereal Chem.* 12, 321.
- Swanson, C.O., 1936. Physical tests to determine quality in wheat varieties. *Cereal Chem.* 13, 179.
- Sullivan, B., Near, C., Foley, G.H., 1936a. The role of the lipids in relation to flour quality. *Cereal Chem.* 13, 318.
- Sullivan, B., Near, C., Foley, G.H., 1936b. The harmful action of wheat germ on the baking quality of flour and the constituents responsible for this effect. *Cereal Chem.* 13, 453.
- Sullivan, B., Howe, M., Schmalz, F.D., 1936. On the presence of glutathione in wheat germ. *Cereal Chem.* 13, 665.
- Sullivan, B., Howe, M., Schmalz, F., 1937. An explanation of the effect of heat treatment on wheat germ. *Cereal Chem.* 14, 489.
- Rupp, E., Bailey, C.H., 1937. The effects of protease increments on the plasticity of doughs. *Cereal Chem.* 14, 496.
- Stamberg, O.E., Bailey, C.H., 1938. Relationship of mixing speed to dough development. *Cereal Chem.* 15, 739.
- Pulkki, L.H., 1938. Particle size in relation to flour characteristics and starch cells of wheat. *Cereal Chem.* 15, 749.
- Singh, R., Bailey, C.H., 1940. A biochemical and technological study of Punjab wheat varieties. *Cereal Chem.* 17, 169.
- Ziegler, E., 1940a. Dough improvement studies. II. The effect of adding oxidized glutathione to wheat-flour doughs. *Cereal Chem.* 17, 551.
- Ziegler, E., 1940b. Dough improvement studies. III. Further studies on the oxidation of glutathione by bromate, chlorate, and persulphate. *Cereal Chem.* 17, 556.
- Staudt, E., 1940. Russian export wheats-composition and character of the 1938 crop. *Cereal Chem.* 17, 565.
- Stamberg, O.E., Merritt, P.P., 1941. Quantity of dough in relation to the use of the farinograph. *Cereal Chem.* 18, 627.
- Stamberg, O.E., Bailey, C.H., 1942. The effect of heat treatment of milk in relation to baking quality as shown by polarograph and farinograph studies. *Cereal Chem.* 19, 507.

- Schoonover, F., Freilich, J., Redfern, S., 1946. Some effects of cabinet fermentation on sponge temperatures and dough and bread characteristics. *Cereal Chem.* 23, 186.
- Sullivan, B., Richards, W.A., 1946. Open trough and cabinet fermentation of bread sponges. *Cereal Chem.* 23, 365.
- Sullivan, B., 1952. The reaction of flour proteins with surface active compounds. *Cereal Chem.* 29, 282.
- Thompson, J.B., Buddemeyer, B.D., 1954. Improvement of flour mixing characteristics by a stearyl lactylic acid salt. *Cereal Chem.* 31, 296.
- Shogren, M.D., Shellenberger, J.A., 1954. The design, construction and use of micro baking equipment. *Cereal Chem.* 31, 475.
- Smith, D.E., Andrews, J.S., 1957. The uptake of oxygen by flour dough. *Cereal Chem.* 34, 323.
- Smith, D.E., Van Buren, J.P., Andrews, J.S., 1957. Some effects of oxygen and fat upon the physical and chemical properties of flour doughs. *Cereal Chem.* 34, 337.
- Schlesinger, J., 1957. A rapid method for the production of flour for testing by farinography. *Cereal Chem.* 34, 443.
- Wilham, C.A., Dimler, R.J., Senti, F.R., 1959. A note on the effect of neutral polysaccharides on dough mixing properties. *Cereal Chem.* 36, 558.
- Pollock, J.M., Geddes, W.F., 1960. Soy flour as a white bread ingredient. *Cereal Chem.* 37, 19.
- Sokol, H.A., Mecham, D.K., Pence, J.W., 1960a. Observations on the reactivity of sulphydryl groups in wheat flours. *Cereal Chem.* 37, 151.
- Sokol, H.A., Mecham, D.K., Pence, J.W., 1960b. Sulphydryl losses during mixing of doughs: comparison of flours having various mixing characteristics. *Cereal Chem.* 37, 739.
- Sullivan, B., Dahle, L., Nelson, O.R., 1961. The oxidation of wheat flour. II. Effect of sulphydryl-blocking agents. *Cereal Chem.* 38, 281.
- Yasumatsu, K., Fujita, E., 1962. Studies on the cooking quality of rice. On the plastogram of rice. *Cereal Chem.* 39, 364.
- Ponte Jr., J.G., Titcomb, S.T., Cotton, R.H., 1964. Dough-improving effect of some aliphatic hydrocarbons. I. Baking and physical dough studies. *Cereal Chem.* 41, 203.
- Unrau, A.M., Jenkins, B.C., 1964. Investigations on synthetic cereal species. Milling, baking, and some compositional characteristics of some "triticale" and parental species. *Cereal Chem.* 41, 365.
- Smith, D.E., Mullen, J.D., 1965a. Studies on short and long-mixing flours. II. Relationship of solubility and electrophoretic composition of flour proteins to mixing properties. *Cereal Chem.* 42, 275.
- Smith, D.E., Mullen, J.D., 1965b. Studies on short- and long-mixing flours. III. Mixing properties, protein and lipid composition of various fractions. *Cereal Chem.* 42, 515.
- Tanaka, K., Kazuyo, F., Matsumoto, H., 1967. The effect of acid and salt on the farinogram and extensigram of dough. *Cereal Chem.* 44, 675.
- Tsen, C.C., Bushuk, W., 1968. Reactive and total sulphydryl and disulfide contents of flours of different mixing properties. *Cereal Chem.* 45, 58.
- Tkachuk, R., Hlynka, I., 1968. Some properties of dough and gluten in D₂O. *Cereal Chem.* 45, 80.
- Tanaka, K., Furukawa, K., Kuroiwa, R., Matsumoto, H., 1968. Association of synthetic anionic polymers with gluten. *Cereal Chem.* 45, 386.
- Pomeranz, Y., Shogren, M.D., Finney, K.F., 1969. Improving bread making properties with glycolipids. I. Improving soy products with sucroesters. *Cereal Chem.* 46, 503.
- Yoneyama, T., Suzuki, I., Murohashi, M., 1970. Natural maturing of wheat flour. I. Changes in some chemical components and in farinograph and extensigraph properties. *Cereal Chem.* 47, 19.

Index

Note: Page numbers followed by *f* indicate figures and *t* indicate tables.

A

- Acid-hydrolyzed corn stover, 143–145
- Amylolytic enzymes, 115
- ANSYS Polyflow company, 184
- Antibodies, 170–171
- Arabinoxylans, 100
- Arrival time (AT), 35–36, 169, 169*f*
- Australian Farrer-Guthrie collaboration, 6
- Autofluorescence, 172–183

B

- Baking quality, 4–5
- Bingham model, 133, 141
- Biomass type, 146–148
- Bird-Carreau constitutive model, 184
- Bozkurt's study, 169–170
- Brabender's Farinograph, 16
 - dough-mixing properties, 34
 - extension rate magnitudes, 184–188
 - maximum stable bubble sizes, 184–188
 - shear rate magnitudes, 184–188
- Brabender torque rheometers
 - accessories, 129, 130*f*
 - components, 129
 - for high solids biomass research
 - calibration procedure, 132
 - drive system, 131, 131*f*
 - wheat flour dough at peak development, 134–136, 138–141
 - instrument calibration, 150–155
 - schematic diagram, 132*f*
- Brabender units (BU), 177
- Bran, 100
- Bread production
 - dough consistency, 82–83
 - key elements of, 81–82
- Breakdown time (BT), 169, 169*f*
- Breeder's needs, 6, 15–17
- Buckwheat flour, 118
- Budapest University of Technology and Economics (BUTE), 17

C

- Calibration procedure, 132
- Carboxymethyl cellulose (CMC), 146–148
- Cereal chemistry testing, 4

Cereal proteins, 163

- Chart paper, 15
- Chickpea flours, 121, 122–123*f*
- Chinese wheat flour, 58–60
- Choice of breadmaking method, 85
- Chopin Alveograph, 9*f*
- Circulating water temperature, 104–107*f*, 105–106
- Clear flour products, 76, 76*t*, 78*f*
- Colocalization analysis, 174–175, 178*t*, 180*t*, 183*t*
- Commercial dough mixing, 85–87
- Commercial refined flour product, 75, 79*t*
- Computer screen, 15
- Confocal laser scanning microscopy (CLSM), 168–170

Consistency, 81–83

- Constant dough weight method, 39–40
- Constant flour weight method, 37–40, 93
- Corn flour, 113–114
- Cracker doughs
 - characteristics, 96*t*
 - Farinograph method, 94–96
 - flour-quality requirements, 92–93
 - processing, 92
- Critical capillary number, 184, 186–188

D

- Departure time (DT), 169, 169*f*
- Development time, 103–105, 104–105*f*
- Dietary fibers, 100
- Dietary Guidelines for Americans, 99
- Double-peak Farinograms, 25–26, 37, 39*f*
- Dough
 - consistency, 65–66, 81–83
 - development, 46–57, 85–87, 163–166
 - peak resistance, 64–66
 - physical properties, 58–66
 - processing, 84–85
 - processing equipment and methods, 85
 - properties, 4–5
 - real life of bakery, 17–18
 - rheology, 44–46
 - temperature, 85, 87

Dough development time (DDT), 36, 162

- Dough mixing, 99–100, 105–106
- Drop time, 146

E

- Electrical contacts, alternative solutions, 18–20
- Electronic recording, 15
- Energy consumption patterns, 86–87, 86*f*
- Enzymatic hydrolysis, 148–149
- Evaluation points, breakdown of, 35*f*
- Experimental mill-refined flour, 75
- Extension rate magnitudes, 184–188, 186–187*f*

F

- FarinoAdd-S300 GF accessory kit, 112–115, 112*f*
- Farinograph, 34, 74*f*, 99–101
 - alternate commercial uses, 87–88, 88*f*
 - for classifying flour strength, 36, 37*t*
 - communicating factor, 27–31
 - data for blends of two wheats, 75*t*
 - double-peak, 37, 38–39*f*
 - dough curves, 45*f*
 - excessively strong flours, 95*f*
 - gluten-free (GF) cereals, 111–118, 124
 - instrumental factor, 26
 - methods, 37–41
 - ongoing development and adoption, 13–14
 - operator factor, 25–26
 - “optimal” cracker flour, 94*f*
 - temperature factor, 23–24
 - torque curve, 35–36
 - water absorption factor, 24–25
- Fibers, 84
- Finagle's Law, 19–20
- Finite element method (FEM) codes, 184
- Flour
 - composition, 33–34
 - quality, 33–34
 - assessment, 34
 - strength classification, 36, 37*t*
 - temperature, 24
- Flow behavior index, 140–141

Fluorescence fingerprint (FF), 166
Fluorescent nanoparticles, 168–170

G

Gel-proteins
 disaggregation, 46–52
 fate of, 63–64
Germinated amaranth flour, 118
Gliadins, 163–166, 168–170, 177
Gluten-free (GF) cereals, 111–118, 124
Glutenin aggregates
 dough peak resistance, 64–66
 flow regimes, 58–59, 58*f*
 gel-proteins, fate of, 63–64
Glutenin macropolymer (GMP), 165–166, 165*f*
Gluten network, 81–82
Gluten proteins
 classification, 163–164
 visualization, 166–168, 170–183
Gums, 84

H

Hammer-milled corn stover, torque response for, 137, 137–138*f*, 142*t*
Hankóczy–Brabender relationship, 11, 13*f*
Hankóczy’s dough-testing equipment, 4, 5*f*
Hard wheat flour Farinogram, 91, 174*f*
High molecular weight glutenins, 164–165, 170–183, 173*f*, 179*f*
High protein “strong” soft wheats, 93
Hogarth’s recording drough mixer, 3–4, 7*f*, 8
Hooke, 6–8
Huggins constant, 55–57
Hydrate pulse flours, 119
Hydrocolloids, 115–118, 116*t*
Hyperaggregation model, 47–50, 66–67

I

Immunofluorescent imaging, 168–171
In-process stream selection, 76–77
Insoluble glutenin-gel fraction, 61–62
Instrumental factor, 26

K

Kick’s law, 50–51, 61–62

L

Legumes, 119
Lignocellulosic biomass, 128–129, 143, 146–148

Liquid-like doughs, 113–114
Low molecular weight glutenins, 164–165, 170–183, 173*f*, 179*f*

M

Macro-rheological phenomena, 63–64
Macroscopic level (Level III) aggregation, 67
Manders colocalization coefficient, 174–175
Maximum stable bubble sizes, 184–188, 186–187*f*
Medium strength flour, 162, 162*f*
Mesoscopic level (Level II) aggregation, 67
micro-doughLab, 17
Milk solids, 84
Mixer rheometry, 128
Mixing conditions, 85
Mixing tolerance index (MTI), 36
Mixograph, 8
Molecular level (Level I) aggregation, 67
Museum of Hungarian Agriculture, 4

N

Nanofluorescent quantum dots, 166–168
Navier-Stokes equation, 132
New crop wheat transition, 76
Newton, 6–8
Noninvasive monitoring, 18
Nonwheat grains and seeds, 84

O

Operator factor, 25–26
Osborne classification, 163

P

Patent flours, 76, 76*t*, 78*f*
Peak time (PT), 169, 169*f*
Plateau torques, 142, 142*t*
Polymers, rheological properties of, 64
Postmilling, 73
Power-law model, 133, 139, 140*t*, 140*f*
Pregelatinizing pulses, 121–124, 123*f*
Premilling, 73
Product type, 85
Protein network analysis technique, 175, 175*f*, 177, 178*t*, 180*t*, 183*t*
Pseudocereals, 118
Pugh matrix, 27, 28*f*
Pulses, 119–124, 120*f*

Q

Quantum dots, 166–169

R

Recipe water absorption factor, 83–85
Recipe water levels, 83–85
Red lentil flours, 121, 122–123*f*
Refined flour, 100
Researcher’s needs, 15–17
Rheological models, 133–134, 155–158
Rheological modifiers, 145–146
Rice flour, 114–115
Roller milling, 3–4

S

Salt, 84
SDS-dispersible/extractable (SP) fraction, 60–61
SDS-gel protein (SIP) fraction, 61–62
SDS insoluble glutenin particles, 52
Shape factors, 64–65, 65*f*
Shear rate magnitudes, 184–188, 186–187*f*
Sheeted cracker doughs, 96*f*
Sodium carboxymethyl cellulose (NaCMC), 117
Soft wheat flour
 cracker doughs, 92
 Farinograph, 94–96
 flour-quality requirements, 92–93
 uses, 91–92
Solid-like doughs, 113–114
Soya, 84
Starch
 enzymatic removal, 164*f*
 visualization, 166
Steady-state dough temperature, 24
Straight grade flours, 76, 76*t*, 77*f*
Stream pipes, 80, 80*f*
Strong flour, dough development time, 162, 162*f*
Sugar, 84
Supernatant (SUP) fraction, 47–50, 57

T

Temperature, 23–24
Thermostat reservoir, 23
Time to breakdown (TBD), 36
Titrating water, 24

Torque reduction (TR), 146

Torque rheometers. *See* Brabender torque rheometers

Torque-rotation rate data, 132–133

20-minute drop, 36

U

Unmixing experiment, 64

V

Valorigraph, 10–11

Very strong flour, dough development time, 162, 162 f

Viscosity curves, 139, 139 f

Voluminosity, 47–52, 51 f , 60–61

W

WAC calculation, 40

WAM calculation, 40

Water absorption (WA), 24–25, 35, 83–85, 99–100

Water soluble polymers (WSPs), 145–146

Weak flour, dough development time, 162, 162 f

Wheat flour doughs, 162

Wheat kernel, composition of, 33

Wheat milling operations

Farinograph testing

final product flour blends, 77–78

in-process stream selection,

76–77

limitations, 79–80

mill input, 74–76

purpose, 73–74

Whole wheat flour

(WWF)

composition, 99–101

Farinograph

dough stability time, 106–107 f

mixing water absorption,

102 f

WZ calculation, 40

X

Xanthan gum, 115–116

Y

Yield stress, 144–145, 144–145 f , 148 f

This page intentionally left blank

The Farinograph Handbook

Advances in Technology, Science, and Applications

Fourth Edition

Edited by

Jayne E. Bock, Ph.D., Technical Director, Wheat Marketing Center, Portland, OR, USA

Clyde Don, Ph.D., Managing Director of the FoodPhysica R&D Laboratory, The Netherlands

Full coverage of the principles governing the instrument, its operation, and application of results

The Farinograph Handbook is intended to enable any user to find information on how the different Farinograph models work, how to properly run a standard test and interpret the results, and how to explore standard and unconventional applications for the instrument. Advanced users will find new information on dough rheology and unconventional applications, whereas more traditional users will find new information on using results for process control in traditional bakery applications.

This new edition is a valuable reference for dough rheologists, cereal scientists, food scientists (specifically those working with bread products), millers, grain developers, academics, researchers, and students.

Key Features

- Provides an authoritative source for information regarding the Farinograph and its use
- Includes content on unconventional Farinograph applications
- Offers a troubleshooting section which addresses common issues encountered with the instrument
- Contains information on potential sources of error and how to avoid or control them
- Equips the reader to determine when an instrument requires maintenance and/or repair



WP

WOODHEAD
PUBLISHING

An imprint of Elsevier
elsevier.com/books-and-journals



ISBN 978-0-12-819546-8



9 780128 195468